

**SEDIMENTOLOGY AND GEOCHEMISTRY OF CORE  
SEDIMENTS FROM THE ASHTAMUDI ESTUARY AND THE  
ADJOINING COASTAL PLAIN, CENTRAL KERALA, INDIA**

*Thesis submitted to*  
**THE COCHIN UNIVERSITY OF SCIENCE AND TECHNOLOGY**

*In partial fulfillment of the requirements for the award of the Degree of*  
**DOCTOR OF PHILOSOPHY**  
*in*  
**MARINE GEOLOGY**

***Under the Faculty of Marine Sciences***

*By*

**TIJU I. VARGHESE**



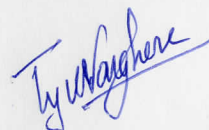
**NATIONAL CENTRE FOR EARTH SCIENCE STUDIES**  
THIRUVANANTHAPURAM, KERALA, INDIA-695011

**DECEMBER 2014**

## DECLARATION

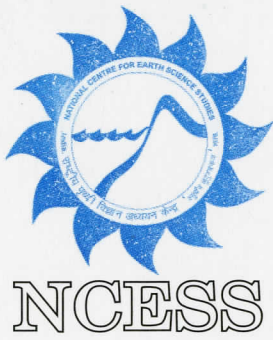
I hereby declare that the thesis entitled “Sedimentology and Geochemistry of Core Sediments from the Ashtamudi Estuary and the Adjoining Coastal Plain, Central Kerala, India” is an authentic record of research work carried out by me under the supervision and guidance of Dr. T.N. Prakash, Scientist-G & Group Head, Coastal Processes Group, National Centre for Earth Science Studies, Thiruvananthapuram, in partial fulfillment of the requirements for the Ph.D. Degree of Cochin University of Science & Technology and that no part thereof has been presented for the award of any other degree in any University.

Thiruvananthapuram  
December 18, 2014



Tiju I. Varghese  
(Reg. No. 3515)

National Centre for Earth Science Studies  
Thiruvananthapuram - 695011



राष्ट्रीय पृथ्वी विज्ञान अध्ययन केन्द्र  
NATIONAL CENTRE FOR EARTH SCIENCE STUDIES

पृथ्वी विज्ञान मंत्रालय, भारत सरकार  
Ministry of Earth Sciences, Government of India

पी.बी.नं. 7250, आक्कुलम, तिरुवनन्तपुरम - 695011, भारत  
PB No. 7250, Akkulam, Thiruvananthapuram-695011, India

**CERTIFICATE**

This is to certify that this thesis entitled "Sedimentology and Geochemistry of Core Sediments from the Ashtamudi Estuary and the Adjoining Coastal Plain, Central Kerala, India" is an authentic record of the research work carried out by Mr. Tiju I. Varghese (Reg. No. 3515) under my supervision and guidance at the National Centre for Earth Science Studies, Thiruvananthapuram, in partial fulfillment of the requirements for the Ph.D. Degree of Cochin University of Science and Technology under the Faculty of Marine Sciences and no part thereof has been presented for the award of any degree in any University.

Thiruvananthapuram  
December 18, 2014

Dr. T. N. Prakash  
(Research Guide)  
Scientist-G & Group Head  
Coastal Processes Group  
National Centre for Earth Science Studies  
Thiruvananthapuram - 695011

*Bible says in Philippians 4:13*

*"I can do all things through Christ which strengtheneth me"*

*To  
My beloved family*

## ACKNOWLEDGEMENTS

*I wish to place on record my deep sense of gratitude to my research guide Dr. T.N. Prakash, Group Head (Coastal Processes), National Centre for Earth Science Studies (NCESS), who has been a source of inspiration and support to me throughout the course of my research work. I owe him a lot for the constant encouragement and guidance and also for sparing his invaluable time, without which this work wouldn't have taken this shape.*

*I am grateful to Dr. N.P. Kurian, Director, NCESS for the support and encouragement rendered throughout this work. I consider myself extremely fortunate to have worked with him, since I found every discussion with him inspiring and enlightening. Thanks are also due to him for providing all the necessary facilities of the institute for the successful completion of my research work.*

*I express my immense gratitude to Dr. L. Sheela Nair, Scientist-E, Coastal Processes Group, NCESS for the constant guidance and encouragement received for the research work and for the support in the preparation of this thesis.*

*Prof. R. Nagendra, Dept. of Geology, Anna University, Chennai and Dr. N. Nagarajan, Asst. Professor, Dept. of Applied Geology, Curtin University, Malaysia are greatly acknowledged for fruitful discussion on geochemical aspects.*

*It is with great pleasure and gratitude that I acknowledge the valuable guidance received from Dr. K.V. Thomas, former Group Head and Dr. T.S. Shahul Hameed, Scientist-G, Coastal Processes Group during the course of my work.*

*I am grateful to Dr. G.R. RavindraKumar, Scientist G and Senior Consultant of Coastal Processes Group, for the guidance in final preparation of the thesis. I am thankful to Dr. M. Baba, former Director, NCESS, for the constant encouragement.*

*I acknowledge with gratitude the help received from M/s. D. Raju, Vijayakumaran Nair, Ajith Kumar, Ramesh Kumar and S. Mohanan, Scientific Officers at various stages of this study.*

*Prof. P. Seralathan, former Head, Dept. of Marine Geology and Geophysics, School of Marine Sciences, CUSAT has provided me valuable support and guidance in his capacity as Doctoral Committee member.*

*I am thankful to the Department of Science and Technology for financial support in the form of Senior Research Fellow under the Project No. SR/S4/ES-310/2007.*

*I acknowledge with thanks the administrative support provided by M/s. P. Sudeep, Chief Manager, M.A.K.H. Rasheed, Manager (F & A) and other officers and staff of the Administrative and Accounts sections of NCESS. Special thanks are due to Librarian and other staff of the library for extending the Library facilities.*

*It is my pleasure to put on record the support and friendliness I have enjoyed from the company of Dr. V.R. Shamji, Mr. C. Sreejith, Dr. C.S. Prasanth, Mr. N. Nishanth during my tenure at NCESS.*

*I have pleasure in acknowledging Mr. R. Prasad and Mr. Anish S. Anand for their unstinting support and timely help from the starting stages of my research work till the submission of this thesis.*

*Thanks are due to Dr. K.O. Badarees, Dr. K. Rajith, and Dr. Reji Srinivas for their support and encouragement at various stages of my research work.*

*Thanks are due to Dr. S.S. Praveen, Mr. S. Arjun, Mr. Arun J. John, Mr. Sreeraj M.K., Mr. Eldhose Kuriakose, Mrs. Krishna R. Prasad, Mrs. Raji S. Nair, Ms. Kalarani, Mrs. Gopika R. Nair and Mrs. Sindhu, NCESS for the help and support extended to me in various stages of the work. I also thank Ms. Gayathri and Mr. Sathyamurthy Research Scholars, Anna University for their help in laboratory computation.*

*Last but not the least I am to express my deep gratitude to my father (K.I. Varghese), my mother (Aleyamma), my loving brothers (Biju and Liju) and my sister-in-law (Raji Liju) for their prayers and unflinching support for completion of this work.*

*Tiju I. Varghese*

---

## *CONTENTS*

---

*Acknowledgements*

*List of Tables*

*List of Figures*

*Abstract*

### **Chapter 1 INTRODUCTION**

1.1	Introduction	1
1.2	Scientific Rationale	2
1.3	Objectives of the Present study	3
1.4	Study Area	3
1.4.1	Ashtamudi Estuary	5
1.4.2	Kayamkulam Lagoon	5
1.5	Physiography	6
1.6	Geology	7
1.6.1	Geological Setting of the Ashtamudi Estuary	7
1.6.2	Geological Setting of the Kayamkulam Lagoon	9
1.7	Geomorphology	9
1.7.1	Coastal Cliff	9
1.7.2	Coastal Plain with Ridge-Runnel Systems	9
1.7.3	Flood Plains	11
1.8	Climate and Rainfall	12
1.9	Physio-chemical Properties	12

### **Chapter 2 LITERATURE REVIEW**

2.1	Introduction	14
2.2	Quaternary Studies	14
2.2.1	International Status	14
2.2.2	National Status	15
2.2.2.1	Studies on the East Coast of India	16
2.2.2.2	Studies on the West Coast of India	17
2.3	Kerala Scenario	19

### **Chapter 3 FIELD DATA COLLECTION AND ANALYSES**

3.1	Introduction	26
3.2	Field Mapping and Collection of Sediment Cores	26
3.2.1	Field Mapping	26
3.2.2	Collection of Sediment Cores	26
3.3	Analyses of Sediment Core Samples	31
3.3.1	Textural Analysis	31
3.3.2	Surface Texture Analysis	33
3.3.3	Clay Mineral Analysis	33
3.3.4	Organic Matter Estimation	34
3.3.5	Determination of Calcium Carbonate	35
3.3.6	Geochemical Analysis	35
3.3.6.1	Sample Preparation and Instruments Used	36
3.3.6.2	Major Elements	37
3.3.6.3	Trace Elements	37
3.3.7	Radiocarbon Dating	37



## **Chapter 4 SEDIMENTOLOGY OF CORE SEDIMENTS**

4.1	Introduction	39
4.2	Lithological Variation	40
4.2.1	Sediment core along the southern transect (Kollam)	40
4.2.1.1	Coastal Plain (Core 1)	40
4.2.1.2	Ashtamudi Estuary (Core 2)	42
4.2.1.3	Ashtamudi Estuary (Core 3)	43
4.2.1.4	Ashtamudi Estuary (Core 4)	44
4.2.1.5	Offshore (Core 5)	45
4.2.2	Sediment core along the northern Transect	46
4.2.2.1	Coastal Plain (Core 6)	40
4.2.2.2	Kayamkulam Lagoon (Core 7)	49
4.2.2.3	Offshore (Core 8)	50
4.3	Textural Parameters	51
4.3.1	Southern Transect	52
4.3.1.1	Coastal Plain	52
4.3.1.2	Ashtamudi Estuary	53
4.3.1.3	Offshore	54
4.3.2	Northern Transect	55
4.3.2.1	Coastal plain	55
4.3.2.2	Lagoon	56
4.3.2.3	Offshore	56
4.4	Sediment classification	57
4.5	Depositional Environment	57
4.5.1	Hydrodynamic condition	58
4.5.2	Suite Statistics	60
4.6	Clay Minerals	62
4.7	Radiocarbon Dating	64
4.8	Discussion	66
4.9	Summary	69

## **Chapter 5 MICROMORPHOLOGICAL CHARACTERISTICS OF QUARTZ GRAINS – IMPLICATIONS ON DEPOSITIONAL ENVIRONMENT**

5.1	Introduction	71
5.2	Microtextural Characteristics	72
5.2.1	Southern Transect	72
5.2.1.1	Coastal Plain	72
5.2.1.2	Estuary	78
5.2.1.3	Offshore	81
5.2.2	Northern transect	82
5.2.2.1	Coastal Plain	82
5.2.2.2	Offshore	90
5.3	Transport Mechanism and Depositional History	92
5.4	Summary	95

<b>Chapter 6</b>	<b>MAJOR AND TRACE ELEMENT GEOCHEMISTRY OF SEDIMENT CORES</b>	
6.1	Introduction	97
6.2	Distribution of Major elements	98
6.2.1	Normalisation of major and trace elements with UCC	98
6.3	Geochemical Classification	112
6.4	Paleoweathering and Sediment Maturity	113
6.4.1	Chemical Index of Alteration	113
6.4.2	ICV Relation to Recycling and Weathering Intensity	117
6.4.3	Textural maturity	118
6.5	Provenance	120
6.6	Environment of Deposition	126
6.7	Geoaccumulation index (Igeo)	126
6.8	Summary	129
<b>Chapter 7</b>	<b>DEPOSITIONAL ENVIRONMENTS AND COASTAL EVOLUTION</b>	
7.1	Introduction	130
7.2	Depositional Environment	130
7.3	Relationship between Organic matter and Calcium Carbonate	131
7.4	Geochemical Proxies	131
7.5	Bathymetry	132
7.6	Holocene sea level changes	134
7.7	Evolution of the coast	135
7.8	Evolution of Ashtamudi Estuary	138
<b>Chapter 8</b>	<b>SUMMARY AND CONCLUSIONS</b>	
8.1	Summary	140
8.2	Evolution of the coast	143
8.3	Evolution of Asthamudi Estuary	144
8.4	Recommendations for Future Work	145
	<b>REFERENCES</b>	146
	<b>PUBLICATIONS</b>	179

---

### *List of Tables*

---

3.1	Details of the sediment cores collected from the different coastal environment of the study area	28
4.1	Sand silt and clay percentages, statistical parameters, organic matter and calcium carbonate contents of the coastal plain core (Core 1) of the southern transect	42
4.2	Sand silt and clay percentages, statistical parameters, organic matter and calcium carbonate contents of the Core 2 (Ashtamudi Estuary) of the southern transect	43
4.3	Sand silt and clay percentages, statistical parameters, organic matter and calcium carbonate contents of the Core 3 (Ashtamudi Estuary) of the southern transect	44
4.4	Sand silt and clay percentages, statistical parameters, organic matter and calcium carbonate contents of the Core 4 (Ashtamudi Estuary) of the southern transect	45
4.5	Sand silt and clay percentages, statistical parameters, organic matter and calcium carbonate contents of the Core 5 (Offshore) of the southern transect	46
4.6	Sand, silt and clay percentages as well as the textural parameters of the coastal plain core (Core 6) in the northern transect	48
4.7	Sand, silt, clay percentages as well as the textural parameters of the Kayamkulam lagoon core (Core 7) in the northern transect	50
4.8	Sand, silt, clay percentages as well as the textural parameters of the offshore core (Core 8) in the northern transect	51
4.9	Classification of grain size parameters based on Folk and Ward (1957)	52
4.10	Radiocarbon dating results in the present study	64
4.11	Published <sup>14</sup> C dates from the coastal sediments of the Kollam and Kayamkulam region	65
6.1	Major and trace element composition of sediments	99-108
6.2	Geoaccumulation index (Igeo) for core sediments of Ashtamudi Estuary	128

---

## *List of Figures*

---

1.1	Location Map showing two transects East-West, cutting across the inland, lagoon/estuary and offshore region of the Kollam and Kayamkulam coast	4
1.2	Geological map of study area	8
1.3	Geomorphological features of the study area representing floodplains, swales, ridges in different orientation ( <i>after</i> Samsuddin et al., 2008)	10
3.1	Map showing the locations of sediment cores collected from the coastal plain, estuary and offshore region along the Kollam-Kayamkulam coast	27
3.2	Field Photographs of the Kollam coastal plain (southern boundary of the study area) showing (a) location of sample collection - Kallada River debouching into the Ashtamudi Estuary, (b) Rotary drilling in operation, (c) collection of undisturbed sediment core in a spoon after drilling and (d) sub-sampling of the core	29
3.3	Field photographs of core sample collection from the Kayamkulam coastal plain (northern boundary of the study area) showing (a) site area east of Kayamkulam Lagoon, (b) Rotary drilling in operation, (c) undisturbed sediment core and (d) lithological observation as well as packing of the samples	30
3.4	Photographs showing the lithology of the collected core samples	30
3.5	Photographs showing (a) Panoramic view of the Ashtamudi Estuary (central portion), (b) Piston Corer used for the collection of core samples, (c) cutting of sediment core using core cutter in the laboratory and (d) sub-sampling of undisturbed sediment core samples	31
3.6	Flowchart showing different types of analysis on sediment core samples	32
4.1	(a) Lithological variation of sand silt clay percentages and (b) Sediment type variations in the coastal plain, estuary and offshore region of the southern transect	41
4.2	(a) Lithological variation of sand silt clay percentages and (b) Sediment type variations in the coastal plain, lagoon and the offshore region of the northern transect	47
4.3	Hydrodynamic deposition of sediments ( <i>after</i> Pejrup, 1988) for (a) the southern and (b) northern transects	59
4.4	Depositional environment based on Mean vs Sorting ( <i>after</i> Tanner, 1991) for the sediment cores of the (a) southern and (b) northern transect	61
4.5	Showing down core variation of X- ray diffraction pattern of clay minerals (K- Kaolinite, I- Illite, and G- Gibbsite) in the coastal plain Core 1 of southern transect	63
4.6	Showing down core variation of X- ray diffraction pattern of clay minerals (K- Kaolinite, I- Illite, G- Gibbsite, and C- Chlorite) in the coastal plain Core 6 of northern transect	64
5.1	SEM photographs of the quartz grains at the depth of 3.0 m showing mechanical features	73
5.2	SEM photographs of the quartz grains at the depth of 9.0 m (a) showing large conchoidal fracture with high relief and angular in outline (b) V-etch pits	73
5.3	SEM photographs of the quartz grains at the depth of 10.9 m (a) showing sub-rounded in outline (b) solution features in the form of branching solution and centipede types	74
5.4	SEM photographs of the quartz grains at the depth of 11.8 m showing (a) totally distorted shape with sub-rounded in outline (b) with chemically etched fractured plates	75
5.5	SEM photographs of the quartz grains at the depth of 12 m showing (a) sub rounded in outline dominating chemical features such as (b) anatomising	76

	pattern, silica pellicle, silica precipitation in conchoidal pattern leading to silica plastering (c) and pressure solution feature (d) indicating diagenesis	
5.6	SEM photographs of the quartz grains at the depth of 15.5 m showing chemical features in the form of (a) dissolution etching and (b) honey comb structure indicating prolong diagenesis	77
5.7	SEM photographs of the quartz grains of Core 2 showing (a) large conchoidal fracture (b) silica solution	79
5.8	photographs of the quartz grains of Ashtamudi estuary Core 3 at the depth of 0.80 m showing (a) sub-rounded with prismatic shape (b) series of fracture plates (c) retainment of mechanical plates (d) erosion of silica overgrowth	80
5.9	SEM photographs of the quartz grains of the southern offshore core (a) Grain breakage associated with fracture (b) chemical upturned plates (c) silica solution (d) silica dissolution	81
5.10	SEM photographs of the quartz grains at the depth of 3.0 m showing (a) mechanical features such as impact pits, chattermarks (b) crescentic groups with friction marks (c) deep grooves with elongate scratches and troughs (d) grooves oriented in a preferred direction	83
5.11	SEM photographs of the quartz grains at the depth of 8.9 m showing (a) sub-rounded with bulbous projection, linear grooves (b) fracture plates with slight chemical modification	84
5.12	SEM photographs of the quartz grains at the depth of 10.9 m showing (a) low relief distorted in nature with solution pits and crevasses (b) different oriented etch pits	85
5.13	SEM photographs of the quartz grains at the depth of 11.6 m showing (a) cross hatching network, deep haloes (b) smoothness of breakage blocks indicating silica precipitation	87
5.14	SEM photographs of the quartz grains at the depth of 16.0 m (a) showing mechanical features such as sub rounded in outline; (b) chemical features such as pressure solution, and (c) deep triangle within triangle indicating intense chemical weathering	88
5.15	SEM photographs of the quartz grains at the depth of 19.7 m showing (a) total etching of the grains (b) silica plastering, silica pellicle, and (c) leaf like structure	89
5.16	SEM photographs of the quartz grains (0.60 m) of northern offshore at the depth of 10 m showing (a) large breakage conchoidal fracture (b) solution crevasses (c) chatter mark trails on upturned plates (d) crystalline overgrowth with irregular solution pits	91
6.1	Normalisation of Major elements (a) and Trace elements(b) diagram against Upper Continental Crust (UCC: Taylor and McLennan, 1985; McLennan, 2001)	109
6.2	Fig. 6.2 $\text{SiO}_2/\text{Al}_2\text{O}_3$ vs $\text{K}_2\text{O}/\text{Na}_2\text{O}$ plot for the core sediments representing the coastal plain, estuary and offshore compared with different possible source rocks	112
6.3	Geochemical classification diagram of sediment cores representing coastal plain, estuary/lagoon and offshore core sediments (after Herron, 1988)	113
6.4	A-CN-K ( $\text{Al}_2\text{O}_3\text{-CaO+Na}_2\text{O+K}_2\text{O}$ ) ternary diagram showing the general weathering trend and intensity of weathering in the source region for the coastal plain, estuary and offshore (after Nesbitt and Young, 1984)	116
6.5	ICV vs CIA plot shows the maturity and intensity of chemical weathering for the sediment cores representing coastal plain, estuary and offshore (after Long et al., 2012b)	119
6.6	$\text{TiO}_2$ vs $\text{Al}_2\text{O}_3$ (after Flyod et al., 1989) bivariate plot showing the possible provenance for the core sediments representing coastal plain, estuary and offshore	121

6.7	K <sub>2</sub> O vs Rb plot shows the provenance field for core sediments representing coastal plain, estuary and offshore	122
6.8	Discriminant function diagram for the provenance signatures of the core sediments using major elements (after Roser and Korsch, 1988)	123
6.9	TiO <sub>2</sub> vs Ni diagram (after Flyod et al., 1989) for the core sediments representing coastal plain, Ashtamudi estuary and offshore	125
6.10	MgO/Al <sub>2</sub> O <sub>3</sub> and K <sub>2</sub> O/Al <sub>2</sub> O <sub>3</sub> diagram (after Roaldset, 1978) to differentiate between marine and non-marine clays representing coastal plain, estuary and offshore region	126
7.1	Kayals of the Ashtamudi estuary	133
7.2	Paleo-shoreline derived from geomorphological signatures and radiocarbon dating during Late Holocene (5,000 to 6,000 Yrs BP) and Late Pleistocene (42,000 Yrs BP). Borehole lithology of 1 & 6 showing peat and corresponding <sup>14</sup> C dates. Sea level fall cause marine regression exposing shelf region even up to 80 m during LGM.	136
7.3	Conceptual model showing the evolution of the coast during the Quaternary	137

## ABSTRACT

The evolution of coast through geological time scale is dependent on the transgression-regression event subsequent to the rise or fall of sea level. This event is accounted by investigation of the vertical sediment deposition patterns and their interrelationship for paleo-environmental reconstruction. Different methods like sedimentological (grain size and micro-morphological) and geochemical (elemental relationship) analyses as well as radiocarbon dating are generally used to decipher the sea level changes and paleoclimatic conditions of the Quaternary sediment sequence. For the Indian coast with a coastline length of about 7500 km, studies on geological and geomorphological signatures of sea level changes during the Quaternary were reported in general by researchers during the last two decades. However, for the southwest coast of India particularly Kerala which is famous for its coastal landforms comprising of estuaries, lagoons, backwaters, coastal plains, cliffs and barrier beaches, studies pertaining to the marine transgression-regression events in the southern region are limited. The Neendakara-Kayamkulam coastal stretch in central Kerala where the coast is manifested with shore parallel Kayamkulam Lagoon on one side and shore perpendicular Ashtamudi Estuary on the other side indicating existence of an uplifted prograded coastal margin followed by barrier beaches, backwater channels, ridge and runnel topography is an ideal site for studying such events. Hence the present study has been taken up in this context to address the gap area. The location for collection of core samples representing coastal plain, estuary-lagoon and offshore regions have been identified based on published literature and available sedimentary records. The objectives of the research work are:

- To study the lithological variations and depositional environments of sediment cores along the coastal plain, estuary-lagoon and offshore regions between Kollam and Kayamkulam in the central Kerala coast
- To study the transportation and diagenetic history of sediments in the area
- To investigate the geochemical characterization of sediments and to elucidate the source-sink relationship

- To understand the marine transgression-regression events and to propose a conceptual model for the region

The thesis comprises of 8 chapters. The first chapter embodies the preamble for the selection and significance of this research work. The study area is introduced with details on its physiographical, geological, geomorphological, rainfall and climate information.

A review of literature, compiling the research on different aspects such as physico-chemical, geomorphological, tectonics, transgression-regression events are presented in the second chapter and they are broadly classified into three viz:- International, National and Kerala.

The field data collection and laboratory analyses adopted in the research work are discussed in the third chapter. For collection of sediment core samples from the coastal plains, rotary drilling method was employed whereas for the estuary-lagoon and offshore locations the gravity/piston corer method was adopted. The collected subsurficial samples were analysed for texture, surface micro-texture, elemental analysis, XRD and radiocarbon dating techniques for age determination.

The fourth chapter deals with the textural analysis of the core samples collected from various predefined locations of the study area. The result reveals that the Ashtamudi Estuary is composed of silty clay to clayey type of sediments whereas offshore cores are carpeted with silty clay to relict sand. Investigation of the source of sediments deposited in the coastal plain located on either side of the estuary indicates the dominance of terrigenous to marine origin in the southern region whereas it is predominantly of marine origin towards the north. Further the hydrodynamic conditions as well as the depositional environment of the sediment cores are elucidated based on statistical parameters that decipher the deposition pattern at various locations viz., coastal plain (open to closed basin), Ashtamudi Estuary (partially open to restricted estuary to closed basin) and offshore (open channel). The intensity of clay minerals is also discussed. From the results of radiocarbon dating the sediment depositional environments were deciphered.



The results of the microtextural study of sediment samples (quartz grains) using Scanning Electron Microscope (SEM) are presented in the fifth chapter. These results throw light on the processes of transport and diagenetic history of the detrital sediments. Based on the lithological variations, selected quartz grains of different environments were also analysed. The study indicates that the southern coastal plain sediments were transported and deposited mechanically under fluvial environment followed by diagenesis under prolonged marine incursion. But in the case of the northern coastal plain, the sediments were transported and deposited under littoral environment indicating the dominance of marine incursion through mechanical as well as chemical processes. The quartz grains of the Ashtamudi Estuary indicate fluvial origin. The surface texture features of the offshore sediments suggest that the quartz grains are of littoral origin and represent the relict beach deposits.

The geochemical characterisation of sediment cores based on geochemical classification, sediment maturity, palaeo-weathering and provenance in different environments are discussed in the sixth chapter.

In the seventh chapter the integration of multiproxies data along with radiocarbon dates are presented and finally evolution and depositional history based on transgression–regression events is deciphered.

The eighth chapter summarizes the major findings and conclusions of the study with recommendation for future work.

# CHAPTER 1

## INTRODUCTION

### 1.1. Introduction

Coastal areas are one of the most populated, diverse and dynamic landscapes on earth. The coastal environment is characterized by a range of erosional and depositional landforms that undergoes constant changes. Natural processes such as the eustatic and isostatic sea level changes, neotectonic activity and other environmental and weather related phenomena play a significant role in reshaping the coastline. Hence, for understanding the formation and evolution of coasts, the use of a reliable and useful chronological tool is needed (Jacob, 2008). A better understanding of the sediment proxy data in sedimentary archives is vital as it is a valuable source of information on the changes in environmental conditions and sediment supply. For an efficient interpretation of the coastal evolution, a synthesis of all inferences derived from various lithological units that encompasses the sedimentary architecture is a prerequisite. The changes in sea level and sediment supply within a geological cycle and their interrelationship can be deciphered from a detailed analysis of the lithological constituents. One of the direct methods used for investigation is by conducting detailed analyses of sediment samples collected from the outcrops and drilled cores. Knowledge of the vertical sequences of sedimentary depositional pattern on the areal distribution particularly their interrelationship as well as temporal variation can lead to a total understanding of the geological evolution of an area (Bateman, 1985).

The evolution of various coastal landforms like estuaries, deltas, lagoons, mangroves, marshes, barrier, dunes, etc, can be linked to the interaction of coastal geomorphology with waves, tides, fluvial supplies as well as relative sea level changes, and anthropogenic activities (Davies, 1964; Chiverrell, 2001). This can lead to changes in the local sedimentation rates, creation of geomorphological formations (spits, cheniers, levees), alteration of the natural hydrodynamics (Leduc et al., 2002; Gerdes et al., 2003; Ybert et al., 2003). For a detailed understanding of these changes in the coastal landforms a thorough analysis combining geomorphological, sedimentological, faunal and mineralogical features is inevitable (Chamley, 1989; Dalrymple et al., 1992; De la Vega et al., 2000; Edwards, 2001; Umitzu et al., 2001).

Sea level and climatic changes during the Quaternary period have strongly influenced the geomorphic and sedimentation processes in the coastal regions. Major portion of the coastal land formed during the late Quaternary period and geomorphic evolution has greatly influence the history of mankind (Narayana and Priju, 2004). The study of Quaternary deposits on continental margins provides the opportunity for explaining the relations between surfaces and deposits that originate during one cycle of relative sea-level fluctuation (Posamentier et al., 1988).

India has a vast coastline of about 7,500 km length, covering both west and east coasts. The west coast particularly the Kerala coast located in the southwest part of Indian peninsula is highly dynamic compared to the east coast. Out of the 560 km coastline of Kerala, a cumulative length of 360 km show dynamic changes in terms of erosion and deposition patterns (Narayana and Priju, 2004). Tectonic processes, resulting in uplift/subsidence alter the fluvial regime (Valdiya and Narayana, 2007) with subsequent changes in the rates of erosion and deposition of sediments (Soman, 1997). Occurrence of prograding coastlines are also observed along the Kerala coast as evident from the chain of coast-parallel estuaries/lagoons with rivers debouching into them and separated from the sea by spits/bars (Narayana and Priju, 2004).

## **1.2. Scientific Rationale**

The evolution of coast through geological time scale is dependent on the transgression-regression event subsequent to the rise or fall of sea level. This event is accounted by investigation of the vertical sediment deposition patterns and their interrelationship for paleo-environmental reconstruction. Different methods like sedimentological (grain size and micro-morphological) and geochemical (elemental relationship) analyses as well as radiocarbon dating are generally used to decipher the sea level changes and paleoclimatic conditions of the Quaternary sediment sequence. For the Indian coast, studies on geological and geomorphological signatures of sea level changes during the Quaternary were reported in general by researchers during the last two decades. However, for the southwest coast of India particularly Kerala which is famous for its coastal landforms comprising of estuaries, lagoons, backwaters, coastal plains, cliffs and barrier beaches, studies pertaining to the marine transgression-regression events in the southern region are limited.

The Neendakara-Kayamkulam coastal stretch in central Kerala where the coast is manifested with shore parallel Kayamkulam Lagoon on one side and shore perpendicular Ashtamudi Estuary on the other side indicating existence of an uplifted prograded coastal margin followed by barrier beaches, backwater channels, ridge and runnel topography is an ideal site for studying such events. Hence the present study has been taken up in this context to address the gap area. The location for collection of core samples representing coastal plain, estuary-lagoon and offshore regions have been identified based on published literature and available sedimentary records. The present research work aims to study the evolution history of the Neendakara-Kayamkulam coastal region utilizing the sub-surface sediment cores for sedimentological and geochemical characteristics supported with proxy environmental indicators. The field and laboratory test results of the sediment cores, being a source of primary information on marine geological processes is expected to unravel the evolutionary history of the Ashtamudi Estuary and its surrounding region.

### **1.3. Objectives of the Present study**

The present study envisages:

1. To study the lithological variations and depositional environments of sediment cores along the coastal plain, estuary-lagoon and offshore regions between Kollam and Kayamkulam in the central Kerala coast
2. To study the transportation and diagenetic history of sediments in the area
3. To investigate the geochemical characterization of sediments and to elucidate the source-sink relationship
4. To understand the marine transgression-regression events and to propose a conceptual model for the region

### **1.4. Study Area**

To understand the coastal evolution during the Pleistocene-Holocene period, a systematic study along two East-West transects originating from the coastal plain and cutting across the estuary/lagoon to the near inner shelf domain has been considered. The study is carried out for the coastal stretch along Kollam and Kayamkulam regions of the central Kerala, India (Fig. 1.1).

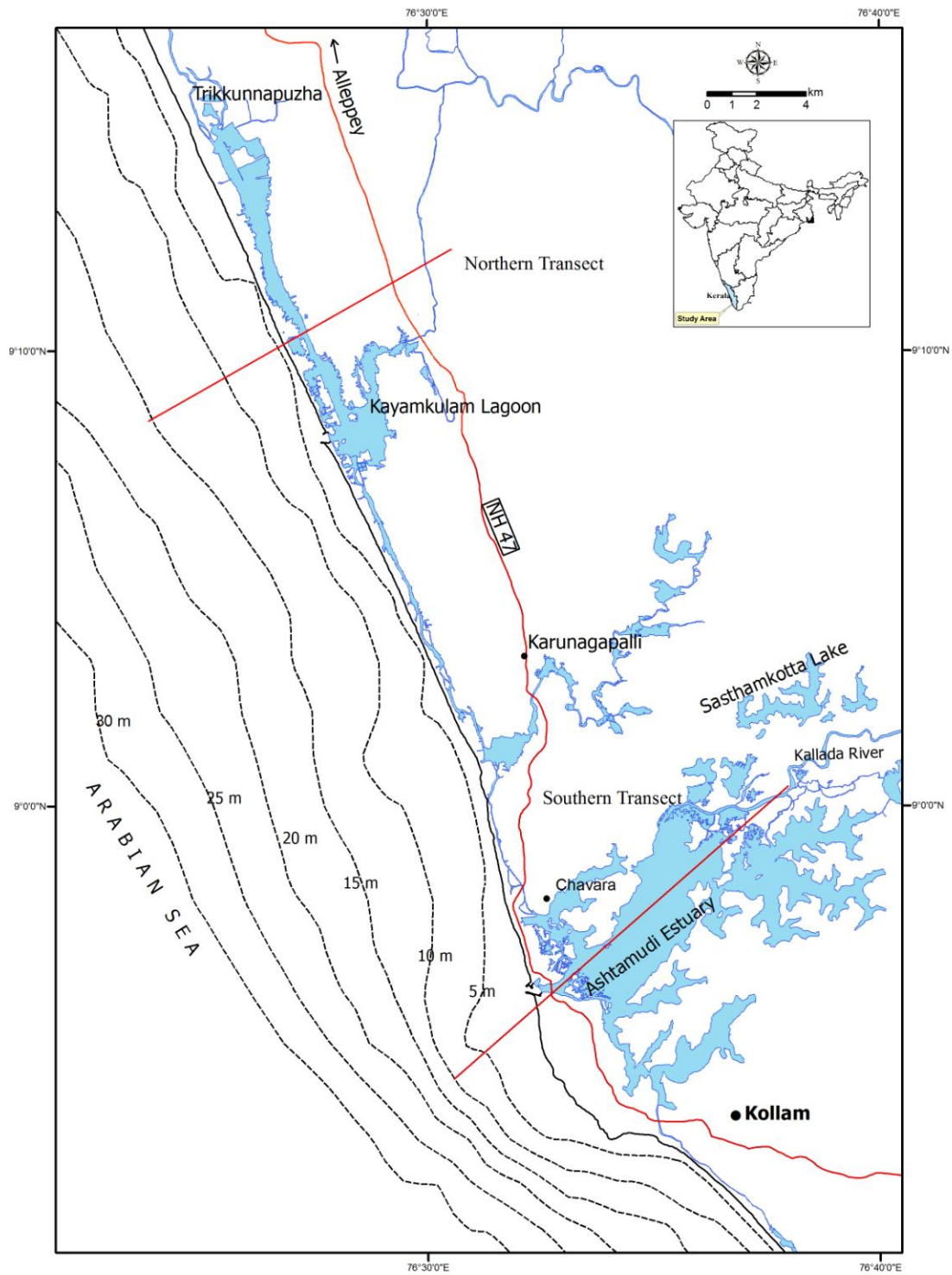


*Fig. 1.1 Location Map showing two transects East-West, cutting across the inland, lagoon/estuary and offshore region of the Kollam and Kayamkulam coast*

#### **1.4.1. Ashtamudi Estuary**

The Ashtamudi Estuary is the second largest in Kerala located between the latitudes of 8° 31'–9° 02' N and 76° 31'–76 ° 41' E respectively. It has an unique configuration characterised by a palm-shaped extensive water body with eight prominent arms/heads, justifying its name 'Ashta' (eight), 'mudi' (head) adjoining the Kollam town. The estuary drains into the Arabian Sea through a 200 m wide mouth that serves as a permanent connection. It has an average depth of 2.14 m in the Neendakara area where fishing harbour has been developed. This is one of the biggest fish-landing centres of the southwest coast in the country (Nair et al., 1983). The Ashtamudi estuary has a length of 16 km with an area of 54 km<sup>2</sup>. Steep slopes of lateritic capping and escarpments are exposed around the estuary like Padappakara area. The estuary is characterised with a long-axis perpendicular to the shoreline and the sides are fringed with escarpments of laterite developed over Tertiary formations (Prakash et al., 2001; Sabu and Thrivikramaji, 2002).

The tides in the estuary are semidiurnal with a range of about 1 m. Thus, the sources of sedimentation in the estuary are from the enormous quantities of silt-laden fresh water inflow from the rivers and the stirred up sediments brought into the estuary during the flood tides (Nair and Azis, 1987). The major fresh water input to the estuary is from the 121 km long Kallada River formed by the confluence of the Kulathupuzha, Chendurni and Kalthuruthy tributaries that originate in the highlands of the Western Ghats. The area of the drainage basin is 1,919 km<sup>2</sup>. The annual run off to the basin is 2,270 million m<sup>3</sup> (PWD, 1976). A few individual islets (thuruths) with very steep side slopes are also observed within the estuary. The deltaic island of Monrothuruth is located at the mouth of the Kallada River where it discharges into the estuary. The presence of a number of water bodies on both sides of the Kallada River and paleo-river channels that connect them with the river indicates that the estuary was more extensive in the past. Soman (1997) reported that the area of the estuary has reduced from 53.80 km<sup>2</sup> in 1968 to 44.77 km<sup>2</sup> in 1983 due to reclamation.

#### **1.4.2. Kayamkulam Lagoon**

The Kayamkulam Lagoon is located in the coastal lands of Kollam and Alappuzha districts (9° 2'–9° 16' N; 76° 25'–76° 32' E) in the form of a linear water

body extending from Sankaramangalam (Kollam district) in the south to Karthikapalli (Alappuzha district) in the north. It covers a length of about 25 km and the width varies between 0.1 and 1 km. The depth ranges from 0.5 m to 2.5 m. The lagoon, which is connected to the Arabian Sea, is separated from the sea by a barrier beach. The barrier beach has a total length of 22 km with a varying width of 2 to 5 km and is enriched with the beach placer deposits. The foreshore slopes vary between 4–10°, and the direction of longshore currents remain predominantly northerly in this segment (Prakash et al., 1987). Three major drainage channels that drain the lagoon basin are the Pallikkal thodu in the south; the Krishnapuram Ar and the Kayamkulam Canal in the central region and Thrikkunnappuzha in the north (Fig. 1.1). In addition to these, a few low order streams and minor canals as well as distributaries of Pamba and Achankovil Rivers also debouch into the Kayamkulam basin at different locations. The general drainage pattern is dendritic reflecting the homogenous terrain. The lake is connected through inland waterways canal to the Vembanad in the north and Ashtamudi in the south.

### **1.5. Physiography**

Kerala is a narrow strip of land on the south western part of the Peninsular India, with width varying from 30 km at the two ends (north and south) and to about 130 km in the central region. The total geographic area of the state is only 38,854.97 km (approximately 1% of India's total area). Physiographically, Kerala can be divided into three well-defined natural divisions viz. low lands, midlands and high lands. These physiographic zones determine the drainage systems, vegetational pattern and resources in the area.

The physical features exhibit wide-ranging variation occasionally broken by a few passes. The Western Ghats, which form an almost continuous mountain chain, borders the eastern part of the state. Kerala has a total of 7 lagoons and 27 estuaries (Nair et al., 1988) of which the Vembanad Lake is the largest estuary with an area of 205 km<sup>2</sup>. The state of Kerala is enriched with 44 rivers of which 41 are west flowing eventually draining into the Arabian Sea (Soman, 1997). The total run-off from all the rivers is about 2,50,000 million cubic feet i.e. about 5% of India's total water potential (Shajan, 1998).

The Kollam district consists of three distinct physiographic zones, the lowland (< 8 m above MSL) the midland (8-75 m above MSL) and the high land (< 75 m above MSL) (KSUB, 1995).

It has been reported that about 63% of the total area of the district comprises of lowland, 23% midland and the remaining 14% highland (Shaji, 2003). The physiographic zone surrounding the Kayamkulam region can be divided into two broad zones – the lowland (< 8 m above MSL) and the midland (8-75 above MSL) (KSUB, 1995). The region is devoid of mountains and hills except for some residual hillocks lying between the Bharnikavau and Chengannur blocks in the eastern part of the district (EDGI, 1998).

## **1.6. Geology**

Geologically, Kerala region is characterised by Precambrian crystallines, coastal Tertiary and Quaternary formations. With reference to the study area, the region can be divided into two sections based on the geological settings, which are discussed below:

### **1.6.1. Geological Setting of the Ashtamudi Estuary**

The area surrounding the Ashtamudi Estuary forms an important geological segment of the southern Indian peninsular shield. The area is surrounded by three major rock formations viz., the Archaean crystalline basement, the Tertiary and the Quaternary sedimentary sequences (Fig. 1.2). The Archaean crystalline basement, represented by the garnet–biotite gneisses, khondalites and charnockites, are dominant in the eastern and southeastern parts of the Kallada basin. The Tertiary sediments are represented by the Quilon and Warkalli Formations of Lower Miocene age. The Warkalli formation composed of sandstones and clays is exposed on the laterite hillocks surrounding the Sasthamkotta and Chelupola Lakes. The Quilon formation, occurring below the Warkalli formation is represented by fossiliferous limestones and sandy carbonaceous clays. The Archaean crystalline basement and the Tertiary sedimentary sequences are lateralized at the top. The cliff section on the banks of estuary is the Quilon bed type. The Quaternary formations are represented by alluvial clays, sandy clays and peat on the southeastern side of the lake.



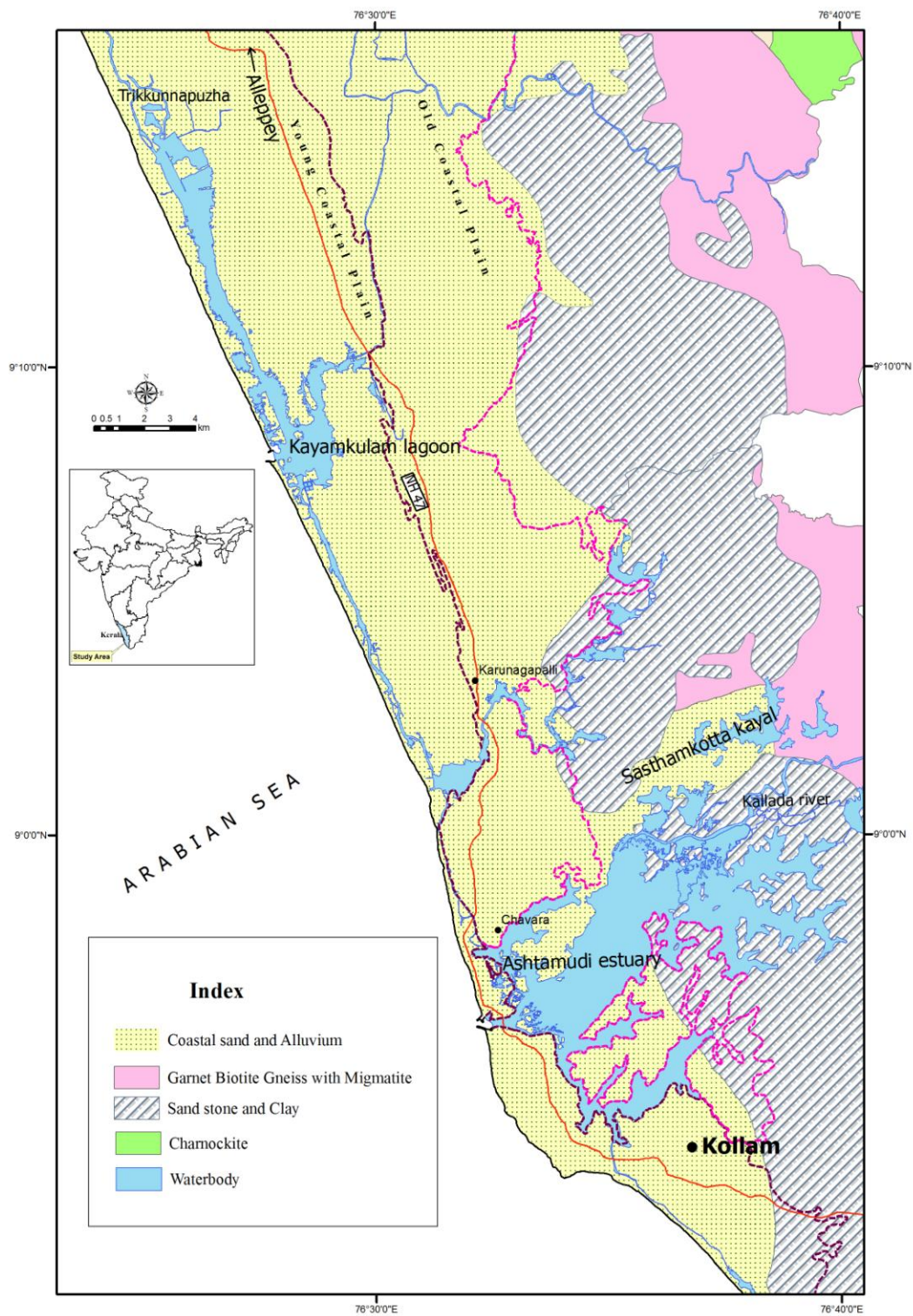


Fig. 1.2 Geological map of study area

### **1.6.2. Geological Setting of the Kayamkulam Lagoon**

The area surrounding the lagoon can be classified into three distinct units, viz., the Precambrian crystallines, the Tertiary sedimentaries and the Quaternary deposits (Fig. 1.2). As mentioned earlier, laterite is exposed as cap rocks at some places.

The Precambrian crystallines are composed predominantly of garnet-biotite gneisses with associated migmatites, garnet-sillimanite gneisses with graphites (Khondalite) and patches of quartz-feldspar-hypersthene granulite (Charnockite). These rocks are found to be intruded at many places by acidic (pegmatites and quartz veins) and basic (pyroxene granulite) dykes. The Precambrians are confined mainly to the eastern part of the watershed area of the estuary. Towards west the Tertiary sediments represented by sandstones and claystones with seams of lignite (Warkali Formation) are observed. Coastal sands and alluvium of Quaternary age dominates the western part close to the estuarine basin. This zone is marked by a series of ridges and runnels that can be attributed to the Quaternary sea level oscillations.

## **1.7. Geomorphology**

The evolution and subsequent changes of the coastal landforms are influenced by factors like the coastal processes, sea level changes, climate, tectonic settings, etc. Several landform units can be seen in the coastal lowlands of the study area. The major landforms of the study area are described below:

### **1.7.1. Coastal Cliff**

These are erosional features of marine origin. Laterite cliff is present in the Thangasseri area (southern boundary of the study area). The cliff occupies an area of 0.14 km<sup>2</sup> with a slope of nearly 20 % (CESS, 1998).

### **1.7.2. Coastal Plain with Ridge-Runnel Systems**

The coastal plain has an area of about 169.0 km<sup>2</sup> extending more towards the northern portion of the district, i.e. beyond the Ashtamudi Estuary (Fig. 1.3). The coastal plain is more or less flat with an average slope of 10% and extends upto Chuarnad and Todiur in the north and towards the south, it decreases considerably.

The coastal plain covers all the backwaters, lakes, small wetlands like Valumel, Punja and Vatta Kayal in the north. Ridge and runnel topography within the coastal plain is dominant from Karunagapally in the north. N-S trending sand ridges and intermittent longitudinal valleys of small tributary streams of Pallikkal Thodu are also present.

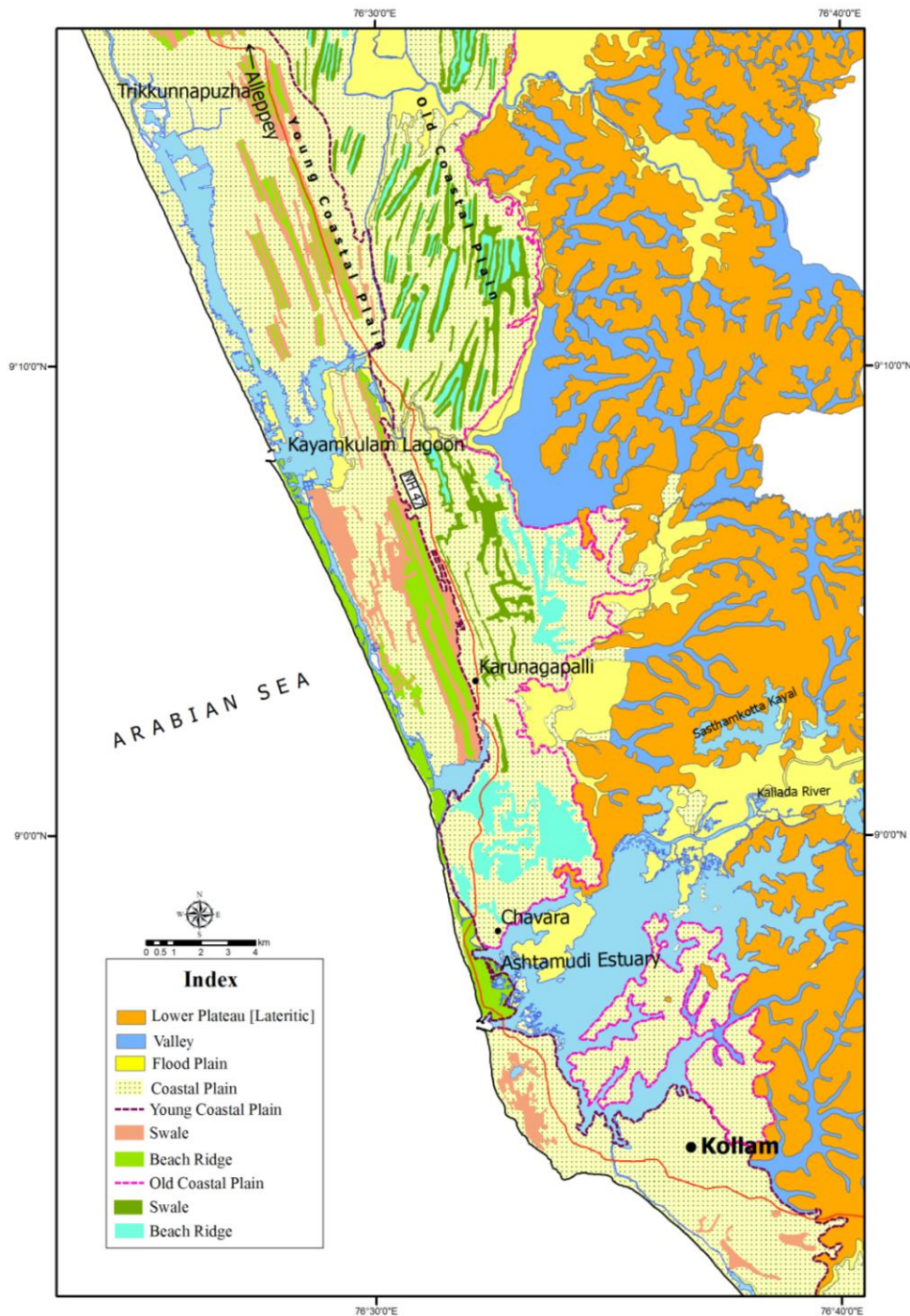


Fig. 1.3 Geomorphological features of the study area representing floodplains, swales, ridges in different orientation (after Samsuddin et al., 2008)

Plains with paleostrandlines with beach ridge is categorised as complex system (CESS, 1998). The width of the ridge, which comprises sand of various grade ranges from 50 to 180 m and height, varies between 0.5 and 1.0 m. The width of the runnels ranges from 50 to 200 m. These features represent successive stillstand position of an advancing shoreline in relation to the sea (Narayana and Priju, 2006). The coastal plain is carpeted by rich placer deposits particularly along the Chavara coast. Chavara is world famous for its ilmenite rich sand and has an estimated reserve of 36 million tonnes (Soman, 1997).

### **1.7.3. Flood Plains**

Terraces adjoining the main rivers, levees, back swamps and alluvial fans constitute the flood plains. About 211 km<sup>2</sup> of area come under this category. It is flat bottomed and occasionally stepped and sloping in the upper part within the midland and highland region. Wide flood plains are noticed in the Kallada, Ittikara and Pallikal Rivers. Side slopes bounding these valleys belong to moderate to steep category. The elongated NW-SE trending valleys indicate structural control in formation over the Precambrian crystalline rocks traversed by lineaments and joints that have facilitated the formation of straight course of these valleys. In the case of the Kallada River, with the exception of wide floodplains in the downstream reaches near Naduvelikara, Mullikala broad N-S trending floodplains are observed around Anthamam thodu near Kulakkada and Pazhi thodu near Manjakkala (Fig. 1.3). Low rolling terrain with gentle side slopes < 15% occupies 340 km<sup>2</sup> of the Kollam district.

Gentle undulations with small ridges are characteristic features of the coastal plain upto Kootangara Chattanpu and Talakulam region. Low rolling terrain gradually merges with moderate undulating terrain with moderate side slope of 15-25%. This unit spread over 317 km<sup>2</sup> of area in the district is dissected and ridges lines are prominent. Highly undulated terrain with moderately steep side slopes of 25 to 38% characterise 350 km<sup>2</sup> of the area of the district. The stream traversing through this undulated terrain form calaracts and small water falls relative relief is as high as 250 m. High undualting terrain with steep slopes ranging from 38.55% bordering the foothills zone of Western Ghats occupies nearly 319 Km<sup>2</sup> (CESS, 1988).

## **1.8 Climate and Rainfall**

The Kerala coast in general experiences tropical monsoon climate. Based on hydro-meteorological conditions, three seasons are identified namely, premonsoon or hot weather period (March-May), southwest monsoon (June-September) and post-monsoon (October-December).

The southwest monsoon constitutes the principal and primary rainy season, which gives about 75 % of the annual rainfall while the post-monsoon is the secondary rainy season with less rainfall. The total annual rainfall of the state varies from about 4,500 mm in the north to about 2,000 mm in the south (average 3,010 mm). The study area has the typical tropical humid climate. A dry summer season from February to May (Pre-monsoon) is followed by the southwest monsoon (June to September) of heavy rain and then the post-monsoon season (October to December) with relatively low rainfall and occasional scanty thunderstorms. The climate has been identified as an important parameter that affects the various stages of morphogenic processes, and the quality and quantity of particulate materials within the estuarine system.

Mean maximum temperatures vary between 30 °C and 32 °C in the coastal belts but rises up to 38 °C in the interior part of the watershed areas of the estuary (Pisharody, 1992). The seasonal and diurnal variations of temperature are not uniform. The stations located near the coasts are influenced by the land and sea breezes and have seasonal and diurnal variations of temperature, which are more or less of the same range.

## **1.9 Physio-chemical Properties**

The salinity of the Kayamkulam lagoon ranges from 0.5 to 33 parts per thousand (ppt) and temperature varies between 26.9 and 32 °C (Kuttiyamma, 1980). The dissolved oxygen recorded in the estuarine water ranges from 3.2 ml/L to 6.5 ml/L. The maximum tidal range is about 1.25 m near the bar mouth at Vallivathukkal Tura. The tidal range exhibits a progressive decrease far inland (Nair, 1971).

The minimum temperature recorded in the Ashtamudi estuary is 26 °C in June/July and maximum is 35 °C in April/May. The sediment pH in the estuary is

noticeably acidic (Soumya et al., 2011). The dissolved oxygen ranges from 7.23 to 9.83 ml/L (Qazim, 2002). Salinity gradient exists from upstream to downstream, with average salinity values of 28.4 ppt and 4.13 ppt during the pre-monsoon and the monsoon periods respectively (Black and Baba, 2001).

## **CHAPTER 2**

### **LITERATURE REVIEW**

#### **2.1. Introduction**

The regional and global variations in sea level during the Quaternary have brought out many episodes of marine transgression and regression around the world. Often these have influenced the coastal geomorphologic settings of the region resulting in the formation of beach ridges, strandlines, drowning of river valleys including estuarine systems. The studies carried out nationally and internationally on these aspects are reviewed here.

#### **2.2. Quaternary Studies**

##### **2.2.1. International Status**

The beginning of the Holocene studies based on the fluctuations or rising gradually of the curve representing global sea level changes Fairbridge (1961) and Shepard (1964). The global sea level data confirmed the existence of Holocene sea level histories varying considerably around the world (Pirazolli, 1976; Bloom, 1977). The Holocene sea level curve proposed by Jelgersma (1966) indicated, that the eustatic sea level changes during the last 10,000 years ie. Holocene were divergent. Pirazolli (1991) proposed three possibilities: (i) an oscillating eustatic sea level, (ii) a steady sea level after 5,000 Yrs BP and (iii) a continuously rising sea level. Subsequently investigators around the world have worked on one or other of these possibilities. Morner (1976) recognised the regional sea-level curves after compilations of age/altitude graphs of sea level curves from different areas. This paper contribution marks the milestones in the sea level record and work models. Goring-Morris and Belfer-Cohen (1998) had reported that the Earth experienced relatively warm, wet, stable, CO<sub>2</sub> rich environments since 11,600 Yrs BP. According to Lamb et al. (1995), Cronin (1999), Partridge et al. (1999), and Satkunas and Stancikaite (2009) the Quaternary history reveals that the environment varied drastically from place to place inferred by climatic and other aspects. Williams and Clarke (1995) and Sinha et al. (2005) reported that the unconsolidated sediment accumulation is the characteristic lithology of Quaternary.

Fairbridge (1983) has shown that the interplay between the marine sediments and submerged deposits can be used to reconstruct various episodes of high and low sea levels, enable to establish a sea level curve along the coast. As the result of eustatic rise, large quantity of sand got accumulated in many of the coastal parts of the world. They are considered as prominent geoscientific tool in deciphering former sea level strands. In general, the longer the sea level rise is, the higher the possibility of its burial or drowning by marine sediments. Longer the fall in sea level, the more probable is their preservation as depositional bodies such as beach ridges and coastal dunes.

According to Intergovernmental Panel on Climate Change (IPCC), the global sea level rise for this century is in the order of 18 to 59 cm (IPCC, 2007), while Kerr (2008) contends that it would be between 80 and 200 cm, taking into account of the retreating rate of glaciers and runoff rate of surface water into the sea. Fairbridge (1983) observed that the world has undergone geological disturbances at the advent of Holocene, manifested by transgressions and regressions. Curran and Moore (1971) illustrated the formation of beach ridges and their importance in elucidating sea level changes.

The studies of Schumm (1969), William and Faure (1980), Butzer (1980), and Goudie (1981) have brought out paleogeomorphic environments from the geomorphology, palynology, micropaleontology and geoarchaeology of the Quaternary deposits in Europe, North America, Africa and Australia. Semeniuk and Searle (1985) studied the Holocene coastal sand in south western Australia based on Calcrete. Mid-Late Holocene sea level curves in the southern hemisphere are invariably characterized by either a falling or a fluctuating trend as per the studies of Pirazzoli (1991). Prentice et al. (2000) reported that the Mid-Holocene proxy play an important role in delineating changes in vegetation and lake levels in the monsoon regions of Asia and northern Africa.

### **2.2.2. National Status**

The sea level changes along the Indian coast are sporadic, qualitative, and pertaining to the strandline generated through erosional and depositional processes (Merh, 1982). Ahmad (1972) described the morphology of the Indian coastline through



sea level changes and correlated the land features to the global interglacial transgression/regression. During the last two decades, attempts are being made to integrate the knowledge globally along the coast by correlating strandline features to the glacio-eustatic sea level changes of the Quaternary.

#### **2.2.2.1. Studies on the East Coast of India**

On the east coast of India, Quaternary studies are sporadic and restricted to the major river mouths and with the depositional and erosional landforms like inland beach ridges rock terrace caves etc. Along the West Bengal coast, Sen (1985) investigated the subsurface Holocene sediments around Calcutta. The presence of rich floral and faunal assemblages indicating flourished tidal mangroove forest further north of the present Sunderbans about 6,000 to 7,000 Yrs BP. Niyogi (1968, 1971) reported 3 terraces in the Subarnekha river delta at altitude of 6.1, 4.7 and 3.8 m above the MSL during the post Pleistocene.

During the Holocene, the eastern coast of India experienced a number of marine transgressions, which reached its maximum during the postglacial Flandrian transgression (Selby, 1985) i.e., between 7,000 and 6,000 Yrs BP when the shoreline shifted far inland with respect to the present coast (Banerjee and Sen, 1987; Chakraborti, 1991). Banerjee and Sen (1987) systematically dated several sets of ancient mud from the Bengal basin, which ranged from 7,000 to 3,000 Yrs BP using radiocarbon dating. The study documented that sea level rise was rapid and accompanied by quick siltation.

Several records relating to maximum humidity and strong monsoon during the early–Mid Holocene over India at 10°N and 15°N were reported by Williams and Clarke (1984), Swain et al. (1983) and Cullen (1981). Farooqui and Vaz (2000) studied Holocene sea level and climatic fluctuations of Pulicat Lagoon found that the maximum fluctuation of sea level was observed around 6,650 Yrs BP based on radiocarbon dates. The occurrences of the organic rich peat layer below the shell bed at 9 m and 15 m can be linked to the deposition during the transgressive phase. The plant organic matter in the peat layer was deposited in  $6,650 \pm 10$  and  $4,800 \pm 780$  Yrs BP, during the transgressive and regressive phases of sea level changes respectively in the dried part of the present Pulicat Lagoon in Palar Basin (southeast coast of India).

Stanley and Hait (2000) differentiated distribution and geometry of subsurface Holocene sedimentation of the Ganges-Brahmaputra related to the neotectonic activity. The study distinguishes the Holocene deltaic and underlying transgressive units and late Pleistocene alluvial deposits. Late Pleistocene muds are slightly stiff with low amount of dispersed plant matter and without interbedded peat layers whereas the Holocene muds are comparatively very soft to moderately compact grey to dark olive grey and black in colour with high organic matter content with the presence of large amount of plant material and interbedded peat.

Rao et al. (1992) studied the sediment cores from eastern continental margin of India in a water depth of 1,200 m and inferred that the sedimentary environment were attributed to climate and sea level changes during Pleistocene and Holocene based on sedimentological and geochemical records. Mohana Rao et al. (1989, 1990) and Srinivasa Rao et al. (1990) reported the occurrences of coarse sand deposits in the deeper parts of the innershelf viz., Gopalpur, Visakhapatnam and Nizampatnam. According to these authors, the sediments were formed during the Holocene stagnation of the sea level at that depth. Mohana Rao and Rao (1994) identified the strandline deposits consisting of coarse sand having mean size of around  $1.0 \phi$  between 20 and 30 m depth off Visakhapatnam, formed due to low sea level during Holocene has been identified. Hence, the accurate study of grain size parameter is essential and important to establish the palaeoclimatic conditions and depositional environments. A confirmed linear patch of coarse sand with higher concentration of  $\text{CaCO}_3$  (>15%) low organic matter (<0.4%) and SEM photomicrographs features at a depth around 50-53 m in the innershelf sediments, off Kalpakkam, southeast coast of India showing the existence of the paleoshoreline, formed probably during the Holocene low sea level (Selvaraj and Mohan, 2003).

#### **2.2.2.2. Studies on the West Coast of India**

The transgression and regression along the Maharashtra coast based on radiocarbon dates were first reported by Agrawal and Kusumgar (1974) and Kale et al. (1984). Accordingly, before 35,000 to 30,000 Yrs BP, the sea level was considered to be lower than the present, but started rising from 30,000 Yrs BP. This was followed by a regression, coupled with a rise in sea level around 15,000 Yrs BP. The sea level attained its maximum level during the mid-Holocene. It was also observed that at

about 6,000 Yrs BP the sea level was almost the same as that at present, but in subsequent periods, i.e., between 6,000 and 2,000 Yrs BP, a further rise of 1 m to 6 m was reported. Similarly, Sukhthankar and Pandian (1990) identified various geomorphic features related to marine regression during Holocene in the Maharashtra coast and highlighted the significance of neotectonism in shaping the shoreline.

Nair (1975) first reported Holocene event in the western continental shelf oolitic limestone based on radiocarbon dates. The outer shelf samples had recorded radiocarbon dates of 11,000-9,000 Yrs BP. Formation of submerged terrace at -92, -85, -75 and -55 m indicated steady sea level dated between 11,000 and 9,000 Yrs BP during Holocene. Hashimi et al. (1995) generated a new Holocene curve for the western continental margin based on dated material. The curve shows a fall at 100 m depth around 14,500 Yrs BP and a rise of 80 m around 12,000 Yrs BP showing a rate of approx. 10m/1,000 years which was followed by constant condition for about 2,000 years. From 10,000 to 7,000 years it rose at a very high rate (20m/1,000 years). Beyond 7,000 years it showed minor fluctuations.

Kale and Rajaguru (1985) reconstructed the late Quaternary transgressional and regressional history of the west coast. They postulated a rise from 12,000 Yrs BP the rate being very rapid (18mm/year) during early Holocene. The sea level along the west coast reached very close to the current level.

Manjunath and Shankar (1992) studied sub-surface samples off Mangalore, which indicates the occurrence of outer shelf sand ranging in age from 11,000 to 9,000 Yrs BP at various depths below mean sea level in the northern and southern parts of the western continental shelf. Radiocarbon dating of carbonised wood samples from the inner continental shelf of Taingapatnam in the southwestern coast of India depicts 9,400-8,400 Yrs BP and correlated with the ages of carbonised wood from inner continental shelf of Ponnani and Karwar. The occurrence of carbonised wood in widely spread offshore areas represents a regional transgressive event in the west coast, which resulted in submergence and destruction of coastal mangroves as reported by Nambiar and Rajagopalan (1995). It has long been recognised that the west coast of India represents a drowned coast (Nair, 1974) and the rise in sea level due to late Pleistocene glaciation affected continental shelf sedimentation. The Holocene transgression permitted a variety of terrestrial and marine processes to

operate over the shelf with the result the nature of the shelf sediments varied significantly with rise in sea level and changing climatic conditions (Reddy and Rao, 1992).

### **2.3. Kerala Scenario**

In the Kerala coast the studies have been carried out on sea level changes from the point of view of stratigraphic, lithological, geochronological and paleontological framework (Jacob and Sastri, 1952; Paulose and Narayanaswamy, 1968; Aditya and Sinha, 1976; Raha et al., 1983, 1987; Ramanujam, 1987). From the study of beach rocks along the southwest coast of India, Thrivikramji and Ramasarma (1981) inferred a 4 to 5 m fall in sea level during the Holocene period. Sawarkar (1969) has located auriferous alluvial gravels farther inland in the Nilambur valley at an elevation of 150 m above mean sea level. Guzder (1980) attributed the alluvial gravels in Nilambur valley to sea level changes during the early late Pleistocene period.

The peat beds that form prominent Quaternary units in Kerala were considered to be developed from the submergence of coastal forests, thereby representing series of transgression and regression events (Powar et al., 1983; Rajendran et al., 1989). Nair and Hashimi (1980) ascribed the formation of oolitic limestone in the Kerala shelf to warmer conditions and low terrestrial run off during the Holocene period (11,000-9,000 Yrs BP). Agarwal (1990) considered the west coast of India to be an emergent type and identified a rise in sea level of the order of 0.3 m during the past 57 years. Nair et al. (1978) and Hashimi et al. (1978) identified three distinct sedimentary facies, the first two consisting of sand and mud, which are of recent origin, while the third outer shelf comprising of relict carbonates, sand facies of late Pleistocene formed at the time of lowest sea level. From the study of carbonate sediments and size of the quartz grains, Nair and Hashimi (1980) inferred a warmer climate and low terrestrial run off during the Holocene (about 10,000 Yrs BP). Further, feldspar content in the sediments has also been used by Hashimi and Nair (1986) to infer the climatic aridity over India around 11,000 Yrs BP. These evidences indicate contrasting climatic changes in the deposition of the carbonate and clastic sediments on the shelf, thus suggesting rapid changes in climate from arid to humid. A review article by Rao and Wagle (1997) gives an elaborate account of the geomorphology and the surficial sediments of the continental margins of India.

Krishnan Nair (1987) studied the morphostratigraphic Quaternary surface of the Kasargod-Cannanore districts and identified the Payyannur strandline as retreated deposit representing palaeo-coastal plain of late Pleistocene to early Holocene period. Rajendran et al. (1989) dated the peat sample of Tannisseri to be  $7,230 \pm 120$  Yrs BP indicating transgression of the sea and lime shell of Payyannur in Cannanore district. These authors have estimated an age of  $4,370 \pm 100$  Yrs BP for the regression.

Samsuddin et al. (1992) considered the strand plain deposits along the northern Kerala coast to be the morphological manifestations of marine transgression/regressions event. Haneesh (2001) studied sea level variations during the late Quaternary and coastal evolution along the northern Kerala coast. Radiocarbon dating of shell samples collected from a depth of 6.3 m from the Thekkekad Island gave an age of  $2,830 \pm 30$  Yrs BP. This shows that the deposition of shells was associated with a regressive phase, which took place at around 3,000 Yrs BP. The radiocarbon dates obtained from the shell and peat samples in dark gray coloured fine and very fine sands from the Onakkunnu transect at a depth of 3.2 m and 10.4 m inferred an age of  $5,650 \pm 110$  Yrs BP and  $>30,000$  Yrs BP respectively. The chronostratigraphy illustrates eight episodes of regressive events corresponding to eight sets of ridges and swales. The innermost ridge event took place around 6,000 Yrs BP and the fore dune adjacent to the beach is a morphologic continuum since 1,000 Yrs BP. From the morphostratigraphic study of strandlines, the innermost ridges are the morphological manifestation of sea level maxima during mid-Holocene (Suchindan et al., 1996). An earlier report by Rajendran et al. (1989) on the origin of sand bar along this coast also attributed to the regression of the sea during 5,000-3,000 Yrs BP.

Sedimentological studies indicate that a palaeo-beach that existed off Kerala coast during late Quaternary low stand of sea level, which, at present, remain detached from the mainland due to the subsequent transgression. The expanse of sandy sediments at a water depth of 40 m in the mid-shelf has an age of 8,000-7,000 Yrs BP. Haneesh (2001) reported that the radiocarbon dating on shells from the innershelf and outershelf cores collected at 40 m and 150 m water depths indicates a sedimentation rate of 0.12 mm/yr for the innershelf and 0.05 mm/yr for the outershelf.

Relict terrigenous sediments in the outer shelf between Mangalore and Cochin indicate that the Holocene sedimentation to the outer shelf is minimal and were not sufficient to cover the Late Pleistocene sediments (Rao and Thamban, 1997). They also confirmed the results by observing the exposure of terrestrial carbonates such as calcretes and paleosols of Pleistocene age at 50 to 60 m water depth.

Rajan et al. (1992) analysed the radiocarbon dating of decayed wood from carbonaceous clay from Ponnani inferred an age of 10,240-8,230 Yrs BP indicating transgression of the sea during early Holocene period which ultimately resulted in destruction of the coastal mangroves. According to Mathai and Nair (1988), the strandlines and linear sand dunes of the Kodungallur area are evidences for a periodic cyclicity in the regression of the sea, indicating dominance of marine forces in the evolution of various landforms. Rajendran et al. (1989) after analysing the peat sample in the Irinjalakuda region estimated an age of  $6,420 \pm 120$  Yrs BP indicating early to middle Holocene. Prithviraj and Prakash (1991) based on the sediment granulometry and quartz grain microtextural features in the outer and near innershelf inferred that the sands are of beach deposits indicating Holocene. Further, distribution and geochemical association of clay minerals on the innershelf of central Kerala was studied by Prithviraj and Prakash (1991). Kaolinite and montmorillonite exhibited an inverse relationship in spatial distribution which has been attributed to the differential settling velocities of the minerals. The geochemical association indicated a terrestrial origin for all the clay minerals.

Agrawal et al. (1970) initiated the Holocene studies along the Ernakulam area and they estimated the age of Wellington Island near Cochin as  $8,080 \pm 120$  Yrs BP indicating the Holocene period based on peat. The studies were further strengthened the ages reported by Agrawal and Kusumgar (1974, 1975), Agrawal et al. (1979) based on carbon dating of samples. Based on the study of satellite images, Mallik and Suchindan (1984) observed striking parallelism of Vembanad Lake with that of the series of strandlines in the central Kerala coast, which is an example of the transgressive-regressive episodes. Their orientation is controlled by changes in direction of approach of wave front. Narayana et al. (2001) have reported the abundance of peat deposits at many onshore locations adjacent to the present shoreline of the west coast showing varying ages between 45,000 and 7,200 Yrs BP.

Narayana and Priju (2004) reported the progradation of the coastline during late Quaternary by observing a number of parallel strandlines that stand out a signature of marine transgression and regression phenomena in the Vembanad Lake.

Narayana (2007) studied the environmental and climate change during the late Quaternary from the coastal land of Cochin based on peat deposit. The study emphasised that the peat deposits which occurring in association with the Quaternary sediments indicated their origin from the submergence of the coastal tract and consequent transgression of the sea. It was proposed that the flooding could be related to transgression occurred likely during 8,000-6,000 Yrs BP destroyed the mangrove vegetation and gave rise to the formation of peat layers. Usually the peat layers occur at 2 m, 6 m, 20 m and 40 m below the surface of the coastal alluvium (Narayana and Priju, 2002). The presence of peat suggests intense plant productivity and luxuriant growth of forests in the immediate vicinity. Priju and Narayana (2007) studied the particle size characterization and late Holocene depositional processes in Vembanad Lake based on Tanner's bivariate plot of grain size parameters.

Reddy et al. (1992) studied the clay mineralogy of innershelf sediments of Cochin west coast of India. The clay minerals Kaolinite and illite were found to occur in decrease order of abundance in the Holocene sediments of the innershelf and adjacent coastal environment of Cochin region. Higher proportions of Kaolinite in sediments of outer parts of innershelf are considered to have been deposited during a fall in sea level in the Holocene. The innershelf sediments of Cochin coast exhibit lens of coarse sands at 30 m water depth, which indicates that they have been deposited during a still stand of Holocene transgression at that level and is therefore relict in nature (Reddy and Rao, 1992).

Rajendran et al. (1989) estimated an age of  $3,130 \pm 100$  Yrs BP in the Muhama region of Alleppey district based on carbon dating of lime shell samples indicating the regression of sea. Nair et al. (2006) estimated an age of  $6,740 \pm 120$  Yrs BP based on dating of sediment collected from a depth of 8.45 m in the Kalarkod region confirming the Holocene period. Based on the sedimentological radiocarbon dating and palynological studies, the presence of a marine and marginal marine environmental complex during Holocene was confirmed. The oldest Holocene sediments dated 8,000-7,000 Yrs BP, and those upto approx. 4,000 Yrs BP had an

abundance of terrestrial organic matter, which probably could be from a period of higher precipitation. A detailed palynological study in the region indicating occurrence and relative abundance of *Cullenia exarillata* pollen along with other wet evergreen forest members at certain intervals indicate the prevalence of heavy rainfall during the early Holocene. This aspect is further complemented by the presence of a large number of fungal remains. In contrast, their scarcity and even absence at higher levels in boreholes point towards relatively dry climate during late Holocene (Kumaran, 2008).

Nair (1990) and Soman (1997) based on their studies reported that the NE-SW to ENE-WSW trending lineaments marked in the coastal belt is considered to be youngest. Chattopadhyay (2001) interpreted two sets of regression-transgression sand ridges along the Kayamkulam sector during Holocene. The N-S trending sand ridges are associated with Holocene sea level rise along with tectonic disturbances that had caused further sea level change. The NNW-SSE sand ridges formed as a result of mid Holocene (6,000-4,000 Yrs BP) sea level changes. Apart from transgression and regression events, which cause alternate waterlogging and fast drainage of the valleys, there are evidences of high rainfall in different spells during early to mid-Holocene (Nair and Hashimi, 1980). Nair and Padmalal (2004) presented that thickest Quaternary sediments is best exposed in the south Kerala sedimentary basin which extends from Kollam to Kodungallur in a form of curvilinear area with a maximum width of approx. 25 km and a thickness of approx. 80 m. The basin is divided into Central Depression (CD) flanked by Southern Block (SB) and Northern Block (NB). The first marine transgression in the basin took place around 42,000 Yrs BP. The Holocene marine transgression was experienced by about 7,000 Yrs BP. This was followed by a regression, which left the present landscape of lagoons, wetlands and the ridge-runnel topography.

Jayalakshmi et al. (2004) analysed two boreholes one at Eruva and another at Muthukulam near Kayamkulam for delineating the late Pleistocene-Holocene history of the southern western Kerala basin. Carbon dating age determination of the wood fragments from the Muthukulam core sample (depth: 1.27-3.0 m) showed the range of 3,700 to 7,200 Yrs BP, indicating a Holocene history. The upper part of the section shows a progressively reduced rainfall pattern culminating in a period of very low



precipitation with the development of a paleosol, which is traceable all over the south Kerala sedimentary basin where late Holocene sediments are available. This period witnessed aeolian activity modifying the sand ridges in the ridge-runnel systems formed by the Holocene regression. The study linked the Quaternary transgression to abnormally high intensity of Asian summer monsoons. Limaye et al. (2010) studied late Quaternary sediments from the boreholes of Panavally and Ayiramthengu of Kollam districts based on cyanobacteria. The beds at Warkalli (Kerala) which probably accumulated in coastal lagoons of Pleistocene, suggest high sea level (Kale and Rajaguru, 1985). Pascoe (1964) has also reported the existence of an old sea beach at the base of Warkalli cliff.

The studies on Ashtamudi Estuary are also reviewed. The study was first taken by Prabhakara Rao (1962) in which he discussed the sediments of nearshore region of Neendakara-Kayamkulam coast adjoining the Ashtamudi and Vatta Estuaries. The recent studies conducted on Ashtamudi Estuary during the last two decades are mainly focused on the physico-chemical features of water and sediment nutrients primary productivity, organic carbon (Nair et al., 1983), and calcium carbonate (Damodran and Sajan, 1983). Sajan (1988) studied the surficial sediments of Ashtamudi Estuary for mineralogy and geochemistry. The variations in the mineralogy of heavy, light and clay minerals directly reflect the variation in their respective sources. The progressive depletion of feldspars and corresponding enrichment of quartz from the eastern to the western part can be attributed to the selective abrasion and chemical weathering. The dual source of supply of sediments to the lake was brought out from the mineralogical studies. The results of the geochemical analysis for the bulk sediments and clay fractions showed that most of the elements were concentrated in the finer fractions and the variation in their content was due to the different geochemical environment in the estuary.

In 2011, the Ashtamudi Management Plan was prepared by the Centre for Earth Science Studies (CESS) based on detailed study of socio-economics, gender, fisheries and tourism in the context of the physical, chemical and biological aspect of the Ashtamudi Estuary (Black and Baba, 2001). The geology and surficial sediment characteristics of the estuary were well documented by Prakash et al. (2001) and it was found that silt and clayey silt were the dominant sediment type in the estuary.

Kurian et al. (2001) after examining the bathymetric data of the Ashtamudi Estuary inferred that the major part of the estuary is shallow (<3 m) with a maximum depth of 14 m near the Kallada River confluence.

Nair et al. (2010) discussed the sedimentological and palynological analysis of two boreholes collected near the confluence of Kallada River with Ashtamudi Estuary to decipher the late Quaternary evolution of this region. The palynoflora analysis revealed that the depositional site was within the tidal limit and deposition occurred under high precipitation and atmospheric humidity. The similarity in  $^{14}\text{C}$  dates of wood sample at 5 m bgl ( $7,490\pm 90$  Yrs BP) and the embedding sediments ( $7,480\pm 80$  Yrs BP) indicate quick burial of the riparian vegetation. The West Kallada borehole reveals middle to late Holocene sequence of clayey silt ( $6,250\pm 110$  Yrs BP;  $3,880\pm 80$  Yrs BP) and sand resting unconformably over greyish white, clayey sand with pebbles and granules derived from laterite provenance. Palynological analysis shows that the Holocene sedimentation took place under marine/nearly marine environment and later changed to brackish water and finally to freshwater environment. Marine transgression approximately 6,000 Yrs BP coupled with heavy rainfall in the hinterlands was responsible for faster sedimentation in the region. The heavy mineral contents, especially opaques, garnet and sillimanite in the sediment samples of the study area as well as the bathymetric configuration of the Ashtamudi, Sasthamkotta and Chelupola Lakes reiterate the fact that these lakes have been evolved from an embayment consequent to incomplete/partial silting up during early to middle Holocene higher sea levels and high rainfall of the Holocene climatic optimum of around 10,000–7,000 yrs.

## **CHAPTER 3**

### **FIELD DATA COLLECTION AND ANALYSES**

#### **3.1. Introduction**

Detailed field mapping and collection of sediment cores from the coastal plain, estuary/lagoon and offshore regions of the Kollam-Kayamkulam coast were carried out to achieve the objectives as outlined in the Chapter 1. The field mapping work involved identification of various geomorphologic units and signatures of past sea level changes in the form of beach ridges and swales present in the study area. For studying the downcore lithological variations, organic matter and calcium carbonate contents, clay mineralogy, major and trace element geochemistry sediment core collections were needed. The peat/organic rich sediments from the core sections were dated with radiocarbon technique for age determination.

#### **3.2. Field Mapping and Collection of Sediment Cores**

The work related to the field mapping and core sample collections are discussed in this section.

##### **3.2.1. Field Mapping**

The first and foremost step in field mapping is to identify the study area, which consist of three segment viz., the coastal region, the estuarine/lagoon system and the offshore region. The study area encompasses the coastal region showing coast perpendicular Ashtamudi Estuary (locally known as the Ashtamudi Kayal) and coast parallel Kayamkulam Lagoon situated in the southern and northern part respectively. In addition to this, the Sasthamkotta, the largest freshwater lake, and other wetland bodies like Chelupola, Cherayattu Lake, and Chittumala Chira are also situated along this coastal belt. Following the base map of Samsuddin et al. (2008) various landuse and landforms features such as beach ridges and swales were mapped for this study.

##### **3.2.2. Collection of Sediment Cores**

The collection of sediment cores is necessary for obtaining accurate and reliable data thereby deducing environmental reconstructions from lacustrine and marine realms (Tomkins et al., 2007). The sediment cores are collected along the two

transects representing the Kollam and Kayamkulam coast as part of this study (Fig. 3.1) and details of core collection with recovery are presented in Table 3.1.

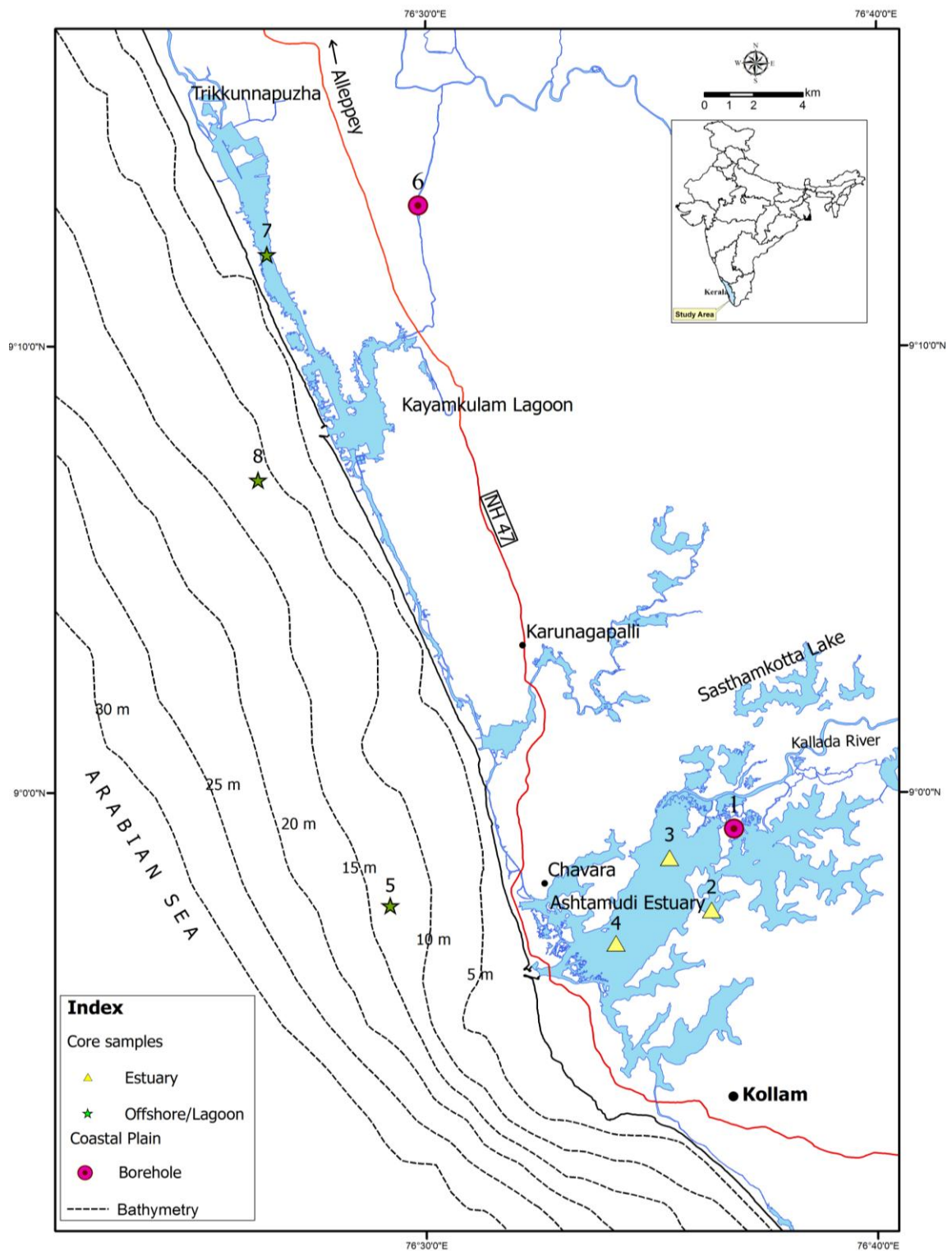


Fig. 3.1 Map showing the locations of sediment cores collected from the coastal plain, estuary and offshore region along the Kollam-Kayamkulam coast

*Table 3.1 Details of the sediment cores collected from the different coastal environment of the study area*

<b>Location</b>	<b>Core No.</b>	<b>Environment</b>	<b>Sample collection</b>	<b>Water depth (m)</b>	<b>Core retrieved (m)</b>
South Transect-I (Kollam)	1	Coastal Plain	Borehole (Rotary Drilling)	--	15.5
	2	Ashtamudi Estuary	Piston Corer	2.5	1.08
	3	Ashtamudi Estuary	Piston Corer	4.5	1.48
	4	Ashtamudi Estuary	Gravity Corer	2.5	0.75
	5	Kollam Offshore	Gravity Corer	12.5	0.88
North Transect-II (Kayamkulam)	6	Coastal Plain	Borehole (Rotary Drilling)	--	20
	7	Kayamkulam Lagoon	Gravity Corer	3	0.65
	8	Kayamkulam Offshore	Gravity Corer	10	0.73

The sediment cores are collected by employing rotary drilling and gravity/piston core methods. In the coastal plain, the sediment cores are collected using rotary drilling. Based on this technique, first every 1 m drilling is done. Then a split spoon sampler (108 cm length and 1.6 cm diameter) is attached to the bottom of a core barrel with a mark of 50 and 75 cm and is forced into the sediment by a drive weight, which is dropped repeatedly onto the drive head located at the top of the drill rod. As a result undisturbed sediment core is collected in the split spoon. When the split spoon is brought to the surface, it is splitted apart and the core section is then sub-sampled at every 10 cm interval (Figs. 3.2, 3.3 and 3.4). The sub-samples are transferred into a plastic bag and are preserved in the deep freezer at 4 °C.

Estuarine cores are collected using the Piston corer (Fig. 3.5). The Corer is assembled onboard a fishing vessel and operated with the help of a davit and pulley system. A piston inside the core pipe is attached to the wire that lowers the corer to the bottom. The corer itself is held in place temporarily by release mechanism activated by a trigger weight hanging about some weight below the bottom of the core

pipe. During lowering, the piston is at the bottom of the pipe. When the trigger weight reaches at the bottom, the coring apparatus falls freely while the piston remains stationary at the sediment–water interface. Thus the Piston breaks the friction and provides pumping action that allows recovery of long core. The recovery of sediment depends upon the nature of sediment present. Immediately after the retrieval of the piston core, core catcher as well as core cutter fitted at the bottom is removed. The Core liner is pulled out from the core barrel and both ends plugged with end cap and the top and bottom ends of the retrieved core are marked for identification. The cores are then brought to the laboratory, sub-sampled at 10 cm interval, and kept in deep freezer at 4 °C until further analyses are carried out.



*Fig. 3.2 Field Photographs of the Kollam coastal plain (southern boundary of the study area) showing (a) location of sample collection - Kallada River debouching into the Ashtamudi Estuary, (b) Rotary drilling in operation, (c) collection of undisturbed sediment core in a spoon after drilling and (d) sub-sampling of the core*

Offshore cores representing the northern as well as southern transect of the study area are collected using the gravity corer. The maximum core retrieval is approximately 1.0 m length and is sub-sampled for detailed analysis.



*Fig. 3.3 Field photographs of core sample collection from the Kayamkulam coastal plain (northern boundary of the study area) showing (a) site area east of Kayamkulam Lagoon, (b) Rotary drilling in operation, (c) undisturbed sediment core and (d) lithological observation as well as packing of the samples*

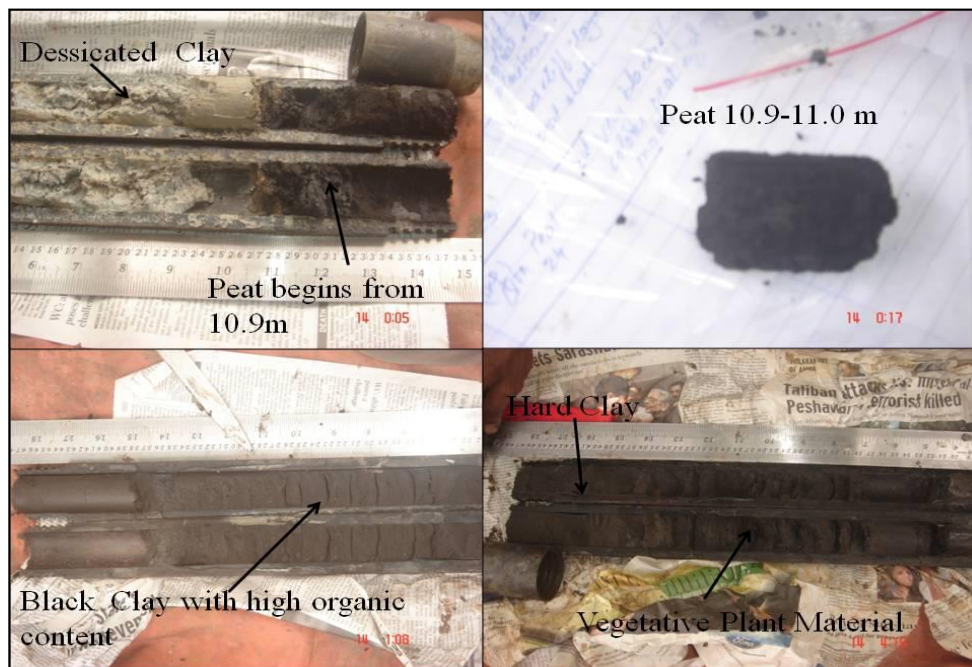


*Fig. 3.4 Photographs showing the lithology of the collected core samples*

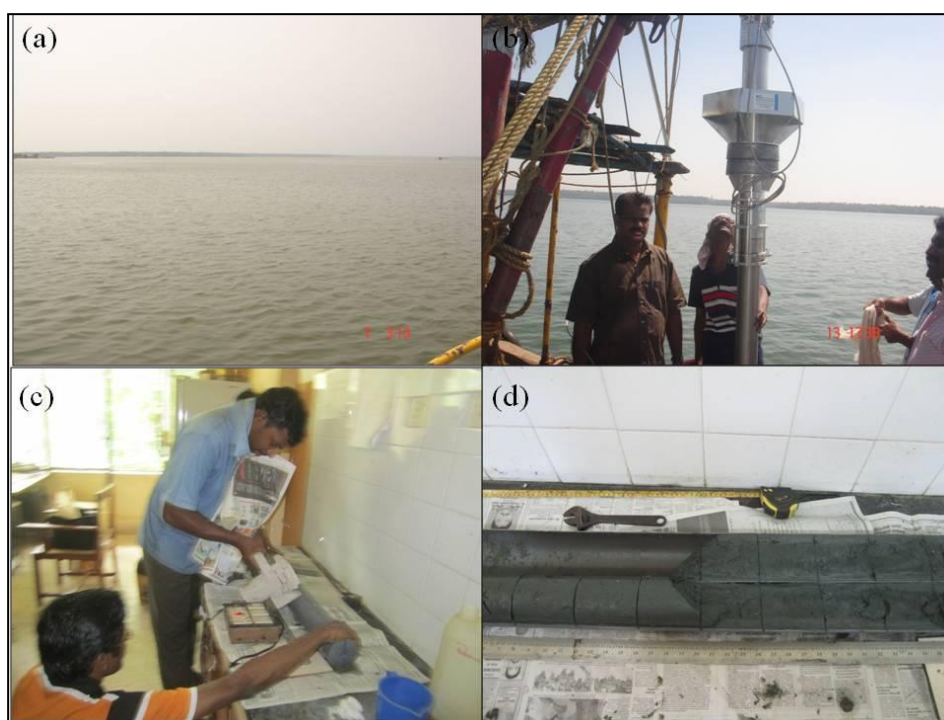


*Fig. 3.5 Photographs showing (a) Panoramic view of the Ashtamudi Estuary (central portion), (b) Piston Corer used for the collection of core samples, (c) cutting of sediment core using core cutter in the laboratory and (d) sub-sampling of undisturbed sediment core samples*

### **3.3. Analyses of Sediment Core Samples**

The sediment cores collected are subjected to detailed textural analysis of, clay mineralogy, organic and calcium carbonate content, geochemical parameters, radiocarbon dating etc. as highlighted in the flow chart (Fig. 3.6). The details on various analysis carried out are briefly given below.

#### **3.3.1. Textural Analysis**

In general, the term texture represents size, shape, roundness, grain surface features and fabric of grains (Pettijohn, 1963). The deposition sequence and environmental reconstruction can be studied by determining the particle size distributions of sediments (Lario et al., 2002). The percentage of sand, silt and clay contents and statistical parameters of the sediment core samples are estimated using standard method (Carver, 1971). The textural analysis for this work is discussed in detail below.



About 50 g of sediment sample is taken and washed repeatedly using deionised water for removal of the salt content. The salt free sample is then treated with dilute hydrochloric acid (to remove calcium carbonate content) and washed repeatedly with deionised water. The sample is further treated with 30 % hydrogen peroxide (to remove the organic matter content) followed by repeated washings with deionised water. After removal of calcium carbonate and organic matter content, the samples is made into paste form by oven drying at about 40 °C for further analysis adopting the moisture replica method.

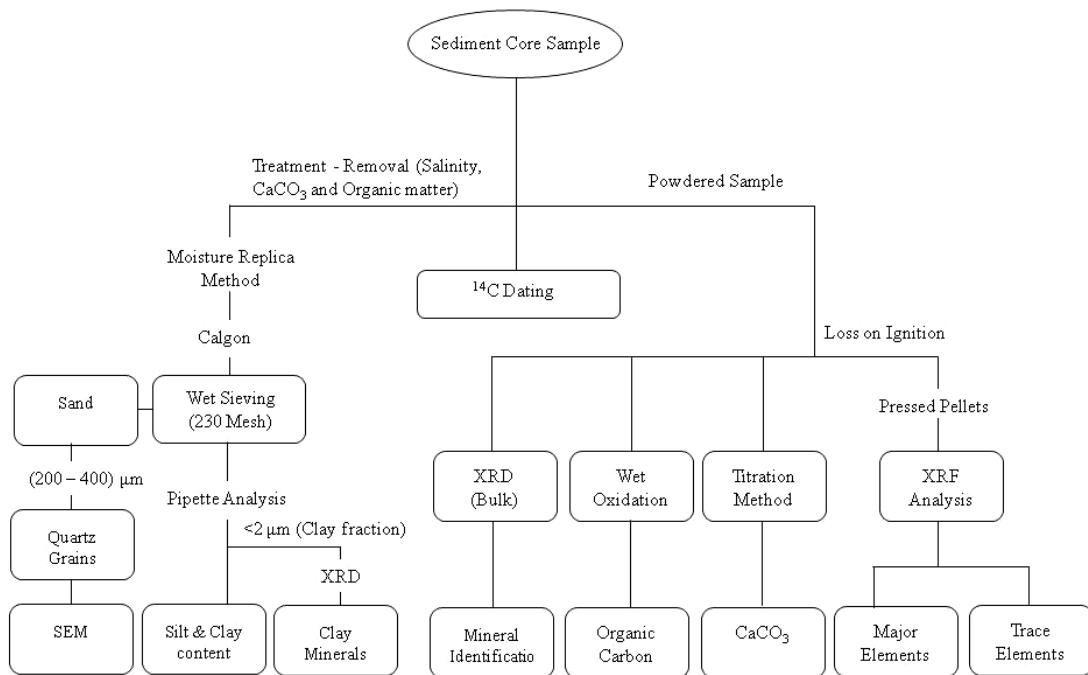


Fig. 3.6 Flowchart showing different types of analysis on sediment core samples

As per the moisture replica method, two watch glasses having samples with approximate weight of 5 g and 25 g respectively are taken. Out of these two watch glasses, the one with 5 gm is dried at 110 °C for the estimation of moisture content whereas the other watch glass with sample is allowed to soak overnight after adding 20 ml sodium hexametaphosphate (Calgon). The soaked sample is wet sieved through a 63 μm sieve to separate sand and mud fraction. The sand fraction (>63 μm) retained in the sieve is dried and weighed, while the mud fraction is collected in a 1,000 ml measuring glass cylinder and subjected to pipette analysis to estimate the silt and clay fractions following the method of Folk (1980). The percentage of sand, silt and clay contents as well as statistical parameters in each of the sample are then determined

using the Gradistat software (Simon, 2007). The sand-silt-clay ratios are plotted on trilinear diagram for textural nomenclature based on Shepard (1954) classification.

### **3.3.2. Surface Texture Analysis**

The study of surface features of quartz grains using Scanning Electron Microscopy (SEM) techniques has been developed into a method for relating microtexture of the samples to specific sedimentary environments (Krinsley et al., 1964; Le Ribault, 1975).

For surface textural analysis of quartz grains, sand fraction of the treated samples are separated from the mud content by sieving using 63  $\mu\text{m}$  sieve based on Carver (1971) method discussed in the previous section. Sand grain fractions between 200 and 400  $\mu\text{m}$  sizes are further separated from the total grains by sieving for SEM analysis (Krinsley and Doornkamp, 1973). The Monocrystalline quartz grains are then hand-picked after examination using stereozoom binocular microscope and then treated with stannous chloride solution to remove the iron stains (Krinsley and Doornkamp, 1973; Helland and Holmes, 1997). On an average, about twenty-five quartz grains are selected from the sand size fraction of each sample to understand the microtextural variations present and also to interpret the depositional history (Krinsley and Doornkamp, 1973; Baker, 1976). The selected quartz grains mounted on stubs, sputter-coated with silver tape are examined using a Hitachi S-3400N Variable Pressure Scanning Electron Microscope (SEM) with Deben Peltier Coolstage. The SEM available with the Department of Civil Engineering, Anna University, Chennai, India has been used for the present study. The various types of quartz grain microtextures seen in the sample have been analyzed and studied in detail by comparing with the published literatures (Krinsley and Donahue, 1968; Krinsley and Margolis, 1971; Margolis and Kennet, 1971; Krinsley and Doornkamp, 1973; Le Ribault, 1975; Higgs, 1979).

### **3.3.3. Clay Mineral Analysis**

Clay mineral analysis of samples is essential, as they are indicators of environmental changes (Chamley, 1989; Weaver, 1989). The species and proportions of individual clay minerals in sediments depend mainly on the climatic conditions and

on the nature of the source rocks (Biscaye, 1965; Griffin et al., 1968). The steps involved in clay mineral analysis adopted for the present study are summarised below.

Based on the settling velocity (Stokes' law) of the sediment particles (following the procedure of Carver, 1971) discussed in section 3.3.1, the sample is allowed to stand for 6 hours 54 minute and the clay suspension ( $< 2 \mu\text{m}$ ) from the top 10 cm of the column (approx. 300 ml) is siphoned out. The siphoned liquid is centrifuged for 15 minutes to form thick suspension of clay slurry. Clay slurry is then mounted on a grounded slide following the smearing technique proposed by Gibbs (1965). The glass slides are allowed to dry at room temperature without any contamination (Biscaye, 1964; Gibbs, 1965). The clay slides are then subjected to X-ray diffraction analysis using the Philips X'PERT PRO X-ray diffractometer installed in the XRD laboratory of the National Centre for Earth Science Studies, Thiruvananthapuram.

The clay slide is scanned from  $5^\circ$  to  $40^\circ$  at  $2^\circ 2\theta$  /minute with a copper target and nickel filter at a setting of 40 KV and 30 mA. The resultant scanned peak is generated and the presence of clay minerals like kaolinite ( $7 \text{ \AA}$ ), gibbsite ( $4.85 \text{ \AA}$ ), chlorite ( $14 \text{ \AA}$ ), illite ( $10 \text{ \AA}$ ) and montmorillonite ( $15-17 \text{ \AA}$ ) (Rao and Rao, 1996) are confirmed by running the High Score Plus software consisting of ICDD and JCPDS data. Further to differentiate the kaolinite and chlorite peaks, the samples are also rescanned from  $24$  to  $26^\circ 2\theta$  at  $0.5^\circ 2\theta$ /minute (Biscaye, 1964).

#### **3.3.4. Organic Matter Estimation**

Organic matter in soils and sediments is widely distributed over the earth's surface occurring in almost all terrestrial and aquatic environments (Schnitzer, 1978). Organic matter is a good index of the environment in which the sediments are deposited. For the present study, the procedure proposed by Gaudette et al. (1974) modified version of El Wakeel and Riley (1957) method has been adopted. The various steps in laboratory analysis are enumerated below.

The selected core samples is dried in an oven at  $50^\circ\text{C}$  and finely powdered in agate mortar. Precisely 0.5 gm of sample is weighed and treated with 10 ml of potassium dichromate solution and 20 ml of Conc.  $\text{H}_2\text{SO}_4$  (1.25 g  $\text{Ag}_2\text{SO}_4$  dissolved in 500 ml conc.  $\text{H}_2\text{SO}_4$ ) which is mixed gently by rotating the flask for a minute. The

mixture is kept for an hour and then diluted by adding 200 ml of distilled water. After acquiring normal conditions, 7 to 8 drops of ferroin indicator is added. The solution is titrated against the 0.5 N Ferrous Ammonium Sulphates in a burette to a single drop end point (brilliant red wine). A standard blank without sediment is run with each of the new batch of samples. Organic carbon is calculated and then multiplied with a scale factor of 1.74 (Nelson and Sommers, 1996) to obtain the organic matter content.

### **3.3.5. Determination of Calcium Carbonate**

Calcium carbonate content of the sediment (being a function of production, dissolution and dilution) has been widely used for stratigraphic correlation, and interpretation of palaeo-oceanographic changes (Dunn et al., 1981; Gardner, 1982; Piasias et al., 1985). For accurate interpretation of the marine sediment record in-depth knowledge of the processes controlling the preservation of  $\text{CaCO}_3$  is needed (Milliman et al., 1999). The variations in the carbonate contents reflect the differences in the environmental conditions of deposition (Setty and Madhusudhana Rao, 1972).

In this study, the percentage of  $\text{CaCO}_3$  in sediment samples is determined adopting the Hutchinson and Mcheman (1947) method. The principle involves, treating the sample with a known quantity of HCl and estimating the excess of HCl by back titration with standard NaOH using phenolphthalein indicator. The different steps used in this method are described in the following paragraph.

A known weight (approx. 1 gm) is taken in an Ermelyer flask and 50 ml of 0.2 N dil. HCl is added. It is mixed gently and kept for half an hour. About 25 ml from the dissolved carbonate solution is then transferred into another Ermelyer flask and 3 to 4 drops of phenolphthalein indicator is added for titration against 0.2 N NaOH solutions. The end point is indicated by light pink colour.

### **3.3.6. Geochemical Analysis**

Geochemistry is the functional characterization, evaluation of elemental distribution and concentration of chemical elements in the rock, soil and water. The study further includes understanding of chemical processes and reactions that govern the composition and chemical flux between various states (Kabata-Pendias and Pendias, 2001; Neuendorf et al., 2005). The geochemical signature of sediment is a

reflection of its source material and also the processes within the sedimentary cycle that can result in chemical fractionation (Taylor and McLennan, 1985).

X-ray Fluorescence (XRF) is a well-established technique adopted for the analysis of geological materials due to its precision, accuracy, versatility, automation, sensitivity and selectivity. It is one of the most rapid and relevant method of geochemical analysis for obtaining qualitative and quantitative elemental analysis. The steps involved are described below.

#### **3.3.6.1. Sample Preparation and Instruments Used**

The sediment cores samples collected from the different coastal environment is washed thoroughly to remove salt and then dried at 50 °C. The sediment is powdered with help of pestle and mortar and then sieved through 230 mesh. The powder sample passing through 230 mesh (< 63 µm) is collected and then dried at 110 °C overnight in order to remove the moisture content. After removing moisture content the sample is then subjected to Loss on Ignition (LOI).

LOI is a widely used technique in geological marine and soil science investigation (Bisutti et al., 2004). The dried powder samples are heated in a muffle furnace at 950 °C for one hour in order to eliminate the volatile constituents like organic matter, calcium carbonate contents and interstitial waters etc. Pressed pellets are prepared by using collapsible aluminium cups (Govil, 1985). These cups are filled with boric acid as binder and about 1 g of the finely powdered sample (after LOI) is put on the top of the boric acid and pressed under a hydraulic press at 20 tons pressure to obtain a 40 mm diameter pellet.

Bruker model S4 Pioneer sequential wavelength-dispersive X-ray spectrometer equipped with a goniometer (which holds seven analyzing crystals) with 4 kW Rh X-ray tube and 60 samples automatic loading system available at XRF Laboratory, National Centre for Earth Science Studies is used to measure different peaks and background counts for the major and trace elements. The supporting software used for computer analyses is able to take care of dead time correction, background, line overlap corrections and matrix effects giving the output directly as the concentration in weight percentage or in ppm after converting the counts into concentration with the help of calibration curves.

### **3.3.6.2. Major Elements**

Major element concentrations are determined adopting the X-ray fluorescence spectrometry method following the procedures given by Calvert (1990). The XRF intensities measured from elements in dry samples show variations depending on the XRF absorption rates (Tertian and Claisse, 1982). The major elements determined are: Si, Al, Fe, Ti, Ca, Na, K, Mg, Mn and P.

### **3.3.6.3. Trace Elements**

Determination of the Trace element abundances in sediments allow us to reconstruct the paleodepositional conditions (Weme et al., 2003; Riboulleau et al., 2003; Algeo, 2004; Nameroff et al., 2004; Rimmer, 2004). While using trace element concentrations to reconstruct paleoenvironmental conditions, one must assess whether they are relatively enriched or depleted. In general, the degree of enrichment or depletion of a trace element in a sample is evaluated relative to its concentration in a reference that is usually average shale value (Wedepohl, 1971, 1991; McLennan, 2001). The trace elements consisting mainly of Cr, Co, Ni, Cu, Zn, Ga, Rb, Y, Zr, Nb, Ba, La, Ce, Sm are analysed using XRF.

### **3.3.7. Radiocarbon Dating**

Recent scientific work has demonstrated the capability of peat and organic rich muddy sediment to store information of the past environments with a high temporal resolution (Goodsite et al., 2001). Peat sections have served as archives of heavy metal pollutants of the atmosphere (Benoit et al., 1998; Shotyk et al., 1998) and yielded records of both climate and atmospheric CO<sub>2</sub> content (White et al., 1994; Martinez-Cortizas et al., 1999). For the present study, the Radiocarbon dating (<sup>14</sup>C) analysis is carried out in the Radiocarbon Laboratory at Birbal Sahni Institute of Paleobotany (BSIP), Lucknow. The process involved following steps.

Combustion of the cleaned and pre-treated (using 10% HCl) sediment sample is carried out in a quartz electrical furnace in presence of clean and dry oxygen-flow at 750 to 900 °C. This is followed by allowing the reaction with copper oxide to convert carbon monoxide, if any left over, to the carbon dioxide. Since the sample carbon dioxide may contain several impurities like sulfur and halides in addition to moisture, multi-stage cleaning using acidified

potassium permanganate, potassium dichromate, silver chloride in definite concentrations and moisture absorbers like cooled silica gel and molecular sieve are carried out. The cleaned and dried carbon dioxide is collected using liquid nitrogen. It is freed from oxygen followed by formation of lithium carbide in the presence of catalyst (molten lithium) and slow hydrolysis to obtain acetylene. In the presence of a catalyst, the acetylene is trimerised to obtain benzene. After careful weighing of sample benzene, a calculated amount of scintillator (PBD Butyle purum) is added to benzene vial and the vial is placed in the counter Quantulus 1220 for 25 cycles of counting. Appropriate SQP correction is applied to estimate the radiocarbon amount and ages calculated using the standard formula based on radioactive decay of radiocarbon. While determining the age, the half-life used is 5,530 years as per the traditional method even though the accepted present value is 5,730 years. The obtained radiocarbon dates is calibrated using IntCal09 software of the Washington University.

## CHAPTER 4

# SEDIMENTOLOGY OF CORE SEDIMENTS

### 4.1. Introduction

Sedimentary deposits are often considered as the pages of the earth's history. A better understanding of the proxy evidences in sedimentary archives would provide a wealth of information including changes in environmental conditions and sediment supply. Interpretation of the depositional and paleoclimate environment requires synthesis of all the inferences that can be retrieved from the various lithological units that encompasses sedimentary architecture. The constituent part of the sedimentary packages/units indicates the position of sea level and also changes in sediment supply within a cycle and enables interpretation of their interrelationship through the time. Studies of sedimentary packages collected from exposed outcrops and or drilled borehole cores are one of the direct methods in sedimentological investigations. A cursory glance of literature reveals that several studies have been undertaken in different parts of the world for achieving the past environmental climatic and sea level changes (Fairbanks, 1989; Prell et al., 1992; Rao et al., 2003; Pandarinath et al., 2004; Verma and Sudhakar, 2006; Nair et al., 2010).

Knowledge of sediment texture is vital to differentiate various depositional environment of ancient as well as recent sediments (Manson and Folk, 1958; Freidman, 1961). Many of the earlier researchers have successfully adopted the granulometric analysis of unconsolidated sediments as an efficient tool for a thorough understanding of the depositional pattern of the sediments. Size parameters can also give insight into the spatial and temporal variations of transportation and depositional processes even within the same environment (Samsuddin, 1986; Samsuddin et al., 1991).

In this chapter, the sedimentological characteristics, like the downcore variations in the sediment facies, organic matter, calcium carbonate, clay mineralogy and radiocarbon dating of the samples collected from predefined locations in the study area are discussed. The collection of sediment cores representing the coastal plain, estuary/lagoon and offshore along the two transects are discussed in Chapter 2.



## **4.2. Lithological Variation**

The lithological variations of the cores representing the coastal plain, estuary/lagoon and offshore of the southern and northern transect are enumerated in the following section.

### **4.2.1. Sediment core along the southern transect (Kollam)**

The sediment cores along the southern transect comprises of 5 cores representing the coastal plain (Core 1), the Ashtamudi Estuary (Core 2, 3, 4) and the Offshore (Core 5) respectively (Fig. 3.1 in Chapter 3).

#### **4.2.1.1. Coastal Plain (Core 1)**

The Core 1 (08° 59' 11" N, 76° 36' 49" E) is located in the coastal plain where the Kallada River joins the Ashtamudi Estuary. The core is sub-divided into 5 litho-units (Figs. 4.1a & b) and the percentage of sand, silt, clay, organic matter and calcium carbonate in each of the units are presented in Table 4.1. The first litho-unit starts with a top soil of 0 to 2 m. This is followed by the second unit of 2 to 7 m where the sand particles are angular to sub-angular in nature ranging from 70.09 to 89.11%. The silt and clay content are much less in this unit and varies from 3.9 to 11% and 6.98 to 18.91% respectively. The organic matter and calcium carbonate contents are least with an average value of 1.53% and 0.66%. The third unit of 7 to 9 m is dominated by sand to silty sand sediments where the sand, silt and clay contents ranges from 66.94 to 78.87%, 5.90 to 20.42% and 5.88 to 12.64% respectively. Broken shells and traces of heavy minerals were also observed. In this unit a marginal increase of calcium carbonate (av. 1%) and a decrease of organic matter (av. 0.56%) are noted.

Muddy sediments dominate the fourth unit representing the 9 to 11 m with clay percentage ranging from 36.97 to 84.06%. The upper part of this unit is soft with brownish to reddish colour with traces of brachiopod shells. However, the lower part is characterised by very hard clay of white to greyish colour. Less percentage of sand and silt was observed. Towards the end of this unit, a thin layer of black peat with an approximate thickness of 0.20 m was observed which has an organic matter of 47%. The last unit (11-15.5 m) comprises of silty clay type sediments. The percentages of sand, silt and clay ranges from 0.41 to 12.65%; 25.11 to 33.26%; and 56.35 to 72.12%

respectively. The unit also shows enrichment of organic sediments ranging from 10 to 14 % with well-preserved vegetative plant material.

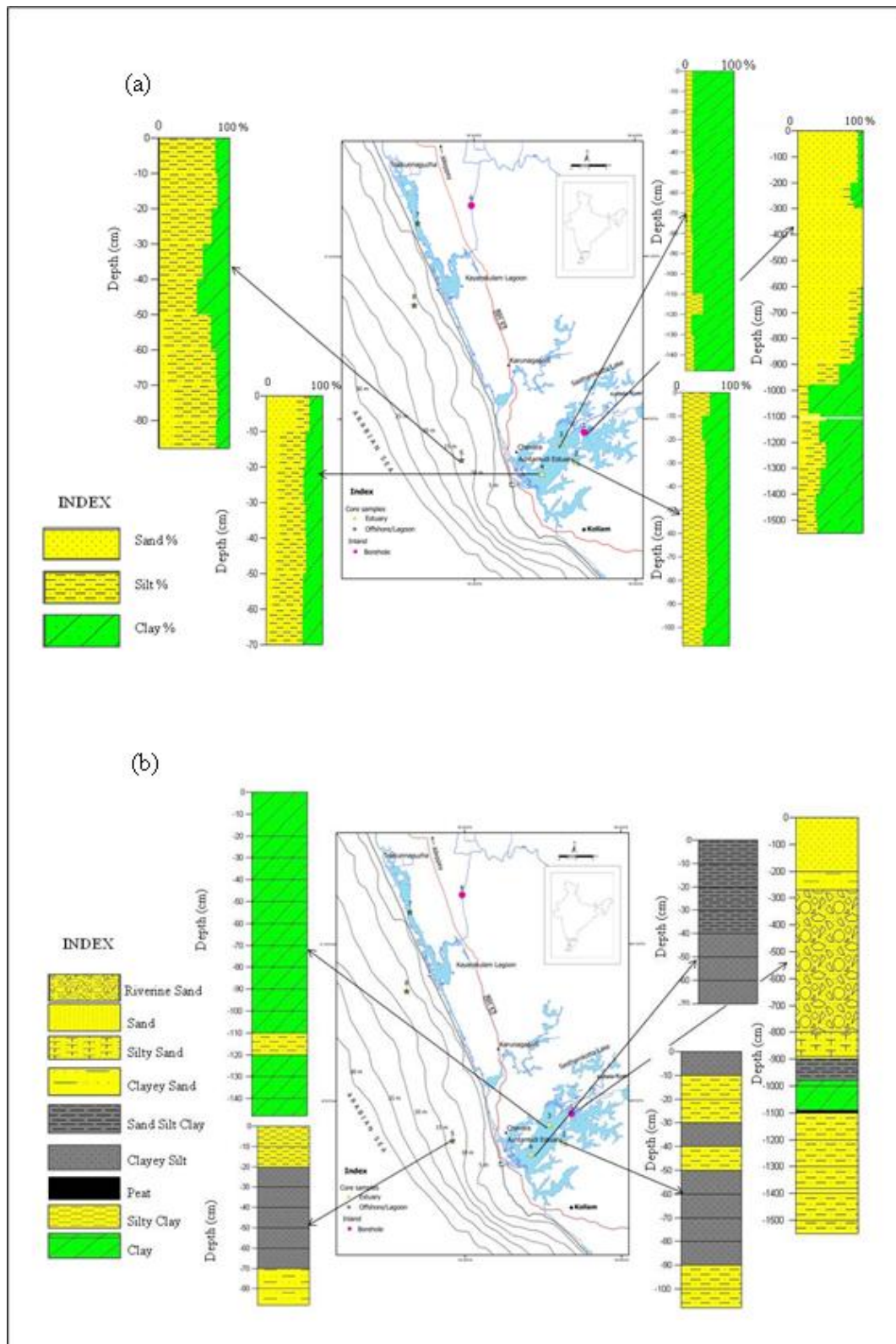


Fig. 4.1 (a) Lithological variation of sand silt clay percentages and (b) Sediment type variations in the coastal plain, estuary and offshore region of the southern transect

*Table 4.1 Sand silt and clay percentages, statistical parameters, organic matter and calcium carbonate contents of the coastal plain core (Core 1) of the southern transect*

Sl No	Depth (m)	Sand (%)	Silt (%)	Clay (%)	Mz ( $\phi$ )	SD ( $\phi$ )	Sk	K <sub>G</sub>	Sediment Type	OM (%)	CaCO <sub>3</sub> (%)
1	2.0	89.11	3.90	6.98	1.85	2.35	0.56	2.01	Sand	2.00	0.6
2	2.7	70.09	11.00	18.91	4.13	4.13	0.51	1.01	Clayey Sand	4.20	1
3	3.0	76.56	9.67	13.74	7.33	3.38	0.09	0.51	Sand	2.70	1
4	4.0	99	-	-	0.36	0.92	0	1.05	Sand	0.59	0.6
5	5.0	99	-	-	0.52	0.91	-0.03	1.22	Sand	0.49	0.2
6	5.9	99	-	-	-0.45	1.27	0.14	0.72	Sand	0.36	0.6
7	7.0	77.81	19.75	2.43	1.78	2.06	0.30	1.05	Sand	0.38	0.6
8	8.0	78.87	15.25	5.88	0.98	3.58	0.34	1.15	Sand	0.67	1
9	8.9	66.94	20.42	12.64	2.25	3.35	0.23	1.40	Silty Sand	0.32	1
10	9.0	76.52	5.90	17.58	4.18	4.46	0.53	2.17	Sand	0.40	1.2
11	9.8	30.67	32.37	36.97	4.71	5.52	-0.01	0.50	Sand Silt Clay	0.30	0.8
12	10	0.60	15.34	84.06	10.32	1.86	-0.75	1.20	Clay	0.23	1.8
13	10.9	3.93	12.62	83.45	10.29	2.25	-0.79	1.89	Clay	1.19	0.8
14	11	3.50	32.19	64.31	8.70	2.83	-0.41	0.72	Silty Clay	47.18	b.d.
15	11.8	12.65	30.99	56.35	8.22	3.14	-0.35	0.57	Silty Clay	10.94	b.d.
16	12.0	8.61	25.11	66.29	9.42	2.68	-0.72	0.76	Silty Clay	12.89	b.d.
17	13.0	12.31	31.10	56.59	8.29	3.06	-0.28	0.64	Silty Clay	7.58	b.d.
18	13.8	2.97	32.90	64.13	9.03	2.68	-0.50	0.67	Silty Clay	14.44	b.d.
19	14.0	0.41	33.26	66.33	9.43	2.23	-0.44	0.64	Silty Clay	11.93	b.d.
20	15.0	0.76	27.11	72.12	9.68	2.25	-0.63	0.75	Silty Clay	12.34	b.d.
21	15.5	0.80	29.68	69.53	9.51	2.38	-0.60	0.72	Silty Clay	12.00	b.d.

Mz = Mean size, SD = Standard Deviation, Sk = Skewness and K<sub>G</sub> = Kurtosis

#### **4.2.1.2. Ashtamudi Estuary (Core 2)**

The Core 2 (08° 57' 06" N, 76° 36' 11.9" E) is located on the eastern part of the Ashtamudi Estuary adjacent to the Velimon Kayal which is considered as a Marine Bioreserve Zone (Black and Baba, 2001). Prakash et al. (2001) have reported that the surficial sediment distribution in this arm is composed of clayey silt sediment.

The downcore lithological variations of sand-silt-clay percentage and sediment type are shown in figures 4.1a and b and also presented in Table 4.2. The lithology of this core consists of three units. In the first unit, the top 0.40 m sediment is composed of silty clay sandwiched between clayey silt. The percentage of sand ranges from 0.39 to 0.81%, silt from 41.58 to 58.22% and clay from 41.39 to 57.84%. A second unit of 0.40 to 0.80 m follows this where the percentage of sand is less which varies from 0.78 to 1.39% whereas silt and clay percentage increases from 47.77 to 51.57% and

47.04 to 51.24% respectively. The third unit 0.80 to 1.08 m is dominated by clayey silt and silty clay type sediments with < 1% of sand.

*Table 4.2 Sand silt and clay percentages, statistical parameters, organic matter and calcium carbonate contents of the Core 2 (Ashtamudi Estuary) of the southern transect*

SL No.	Depth (m)	Sand (%)	Silt (%)	Clay (%)	Mz ( $\phi$ )	SD ( $\phi$ )	Sk	K <sub>G</sub>	Sediment Type	OM (%)	CaCO <sub>3</sub> (%)
1	0.1	0.39	58.22	41.39	8.06	2.54	0.24	0.71	Clayey Silt	4.6	8.4
2	0.2	0.58	41.58	57.84	8.83	2.30	-0.02	0.64	Silty Clay	4.6	7.6
3	0.3	0.81	47.17	52.02	8.33	2.63	0.02	0.63	Silty Clay	5.4	5.7
4	0.4	0.66	50.03	49.31	8.32	2.50	0.12	0.66	Clayey Silt	5.7	6.7
5	0.5	0.99	47.77	51.24	8.48	2.40	0.13	0.66	Silty Clay	5.4	7.8
6	0.6	0.78	51.29	47.94	8.38	2.39	0.20	0.63	Clayey Silt	4.9	6.9
7	0.7	0.92	50.13	48.95	8.34	2.49	0.14	0.65	Clayey Silt	5.0	7.8
8	0.8	1.39	51.57	47.04	8.27	2.50	0.16	0.65	Clayey Silt	5.1	7.9
9	0.9	0.74	51.24	48.02	8.27	2.48	0.15	0.62	Clayey Silt	5.1	8.0
10	1	0.77	49.27	49.96	8.46	2.40	0.17	0.63	Silty Clay	5.3	8.4
11	1.8	0.67	42.68	56.65	8.82	2.24	0.07	0.68	Silty Clay	5.3	7.4

#### 4.2.1.3. Ashtamudi Estuary (Core 3)

The Core 3 (08° 58' 32.1" N, 76° 35' 23.3" E) is located in the south central estuary which is the main channel of the estuary where intense fishing activity is being carried out (Nair et al., 1983). The bathymetry of the surrounding area is shallow (Kurian et al., 2001). The surficial sediments near to the core site indicate the dominance of clayey silt sediments (Prakash et al., 2001). Details of the textural characteristics, organic matter and calcium carbonate of Core 3 are presented in Table 4.3. The lithology of the core is shown in figures 4.1a and b. It consists of three units. The first unit representing the top 0 to 0.30 m comprises of soft greenish clay, where the sand, silt and clay percentages range from 0.54 to 1.65%, 11.67 to 13.57% and 85.89 to 86.69% respectively. The organic matter and calcium carbonate contents in this unit exhibit an average value of 5 %. The second unit of 0.30 to 1.0 m is composed of clay, which is hard sticky and greenish colour.

Occurrences of sand is  $\leq$  1 % with silt varying between 12.90 and 17.24% showing varied percentage at regular intervals. Clay sediments are dominating throughout this unit, ranging from 82.47 to 86.20%. The last lithounit from 1.0 to 1.48 m comprises of clayey type sediments, which is sticky and greenish colour. The

average percentages of silt and clay constitute 19.82% and 79.83% respectively except at the depth of 1.20 m where silty clay dominates with silt and clay percentages of 36.47% and 63.36% respectively. The organic matter and calcium carbonate contents constitute an average percentage of 5.47% and 4.01 % respectively.

*Table 4.3 Sand silt and clay percentages, statistical parameters, organic matter and calcium carbonate contents of the Core 3 (Ashtamudi Estuary) of the southern transect*

SL No	Depth (m)	Sand (%)	Silt (%)	Clay (%)	Mz ( $\phi$ )	SD ( $\phi$ )	Sk	K <sub>G</sub>	Sediment Type	OM (%)	CaCO <sub>3</sub> (%)
1	0.2	0.54	13.57	85.89	10.39	1.71	-0.72	1.06	Clay	5.78	5.58
2	0.3	1.65	11.67	86.69	10.40	1.73	-0.72	1.20	Clay	5.63	5.16
3	0.4	0.39	13.41	86.20	10.39	1.72	-0.73	0.99	Clay	5.49	4.93
4	0.5	0.41	14.53	85.06	10.35	1.80	-0.74	1.09	Clay	6.16	5.38
5	0.6	0.29	17.24	82.47	10.24	1.89	-0.74	0.97	Clay	6.17	4.81
6	0.7	0.20	14.59	85.22	10.34	1.77	-0.73	0.99	Clay	5.82	5.05
7	0.8	0.46	12.90	86.64	10.39	1.71	-0.72	1.06	Clay	6.03	3.90
8	0.9	0.00	15.52	84.48	10.30	1.83	-0.72	1.00	Clay	5.92	3.71
9	1.0	0.25	14.08	85.68	10.35	1.73	-0.72	0.96	Clay	6.01	3.95
10	1.10	0.59	14.51	84.90	10.34	1.77	-0.73	1.06	Clay	5.69	4.76
11	1.20	0.18	36.47	63.36	8.88	2.44	-0.20	0.68	Silty Clay	5.08	3.20
12	1.30	0.38	12.40	87.21	10.43	1.79	-0.73	1.22	Clay	5.37	3.69
13	1.40	0.23	18.02	81.75	10.14	1.89	-0.69	0.89	Clay	5.54	3.73
14	1.48	0.34	17.71	81.95	10.22	1.92	-0.76	1.09	Clay	5.69	4.68

#### **4.2.1.4. Ashtamudi Estuary (Core 4)**

The Core 4 (08° 56' 37" N, 76° 34' 12" E) is located in the central estuary, which has the highest landings of fishes and shrimps (Kurup and Thomas, 2001). The bathymetry data in the central estuary reveals that the depth in the northern central part reaches upto 10 m, where as the southern central is very shallow i.e., about 1m depth (Kurian et al., 2001).

The variation of sand, silt, clay, organic matter and calcium carbonate percentage are presented in Table 4.4. The litholog of this core (Fig. 4.1 a, b) comprises of two units. The first unit from 0 to 0.40 m is composed of sand, silt and

clay sediments where the sand, silt and clay contents ranges from 23.57 to 53.80%, 23.15 to 33.08% and 23.05 to 33.08% respectively. The percentage of calcium carbonate and organic matter shows an average value of 6.5% and 3.4% respectively. This is followed by the second unit of 0.40 to 0.70 m where the sediments are clayey silt with a dominance of silt which is evident from an average value of 54.93%. Here the sand content is less compared to the first unit with the percentage varying between 6.26 and 18.02%. The clay content ranges from 29.63 to 35.14%. An enrichment of calcium carbonate with an average value of 11 % is observed whereas the organic matter remains more or less same (4%) as that of the unit above it.

*Table 4.4 Sand silt and clay percentages, statistical parameters, organic matter and calcium carbonate contents of the Core 4 (Ashtamudi Estuary) of the southern transect*

Sl. No.	Depth (m)	Sand (%)	Silt (%)	Clay (%)	Mz ( $\phi$ )	SD ( $\phi$ )	Sk	K <sub>G</sub>	Sediment Type	OM (%)	CaCO <sub>3</sub> (%)
1	0.10	53.80	23.15	23.05	5.82	2.85	0.86	0.86	Sand Silt Clay	0.71	8.7
2	0.20	24.01	45.73	30.26	6.98	3.02	0.32	0.69	Sand Silt Clay	4.17	6.7
3	0.30	20.95	45.97	33.08	7.07	3.03	0.32	0.68	Sand Silt Clay	4.31	4.4
4	0.40	23.57	46.69	29.74	6.91	3.00	0.36	0.74	Sand Silt Clay	4.16	6.2
5	0.50	18.02	52.35	29.63	7.01	2.99	0.35	0.77	Clayey Silt	3.71	9.4
6	0.60	11.54	53.84	34.62	7.44	2.90	0.19	0.74	Clayey Silt	4.31	10.8
7	0.70	6.26	58.60	35.14	7.59	2.79	0.25	0.77	Clayey Silt	4.35	12.5

#### 4.2.1.5. Offshore (Core 5)

The Core 5 (08° 57' 28" N, 76° 29' 12" E) is collected off Kollam coast at a depth of 12.5 m with a recovery of 0.88m. In general, the offshore areas are carpeted by clayey silt distribution (Prakash, 2000). Table 4.5 gives the percentages of sand, silt, clay, calcium carbonate and organic matter in Core 5. The lithological variation reveals that the core is divided into three units (Figs. 4.1a & b). The first unit from 0 to 0.40 m is dominated by silt varying between 60.22 and 80.47% followed by clay ranging from 20.28 to 37.70%. The sand percentage is less ranging from 1.63 to 3.79%. The calcium carbonate content ranges up to 11% whereas the organic matter constitutes only 3% in this unit. This is followed by the second unit, 0.40 to 0.60 m where the sediments are clayey silt with less percentage of sand. There is a gradual increase of silt (54.46 to 58.59%) down the core whereas the clay percentage

decreased up to 45.23%. The organic matter decreased to <2% whereas the calcium carbonate increased even up to 14 % compared to the first unit. The third unit from 0.60 to 0.88 m comprises of sandy silt sediments where the sand percentage increased from 12.82 to 22.30%. The silt exhibit uniform value as that of the unit above it where as the clay varies between 16.88 and 19.12% showing a decreasing trend down the core as compared to the other two units. The organic matter ranges from 1 to 3 % where as the calcium carbonate increases upto 13%.

*Table 4.5 Sand silt and clay percentages, statistical parameters, organic matter and calcium carbonate contents of the Core 5 (Offshore) of the southern transect*

SL. No	Depth (m)	Sand (%)	Silt (%)	Clay (%)	Mz (φ)	SD (φ)	Sk	K <sub>G</sub>	Sediment Type	OM (%)	CaCO <sub>3</sub> (%)
1	0.10	1.63	78.09	20.28	6.33	2.37	0.62	1.13	Silt	2.84	10
2	0.20	3.38	80.47	16.15	6.09	1.99	0.45	1.49	Silt	3.00	11.4
3	0.30	3.79	71.02	25.19	6.99	2.72	0.52	0.94	Clayey Silt	3.26	11
4	0.40	2.08	60.22	37.70	7.46	2.84	0.38	0.56	Clayey Silt	3.90	10.2
5	0.50	0.31	54.46	45.23	8.19	2.51	0.19	0.65	Clayey Silt	4.98	9
6	0.60	8.38	66.09	25.53	6.79	2.74	0.51	0.91	Clayey Silt	4.05	12.6
7	0.70	12.82	68.31	18.87	6.12	2.40	0.51	1.22	Clayey Silt	2.63	12.1
8	0.80	21.58	61.54	16.88	5.62	2.76	0.22	1.63	Sandy Silt	2.70	13.3
9	0.88	22.30	58.59	19.12	5.32	3.42	0.13	1.77	Sandy Silt	1.36	14.5

#### **4.2.2. Sediment core along the northern Transect**

The sediment cores along the northern transect comprises of 3 cores representing the coastal plain (Core 6), the Kayamkulam Lagoon (Core 7) and the Offshore (Core 8) region respectively. The downcore lithological variations including the calcium carbonate and the organic matter distribution in the sediment cores are briefly discussed below and also presented in figures 4.2a & b.

##### **4.2.2.1. Coastal Plain (Core 6)**

The Core 6 (09°13' 09" N, 76° 29' 50" E) represents the coastal plain of the northern transect located 7.9 km east of the Kayamkulam Lagoon. This core falls within a paleodrainage channel (Chattopadhyay, 2002) and a line separating the young and old shoreline orienting in the NNW-SSE direction (Samsuddin et al., 2008). The details of the core are given in Chapter 3.

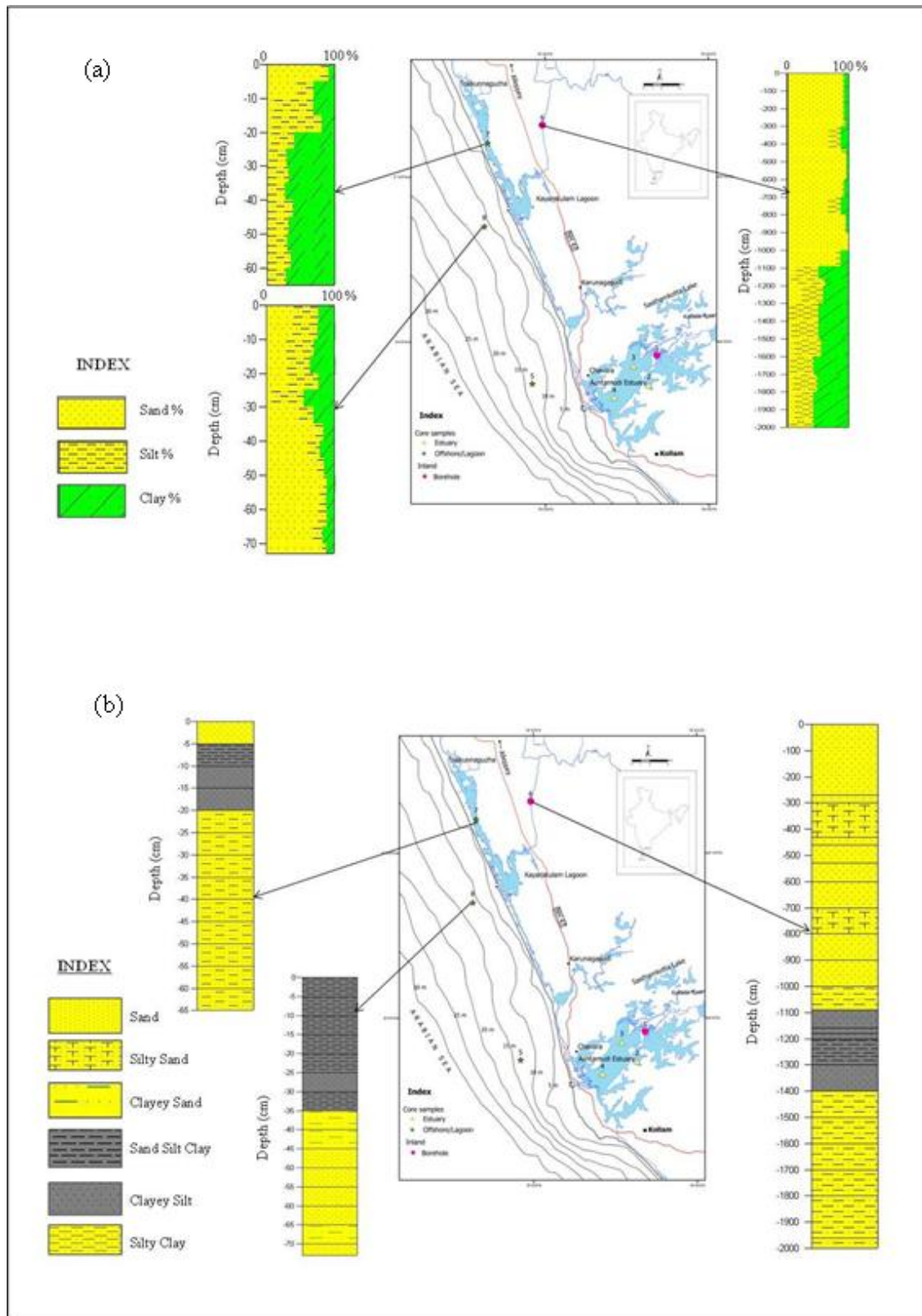


Fig. 4.2 (a) Lithological variation of sand silt clay percentages and (b) Sediment type variations in the coastal plain, lagoon and the offshore region of the northern transect



The percentage of sand, silt, clay, organic matter and calcium carbonate are presented in Table 4.6. The sediment litholog starts with a top soil of 2.5 m and consist of 4 units (Fig. 4.2a & b). The first unit from 2.5 to 4 m comprises of medium to fine sand showing light to brownish colour. Here in this unit the sand dominates ranging from 89.81 to 91.81% (av. 90.81%) where as silt and clay contents are minimum with an average percentage of 3.61% and 5.58% respectively. The percentatge of organic matter and calcium carbonate are least in this unit. This is followed by a second unit, from 4 to 10 m where sand of light greenish colour dominates with an intercalation of silty sand at the top and bottom. The sand content varies between 66.94 and 99% with considerable increase of silt (av. 7.31%) whereas the clay percentage ranges from 2.70 to 7.26% except at the depths of 4.3 and 8 m where an increase of 12% is observed. At the end of this unit (10 m), minute broken shells with considerable amount of heavy minerals are noted. The organic matter and calcium carbonate percentages are insignificant throughout the unit except at 8 and 10 m depths where it increases to 7 and 14% respectively.

*Table 4.6 Sand, silt and clay percentages as well as the textural parameters of the coastal plain core (Core 6) in the northern transect*

Sl. No.	Depth (m)	Sand (%)	Silt (%)	Clay (%)	Mz (φ)	SD (φ)	Sk	K <sub>G</sub>	Sediment Type	OM (%)	CaCO <sub>3</sub> (%)
1	2.7	89.81	2.72	7.47	2.26	2.20	0.37	2.75	Sand	0.20	1.2
2	3.0	91.81	4.50	3.69	1.98	1.50	0.33	1.50	Sand	0.14	0.4
3	4.3	67.38	20.34	12.28	4.10	2.36	0.68	2.15	Silty Sand	0.64	1.2
4	4.6	88.13	7.73	4.14	2.39	1.58	0.31	1.96	Sand	0.15	0.8
5	5.3	95.41	1.89	2.70	1.57	1.03	0.36	1.04	Sand	0.07	0.2
6	6.0	96.36	0.87	2.76	1.61	1.07	0.12	0.99	Sand	0.07	0.6
7	7.0	88.23	4.51	7.26	2.69	1.72	0.70	5.21	Sand	0.31	1.6
8	8.0	66.94	20.42	12.64	3.37	1.58	0.52	6.10	Silty Sand	0.43	7.2
9	8.9	93.49	2.73	3.78	2.92	0.88	0.59	4.12	Sand	0.15	0.8
10	10.0	99	-	-	3.23	0.45	-0.07	1.11	Sand	0.35	14.4
11	10.9	79.78	8.22	12.00	3.76	1.89	0.40	5.30	Sand	0.33	38
12	11.6	13.06	38.27	48.67	8.03	2.92	-0.01	0.67	Silty Clay	1.84	23.6
13	11.8	6.80	53.17	40.03	7.77	2.70	0.25	0.76	Clayey Silt	1.89	19.8
14	12.0	16.56	46.35	37.09	7.28	3.09	0.20	0.69	Clayey Silt	1.79	23
15	13.0	23.33	34.71	41.96	7.31	3.14	0.15	0.54	Sand Silt Clay	1.85	17.8
16	13.9	2.15	49.14	48.70	8.19	2.66	0.10	0.60	Clayey Silt	1.84	25.6
17	15.0	7.68	43.49	48.82	7.91	2.92	0.00	0.56	Silty Clay	1.54	21.8
18	16.0	10.55	44.62	44.82	7.55	3.04	0.19	0.52	Silty Clay	1.51	20
19	17.0	3.31	39.51	57.17	8.47	2.77	-0.19	0.61	Silty Clay	1.70	22.6
20	18.0	9.76	39.65	50.59	7.98	3.00	-0.07	0.55	Silty Clay	1.60	18.8
21	19.7	11.14	31.07	57.80	8.57	3.17	-0.49	0.60	Silty Clay	1.36	23.2
22	20.0	2.63	39.97	57.40	8.52	2.71	-0.16	0.61	Silty Clay	1.96	21

This is followed by a third unit of 10 to 14 m, where the sandy sediments sequence is changed to silty clay/clayey silt type of sediments. Large amount of minute broken shells of brachiopods and pelecypods were observed for a thickness of 1 m showing 38% of calcium carbonate with sand content as high as 80%. At 11 to 12 m the brachiopods and pelecypods shells are completely embedded with the clayey silt type sediments. Towards the lower part of this unit the sandy sediments decreases with an increase in silt and clay content. As a whole, the percentage of sand, silt and clay contents in this unit ranges from 2.15 to 13.06%, 34.71 to 53.17% and 37.09 to 48.70% respectively indicating an abrupt change in the sand-silt-clay content. In general, there is an increase of calcium carbonate along this unit with percentage varying between 14 and 38% where as the organic matter showed a maximum value of 1.89% as compare to the top litho-units.

The fourth unit comprises of 14 to 20 m where silty clay sediments dominate throughout with silt and clay ranging from 31.07 to 44.62% and 44.82 to 57.80% respectively. The sand content which ranges from 2.63 to 11.14% exhibits less variation. A sizeable quantity of broken shells is encountered with the fine sediments down the core with the calcium carbonate ranging from 18 to 25% and organic matter of 1.96%.

#### **4.2.2.2. Kayamkulam Lagoon (Core 7)**

The Core 7 (09° 12' 03" N, 76° 26' 29" E) collected from the Kayamkulam Lagoon consists of three units. The percentages of sand, silt, clay, organic matter and calcium carbonate are given in Table 4.7. The first unit 0 to 0.10 m is dominated by sand ranging from 44.75 to 79.87% followed by clay and silt showing 8.38 to 31.09% and 11.75 to 24.16% respectively. The calcium carbonate shows an average value of 6.25% whereas the organic matter is less (av. 2.58%). In the second unit from 0.10 to 0.30 m the sand percentage decreased from 10.08 to 3.15% with an increase in silt and clay percentage in the range of 25.81 to 72.50% and 19.24 to 71.04% respectively. The organic matter and calcium carbonate content shows an average value of >6%. This is followed by the third unit of 0.30 to 0.65 m where the sediments are of silty clay showing negligible sand (av. 1%) content with the dominance of clay (av. 68.10%) through out this unit. The organic matter (av. 7%) and the calcium carbonate (av. 6%) percentages are high as compared to the first two units.

*Table 4.7 Sand, silt, clay percentages as well as the textural parameters of the Kayamkulam lagoon core (Core 7) in the northern transect*

<b>Sl No.</b>	<b>Depth (m)</b>	<b>Sand (%)</b>	<b>Silt (%)</b>	<b>Clay (%)</b>	<b>Mz (φ)</b>	<b>SD (φ)</b>	<b>Sk</b>	<b>K<sub>G</sub></b>	<b>Sediment Type</b>	<b>OM (%)</b>	<b>CaCO<sub>3</sub> (%)</b>
1	0.05	79.87	11.75	8.38	2.23	2.71	0.69	1.73	Sand	1.18	6.09
2	0.10	44.75	24.16	31.09	5.66	4.27	0.25	0.59	Sand Silt Clay	3.98	6.40
3	0.15	10.08	58.17	31.75	9.16	2.56	-0.37	0.80	Clayey Silt	6.40	7.70
4	0.20	8.26	72.50	19.24	9.15	2.55	-0.34	0.77	Clayey Silt	6.59	6.27
5	0.25	6.48	33.73	59.78	9.20	2.59	-0.48	0.77	Silty Clay	6.53	6.39
6	0.30	3.15	25.81	71.04	9.48	2.05	-0.34	0.64	Silty Clay	6.68	6.13
7	0.35	1.22	30.78	68.00	9.50	2.15	-0.42	0.69	Silty Clay	6.73	5.56
8	0.40	1.03	26.40	72.57	9.64	1.92	-0.29	0.65	Silty Clay	6.58	5.69
9	0.45	0.72	37.35	61.93	9.27	2.19	-0.21	0.63	Silty Clay	6.73	6.18
10	0.50	0.84	31.42	67.74	9.92	2.14	-0.72	0.69	Silty Clay	6.93	5.05
11	0.55	1.23	29.04	69.73	9.82	2.04	-0.64	0.62	Silty Clay	7.22	5.25
12	0.60	0.94	34.74	64.32	9.07	2.50	-0.35	0.71	Silty Clay	7.09	5.36
13	0.65	0.94	26.75	72.31	9.71	2.37	-0.70	0.81	Silty Clay	7.06	5.99

#### **4.2.2.3. Offshore (Core 8)**

The Core 8 (09° 07' 31" N, 76° 26' 17" E) is located 2 km south of the Kayamkulam breakwater. The percentages of sand, silt, clay, organic matter and calcium carbonate are given in Table 4.8. The core is sub-divided into two litho-units. The top 0.35 m comprises of sand-silt-clay (mud) sediments where the percentages of sand, silt and clay contents ranges from 29.04 to 47.90%, 22.4 to 47.39% and 22.36 to 44.18% respectively indicating more or less equal distribution. The calcium carbonate content varies from 8 to 15.4% whereas the organic matter has an average value of 3%. This is followed by a second unit of 0.35 to 0.73 m where the sediment is rich in sand which varies between 60.23 and 83.83% followed by clay and silt ranging from 5.64 to 14.04% and 10.13 to 16.84% respectively. The calcium carbonate percentage is 6.57% and the organic matter < 2%.

*Table 4.8 Sand, silt, clay percentages as well as the textural parameters of the offshore core (Core 8) in the northern transect*

Sl. No.	Depth (cm)	Sand (%)	Silt (%)	Clay (%)	Mz ( $\phi$ )	SD ( $\phi$ )	Sk	K <sub>G</sub>	Sediment Type	OM (%)	CaCO <sub>3</sub> (%)
1	0.05	41.41	36.23	22.36	6.39	3.27	0.64	1.01	Sand Silt Clay	2.09	15.4
2	0.10	38.64	36.73	24.64	6.46	3.27	0.65	0.88	Sand Silt Clay	2.14	11.4
3	0.15	29.04	41.01	29.95	6.86	3.21	0.48	0.50	Sand Silt Clay	2.44	13.6
4	0.20	30.52	33.58	35.9	7.00	3.35	0.33	0.52	Sand Silt Clay	2.85	12
5	0.25	31.62	45.43	22.95	6.33	3.39	0.55	1.06	Sand Silt Clay	2.60	12
6	0.30	8.43	47.39	44.18	7.99	2.85	0.12	0.66	Clayey Silt	5.44	10.8
7	0.35	47.9	22.4	30.06	5.99	3.79	0.52	0.57	Sand Silt Clay	3.00	8
8	0.40	71.99	12.19	15.82	4.07	3.24	0.56	1.59	Clayey Sand	1.93	6.6
9	0.45	60.23	19.22	20.55	5.29	4.08	0.52	0.89	Clayey Sand	2.29	8
10	0.50	75.33	10.05	14.62	3.65	3.24	0.65	1.65	Sand	1.73	6.8
11	0.55	83.83	5.64	10.53	2.16	2.45	0.69	2.37	Sand	1.27	6
12	0.60	79.41	10.46	10.13	2.38	2.60	0.67	1.69	Sand	1.27	6
13	0.65	76.02	13.56	10.42	2.46	2.76	0.67	1.59	Sand	1.12	5.6
14	0.70	69.12	14.04	16.84	4.15	3.56	0.58	1.19	Clayey Sand	1.73	7.4
15	0.73	82.36	6.57	11.08	2.43	2.56	0.66	1.80	Sand	1.22	5.4

### 4.3. Textural Parameters

Grain size parameters form the basis of many schemes for classifying the sedimentary environments. Several researchers during the past 50 years have employed different methods and criteria to distinguish environment of deposition from the grain size distributions (Folk and Ward, 1957; Friedman, 1961, 1979; Sahu, 1964; Moiola and Weiser, 1968; Vincent, 1986). Every environment of deposition may be assumed to have characteristics, typical of the energy conditions as functions of location and time (Sahu, 1964). In the present study from the cumulative weight percentages of the grain size distribution the parameters such as the mean size, standard deviation, skewness and kurtosis are calculated following the Folk and Ward (1957). The classification of grain size parameters is presented in Table. 4.9. The textural characteristics of different locations of the study area representing the coastal plain, estuary/lagoon and offshore for the southern and northern transect are presented in the following sections.

Table 4.9. Classification of grain size parameters based on Folk and Ward (1957)

<b>Mean Size Value</b>	<b>Nature of sediment</b>
$-\infty$ to $-1 \phi$	Gravel
$-1$ to $0 \phi$	Very coarse sand
$0$ to $+1 \phi$	Coarse sand
$+1$ to $+2 \phi$	Medium sand
$+2$ to $+3 \phi$	Fine sand
$+3$ to $+4 \phi$	Very fine
$+4$ to $+8 \phi$	Silt
$+8$ to $-\infty$	Clay
<b>Standard Deviation values</b>	<b>Nature of sediment</b>
$<0.35 \phi$	Very well sorted
$0.35$ to $0.50 \phi$	Well sorted
$0.50$ to $0.70 \phi$	Moderately well sorted
$0.70$ to $1.0 \phi$	Moderately sorted
$1.0$ to $2.0 \phi$	poorly sorted
$2.0$ to $4.0 \phi$	Very poorly sorted
$>4.0 \phi$	Extremely poorly sorted
<b>Skewness values</b>	<b>Nature of Sediment</b>
$+1.00$ to $+0.30$	Very finely skewed
$+0.30$ to $+0.10$	Fine skewed
$+0.10$ to $-0.10$	Nearly symmetrical
$-0.10$ to $-0.30$	Coarse skewed
$-0.30$ to $-1.00$	Very coarse skewed
<b>Kurtosis values</b>	<b>Nature of Sediment</b>
$0.07$ to $0.67$	Very Platykurtic
$0.67$ to $0.90$	Platykurtic
$0.90$ to $1.11$	Mesokurtic
$1.10$ to $1.50$	Leptokurtic
$1.50$ to $3.00$	Very leptokurtic
$3.00$ to $\infty$	Extremely leptokurtic

#### 4.3.1. Southern Transect

The statistical parameters like the mean size, standard deviation, skewness and kurtosis for the coastal plain, estuary and offshore for the southern transect are briefly discussed below.

##### 4.3.1.1. Coastal Plain

The mean grain size of the sediment core of the southern coastal plain represented by Core 1 ranges from  $0.36$  to  $10.32 \phi$  with an average of  $6.05 \phi$  (Table

4.1). The mean grain size from the depth 2.0 to 4.0 m ranges from 0.36 to 7.33  $\phi$  indicating the presence of coarse-medium sand to coarse silt grade. The sediments were very poorly sorted at the beginning and becomes better down the unit with a range of 0.92 to 2.35 $\phi$ . Skewness reveals very fine to symmetrical in nature with a value of 0.55 to 0.09. The peakedness of the sediments in this unit is of very-lepto to very-platykurtic in nature. The mean size decreases further down the core from 4.0 to 7.0 m ranging from 0.52 to 1.78  $\phi$  indicating coarse to very coarse sand. The sediments are poorly sorted with symmetrical to fine skewed nature and mesokurtic in nature. Below this unit (7.0 to 9.0 m) the mean grain size changes from coarse to fine sand grade with a value of 0.98 to 4.18 $\phi$ . The sediments are poorly to very poorly sorted type with a value of 3.58 to 4.46. Moreover the sediments are fine skew to very fine skewed (0.33 to 0.52) with its peakedness dominating in lepto to very leptokurtic region.

Below 9.0 m, the mean size increases sharply from 4.71 to 8.70  $\phi$  showing that the sediments are modified from fine sand to coarse silt except at the depth from 9.9 to 10.9 m, where the mean size exhibits clay type with a value of 10.32  $\phi$ . In this unit the sediments are very poorly to extremely poorly sorted with a value ranging from 1.86 to 5.52 $\phi$ . Symmetry of the sediments is of very coarse skewed with a value ranging from 0.79 to 0.01 with lepto-platykurtic in nature. Further, from 11 m to down the core (15.5 m) the mean size varies from 8.22 to 9.68  $\phi$  with an average of 9.08  $\phi$  indicating fine grade sequence of clayey type sediments. Here the sediments are very poorly sorted in nature with a value ranging from 2.23 to 3.14 and coarse to very coarse skewed with a negative value ranging from 0.28 to 0.72. The peakedness of the sediments reveals the sediments are platykurtic to very platykurtic in nature with a value ranging from 0.57 to 0.75 respectively.

#### **4.3.1.2. Ashtamudi Estuary**

The statistical parameters for the 3 cores from the Ashtamudi estuary namely Core 2, 3 and 4 are discussed below.

In Core 2 (Table 4.2), the mean grain size along the entire core varies from 8.06 to 8.88  $\phi$  with an average of 8.41  $\phi$  indicating the dominance of very fine silt down the core. Sediments are very poorly sorted with a value ranging from 2.24 to

2.63 with finely skewed in nature. Kurtosis show the sediments are of platykurtic in nature with a value ranging from 0.63 to 0.71.

The mean size of Core 3 (Table 4.3) varies from 10.14 to 10.40  $\phi$  with an average of 10.32  $\phi$  indicating clayey type sediments from the top to down the core except at a depth of 1.2 m where the mean size indicates very fine silt type with a value of 8.88 $\phi$ . The sediments are poorly sorted with a value ranging from 1.71 to 2.44 along the entire core. The sediments are of coarse skewed in nature with a value ranging from 0.20 to 0.76. The sediments exhibit mesokurtic in nature upto a depth of 1.10 m but changes to platykurtic down the core.

The statistical parameters of Core 4 (Table 4.4) reveal that the mean size varies from 5.82 to 7.59  $\phi$  with an average of 6.97  $\phi$  indicating fine sediments. The mean size of the estuarine core (Core 4) starts with coarse silt with a value of 5.82  $\phi$  followed by the fining of the grain size revealing fine to medium silt with a value ranging from 6.91 to 7.07  $\phi$  upto a depth of 0.40 m. Below this up to the end of the core the mean size varies from 7.01 to 7.59  $\phi$  indicating fine silt down the core. The entire core exhibits sediments of very poorly sorted nature with a value ranging from 2.79 to 3.03. The skewness value varies between 0.19 and 0.86 indicating that the sediments are of fine to very fine skewed in nature. The peakedness of the sediments along the entire core is of platykurtic in nature with a value ranging from 0.68 to 0.86.

#### **4.3.1.3. Offshore**

The statistical parameters of the core from the southern offshore location are presented in the Table 4.5. The mean grain size of the top 0.40 m core indicates that it is dominated by medium to fine-silt with size ranging from 6.33 to 7.46 $\phi$ . Here the sediments are of very poorly sorted type with a value ranging from 1.99 to 2.84 $\phi$ . The symmetry reveals that the sediments are of very fine skewed in nature with a value ranging from 0.32 to 0.62 $\phi$ . The peakedness of the sediments varies from 0.56-1.14 indicating the variation in the kurtosis value from lepto-meso-platykurtic in nature. From 0.40 to 0.60 m, the mean size varies from 6.79-8.19  $\phi$  showing the dominance of very fine to medium silt which is poorly sorted in nature. The sediments are fine to very fine skewed with a value ranging from 0.19 to 0.51. The peakedness of the sediments reveals very platykurtic in nature. From 0.60 m to down the core, the mean

size exhibits medium to coarse silt with a value ranging from 5.32 to 6.12 $\phi$ . The sediments are very poorly sorted with fine to very fine skewed. The Kurtosis value ranges from 1.22 to 1.77 indicating lepto-very leptokurtic in nature.

#### **4.3.2. Northern Transect**

The statistical parameters of the cores representing the coastal plain, lagoon and offshore locations of the northern transect are discussed below.

##### **4.3.2.1. Coastal plain**

In the northern coastal plain, the average statistical parameters of the entire core sediments (Table 4.6) reveal a mean size of 5.33  $\phi$  and a sorting co-efficient of 2.19. The top 4 m of the core section exhibits a mean size of 1.98 to 2.26  $\phi$  indicating medium to fine sand with a sorting co-efficient of 1.50 to 2.20 indicating poorly sorted sediments. The grains are of very fine skewed with a value of 0.33 and leptokurtic in nature. From 4 to 10.0 m the mean grain size varies considerably from top to bottom with a mean size ranging from 1.57 to 4.10  $\phi$  indicating medium to very fine sand and coarse silt down the unit. The sorting co-efficient shows a decreasing trend down the unit from 2.36 to 0.45 indicating that the poorly sorted nature is changed to moderately to well sorted type.

Skewness reveals the sediments are very fine skewed with a value ranging from 0.12 to 0.70 except at the bottom of the unit where the sediments show a symmetrical nature with a value of 0.07. The peakedness of the sediments reveals very lepto-meso to extremely leptokurtic in nature with a value ranging from 0.99 to 6.10. This unit is followed by the change in the statistical parameters where the mean size changes from fine sand to very fine to fine silt up to a depth of 14 m with a value ranging from 3.76 to 8.19 $\phi$ . The sediments are very poorly sorted with a value ranging from 1.89-3.14. Skewness reveals mixed variety with fine skewed to symmetry in nature with a value ranging from 0.10-0.40. The peakedness of the sediments changes from lepto- platykurtic in nature with a value ranging from 5.30 to 0.54. From 14 m to down the core, the mean size varies between 7.91 and 8.57  $\phi$  indicating alternate layers of fine to very fine silt components of poorly sorted nature with a sorting co-efficient ranging from 2.71 to 3.04 $\phi$ . The skewness exhibits mixed variety in nature



with a value ranging from -0.16 to -0.19. The Kurtosis reveals that the sediments are very platykurtic in nature with a value ranging from 0.52 to 0.61.

#### **4.3.2.2. Lagoon**

The statistical parameters of Core 7 located in the lagoon are presented in Table 4.7. The mean grain size of the top 0.10 m indicates fine sand to coarse silt with a value ranging from 2.23 to 5.65 $\phi$ . From 0.10 to down the core (0.65 m), the sediments are of clay type with a value of 9.46 $\phi$ . The sediments are poorly sorted, coarse skewed and platykurtic as indicated by the average values of 2.3, -0.44 and 0.71 respectively.

#### **4.3.2.3. Offshore**

The textural parameters of the northern offshore core (Table 4.8) indicates that the mean size are of fine to very fine silt grade with a value ranging from 6.33 to 7.0  $\phi$  (avg. 6.6  $\phi$  ) up to a depth of 0.25 m where the sediments are poorly sorted with a value ranging from 3.21 to 3.29. The symmetry reveals that the sediments fall in the category of very fine skewed in nature with a value ranging from 0.33 to 0.64. The peakedness of the sediments starts with mesokurtic in nature with a value of 1.01, which is followed by platy to very-platykurtic in nature with a value ranging from 0.88 to 0.52. From 0.30-0.45 m, the mean size increases from fine to very coarse silt with a value ranging from 7.99 to 5.29. The sediments are poorly to extremely poorly sorted with very fine skewed in nature.

Kurtosis reveals that the sediments are accumulated in the tail position with better sorting value ranging from 0.66 to 0.89. But from 0.50 m onwards to the end of the core, the mean size changes from coarse silt to very fine sand grade with a value ranging from 2.16 to 3.65  $\phi$  indicating a change in the environment except at 0.70 m where the mean size corresponds to very coarse silt grade. However the sorting is very poor with a value ranging from 2.45 to 3.56. The degree of asymmetry in the frequency distribution curve reveals that the sediments falls in the category of very fine skewed nature with a value ranging from 0.58 to 0.69. Kurtosis reveals that the central positions are better sorted with a value ranging from 1.19 to 2.37 indicating very leptokurtic in nature.

#### **4.4. Sediment classification**

Nomenclature describing the sediment distributions is important to geologists and sedimentologists because the grain size is the most basic attribute of sediments (USGS, 2006). Traditionally, geologists have divided sediments into four size fractions namely - gravel, sand, silt and clay based on their grain sizes and classified these sediments based on ratios of the various proportions of the fractions. Several classification schemes exist (Robinson, 1949; Trefethen, 1950; Folk, 1954; Shepard, 1954). Shepard's classification scheme emphasizes the ratios of sand, silt and clay because they reflect sorting and reworking (Poppe et al., 2005). The original classification scheme developed by Shepard (1954) used a single ternary diagram with sand, silt and clay in the corners and 10 categories to graphically represent the relative proportions among these three grades within a sample.

The dominant sediment types in the coastal plain of the southern transect falls under the category of sand, silty sand, clayey sand, silty clay and clay. The estuarine cores fall under the category of silty clay, clayey silt and muddy type of sediments. Silty type sediments are found to dominate in the offshore areas.

In the northern transect the coastal plain core falls under the category of sand, silty clayey, clayey silt and sand silt clay. The lagoon core falls under the silty clay and sand silt clay. Finally the offshore core falls under the category of sand-silt-clay (mud), clayey silt, clayey sand and sand.

#### **4.5. Depositional Environment**

To interpret the depositional environment of sediments many research workers have utilized the textural parameters such as the mean grain size, sorting, skewness and kurtosis (Folk, 1974; Folk and Ward, 1957). In addition to the textural parameters the ratios of sand, silt, clay on the Ternary diagram (Pejrup, 1998) and scatter plots of mean size and sorting (Tanner, 1991 a,b) are used to characterize the energy condition of the environment. For the present study, the above ratios were used to understand the depositional environment and are briefly described below.

#### **4.5.1. Hydrodynamic condition**

The ternary diagram proposed by Pejrup (1988) is used to understand the hydrodynamic condition of deposition. This is basically a distinction between an aggregated fine fraction and non-aggregated coarse fraction which forms the basis for one of the interpretive tools employed to discuss the particle size distributions.

The ternary diagram is divided into four sections and each section is further divided into four classes. The triangle consists of 16 groups, each one of which is named by a letter indicating the type of sediment and a number indicating the hydrodynamic conditions during the deposition. For example, group DII represents sediments containing sand from 0 to 10% deposited under rather quiet hydrodynamic condition. According to Pejrup (1988) section I indicate very calm hydrodynamic conditions rarely found in the estuaries and sections II to IV indicate increasingly violent hydrodynamic conditions.

The sand, silt and clay content of each of the core samples representing the coastal plain, estuary and the offshore of the southern transect (Fig. 4.3a) are plotted in Pejrup's (1988) diagram. Based on the lithological variation the samples of the coastal plain (Core 1) are divided into three units. The core samples of 2.7 to 9.8 m falls in the category of III and IV indicating that the sediments were deposited under violent to the most violent environment. The sediments from 9.9 to 10.9 m fall under the category I indicating quietest environment. Further down the core from 11 to 15.5 m the sediments falls under the category (II) indicating a calm environment.

Out of the three estuarine cores (Core 2, 3, 4), Core 2 sediment falls under the category I representing quietest environment except one sample falling under the category II indicating a calm environment. In Core 3, most of the samples fall near the boundary line of category II and III indicating violent to calm environment. In Core 4, most of the samples fall in the category III indicating violence except one sample which falls in the boundary line of category II and III showing violent to calm environment. The sediment of the offshore Core 5 comes under the category III which falls in the violent environment.

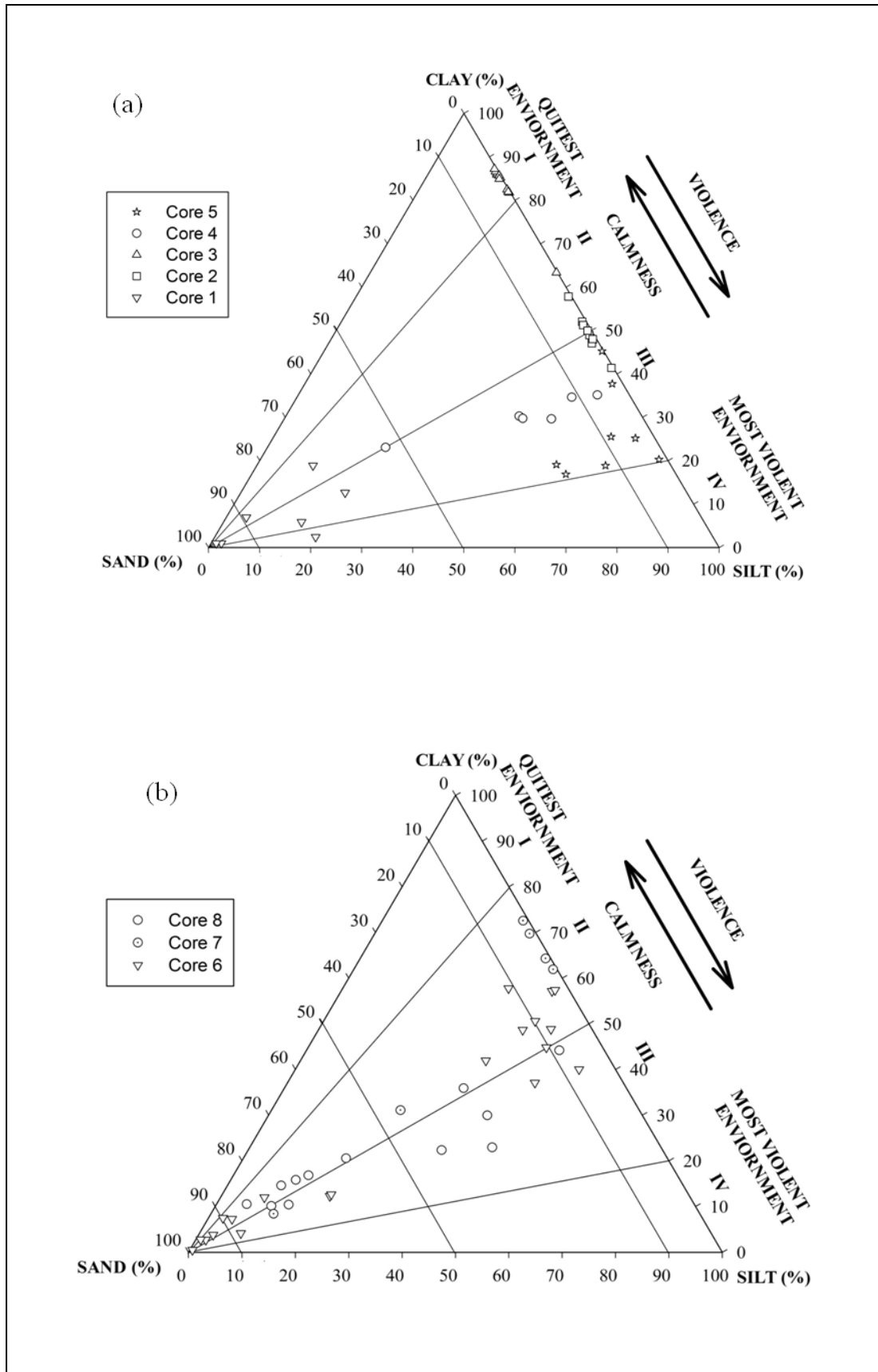


Fig. 4.3 Hydrodynamic deposition of sediments (after *Pejrup, 1988*) for (a) the southern and (b) northern transects

The sand, silt and clay percentages for the coastal plain, lagoon and the offshore cores of the northern transect are also plotted in Pejrup's diagram and are shown in figure 4.3b. The samples representing the top 10.8 m of the coastal plain falls under the category III indicating violent environment whereas from 11 m to down the core the sediments falls under the category II indicating calmness. The sediments of the Core 7 also falls under the category II indicating calmness. In the offshore (Core 8), the top 0.45 m falls under the category II indicating calmness whereas down the core, the sediments falls under the category III indicating violent environment.

#### **4.5.2. Suite Statistics**

The Tanner plot uses the mean size and sorting value to understand the depositional energy condition. The suite statistics model proposed by Tanner (1991a,b) uses the bivariate plots of the mean size and sorting in a logarithmic scale. This plot is sub-divided into three different fields representing the different energy conditions of deposition as (i) fluvial and storm episodes, (ii) partially open to restricted estuary and (iii) closed basin, giving the effective discrimination of depositional environments. Spencer et al. (1998) have modified the plots of Tanner (1991a,b) by including the open channel field in the plot. The biplot adopted from Spencer et al. (1998) focuses on the part of the diagram related to new supply environments and attempts to distinguish between the river and the closed basin or the settling environment. The distinction relates primarily to current energies of the depositional setting. For example, it distinguishes between calm settling conditions and fluvial flood or storm episodes (Lario et al., 2000) or between closed and open conditions related to barrier development (Spencer et al., 1998).

For the present study the mean grain size and sorting of the coastal plain, estuary and the offshore sediments of the southern transect were superimposed on the suite statistics proposed by Tanner (1991a,b) and modified by Spencer et al. (1998). The bivariate plots of the mean size versus standard deviation shows that the sediments of the coastal plain core (Core 1) of southern transect (Fig. 4.4a) falls under two categories. From 2 to 9 m the sediments falls under the open channel conditions indicating high energy whereas from 10.9 to 15.5 m, the sediments falls in the closed

basin indicating low energy. The sediments of the estuarine cores show variation in the depositional environment.

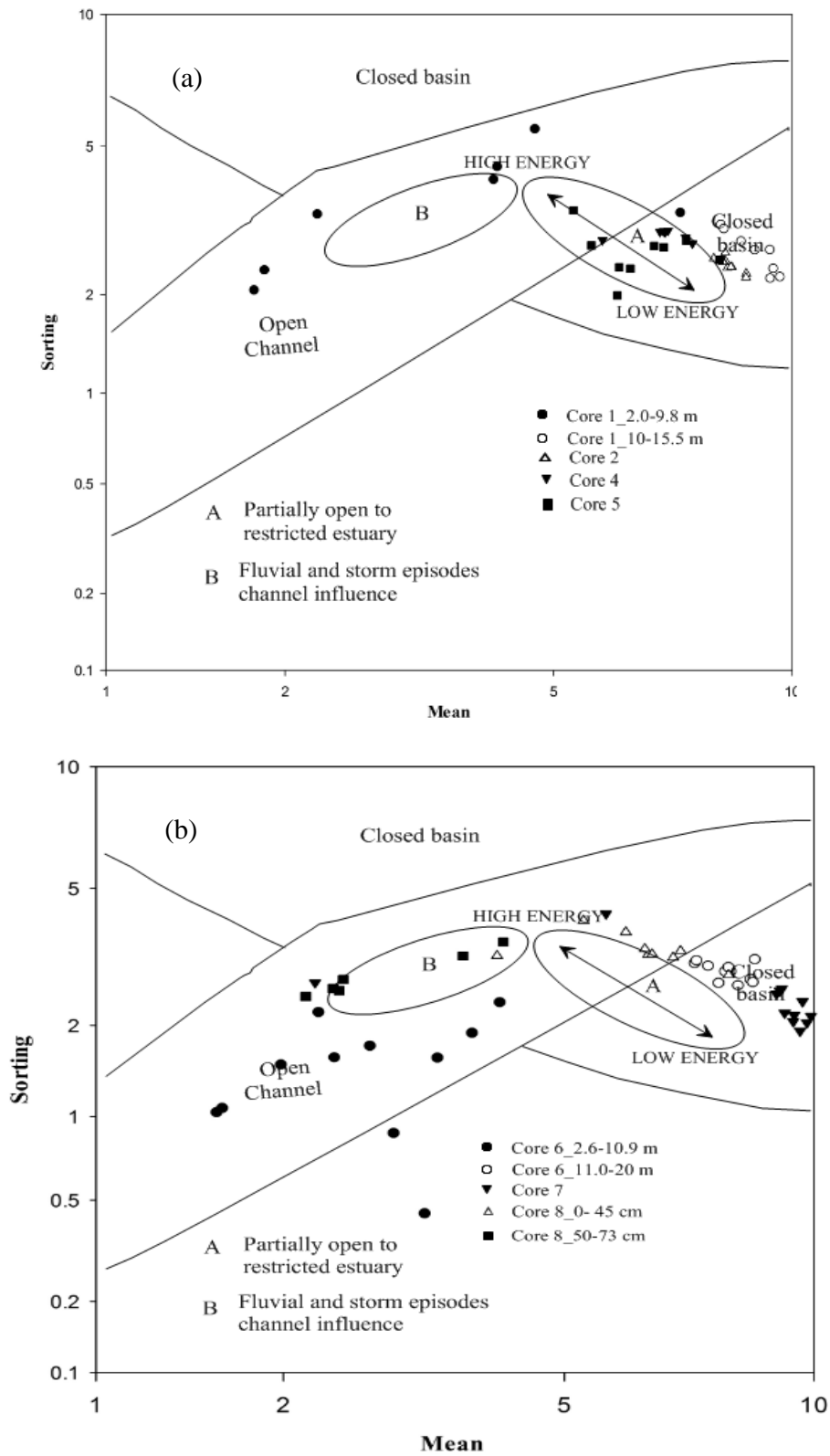


Fig. 4.4 Depositional environment based on Mean vs Sorting (after Tanner, 1991a,b) for the sediment cores of the (a) southern and (b) northern transect

In core 4, all the sediments fall under the partially open to restricted estuary environment whereas the Core 2 sediments fall in the closed basin with some falling in the margin of closed basin and partially open to restricted estuary conditions. The offshore sediments (Core 5) fall in the partially open to restricted estuary.

In the northern transect (Fig. 4.4b), the coastal plain Core 6 is divided into two groups. From 2.6 to 10.9 m the sediments fall under the open channel conditions indicating high energy whereas from 11 to 20 m, the sediments fall under the category of closed basin indicating low energy. The sediments of the lagoon core (Core 7) exhibit a dominance of closed basin condition indicating low energy. In the offshore core (Core 8), the top 0.45 m falls close to the partially open restricted estuary indicating moderate energy whereas from 0.50 to 0.73 m the sediments fall in the fluvial and storm episode conditions.

#### **4.6. Clay Minerals**

The clay mineral composition of the coastal and estuarine sediments is of broad interest because its sensitivity is an indicator of environmental change (Velde, 1995; Stanley et al., 1998). Clay mineral characteristics of the aquatic sediment reflect the prevailing climatic conditions, hydrography, geology and topography of the continental source area (Chamley, 1989). The variation in the clay mineral distribution is therefore a tool for deciphering the sediment sources and transport to the area. The clay mineral composition indicates the intensity of weathering, especially the degree of hydrolysis, at source rock regions which can be used as paleoclimatic indicators (Chamley, 1989).

The dominance of the kaolinite group of minerals followed by gibbsite, illite, chlorite and montmorillonite along the Kerala coast have been reported by many researchers (Rao et al., 1983; Prithviraj and Prakash, 1991).

In the present study, the clay minerals were analysed for the selected cores representing the coastal plains of the southern (Core 1) and the northern (Core 5) transects. In this study the down core clay mineral variation of both cores were studied for intensities and crystallinity characteristics.

The study of core 1 reveals (Fig 4.5) that the clay mineral intensities of kaolinite and gibbsite from 2 to 7 m, show low peak. From 7 to 9 m where the sediments are composed of silty sand as discussed in the previous section, the kaolinite, gibbsite peaks are feeble. From 9 to 10.8 m where the sediment are composed of hard clay, the kaolinite and gibbsite exhibit sharp peaks overlapping each other. This overlapping peak of kaolinite and gibbsite is drastically reduced to trivial content of these minerals at 11 m depth where black peat is encountered. From 11 to 15.5 m the peak for kaolinite and gibbsites are broader and slightly increased to moderate level.

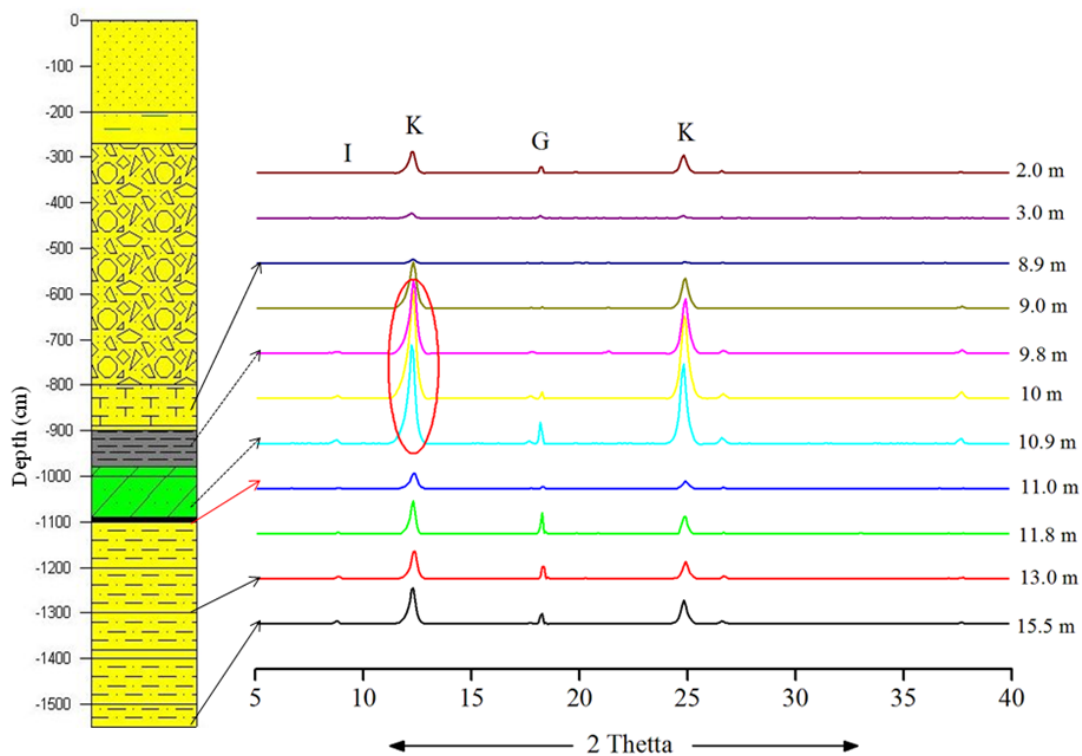


Fig. 4.5 Showing down core variation of X- ray diffraction pattern of clay minerals (K- Kaolinite, I- Illite, and G- Gibbsite) in the coastal plain Core 1 of southern transect

In the northern transect, clay mineral intensities for the coastal plain (Core 6) is shown in figure 4.6. The top 4 m no clay mineral peak is noted since the sediment litholog indicates the dominance of very fine sand except at the depth of 4.2 m where the kaolinite and gibbsite shows sharp peak with feeble peak of chlorite and illite. From 10 to 14 m depth, the peak of kaolinite and gibbsite shows moderate trend where the sediment types are of silty clay. Further down from 14 to 20 m kaolinite



peak exhibit sharp peak indicating well developed crystalline nature. Very feeble peaks of illite and gibbsite are also observed.

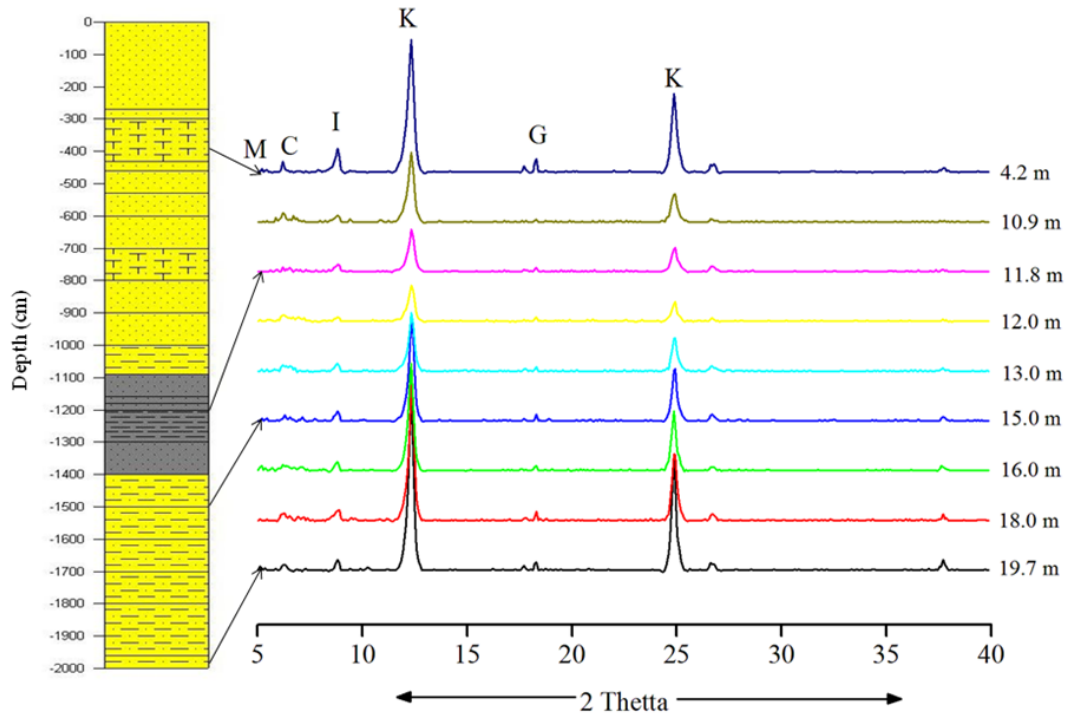


Fig. 4.6 Showing down core variation of X- ray diffraction pattern of clay minerals (K- Kaolinite, I- Illite, G- Gibbsite, and C- Chlorite) in the coastal plain Core 6 of northern transect

#### 4.7. Radiocarbon Dating

The results of  $^{14}\text{C}$  dating analysed from the study area are given in Table 4.10 and the published dates surrounding the study region are presented in Table 4.11.

Table 4.10 Radiocarbon dating results in the present study

Sl No.	Location	Transect	Sample code	Depth (m)	Dating material	Age Yrs BP
1	Coastal Plain			11	Peat/lignite	24670±1860
2	Coastal Plain		Core 1	11.7	Black clay	> 40000
3	Coastal Plain	Southern Transect		15.0-15.5	Black clay	42115 ± 180
5	Ashtamudi Estuary		Core 2	1.0-1.08	Sediment	940 ±180
6	Coastal Plain	Northern Transect	Core 6	11.6 m	Sediment	21340 ±2260

Table 4.11 Published  $^{14}\text{C}$  dates from the coastal sediments of the Kollam and Kayamkulam region

SL No.	Location	Sample Type	Depth (m)	Radiocarbon Dating (Age)	References
1	Munrothuruth	Sediment	11	4350± 90	Padmalal et al. 2011
2	Puthenthuruthu	Sediment	12.5	6117± 101	Padmalal et al. 2011
3		Sediment	21	9376± 140	Padmalal et al. 2011
4	Pangod	Sediment	31	12504± 148	Padmalal et al. 2011
5		Wood	3	5260 ± 120	Nair et al. 2009
6		Wood	5	7490 ± 90	Nair et al. 2009
7		Sediment	5	7480 ± 80	Nair et al. 2009
8		Sediment	6	7550 ± 160	Nair et al. 2009
9	West Kallada	Sediment	10.5	3880 ± 80	Nair et al. 2009
10		Sediment	15.9	4050 ± 80	Nair et al. 2009
11		Sediment	23.5	6250 ± 110	Nair et al. 2009
12	Ashtamudi surface	Lime shell	-	1330 ± 100	Rajenderan et al. 1989
13	Kadapuzha	Sediment	11	6518±119	Padmalal et al. 2013
14		Sediment	16	8269±44	Padmalal et al. 2013
15	Thevalkara	Sediment	10-12	41788 ±574	Padmalal et al. 2013
16	Parayakadavu	Shell	6.5	4610±100	Padmalal et al. 2013
17	Ayiramthengu	Shell	5	2580± 110	Padmalal et al. 2013
18		Sediment	20	40000	Padmalal et al. 2013
19	Ramapuram	Sediment	3	2460±120	Nair et al. 2006
20	Ramapuram	Shell	7.6	39370±1000	Nair et al. 2006
21	Ramapuram	Wood	-	2460 ± 120	Jayalakshmi et al. 2004
22	Muthukulam (Kayamkulam west )	Wood	1.27-1.35	3362 ± 114	Jayalakshmi et al. 2004
23	Muthukulam	Wood	2.07-2.12	6276 ± 112	Jayalakshmi et al. 2004
24	Muthukulam	Shell	3.0-3.10	7176 ± 82	Jayalakshmi et al. 2004

From the Table 4.10, out of the 5 dates, 4 dates are from the southern transect representing the coastal plain and the Ashtamudi Estuary, whereas 1 date represents the coastal plain of the northern transect. Based on the present study the age ranges from 42,115 Yrs BP to 940 Yrs BP indicating the evolution from late Pleistocene to Recent. For the southern transect, selected samples consisting of organic rich sediments and peat for the coastal plain (Core 1) were dated and the results are presented in Table 4.10. The results reveal that the black clay sediments rich in organic matter (14%) at the depth ranging from 15.0 to 11.7 m have an age of 42,115 Yrs BP to 40,000 Yrs BP. The peat sample with an organic matter content of 47% at the depth of 11 m, which is above the black clay rich sediments shows an age of 24,670 Yrs BP. The inferred dates from study indicate the late Pleistocene. The core representing the Ashtamudi Estuary (Core 2) yielded an age of 940 Yrs BP from the core retrieved of 1.0 to 1.08 m indicating recent sediments. In the northern transect

the coastal plain (core 6) of the present study (Table 4.10) at the depth of 11.6 m yields an age of 21,340 Yrs BP indicating the late Pleistocene.

#### **4.8. Discussion**

The study of Quaternary sediments is important in any coastal region since they contain the record of sea level changes, palaeoclimate and tectonics, which have given rise to the present landscape (Nair and Padmalal, 2004). The occurrence of Quaternary formations at various elevations along the Kerala coast speaks of recent uplift. Incidence of a chain of coast-parallel estuaries/lagoons with rivers debouching into them and separated from the sea by spits/bars along the central Kerala coast provides evidence of a prograding coastline (Narayana and Priju, 2004). Many coastal lowland environments can therefore be expected to contain a relatively abundant, well-preserved sedimentary archive that makes high-resolution reconstructions of a regional depositional history in response to the Pleistocene sea level changes (Bowen, 1978; Lowe and Walker, 1997).

In the study area the results of the sediment litholog of the southern transect indicates several depositional as well as erosion episodes. The top 7 m of the sediment column encompasses sand of medium to fine size grade of angular nature. Nair and Padmalal (2004) have reported a Holocene sediment thickness of 8 m in this region. The Holocene sediment is characterised by soft compact clay rich in organic material. But the present study reveals that these Holocene sediments have been replaced by almost equal thickness of modern sediments containing least organic matter content brought by the Kallada River. The fluvial signature has been deciphered through SEM studies and their details are given in Chapter 5. Overpeck et al. (1996) concluded that the monsoon strength increased suddenly in two steps, 13,000–12,500 <sup>14</sup>C Yrs BP and 10,000–9,500 <sup>14</sup>C Yrs BP.

Most climatic proxies suggest that the stronger monsoon in the early Holocene was associated with high lake levels; increased flow discharges floods and scouring (Kale et al., 2004). Moreover the Kallada River which is existing as major depocentre of the Ashtamudi Estuary brought heavy discharge consequent to the stronger monsoon during the mid-Holocene resulting in the incised valley formation leading to the progradation towards the coast. Below 7 to 9 m, the sediments are of medium to

coarse sand with occasional gravel and brachiopods shells indicating a change in the deposition scenario of shallow marine to lagoonal and swamp/marshy environment. Nair and Padmalal (2004) reported similar observations. From 9.0 to 10.8 m the sediment is enriched with clayey type sediments which are hard and greyish to whitish in colour probably indicating the exposure and desiccation during the period of non-deposition (Allen, 1970). Yim et al. (2008) characterised these hard desiccated clay based on their physical properties like stiffness, mottled appearance, lower moisture content and absence of shell fragments. This was also observed in the litho-unit. These desiccated clays could have formed when the sea level was lower exposing the lake bed during the Last Glacial Maximum (LGM). Narayana et al. (2001) also reported paleo-desiccated clay in the core section collected from the Vembanad Estuary during the low sea level stands prior to burial by a Holocene marine transgression event. The clay mineral studies on this section exhibit sharp crystalline peak of kaolinite deposited in quietest environment as confirmed by the Pejrup classification of hydrodynamic conditions. Moreover, an arid climate existed during 22,000 to 18,000 Yrs BP in the Kerala region due to the weak southwest airflow. A drastic reduction of the summer monsoonal rainfall and reduced run off from the Western Ghats Rivers (Van Campo, 1986) has enhanced the hardness of the clay. Further, Meher-Homji and Gupta (1999) based on pollen studies from offshore location of Kerala revealed decline of mangrove forest during the period between 22,000-18,000 Yrs BP along Kerala, which indicates enhanced dry phase. Rajendran (1979) based on the littoral deposits of Kerala reported aridity during low sea level phase at the end of Pleistocene. Yim et al. (2008) have reported the formation of three stiff and mottled palaeo-desiccated crusts by sub-aerial exposure during the last glacial period, the second last glacial period and third last glacial period in the two shallow bays in Hong Kong, China.

A thickness of 0.20 m peat was observed from 10.8 to 11m core section indicating an abrupt change in the sedimentary environment. The peat sample containing an organic matter of 47% was dated in the radiocarbon laboratory at BSIP Lucknow and has inferred an age of  $24,670 \pm 1860$  Yrs BP. This indicates the withdrawal of marine transgression during late Pleistocene period. During the withdrawal, the sediment bed was exposed to a still stand condition leading to the decomposition of vegetative material. Moreover, the kaolinite shows poor peak

intensity further suggesting the absence of clay, related to intense plant productivity and luxuriant growth of forests in the immediate vicinity (Mascarenhas et al., 1993). The peat beds, which form Quaternary units in Kerala, indicate their formation from submerged coastal forests i.e. initial subsidence of the coast and consequent transgression of the sea (Powar et al., 1983; Rajendran et al., 1989). According to Woodroffe (1983), peat formation is normally restricted to sheltered areas where low energy conditions prevail, gently sloping intertidal areas, substrates favourable for plant growth and a relatively stable sea level. Shajan (1998) reported an age of 25,000 to 30,000 Yrs BP from the peat samples at depths of 18 m and 24 m just below the secondary lateritic horizon in the central Kerala coast.

From 11 to 15.5 m the sediments are composed of black clay with high organic content and interblended with vegetative matter. Moreover, the radiocarbon dating estimated an age ranging from 42,000 to 40,000 Yrs BP, which indicates the first marine transgression event surrounding the Ashtamudi Estuary during the late Pleistocene period. This marine transgression event led to the submergence of mangroves and other vegetation forest which might have existed along this region during 40,000 Yrs BP. Narayana et al. (2002) reported that the central Kerala coast i.e. Vembanad region was covered with intensive mangroves and other forest vegetation even at 40,000 Yrs BP and was inundated during higher sea level stands.

Since the estuary are the transition zones between rivers and the sea, the nature of bottom sediment depend upon the hinterland geology and river runoff. The fresh water inflow from the rivers and the tidal inflow near the estuarine mouth largely determine the quantity of sediment deposition in the estuary. The textural characteristics based on surficial sediments of the Ashtamudi Estuary indicate the distribution of silt, clayey silt and sand (Black and Baba, 2001). The present study is related to the sub-surficial sediments of the three cores. Out of the three cores, Core 3 is entirely composed of clay where as Core 2 sediments are dominated by clayey silt to silty clay and Core 4 composed of sand-silt-clay to clayey silt. The ternary plots proposed by Pejrup and suite statistics proposed by Tanner for all the three cores confirms that the sediments were deposited under closed basin indicating low energy environment

In the northern coastal plain core (Core 6), which comprises of 20 m length, the top 10 m sediments comprise of very fine sand associated with minute broken shells deposited under open channel with violent environment indicating beach-littoral environment. Normally the sediments of the beach environment shows well rounded nature. This was studied through SEM analysis and discussed in Chapter 5. Nair et al. (2006) reported that the Ramapuram borehole which is adjacent to the Core 6 consist of medium to fine sand of Holocene age at a depth of 7 m. Similar observations were also noted in the study core which elucidates that sediments above 10 m depth underwent marine transgression event during Holocene period. From 10 to 14 m depth, the sediment rich in sand are completely changed to mud interblended with pelecypods and gastropods shells showing stiffness and maximum occurrence of calcium carbonate content (38%) indicating a lagoonal littoral environment. High calcium carbonate content also indicates the cooling period related to glacial event. Moreover the sand silt clay ratios of Pejrup diagram and Tanner plot for energy condition confirm that the sediments of this litho-unit were deposited under the calmness of low energy environment. The radiocarbon dating analysed at the depth of 11.8 m reveals an age of 21,340 Yrs BP. The dates reveal that the age is close to arid phase and the beginning of Last Glacial Maximum leading to the stiffness of sediment indicating its deposition during the late Pleistocene. From 14 to 20 m the sequence of the sediments that are composed of silty clay with 3% organic content show similiar trend as that of the Core 1 except in the lagoonal deposit below 15 m. The sediment associated with presence of broken shells confirms its deposition under the beach lagoonal environment.

In the offshore region, the sediments of the southern core (Core 5) were deposited under moderate energy environment where as the northern core (Core 8) sediments were deposited under violent environment. Moreover down the core the sediment are composed of sand with less percentage of organic content indicating relict beach deposits.

#### **4.9. Summary**

The study deals with the textural analysis of the core samples collected from various predefined locations of the study area. The result reveals that the Ashtamudi Estuary is composed of silty clay to clayey type of sediments whereas offshore cores

are carpeted with silty clay to relict sand. Investigation of the source of sediments deposited in the coastal plain located on either side of the estuary indicates the dominance of terrigenous to marine origin in the southern region whereas it is predominantly of marine origin towards the north. Further the hydrodynamic conditions as well as the depositional environment of the sediment cores are elucidated based on statistical parameters that decipher the deposition pattern at various locations viz., coastal plain (open to closed basin), Ashtamudi Estuary (partially open to restricted estuary to closed basin) and offshore (open channel). From the results of radiocarbon dating, the coastal region surrounding the Ashtamudi Estuary underwent the first marine transgression event during 40,000 yrs BP which resulted in the submergence of mangroves as well as vegetative material as present in the sediments and this lasted up to 24,000 yrs BP as indicated by the peat deposit.

# CHAPTER 5

## MICROMORPHOLOGICAL CHARACTERISTICS OF QUARTZ GRAINS – IMPLICATIONS ON DEPOSITIONAL ENVIRONMENT

### 5.1. Introduction

Quartz grains are the most commonly occurring particles in the clastic sediments due to high stability and absence of cleavage planes. Because of the overall abundance of quartz grains in siliciclastic successions, petrographers, sedimentologists and soil scientists have long tried to find properties on the surface of quartz that may be related or linked to transport characteristics. With the use of Scanning Electron Microscopy (SEM) to earth sciences applications during the 1960's, the properties of the surface of quartz grains became a focus for researchers, especially for determining the transportation and deposition of sediments. The first atlas on the morphological features of quartz grain (Krinsley and Doornkamp, 1973) included a wide range of surface features related to transport and depositional history. Later, the analysis of detrital grain surfaces became a widely used tool in sedimentology, physical geography, and soil science. Many surface features on detrital sediment grains are considered to be characteristic of the fluid dynamics in distinct sedimentary environments (*see for e.g.*, Krinsley and Doornkamp, 1973; Mahaney, 2002), though different environments can include almost identical mechanical (i.e., grinding, sliding, or cracking) and chemical (i.e., dissolution or precipitation) processes.

The study of quartz grain microtextures (>200  $\mu\text{m}$ ) with SEM technique has been shown to be a valid method in sedimentary petrology for interpreting sedimentary environments and transport mechanisms (Krinsley and McCoy, 1977; Krinsley and Marshall, 1987). The microtextures provide vital information regarding the various processes acting on the grains during transportation and/or after deposition (Doornkamp and Krinsley, 1971; Mahaney, 1998). The criteria for distinguishing mechanical and chemical features and their implications have been well-established (*see*, Rahman and Ahmed, 1996). Thus, the microtextural study on quartz grains is



considered as a powerful tool in the identification of provenance, processes of transport and diagenetic history of the detrital sediments (Krinsley et al., 1976; Madhavaraju et al., 2006). Surface textures of clastic particles are also repositories of information about the physical and chemical processes to which the particles have been subjected (Krinsley and Doornkamp, 1973). A grain of quartz sand taken from the beach bears characteristic texturalsignatures on its surface, which strongly reflects the wave action. This signature is quite distinct from those produced by the action of rivers, wind or glaciers.

Surface textures can be grouped into two categories. One class deals with the dullness or polish of the grain and the other concerns the marking on the grain surface. Many investigators opined that a systematic study of the above two classes can provide an insight into the history of transportation and deposition of clastic particles (Krinsley and Doornkamp, 1973; Baker, 1976; Marshall, 1987).

## **5.2. Microtextural Characteristics**

In order to understand the transport mechanism and post depositional history of sediments of the study area, SEM analyses were carried on the quartz grains selected from sediment cores representing the coastal plain, estuary/lagoon and offshore region of the southern and northern transect (see also Fig. 3.1 in Chapter 3). The detailed microtextural characteristics of the sand grains for the transect is enumerated below following well established guidelines used in literatures applied for SEM features as cited in Chapter 3.

### **5.2.1. Southern Transect**

The microtextural analysis representing the coastal plain (Core 1), Ashtamudi Estuary (Core 2 and Core 3) and offshore core (Core 5) were used for the southern transect. The SEM features are envisaged below.

#### **5.2.1.1. Coastal Plain**

The detailed description of litho-units and textural variation of samples representing the coastal plains are presented in Chapter 4. The SEM analysis have been carried out on the core samples representing southern transect based on lithological variations by selecting the quartz grains from selected depth (3 m, 9 m,

10.9 m, 11.8 m, 12 m, 15.5 m). The surface texture of quartz grains at the depth of 3 m predominantly shows fresh angular features (Fig. 5.1) with series of conchoidal fractures.

At the depth of 9 m, the grains are angular with irregular margins; the edges are sharp and show conchoidal fractures (Figs. 5.2 a & b). The grain exhibits high relief with numerous pits with V-shaped scratches. These are attributed to the fluvial process related to high degree of turbulence in the flow, causing collision and compression of grains against each other (*see*, Krinsley and Doornkamp, 1973; Joshi, 2009).

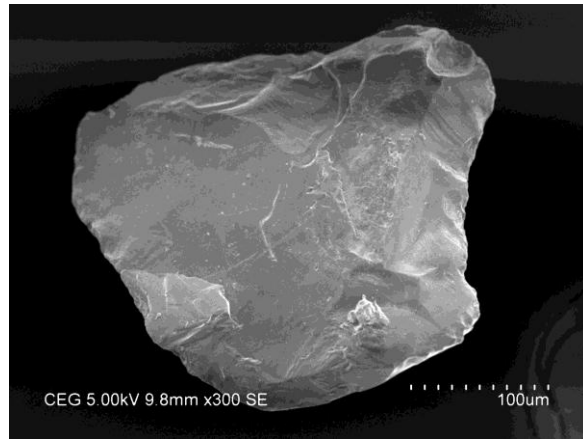


*Fig. 5.1 SEM photographs of the quartz grains at the depth of 3.0 m showing mechanical features*

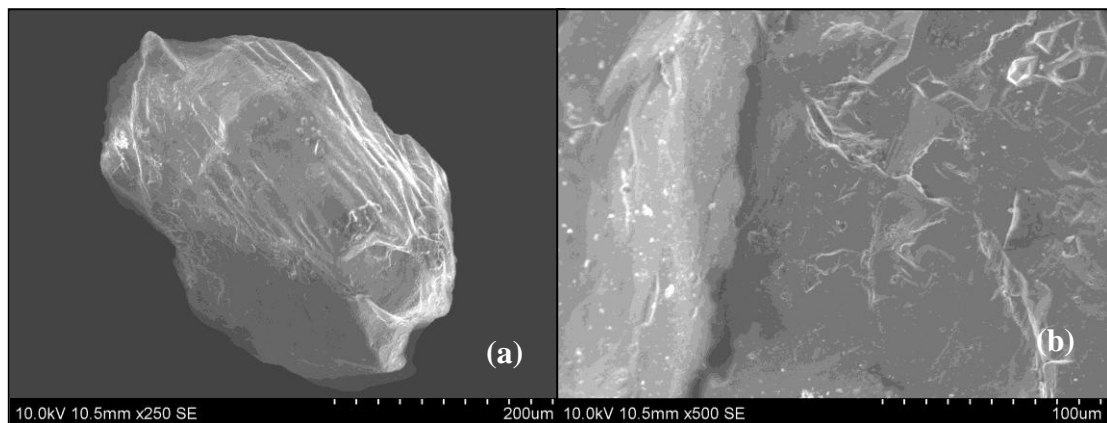


*Fig. 5.2 SEM photographs of the quartz grains at the depth of 9.0 m (a) showing large conchoidal fracture with high relief and angular in outline (b) V-etch pits*

A large number of quartz grains bear the distinct abrasion marks (Fig. 5.2a), which are frequently noticed at the edge of the grains rather than the smooth surface relating to fluvial transport (Krinsley and Takahashi, 1962) and suggestive of moderately long distance of transport in an aqueous medium having a high energy condition (Krinsley and Doornkamp, 1973). However, this type of features may also be formed during transport of the host grains in a turbulent river (Ly, 1978) or at the

beach (Blackwelder and Pilkey, 1972). Locally derived quartz grains tend to exhibit conchoidal fractures and flat surfaces (Krinsley and Doornkamp, 1973; Krinsley and Smalley, 1973). Thus, the mechanical features found on the quartz grains are attributed prominently after its deposition. Later stages of chemical etching have also been found on few grains indicated by an oriented V-etch pits (Fig. 5.2b), with less occurrence of isosceles triangles (Margolis, 1968).

At a depth of 10.9 m, the angularity of quartz grain is changed to sub-rounded (Fig. 5.3a) with smooth edges in outline indicating considerable amount of recycled sediments. During the mechanical process the grain is fractured and V-shaped pits, scratches, curved grooves and linear steps on the fractured surface were developed indicating mechanical abrasion during the deposition in sub-aqueous media (Krinsley and Doornkamp, 1973). However, these mechanical features were later modified by solution-features leading to the formation of linear shaped, branching solution type (Fig. 5.3b) originated and enlarged as primary fracture as well as centipede sub-type feature (Fig. 5.3b), which occurs in groups and are associated with oriented triangular facets.

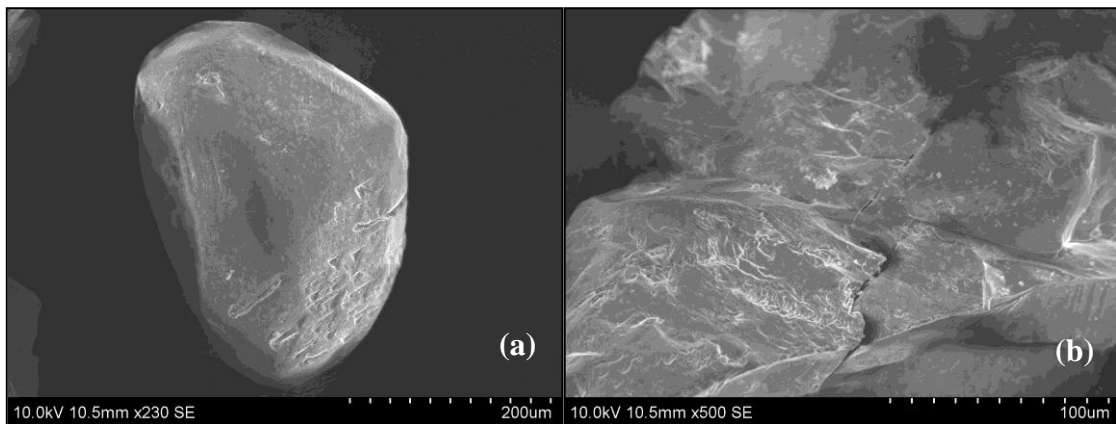


*Fig. 5.3 SEM photographs of the quartz grains at the depth of 10.9 m (a) showing sub-rounded in outline (b) solution features in the form of branching solution and centipede types*

The precipitation of silica in the surface depressions, results in a shallower feature followed with oriented V-shaped etch pits orienting in one direction resembling isosceles in nature indicative of chemical etching (Le Ribault, 1975). The type of surface features produced on the grains depends on the nature of the etching media, size and shape of the grains and the crystal habit (Subramanian, 1975). Conchoidal fracture is common but has smoothed due to silica precipitation as well

as long residence time. The edges are rounded in outline with moderate relief. Due to long period of deposition in an aqueous condition, the impacts pits have smoothed leading to the formation of solution pits. A few solution crevasses are observed further strengthening the chemical activity in the grains. Traces of crescentic grooves (Fig. 5.3b) of mechanical origin is plastered by silica precipitation indicating silica solution followed by oriented V-etch pits indicating chemical etching (Margolis and Krinsley, 1971).

At the depth of 11.8 m the surface texture of the quartz grains reveals a total change in the deposition scenario. The shape as well as mechanical abrasion features of the sub-rounded quartz grains, which are basically of an aqueous transport is totally modified and forms a corroded shape (Fig. 5.4a) with low relief indicating dissolution features indicating chemical etching which is likely to occur when pH is suddenly increased by the contact of alkali solutions (Hurst, 1981) under the influence of marine incursion. Previous work has shown that quartz dissolution often occurs preferentially along certain crystallographic directions probably because of dislocations or defects are more soluble due to strain and high free-surface energy (Margolis, 1968; Hurst, 1981). The fractured plates which are formed due to mechanical action are weathered and chemically etched (Fig. 5.4b) indicating prolonged residence of time (Krinsley and McCoy, 1977).

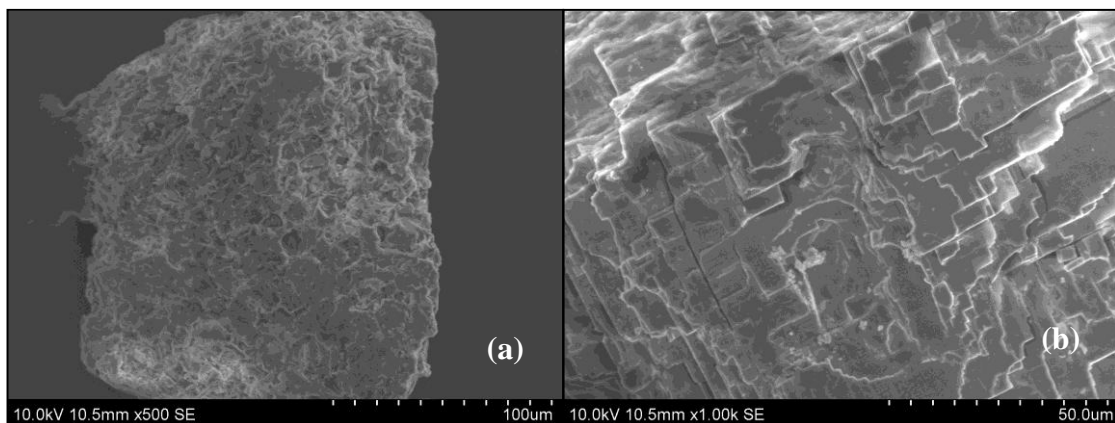


*Fig. 5.4 SEM photographs of the quartz grains at the depth of 11.8 m showing (a) totally distorted shape with sub-rounded in outline (b) with chemically etched fractured plates*

At 12 m depth, the majority of the grains exhibit silica precipitation masking the mechanical features exhibiting a low relief (Fig. 5.5a). The fine anatomising

pattern or deep solution surface (Fig. 5.5b) is observed on the flat surface, which is considered to be formed as a result of etching by alkaline solutions, and is indicative of occasional sub-areal exposure and/or slight diagenesis (*for e.g.*, Margolis and Krinsley, 1971). Small traces of solution pits are also observed on the edges of the grain indicating chemical etching (Margolis, 1968).

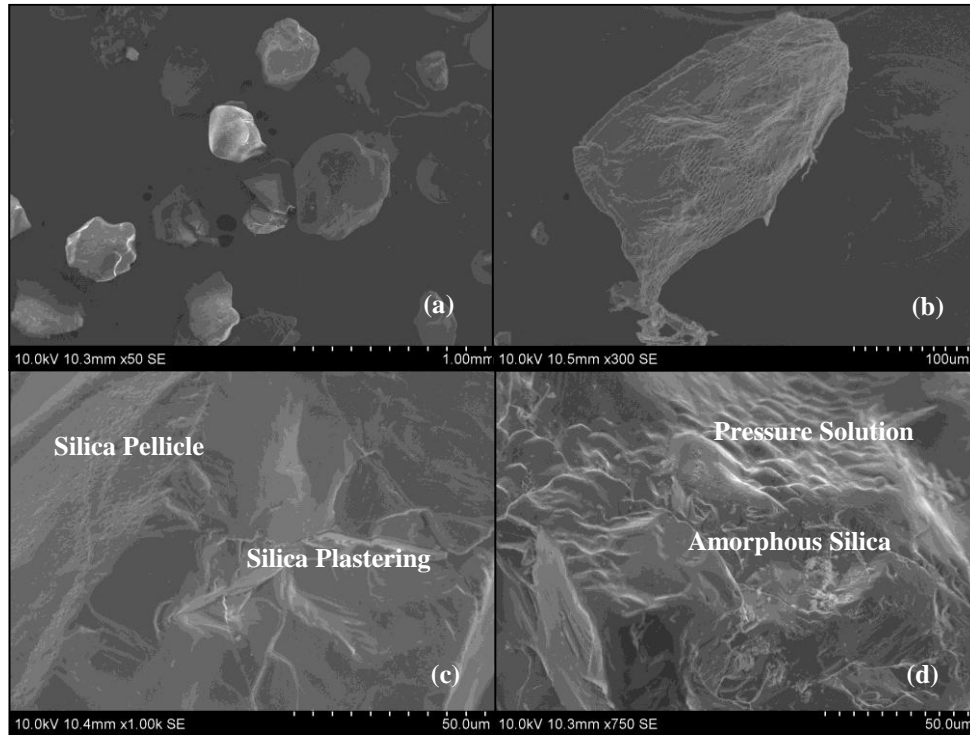


*Fig. 5.5 SEM photographs of the quartz grains at the depth of 12 m showing (a) sub rounded in outline dominating chemical features such as (b) anatomising pattern, silica pellicle, silica precipitation in conchoidal pattern leading to silica plastering (c) and pressure solution feature (d) indicating diagenesis*

A coalescence of tiny globules is observed masking the grain upper surface (Fig. 5.5c) indicating silica pellicle feature, which is formed due to continuous precipitation of silica solution. Silica precipitation in natural system is largely controlled by the pH condition; the lower the value of pH, increases the higher precipitation of silica (Hurst, 1981). Their development on the studied grain surface took place at the sheltered hollows, at the bottom, at the entire and rarely on the broken surface. The nature and distribution of the precipitated silica take place after or during transport, where silica saturated acidic ( $\text{pH} < 7$ ) condition was prevailing. On the other side of silica pellicle feature, the mechanical feature such as conchoidal fractures, fracture plates, straight grooves have been smoothed (Fig. 5.5c) due to silica precipitation leading to the formation of silica plastering indicating diagenetic

process (Krinsley and Donahue, 1968). The deep sub-circular resembling rounded hillocks like features (Fig. 5.5c) observed on the grains have been identified as pressure solutions (*see*, Srivastava, 1989), which is an indication of diagenetic process (Krinsley and Doornkamp, 1973) as well as linked to overburden (Srivastava, 1989). Pressure solution is another mechanism that causes dissolution of silicate grains and is based on the principle that silica solubility increases as pressure is applied to silicate grains (Dewers and Ortoleva, 1990). Isolated patches of amorphous silica (Fig. 5.5c), precipitated from seawater, formed on flat conchoidal surfaces (Krinsley and Margolis, 1969) associated with pressure solution. Closely spaced chemical etch pits form on sand grains by abrasion solution or during diagenesis, when grains are exposed to high pH solution (Margolis and Krinsley, 1971). The grains generally are covered with, what is either amorphous silica or quartz precipitated from sea water; these precipitates forms knobby or bumpy projections on flat, conchoidal surfaces, but follows the upturned plate lithology on irregular surfaces. Commonly, solution and precipitation are found together, perhaps indicating more than one period of chemical action.

At the depth of 15.5 m, the grain is sub-rounded, low relief with solution pits. The grains exhibits dissolution etching (Fig. 5.6a), which is considered as extreme form of weathering and is located on the old fractured surfaces of quartz, which suggests that its formation is assisted by the fractured, which has weakened and later weathered (Mahaney and Kalm, 1995). Long residence time might have lead to the etching on the incipient quartz growth. The overall appearance looks like honey comb structure (Fig. 5.6b).

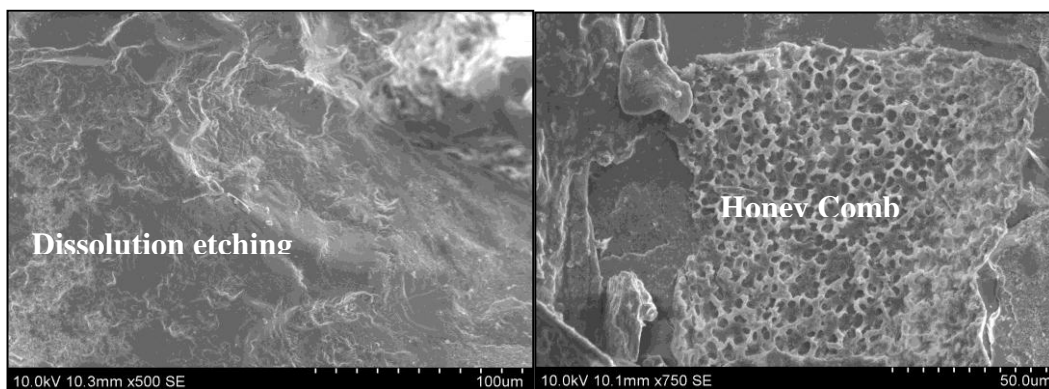


*Fig. 5.6 SEM photographs of the quartz grains at the depth of 15.5 m showing chemical features in the form of (a) dissolution etching and (b) honey comb structure indicating prolong diagenesis*

### 5.2.1.2. Estuary

Two representative samples of Core 2 and Core 3 from Ashtamudi Estuary were used to interpret the various microtexture features.

The Core 2 is retrieved with a length of 1.08 m. Quartz grains at 1 m is examined for SEM analysis. It is interesting to note that majority of the quartz grains are sub-rounded with edges smooth in outline. The majority of the grains show conchoidal fracture (Fig. 5.7a) with range of medium to high as well as series of fracture plates (Fig. 5.7a) indicating mechanical collision (Kransley and Doornkamp, 1973). Breakage block with irregular depression and upon the breakage surface, impact pits (Fig. 5.7a) of various sizes is impounded on it indicating mechanical abrasion features because of high turbulent action (Ly, 1978). Coalescing impact pits (Fig. 5.7a) and curved grooves (Fig. 5.7a) are also noticed. Impregnation of these mechanical features such as impact pits, coalescing pits, oriented fracture depicts that these features were generated by grain to grain and grain to substrate collisions (Manker and Ponder, 1978) indicating transportation of sediments in high energy sub-aqueous medium under fluvial transport (Manker and Ponder, 1978). However, later during post depositional scenario silica solution has impounded on the pre-existing mechanical feature of the grain surface, possibly due to marine incursion (Fig. 5.7b). An isosceles triangle of etch pit is observed indicating chemical etching but it is not fully developed in some places.

Based on these features such as conchoidal fracture, oriented fractures, impact pits it is evident that the quartz grain was first deposited by mechanical alteration under fluvial environment (*see for e.g.*, Ly, 1978). Moreover, Kallada River, which is the major contributor for the Ashtamudi estuary (Prakash et al., 2001) further confirms its original source as fluvial origin. Later, during the post depositional scenario, the grain have undergone chemical etching leading to the formation of etch pits in the form of isosceles triangle, solution pits, silica solution. In some places the triangle pits are not fully pronounced because of short duration of residence time. Hence it is concluded that the quartz grains represents the mechanical origin followed by chemical alteration although not fully pronounced.

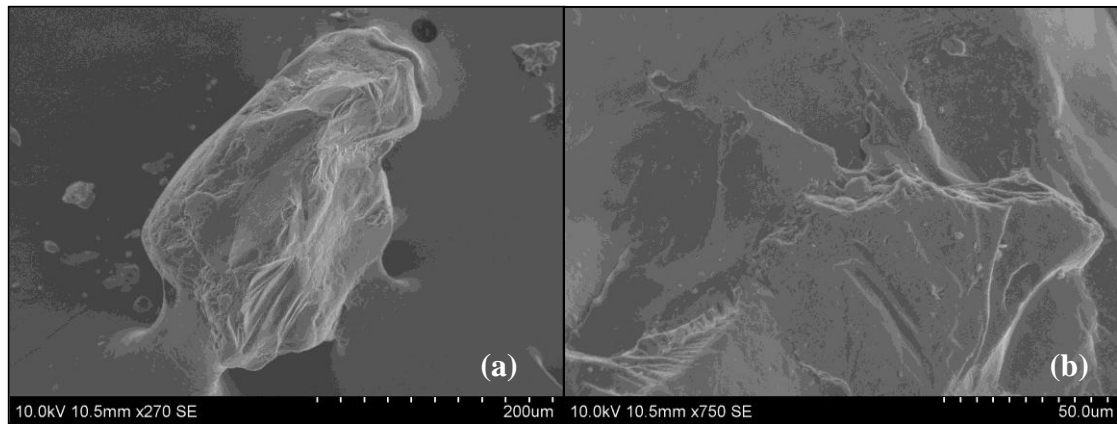


*Fig. 5.7 SEM photographs of the quartz grains of Core 2 showing (a) large conchoidal fracture (b) silica solution*

The quartz grains (0.80 m) of Core 3 core samples taken for SEM analysis. The quartz grain generally show sub-rounded with prismatic (Fig. 5.8a) shape and high relief. Some of the notable features observed are fractured plates (Fig. 5.8b), medium to large conchoidal fracture indicating transported and deposited in high aqueous turbulent medium. Conchoidal fracture patterns vary from regular dish shapes (uncommon) to irregular elongate fan-like or trough-like depressions. The common parallel step-like fractures that curve around the conchoidal depression are thought to be expressions of planes of weakness (Margolis and Krinsley, 1974).

The presence of conchoidal fractures, accurate steps and other mechanical breakage patterns on quartz and grains has been used as an indicator of a glacial environment of transport in first place (Krinsley and Donahue, 1968; Krinsley and Doornkamp, 1973), However, number of studies have been reported from coastal environments evidently shown the presence of the above mentioned features as an indication of transportation and/or deposition associated with fluvio-marine condition (Fitzpatrick and Summerson, 1971; Setlow and Karpovich, 1972).

During the post depositional process, solution of quartz may occur through the abrasion solution phenomenon of Fournier (1960) in the conchoidal surface. This could supply silica in sufficient quantities to the environment to cause local super saturation and precipitation. This is followed by etch pits in the form of oriented V-shaped, isosceles triangle in pattern indicating chemical etching. Another noticeable feature is the mechanical fracture, which was produced in the previous environment



and is retained (Fig. 5.8c) except for the lower part, which is replaced by silica dissolution. The surface on the both side of the mechanical fracture is plastered by silica solution (Fig. 5.8c). At the upper margin of the mechanical fracture because of silica precipitation the quartz inter growth is produced but in an eroded forms (Fig. 5.8c). When closely magnified surface (Fig. 5.8d) pits and crevasses, with precipitated silica on that weathered surface is noticed.

Based on the surface features, the quartz grains of the Core 3 is interpreted as it was first transported and deposited under high turbulent aqueous medium suggested by the presence of mechanical features such as abundance of fracture plates, conchoidal fracture. Later, during post depositional processes, silica solution, etch pits indicating chemical etching as well as solution pits, crevasses on the weathered surface which clearly indicate that the grains underwent high energy chemical environment (Krinsley and Doornkamp, 1973).

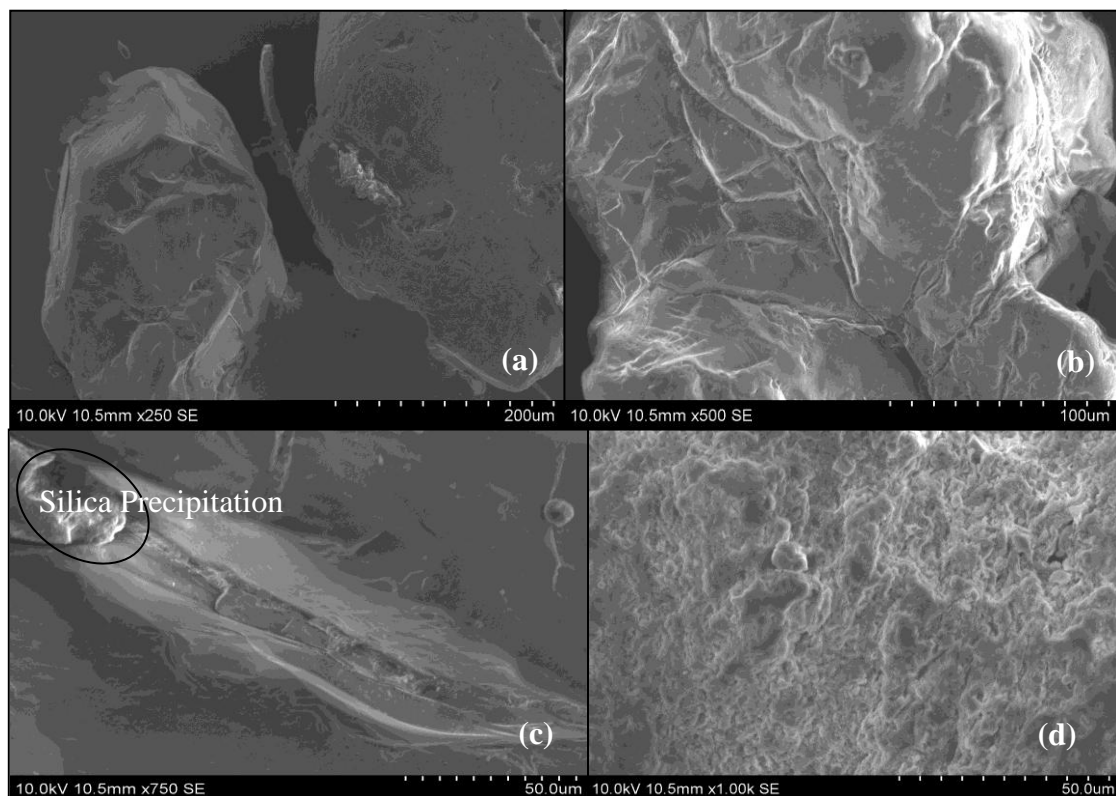


*Fig. 5.8 SEM photographs of the quartz grains of Ashtamudi estuary Core 3 at the depth of 0.80 m showing (a) sub-rounded with prismatic shape (b) series of fracture plates (c) retainment of mechanical plates (d) erosion of silica overgrowth*

### 5.2.1.3. Offshore

The southern shelf representing the Kollam offshore has a core length of 0.88 m retrieved from a depth of 12 m. Quartz grains of 0.80 m taken for SEM analysis. It is observed that the grains are sub-rounded in shape. Grain breakage associated with fracture at regular interval is observed (Fig. 5.9a). Medium to large conchoidal fracture impact pits, mechanical upturned plates, and deep mechanical V-shaped pits are observed, clearly indicating the transportation and deposition of the quartz grain under turbulence subaqueous medium. Sparse polygonal cracks (Fig. 5.9a) are identified on the quartz grains, which may be the result of physical or chemical weathering of salts crystallised on grains when they were at rest (Kransley et al., 1976). During the post depositional scenario, chemically upturned plates are observed in the form of precipitated silica in the deep crack along the grain centre (Fig. 5.9b), when highly magnified (Fig. 5.9c) as well as along the conchoidal fracture surface in the form of step like appearance (Fig. 5.9c). The edges are smoothed by reprecipitation of silica in the form of bouldous projection (Fig. 5.9d) as well as pre-existing mechanical features such as impact pits as well as V-shaped pits, scratches are well preserved.

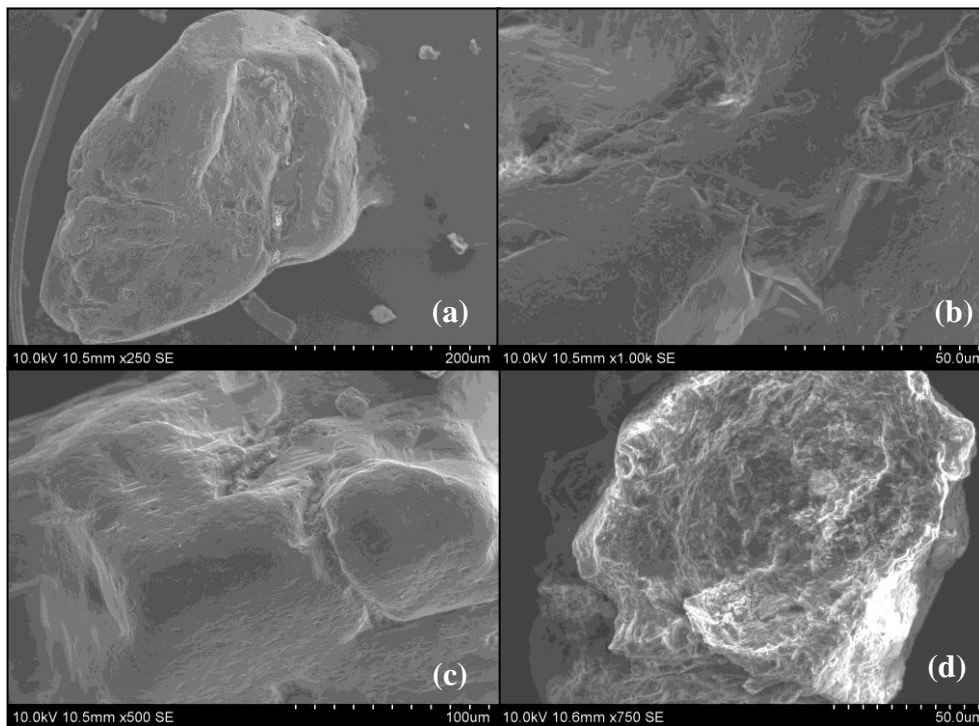


*Fig. 5.9 SEM photographs of the quartz grains of the southern offshore core (a) Grain breakage associated with fracture (b) chemical upturned plates (c) silica solution (d) silica dissolution*

## 5.2.2. Northern transect

For the southern transect, the coastal plain (Core 6) and offshore core (Core 8) were utilised for the microtextural analysis. The SEM features are presented below.

### 5.2.2.1. Coastal plain (Core 6)

SEM analysis were carried out on the sediment cores representing the northern transect, which has a core recovery of 20 m. Based on lithological observation as well as textural analysis, 5 selected samples representing 3 m, 8.9 m, 10.8 m, 11.6 m, 16.7 m and 19.7 m depths were taken for microtextural analyses. The following observations are described below.

At a depth of 3 m, the quartz grains are rounded in shape with high relief. The quartz grains exhibit numerous mechanically V-shaped pits (Fig. 5.10a), which are irregular, differing in shape and size and occur as crescentic or elongate slit like openings oriented in different direction in the order of 3–4 pits per microns squaremeter and are formed as a result of grain to grain collision (Manickam and Barbaroux, 1987). The abundance and size of some of the V-pits are deep indicating the grains are subjected to longer period and higher intensities of sub-aqueous agitation (Manickam and Barbaroux, 1987). Numerous impacts pits (Fig. 5.10a) with small to medium size range and breakage blocks are observed indicating turbulent subaqueous abrasion (Nordstorm and Margolis, 1972). Series of fractured plates (Fig. 5.10a) is inherited indicating fracturing of grains in a high energy transportational system (Higgs, 1979). Inter-clast collision during debris flow can frequently create fracturing of the grains as a genetic feature (Margolis and Kennett, 1971). Chatter marked trails (Fig. 5.10a) are also seen along the edges of the grains indicating mechanical abrasion in a sub-aqueous environment (Gravenor, 1979), which are caused by glancing blow across the face of a grain (Bull, 1980). Medium to large conchoidal fracture associated with deep depression of irregular or parabolic in shape (Fig. 5.10a) is observed along the surface of the grain.

Abundant linear as well as curved scratches (Fig. 5.10b) in different orientation and V's are seen indicating grain-to-grain collisions in an aqueous medium (*e.g.*, Krinsley and Margolis, 1969; Higgs, 1979). The density of the V's appears to be in direct relationship to the number of straight and curved scratches.

Deep grooves with elongate scratches and troughs (Fig. 5.10c) as well as curved such as crescentric in nature (Fig. 5.10c) is also observed reflecting sustained high shear stress (Mahaney and Kalm, 2000; Mahaney, 2002). These grooves are oriented in a preferred direction (Fig. 5.10d), occur with a conchoidal fracture and appear in sets. Linear groove plates occur as a series of linear grooves of different dimensions aligned at an angle to the grain surface.

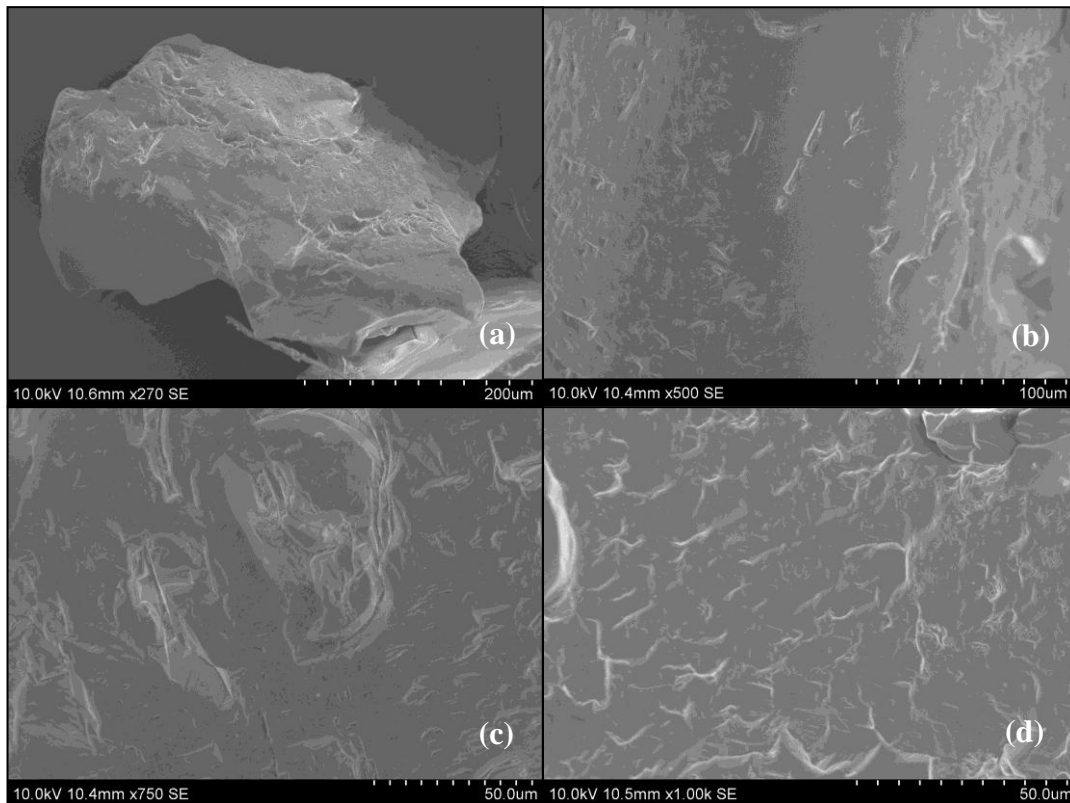


*Fig. 5.10 SEM photographs of the quartz grains at the depth of 3.0 m showing (a) mechanical features such as impact pits, chattermarks (b) crescentric groups with friction marks (c) deep grooves with elongate scratches and troughs (d) grooves oriented in a preferred direction*

The surface texture found include all those modern characteristics of modern beach sand, i.e., V-shaped indentations, straight or slightly curved grooves and blocky conchoidal breakage pattern (Krinsley and Donahue, 1968). The irregular orientations of V-shaped indentations, their average depth, their density per square micron and the groove markings (a creiterion of wave action) further indicate that the specimen is derived from the high energy or surf zone of the littoral environment (Krinsley and Donahue, 1968). Margolis and Kennett (1971) reported V's generally occur on less than 50 % of the grains from the fluvial origin and on more than 50 % of those from

high energy beaches. The main contention for the mechanical abrasion theory is the existence of the chatter mark trails in association with other mechanical features like the V- shaped pits (Bull, 1978), which are observed at this depth. Similar features were observed for ancient beach sands (Hodgson and Scott, 1970), which were also observed in the present study. In the inner-shelf and beach environment of the northern Kerala coast, the chatter marks are very well preserved and are abundant in the quartz grains (Samsuddin, 1991 and present study). Hence the quartz grains undergone more of mechanical breakdown, which is typical of beach and near-shore environment.

At the depth of 8.9 m, the quartz grains are rounded in nature with moderate relief. The grains exhibit numerous impact pits (Fig. 5.11a) associated with conchoidal fracture on the bulbous projection of the edge grains. Straight as well as curved grooves (Fig. 5.11a) with varying length are observed associated with V-shaped mechanical pits on the side of the grooves. Chattermarks is observed on the upper conchoidal surface (Fig. 5.11a) indicating a product of a physical phase followed by a chemical phase (Bull et al., 1980; Orr et al., 1983, 1985). Chattermarks is chemical alteration by dissolution of quartz material. Internal cracks that have not yet reached the surface may become pathways for rapid dissolution when etching processes attack a quartz grain or come into contact with these structural defects due to the fact that the dissolution is a surface-related interaction between solution and quartz (Peterknecht and Tietz, 2011).

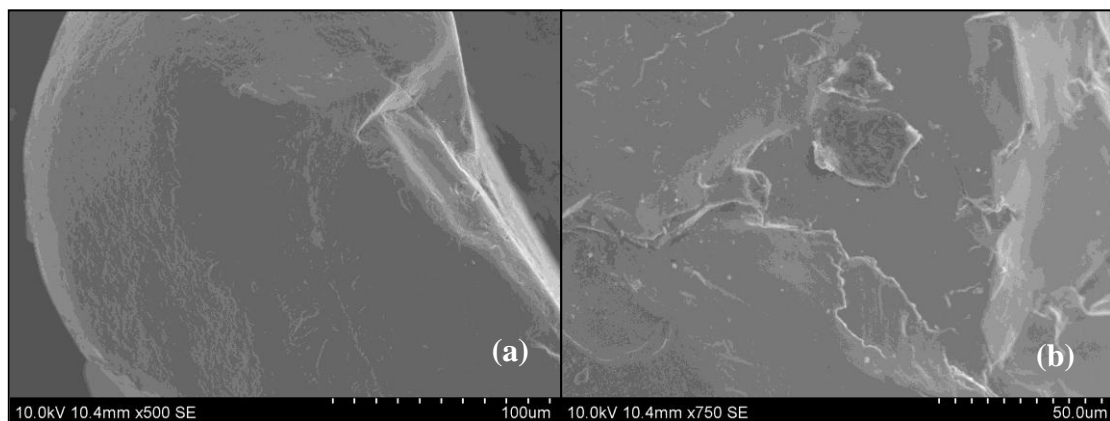


*Fig. 5.11 SEM photographs of the quartz grains at the depth of 8.9 m showing (a) sub-rounded with bulbous projection, linear grooves (b) fracture plates with slight chemical modification*

Curved as well as straight scratches also observed. Compared to the above, mechanical features prevail in these samples but with little chemical action. Series of fractured plate (Fig. 5.11b) are also observed, on which chemical precipitation has undertaken associated with adhering particles (Fig. 5.11b). The above features indicate that at the depth of 8.9 m, beach environment prevailed with slight modification on the features by chemical action.

At the depth of 10.9 m, the shape of the grain exhibits sub-rounded, low relief and corroded (Fig. 5.12a) as well as distorted in nature. The mechanical features produced in the grain have been totally obliterated. Series of solution pits (Fig. 5.12a) highly variable in size, with circular and sub-circular or elongate in shapes (Kransley and Doornkamp, 1973) is impounded on the grain. Conchoidal fractures have been recycled with silica solution (Fig. 5.12a). The effects of solution all over the grain are clearly seen and are rounded in shape. Solution crevasses (Fig. 5.12a) seen on the grains have undergone intense surface disintegration by chemical dissolution.

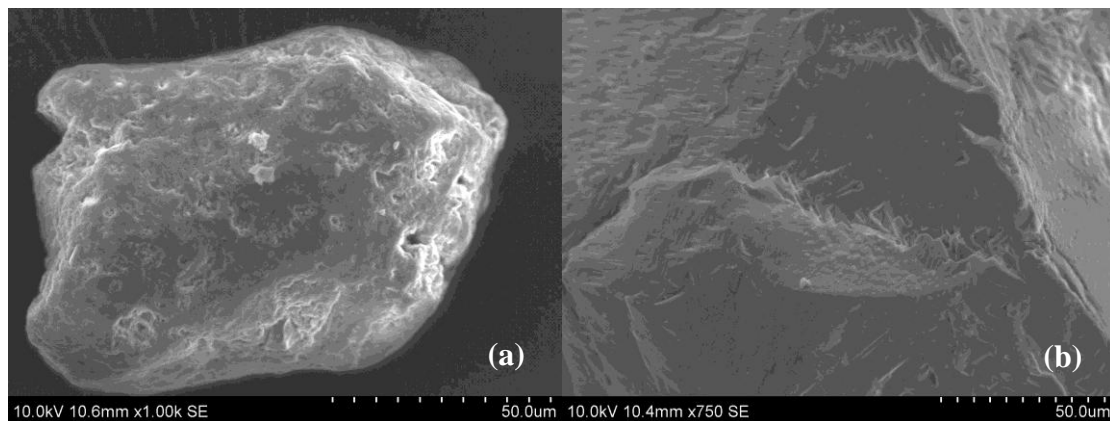


*Fig. 5.12 SEM photographs of the quartz grains at the depth of 10.9 m showing (a) low relief distorted in nature with solution pits and crevasses (b) different oriented etch pits*

Limited quartz dissolution is indicated by solution rounding of primary angularity and by the formation of etch pits. Etch pits ranges from V-shaped deep oriented triangular pits, isosceles triangles, rectangular/rhombohedral pits, anatomising features of ridges and valley and oriented striations pits are observed (Fig. 5.12b). On the other hand, silica pellicle (Fig. 5.12b) masking the mechanical features is also observed. Such differences in etch pit density can be attributed to differences in crystallographic orientation (Hicks, 1985; Gratz et al., 1991) and/or to

variations in micro-weathering environments (Schultz and White, 1999). Conversely, the density and size of etch pits associated with selective weathering of dislocations on the quartz surface increase with decreasing depth (Schultz and White, 1999). The degree of etching also varies according to the residence time (Udayaganesan et al., 2011). These etch features exist more frequently in the marine environments, where the rate of chemical solution exceeds the rate of mechanical abrasion (Margolis, 1968).

A period of solution by sea water in a quietescent environment is indicated by the presence of oriented etch pits superimposed on the earlier mechanical features. The larger triangle is a composite form consisting of a whole series of successively smaller triangles towards the base of the pit. This pit has the form attributed by Krinsley and Donahue (1968) and Margolis (1968) to chemical etching. Margolis (1968) concluded that this etch form is the result of relatively slow chemical solution. Thus, the type of surface produced— V, U, triangular shape, anatomising ridges or oriented patterns depends on the nature of the etching media, size and shape of the grains and the crystal habit (Subramanian, 1975) as well as different crystallography orientations (Hicks, 1985; Brantley et al., 1986; Gratz et al., 1991) and/or to variations in micro-weathering environments (Schultz and White, 1999). Geological time replaces the intensity of etching as an important factor by prolonging the contact between the grains and a solvent, such as sea water. Previous work has shown that quartz dissolution often occurs preferentially along certain crystallographic directions probably because dislocations or defects are more soluble due to strain and high free-surface energy (Margolis, 1968; Hurst, 1981). The most diagenetic features of this environment are the triangular etch depressions where chemical etching along planes of weakness occur extensively. This texture usually indicates a high energy chemical environment. The increasing rate of evaporation and the abundance of salts in the pore water generally increase the pH which affects the quartz grains and influences the development of chemical features (Washmi and Gheith, 2003). Solution crevasses mainly occur in association with solution pits (Krinsley and Doornkamp, 1973).

At the depth of 11.6 m, quartz grains are sub-rounded with intense weathering in the form of cross-hatching network of etch pits (Fig. 5.13a) in the depressed

conchoidal surface indicating prolonged chemical etching (Margolis, 1968). Formation of deep haloes (Fig. 5.13a) at the centre of the grain is observed indicating further prolonged chemical etching during diagenesis. Mechanical abrasion features is totally obliterated. The conchoidal fractures which were produced on the edges of the grain are smoothed by silica precipitation. The breakage block (Fig. 5.13b) has been smoothed with silica precipitation and then dissolution has taken place leading to solution crevasses. Based on these microfeatures, it is evident that due to prolonged residence time, the complete shape of the grain has been modified, which result in chemical alteration of the quartz in prolonged immersion in marine environment.

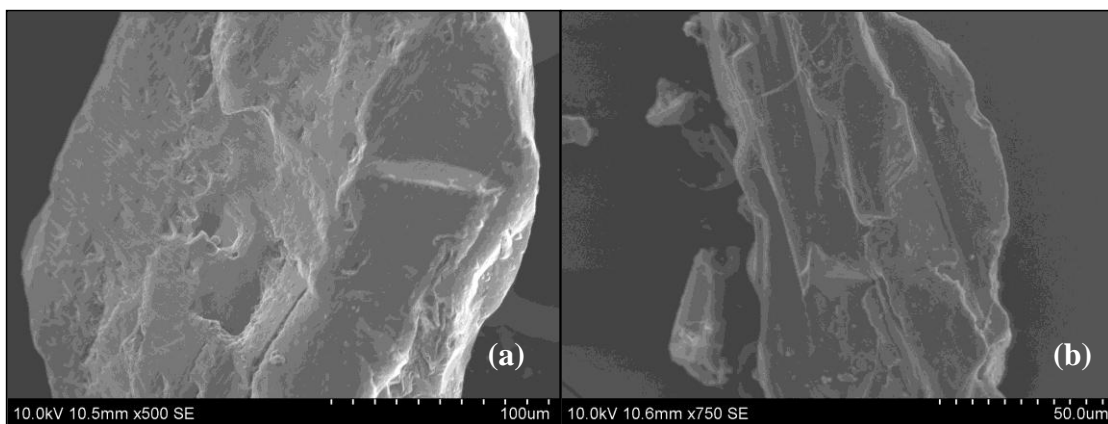


*Fig. 5.13 SEM photographs of the quartz grains at the depth of 11.6 m showing (a) cross hatching network, deep haloes (b) smoothness of breakage blocks indicating silica precipitation*

At the depth of 16.0 m, the surface texture exhibit sub-rounded in shape with moderate relief. In the lower part of the grains, slightly curved grooves with an approximate length of 8 microns, impact pits, straight scratches (Fig. 5.14a), which are the typical features of mechanical abrasion of beach environment (*see for e.g.*, Krinsley and Donahue, 1968) is visible indicating the grain were transported as well as deposited through mechanical process but later during post-depositional process, plastering of silica solution took place leading to the smoothness of the edges indicating reworked sediments. On the upper part, the smooth edges of the grains are etched in the form of irregular in outline. The upper surface is plastered by silica solution over which coalescence of tiny silica globules leading to the formation of soluble silica pellicles (Fig. 5.14a) are observed. Depending upon the available silica solution silica pellicle may grow partly or wholly, which mask the earlier microtextures and are generally formed on the quartz grains during post



deposition/diagenesis on the broken surfaces or conchoidal surface (Madhavaraju et al., 2004).

When magnified closely (Fig. 5.14b), the conchoidal surface, which was formed during mechanical process has been found smoothed chemically through silica solution, giving rise to heap mound of circular to sub-circular hillock like feature such as pressure solution (Fig. 5.14b) associated with solution pits and oriented V-shaped

etch pits (Fig. 5.14b) upon the precipitated upturned plates (Fig. 5.14c). Etch pits of oriented crystallographic direction is observed (Fig. 5.14c) on the other side. Inside the breakage surfaces, the fractured surface has been widened by silica plastering because of silica precipitation. Moreover, precipitated upturned plates in the form of step like appearance is noticed with a deep triangle within triangle at the centre (Fig. 5.14c) is noticed indicating a long period of chemical etching probably in basic environment (Krinsley and Doornkamp, 1973).

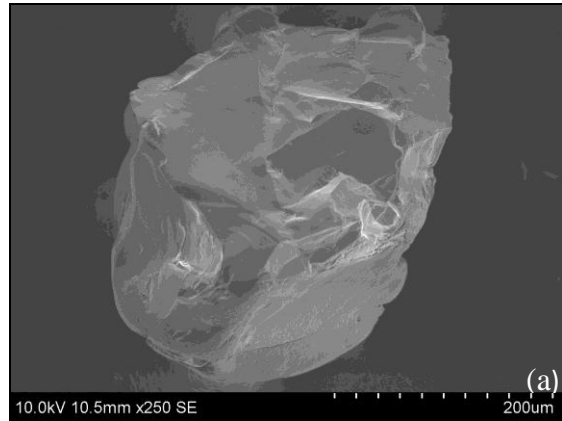


*Fig. 5.14(a) SEM photographs of the quartz grains at the depth of 16.0 m showing mechanical features such as sub rounded in outline*

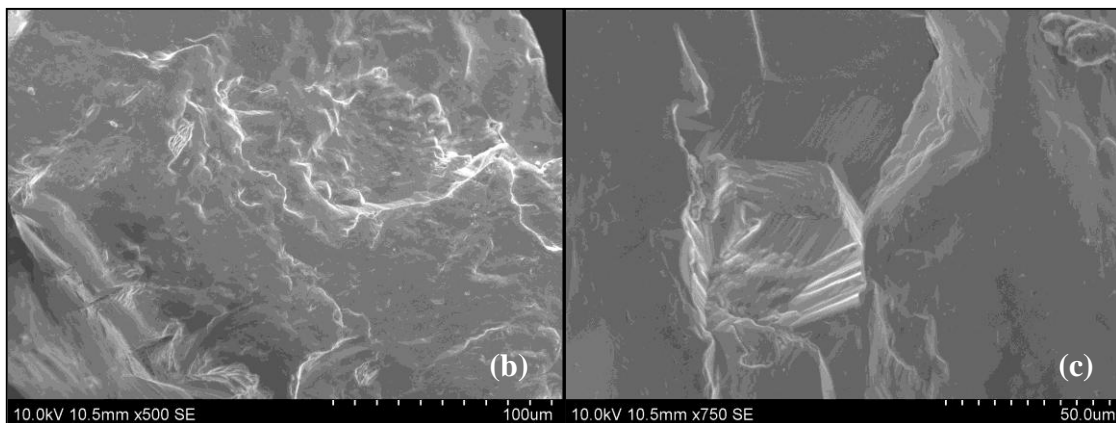


*Fig. 5.14 SEM photographs of the quartz grains at the depth of 16.0 m showing (b) chemical features such as pressure solution and (c) deep triangle within triangle indicating intense chemical weathering*

At the depth of 19.7 m, the quartz grains are totally etched forming irregular in outlines (Fig. 5.15a) indicating prolonged deposition of the grain in the marine

environment. The intense features are developed on the quartz grains when the grains remain immobile under the alkaline environment (Joshi, 2009). The conchoidal surfaces as well as fractured plates, which were formed during mechanical abrasion, have been smoothed by silica solution indicating silica plastering (Fig. 5.12b) upon the pre-existing surface. While on the other side the entire grain surface has been masked by coalescence of tiny globules/crystals indicating silica pellicle (Fig. 5.12b) indicating rapid precipitation of silica (Rahman and Ahmed, 1996). Tiny euhedral crystals are observed representing crystalline overgrowth (Fig. 5.12b) which requires more lapse time during precipitational process as well as more stagnancy of the host particles (Rahman and Ahmed, 1996).

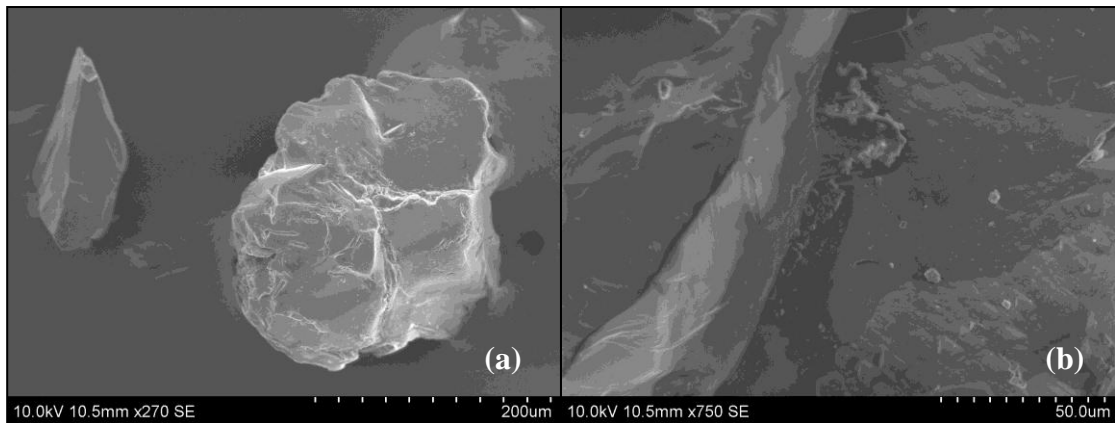


*Fig. 5.15 SEM photographs of the quartz grains at the depth of 19.7 m showing (a) total etching of the grains (b) silica plastering, silica pellicle*

A series of leaf like structures (Fig. 5.12c) on the upturned plates indicating silica solution cum precipitation masking the previous micro-features and forming chemically upturned plates are observed on quartz grains of 19.7 m depth. A series of solution pits (Fig. 5.12c) in elongate as well as etched shape are observed on the leaf like structure resembling intense

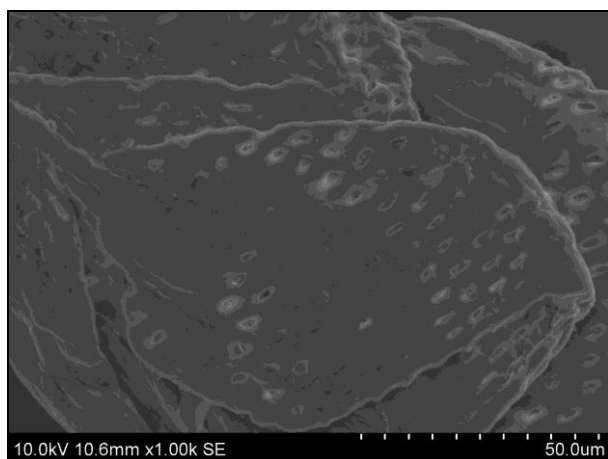


*Fig. 5.15 SEM photographs of the quartz grains at the depth of 19.7 m showing (c) leaf like structure*

chemical etching indicating silica dissolution over a period of long residence time. Hence, it is confirmed that at this depth, quartz grains undergone chemical alteration rigorously in the form of silica precipitation such as silica plastering silica pellicle and crystalline over growth then followed by silica dissolution in the form of solution pits which indicate that diagenesis is the major contributor in the formation of microsurfcae texture features at this depth.

#### **5.2.2.2. Offshore**

In the northern transect offshore core (Core 8), is collected from Kayamkulam offshore at a depth of 10 m with a core length of 0.73 m. Based on lithological observations, quartz grains at 0.60 m depth is taken for SEM analysis.

It is observed that the grain is subrounded in shape with large amount of breakage fracture. Mechanical V-shaped impact pits (Fig. 5.16a), large breakage conchoidal fracture (Fig. 5.16a), fracture plates (Fig. 5.16a) is observed indicating transportation of grains under high turbulent aqueous medium (*e.g.*, Krinsley and Doornkamp, 1973). Linear shaped, branching solution feature originated and enlarged as primary fracture is also observed (Fig. 5.16b) in the quartz grain. Abundance of solution crevasses mainly occur in association with solution pits (Fig. 5.16b) (Krinsley and Doornkamp, 1973) is observed. The solution crevasses (Fig. 5.16b) takes the form of a very thin surface layer peeling backwards away from the linear hollow (Doornkamp and Krinsley, 1971). Processes of solution tend to open up cracks and crevasses along the structural weakness in these quartz grains (Joshi, 2009). Whenever a weak spot is found by the same process, a solution pit is created (Krinsley and Doornkamp, 1973; Joshi, 2009) indicating silica dissolution took place during the post depositional process. Some of the solution is seen in the formation of cracks with much curved edges between the conchoidal fracture (Fig. 5.16b) indicating early stages of development of crevasses (Krinsley and Doornkamp, 1971) leading to the formation of secondary conchoidal fracture. Krinsley and Doornkamp (1971) reported that these conchoidal features will become lines of weakness on the grain surface and will automatically opened-up by chemical action. Therefore, solution and chemical weathering have led to mechanical action, which in turn, has resulted in a new phase of chemical activity.

On the upturned plates (Fig. 5.16c) series of straight to crescent-shaped grooves of chemical alteration by dissolution of quartz material (Bull, 1977) known as chattermarks trails randomly oriented is observed (Fig. 5.16c). These microstructures as observed became wider and deeper with increasing duration of etching (Peterknecht and Tietz, 2011). Internal cracks that have not yet reached the surface may become pathways for rapid dissolution when etching processes attack a quartz grain or come into contact with these structural defects due to the fact that the dissolution is a surface-related interactions between solution and quartz (Peterknecht and Tietz, 2011). In this process, the etching procedure affects the entire surface of the grain and totally destroys the polish by dissolution and subsequent removal of quartz. This removal opens the previously internal cracks for invading solution and further material removal, thus sculpting the grooves of the chattermark trail.

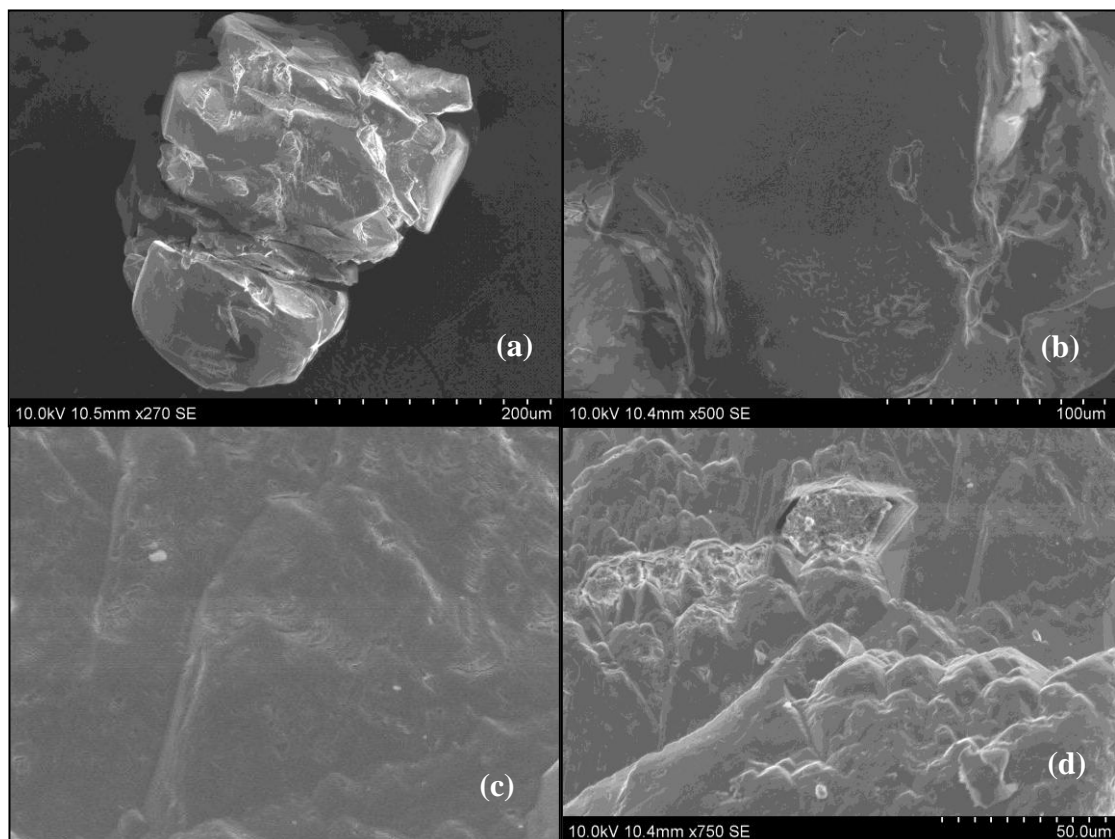


*Fig. 5.16 SEM photographs of the quartz grains (0.60 m) of northern offshore at the depth of 10 m showing (a) large breakage conchoidal fracture (b) solution crevasses (c) chatter mark trails on upturned plates (d) crystalline overgrowth with irregular solution pits*

Another important feature is numerous majority of the precipitated silica represents tiny euhedral crystals crystal faces termed crystalline overgrowth (Fig. 5.16d) have formed on the upturned plates by precipitation. A number of rhombohedral faces are well developed with occasional pyramid faces also present. This chemically precipitated texture represents an acidic environment having lower pH value and capable of silica precipitation (Krauskopf, 1956). Development of euhedral crystalline overgrowth require to lapse more time during precipitational process as well as more stagnancy of the host particles (Rahman and Ahmed, 1996). Upon the crystalline overgrowth in the form columnar shape, irregular solution pits (Fig. 5.16d) with solution crevasses is observed. Moreover, a long period of chemical etching probably in basic environment (Krinsley and Doornkamp, 1973) has produced a deep triangle within triangle form at the centre (Fig. 5.16d). Upon these isosceles triangle as well as along the sides excess of silica solution after prolonged residence time forms etched silica flakes (Fig. 5.16d) indicating dissolution of silica dominated when the pH condition is suddenly increased by the contact of alkali solutions (Hurst, 1981) under the influence of marine ingresson.

### **5.3. Transport Mechanism and Depositional History**

The environment in which the mineral grains were deposited is significant in the study of influence of time on the grain surface textures (Ly, 1978). The microtextural analyses of quartz grains representing the sediment core which is 9.5 km east of the present day coastline shows the dominance of angular grains with high relief, impact pits, imbricated breakage block, medium to large conchoidal fractures, oriented fracture plates, flat cleavage surfaces, which are indicative of the sediments up to a depth of 9 m were transported and deposited under fluvial environment through mechanical processes. This is corroborated with the sediment texture revealing medium to fine sand with angular in nature. Overpeck et al. (1996) based on radiocarbon dating inferred that the southwest Indian monsoon strength increased suddenly during 13,000–12,500 Yrs BP and 10,000–9,500 Yrs BP respectively. The climatic proxies suggest that the stronger monsoon in the early Holocene was associated with high lake levels; increased flow discharges floods and scouring (Kale et al., 2004). Since the Kallada River is a major depocentre for the Ashtamudi Estuary, it may be during the time of stronger monsoon, incised valley has taken place

leading to the huge thickness of fluvial deposits through mechanical processes indicating observed microtextural features of fluvial origin surrounding the estuary.

Below 9.0 to 10.8 m, the fluvial angular grains with mechanical microtextural features has been modified to sub-rounded in shape indicating reworked deposits with the intervention of chemical features in the form of linear branching solution, centipede type indicating chemical etching in aqueous medium. The sediment characteristics reveals with sand-silt-clay (mud) is brown in colour followed by grey to whitish hard-desiccated clay indicative of subaerial exposure during a period of non-deposition corresponding to the LGM and associated lowering of water table and reduced monsoonal activity recorded Worldwide (Nair et al., 2006). Van Campo (1986) reported an arid climate existed during 22,000–18,000 Yrs BP in the Kerala region due to weak southwest air flow, a great reduction of summer monsoonal rainfall and runoff from the Western Ghats Rivers. Because of non-deposition as well as a rid climate the grains remained intact with aqueous medium leading to formation of fluvial chemical features. But below 10.8 to 15.5 m depth, the quartz grains exhibited distorted in shape showing intense chemical microtextures features like silica pellicle, solution pits, pressure solution, with prolong diagenesis features of dissolution etching and honey comb structure indicating chemical alteration under marine environment. The sediments are composed of black clay with peat layer, which affirms the marine transgression event during the late Pleistocene. Similar observations were reported elsewhere (Shajan, 1988; Narayana et al. 2002). Hence, during the late Pleistocene the coastal plain surrounding the Ashtamudi Estuary were deposited under marine realm.

In the northern coastal plain, which is located 7.6 km away from the present shoreline exhibits roundness and high concentration of mechanical V-shaped marks with occasional linear grooves, chattermarks, indicating subaqueous transport under high energy conditions (Krinsley and Doornkamp, 1973) up to a depth of 10 m from the ground level confirming littoral environment. This is followed by the strong chemical alteration features in the form of series of etch pits in the form of V-pits, isocles triangle, rectangular pits, silica pellicle indicating intense chemical etching as well as prolonged chemical dissolution inferring diagenesis under prolonged marine evolution down the core.

Based on the quartz surface texture for the coastal plains of the northern as well as southern transect, it can be concluded that the northern coastal plain underwent more pronounced transgression regression events during late Quaternary. This is also confirmed by radiocarbon dates as well as formation of ridges and swales of different sets of orientation based on series of episodes of transgression as well as regression events, which were reported elsewhere (Chattopadhyay, 2002; Jayalekshmi et al., 2004; Samsuddin et al., 2008). The borehole of the coastal plain in the southern transect is dominated quartz grains of terrigenous characteristics even up to a depth of 10 m indicating absence of marine incursion during Holocene, whereas the chemical alteration is enhanced further down core confirming longer resident time under the low energy marine environment during Late Pleistocene which is also confirmed by the dating results of the peat below 10 m depth.

In the Ashtamudi Estuary, surface textures features such as conchoidal fracture, oriented fractures plates, impact pits are inferred which confirms that the quartz grain was first deposited by mechanical alteration through subaqueous impact under fluvial environment (Krinsley and Doornkamp, 1973; Ly, 1978; Monker and Ponder, 1978). Moreover, the Kallada River, which is the major sediment source of Ashtamudi estuary (Prakash et al., 2001) further confirms its original source from fluvial origin. Later, during the post depositional scenario, the grains have undergone chemical etching leading to the formation of etch pits in the form of isosceles triangle, solution pits, silica solution. At places, the triangle pits are not fully pronounced because of rapid silica reprecipitation as well as short duration of residence time. Hence, it is concluded that the quartz grains were deposited through mechanical process under fluvial origin followed by post depositional process of chemical alteration but not fully pronounced.

In the offshore region, based on microtexture features it is inferred that the quartz grains were first transported and deposited under littoral environment based on the presence of series of fractures plates, conchoidal fracture and V-shaped pits indicating formation of these features in the turbulent aqueous high energy environment (Ly, 1978; Krinsley and Doornkamp, 1973). During the post depositional process, quartz grains underwent chemical alteration process of silica precipitation as well as silica dissolution in the form of quartz intergrowth, solution

pits, crevasses, etch pits, chemical etching in the form of triangle within triangle indicating high chemical energy environment. Moreover, the presence of chattermark observed in the quartz grain reveals a two-phase formation process: the first phase is the mechanical collision of components (Paterson, 1978; Swain, 1979) during sediment transport followed by a second (depositional) phase characterized by the establishment of a chemical reaction upon any quartz surface available for dissolution (Peterknetch and Tietz, 2011).

It has been reported by earlier workers that the coarser sandy sized sediments are not of recent origin supplied from the hinterland by the present day rivers, but, are the beach and nearshore sediments of Holocene period during the lower stand of sea level, which was later submerged by rise in sea level (Nair et al., 1978) and emplaced in the present day outer-innershelf environment. Similar observations with SEM features were reported elsewhere (Prithiviraj and Prakash, 1991) along the Kerala Coast.

Coch and Krinsley (1971) reported that the intensity of chemical action depend on the age of deposits, with stronger etching effects observed in the older sediments. The longer the residence time in the marine environment, more the chemical action for the quartz grain (Prithiviraj and Prakash, 1991). It has also been shown that quartz grains from modern beach environment do not exhibit significant chemical action (Ly, 1978). Therefore, it is confirmed the quartz grains are of littoral origin and also represent some of relict beach deposits. These relict sands were probably deposited on the shelf during the last low stand of sea level and were then submerged as the sea transgressed over the shelf during the Holocene post glacial period. Moreover, the coastal currents in shelf might have reworked these relict sands which were in marine environment for a long period time on the innershelf.

#### **5.4. Summary**

The results of the microtextural study of sediment samples (quartz grains) using Scanning Electron Microscope (SEM) are presented. These results throw light on the processes of transport and diagenetic history of the detrital sediments. Based on the lithological variations, selected quartz grains of different environments were also analysed. The study indicates that the southern coastal plain sediments were



transported and deposited mechanically under fluvial environment followed by diagenesis under prolonged marine incursion. But in the case of the northern coastal plain, the sediments were transported and deposited under littoral environment indicating the dominance of marine incursion through mechanical as well as chemical processes. The quartz grains of the Ashtamudi Estuary indicate fluvial origin. The surface texture features of the offshore sediments suggest that the quartz grains are of littoral origin and represent the relict beach deposits.

## CHAPTER 6

# MAJOR AND TRACE ELEMENT GEOCHEMISTRY OF SEDIMENT CORES

### 6.1. Introduction

The chemical composition of sedimentary rocks is dependent on the depositional processes, including source rocks, weathering, sorting, tectonic setting and paleoclimate (McLennan, 1989; McLennan and Taylor, 1991; McLennan et al., 1993). Therefore, provenance analysis will help in reconstructing the predepositional history of a sediment or sedimentary rock. This includes the distance and direction, size and setting of the source region, climate and relief in the source area, and the specific type of sedimentary rocks (Pettijohn et al., 1987; Von Eynatten and Gaupp, 1999).

Elemental variations observed in sediments can also provide vital information on the environmental conditions like diagenetic processes and pollutant inputs, and can assist in sediment correlation and process studies (e.g., Rothwell and Rack 2006). Certain elements or element ratios can be used as proxies for environmental conditions that are either generally valid or constrained to specific conditions (Koinig et al., 2003). Similarly, trace elements such as Th, Zr, Nb, Sc, Y, Cr and REE such as La, Ce, Nd, Gd, Yb are most suited for discriminates of provenance and tectonic setting since these elements have relatively low mobility during sedimentary processes and have short residence time in seawater (Taylor and McLennan, 1985).

This study presents geochemical analysis of the sediment cores representing coastal plain, estuary and offshore of Kollam region. The close examination of the various major and trace elemental compositions of core sediment and their inter-relationship are studied to understand the paleoenvironmental conditions prevailing in the coastal area. The geochemical proxies are used to identify the origins of the estuarine sediments, especially to infer the provenance and source sink relationship. Furthermore, weathering in the source area and maturity of the sediments is also discussed.

## 6.2. Distribution of Major elements

The distribution of the major elements for the sediment cores representing the coastal plain, estuary and offshore are presented in Table 6.1.  $\text{SiO}_2$  (wt%) is recorded higher in coastal plain sediments ranging between 32.2 and 87.5 wt% with an average of 58.5 wt%, which is higher than the offshore (Core 5) (av. 46.8 wt%) and estuarine sediments of Core 4 – 48.6; Core 3 – 37.9 and Core 2 – 40.3 wt%.  $\text{Al}_2\text{O}_3$  content shows variation among the estuarine sediments (Core 4 – 15.3; Core 3– 21.5 and Core 2 – 18.5 wt%), which are comparable with offshore (15.15 wt %) and coastal plain sediments (18.1 wt%).  $\text{Al}_2\text{O}_3$  in Core 3 sediments varies between 20.1 and 23.8 wt%, which is recorded higher than Core 4 (12.6-16.4 wt%) and Core 2 (18.0-19.3 wt%).

Offshore sediments shows comparatively higher  $\text{TiO}_2$ ,  $\text{Fe}_2\text{O}_3$ ,  $\text{CaO}$ ,  $\text{MgO}$ ,  $\text{Na}_2\text{O}$ ,  $\text{K}_2\text{O}$  and  $\text{P}_2\text{O}_5$  contents than the coastal plain sediments, meanwhile these elements concentration in offshore sediments can be comparable with estuarine sediments particularly for the sediments obtained in Core 4. Among the estuarine sediments,  $\text{SiO}_2$ ,  $\text{CaO}$  and  $\text{P}_2\text{O}_5$  content is recorded higher in Core 4 sediments (av. 48.6 wt%; 7.4 wt%; and 0.4 wt%), whereas  $\text{Al}_2\text{O}_3$ ,  $\text{Fe}_2\text{O}_3$  and  $\text{Na}_2\text{O}$  content is recorded higher in Core 3 (av. 21.5 wt%; 9.8 wt% and 4.6 wt% respectively). Core 2 sediment show an intermediate composition between Core 4 and Core 3 except  $\text{MgO}$  content (av. 4.1 wt%) recorded higher than the other cores.

### 6.2.1. Normalisation of major and trace elements with UCC

The overall major oxides comprising coastal plain, estuary and offshore were normalised against the UCC values based on Taylor and McLennan (1985) and is presented in figure 6.1a. The analysed samples are depleted in  $\text{SiO}_2$ ,  $\text{K}_2\text{O}$  and enriched in  $\text{TiO}_2$ ,  $\text{Fe}_2\text{O}_3$ ,  $\text{MgO}$  (except Core 1 samples), and  $\text{P}_2\text{O}_5$ . In general, the sediments of Core 3 are enriched in  $\text{Al}_2\text{O}_3$ ,  $\text{Fe}_2\text{O}_3$ ,  $\text{MnO}$ ,  $\text{Na}_2\text{O}$  and depleted in  $\text{CaO}$  compared to the sediments of other two cores (Core 4 and Core 2). Sediments of Core Core 4 and Core 2 show relatively similar trend in concentration of major oxides compared to sediments of Core 3. The high concentration of  $\text{Fe}_2\text{O}_3$  in these sediments is an indication of oxidation, hydration and leaching processes involved during weathering (Mikkil and Henderson, 1983).

Table 6.1. Major Element concentration in weight percentages for Coastal Plain (Core 1) sediment core

Element (wt %)	2 (m)	2.7 (m)	3 (m)	4 (m)	5 (m)	6 (m)	7 (m)	8 (m)	8.9 (m)	9 (m)	9.8 (m)	9.9 (m)	10.9 (m)	11.8 (m)	12 (m)	13 (m)	13.8 (m)	14 (m)	15 (m)	15.5 (m)
SiO <sub>2</sub>	75.26	65.06	70.54	84.36	82.87	84.40	87.46	67.73	71.55	70.38	43.96	43.95	44.16	35.74	44.39	41.56	32.18	35.44	34.74	36.64
TiO <sub>2</sub>	0.81	0.74	0.74	0.44	0.38	0.32	0.42	0.55	0.75	0.94	0.98	1.08	0.99	0.80	0.85	0.85	0.79	0.79	0.80	0.85
Al <sub>2</sub> O <sub>3</sub>	12.11	15.57	13.73	8.61	8.82	8.35	6.99	9.93	12.92	16.21	26.56	32.68	31.37	23.40	22.57	23.70	21.57	23.72	23.07	24.31
MnO	0.01	0.008	0.008	ND	ND	ND	ND	ND	0.002	ND	0.001	ND	ND	0.016	ND	ND	0.001	0.058	0.050	0.057
Fe <sub>2</sub> O <sub>3</sub>	3.29	4.47	4.06	2.02	1.93	2.28	1.21	6.47	6.19	4.07	10.19	1.85	1.22	7.19	4.90	3.34	4.52	8.73	9.75	9.01
CaO	0.49	0.53	0.47	0.31	0.33	0.31	0.28	4.91	0.31	0.26	0.33	0.28	0.30	0.35	0.38	0.44	0.45	0.35	0.36	0.37
MgO	1.06	1.10	1.07	0.94	0.98	0.94	0.95	0.91	0.94	0.94	0.91	0.91	0.98	1.26	1.33	1.36	1.39	1.21	1.17	1.15
Na <sub>2</sub> O	0.61	0.69	0.59	0.29	0.38	0.24	0.26	0.30	0.44	0.71	0.97	1.39	1.64	1.85	1.71	1.86	2.02	1.42	1.27	1.27
K <sub>2</sub> O	1.31	1.43	1.30	0.70	0.82	0.55	0.34	0.02	0.03	0.02	0.34	0.46	0.49	1.48	2.04	1.93	1.44	1.56	1.35	1.30
P <sub>2</sub> O <sub>5</sub>	0.07	0.08	0.08	0.06	0.06	0.06	0.04	0.14	0.11	0.11	0.16	0.08	0.10	0.08	0.08	0.11	0.09	0.10	0.10	0.10
LOI	4.95	10.28	7.36	2.27	3.36	2.59	2.01	8.95	6.69	6.37	15.54	17.28	18.64	27.78	21.69	24.76	35.48	26.55	27.25	24.89
CIA	78.06	80.31	80.4	83.42	80.55	85.75	84.97	90.83	89.66	87.27	88.17	86.57	84.14	75.31	74.23	74.29	72.47	78.88	80.35	81.29
ICV	0.62	0.58	0.60	0.55	0.55	0.56	0.50	1.33	0.67	0.43	0.52	0.18	0.18	0.55	0.50	0.41	0.49	0.59	0.64	0.574
Al/Ti	15.00	21.18	18.66	19.48	22.96	26.49	16.84	17.98	17.29	17.34	27.10	30.20	31.82	29.21	26.49	28.01	27.24	29.91	28.73	28.57
K/Na	2.16	2.08	2.20	2.43	2.19	2.26	1.30	0.08	0.06	0.02	0.35	0.33	0.30	0.80	1.19	1.04	0.72	1.10	1.07	1.02
Si/Al	6.21	4.18	5.14	9.80	9.40	10.11	12.51	6.82	5.54	4.34	1.66	1.34	1.41	1.53	1.97	1.75	1.49	1.49	1.51	1.51
K/Al	0.108	0.092	0.095	0.082	0.093	0.065	0.049	0.002	0.002	0.001	0.013	0.014	0.015	0.063	0.090	0.082	0.067	0.066	0.059	0.054
Mg/Al	0.087	0.071	0.078	0.109	0.111	0.113	0.136	0.092	0.073	0.058	0.034	0.028	0.031	0.054	0.059	0.057	0.065	0.051	0.051	0.047

Table 6.1 Cont'd. Trace Element concentration in ppm for Coastal Plain (Core 1) sediment core

Element (ppm)	2 (m)	2.7 (m)	3 (m)	4 (m)	5 (m)	6 (m)	7 (m)	8 (m)	8.9 (m)	9 (m)	9.8 (m)	9.9 (m)	10.9 (m)	11.8 (m)	12 (m)	13 (m)	13.8 (m)	14 (m)	15 (m)	15.5 (m)
V	75	100	83	76	68	79	67	102	131	122	155	137	112	125	111	120	125	126	133	142
Cr	66	80	81	54	38	60	52	128	106	86	190	164	131	108	111	113	108	116	118	113
Co	ND	7	2	ND	ND	ND	ND	ND	ND	ND	4	ND	ND	31	27	32	18	21	24	16
Ni	19	30	32	19	7	16	22	10	16	26	62	124	107	61	71	86	75	70	65	63
Cu	2	18	21	ND	ND	ND	12	ND	ND	ND	ND	24	58	42	55	61	51	30	12	10
Ga	11	18	21	ND	3	ND	ND	13	15	17	56	77	74	36	38	47	34	37	35	40
Rb	44	59	51	30	37	26	23	16	16	16	32	46	50	49	68	93	70	60	58	49
Sr	59	78	62	23	34	17	7	232	ND	ND	14	26	24	32	52	81	45	27	23	15
Nb	19	14	16	5	6	4	5	15	15	17	15	11	4	8	12	8	5	6	8	10
Ba	259	292	261	116	149	85	38	ND	ND	16	ND	108	98	334	387	347	294	273	224	219
La	51	73	39	21	13	4	22	32	32	ND	61	69	75	65	60	54	71	52	66	68
Pb	18	24	19	11	12	ND	ND	ND	ND	16	29	41	68	12	ND	ND	15	20	20	23
Ce	90	83	84	52	41	40	47	61	77	ND	81	83	70	142	99	109	107	111	119	101
Sm	5	5	5	4	3	ND	4	4	4	53	4	5	5	7	6	6	6	6	6	5
Th	17	17	21	14	14	14	14	15	15	16	14	13	14	14	15	15	14	14	14	15

Table 6.1 Cont'd. Major Element concentration in weight percentages for Ashtamudi Estuary (Core 2) sediment core

<b>Element (wt %)</b>	<b>10 (m)</b>	<b>0.20 (m)</b>	<b>0.30 (m)</b>	<b>0.40 (m)</b>	<b>0.50 (m)</b>	<b>0.60 (m)</b>	<b>0.70 (m)</b>	<b>0.80 (m)</b>	<b>0.90 (m)</b>	<b>1.0 (m)</b>	<b>1.08 (m)</b>
SiO <sub>2</sub>	40.59	39.62	39.84	40.23	40.73	40.25	39.72	39.91	40.44	40.05	41.19
TiO <sub>2</sub>	0.96	0.89	0.88	0.84	0.88	0.88	0.86	0.84	0.85	0.83	0.84
Al <sub>2</sub> O <sub>3</sub>	17.96	19.04	19.02	18.67	19.25	18.19	17.99	18.37	18.47	18.18	18.62
MnO	0.03	0.04	0.05	0.04	0.05	0.04	0.05	0.04	0.04	0.04	0.05
Fe <sub>2</sub> O <sub>3</sub>	8.52	9.28	9.20	8.71	9.55	10.08	9.70	9.32	9.23	9.11	8.96
CaO	3.90	3.03	3.35	4.30	3.14	3.74	3.97	4.24	3.77	4.59	4.08
MgO	3.89	3.96	4.11	3.97	4.21	4.24	4.22	4.19	4.33	3.96	4.35
Na <sub>2</sub> O	4.83	4.15	3.79	3.81	3.74	3.40	3.38	3.57	3.52	3.67	3.71
K <sub>2</sub> O	1.51	1.49	1.47	1.41	1.50	1.53	1.51	1.44	1.51	1.40	1.53
P <sub>2</sub> O <sub>5</sub>	0.49	0.44	0.42	0.44	0.42	0.44	0.44	0.44	0.44	0.44	0.46
LOI	17.21	17.96	17.77	17.47	16.44	17.96	18.07	17.54	17.31	17.64	16.11
CIA	53.65	59.63	59.58	57.02	60.70	58.64	58.50	58.01	58.27	57.21	57.33
ICV	1.32	1.20	1.20	1.23	1.20	1.31	1.32	1.29	1.26	1.30	1.26
Al <sub>2</sub> O <sub>3</sub> /TiO <sub>2</sub>	18.70	21.34	21.57	22.34	21.98	20.72	20.94	21.84	21.78	22.01	22.11
K <sub>2</sub> O/Na <sub>2</sub> O	0.31	0.36	0.39	0.37	0.40	0.45	0.45	0.40	0.43	0.38	0.41
SiO <sub>2</sub> /Al <sub>2</sub> O <sub>3</sub>	2.26	2.08	2.09	2.15	2.12	2.21	2.21	2.17	2.19	2.20	2.21
K <sub>2</sub> O/Al <sub>2</sub> O <sub>3</sub>	0.08	0.08	0.08	0.08	0.08	0.08	0.08	0.08	0.08	0.08	0.08
MgO/Al <sub>2</sub> O <sub>3</sub>	0.22	0.21	0.22	0.21	0.22	0.23	0.23	0.23	0.23	0.22	0.23

*Table 6.1 Cont'd. Trace Element concentration in ppm for Ashtamudi Estuary (Core 2) sediment core*

<b>Element (ppm)</b>	<b>0.1 (m)</b>	<b>0.2 (m)</b>	<b>0.3 (m)</b>	<b>0.4 (m)</b>	<b>0.5 (m)</b>	<b>0.6 (m)</b>	<b>0.7 (m)</b>	<b>0.8 (m)</b>	<b>0.9 (m)</b>	<b>1.0 (m)</b>	<b>1.08 (m)</b>
Cr	191	188	184	183	184	193	188	184	184	182	182
Co	11	12	12	12	13	14	13	13	13	13	13
Ni	79	83	82	77	80	81	80	82	80	80	81
Cu	13	21	17	25	29	25	21	32	27	29	21
Zn	ND	7	2	ND	18	18	11	8	2	ND	ND
Ga	19	25	27	24	26	25	24	19	22	18	26
Rb	72	83	85	83	79	75	81	60	80	65	100
Y	17	16	12	17	16	22	16	23	14	20	12
Zr	176	72	96	72	111	99	81	109	59	78	34
Nb	10	10	10	10	9	9	9	6	9	7	12
Ba	306	278	274	275	299	275	283	269	282	250	268
La	49	56	49	47	44	52	50	46	53	48	49
Ce	76	88	97	95	84	78	85	86	90	83	75
Sm	6	6	5	5	6	5	5	6	6	6	5

Table 6.1 Cont'd. Major Element concentration in weight percentages for Ashtamudi Estuary (Core 3) sediment core

<b>Element</b>	<b>0.2</b>	<b>0.3</b>	<b>0.4</b>	<b>0.5</b>	<b>0.6</b>	<b>0.7</b>	<b>0.8</b>	<b>0.9</b>	<b>1.0</b>	<b>1.1</b>	<b>1.2</b>	<b>1.3</b>	<b>1.4</b>	<b>1.48</b>
<b>(%)</b>	<b>(m)</b>	<b>(m)</b>	<b>(m)</b>	<b>(m)</b>	<b>(m)</b>	<b>(m)</b>	<b>(m)</b>	<b>(m)</b>	<b>(m)</b>	<b>(m)</b>	<b>(m)</b>	<b>(m)</b>	<b>(m)</b>	<b>(m)</b>
SiO <sub>2</sub>	37.39	37.34	37.85	39.04	NA	37.16	37.17	37.20	37.36	39.18	38.39	38.45	38.57	37.77
TiO <sub>2</sub>	0.81	0.78	0.83	0.85	NA	0.84	0.87	0.85	0.83	0.86	0.86	0.86	0.85	0.83
Al <sub>2</sub> O <sub>3</sub>	20.20	23.77	20.12	20.63	NA	20.98	21.47	21.54	21.86	22.42	21.29	21.71	21.95	22.83
MnO	0.08	0.06	0.08	0.08	NA	0.10	0.09	0.09	0.08	0.09	0.09	0.10	0.12	0.10
Fe <sub>2</sub> O <sub>3</sub>	9.06	9.32	9.35	9.26	NA	9.68	10.27	10.08	9.85	10.21	10.11	10.23	10.63	10.01
CaO	1.85	0.92	1.90	1.93	NA	2.03	1.27	1.07	1.40	1.28	1.34	0.96	1.70	1.43
MgO	3.78	2.67	3.89	3.92	NA	3.63	3.42	3.31	3.33	3.22	3.51	3.43	3.62	3.36
Na <sub>2</sub> O	5.63	4.20	4.89	4.96	NA	4.56	4.26	4.40	4.17	4.39	4.48	4.27	4.01	3.90
K <sub>2</sub> O	1.40	1.68	1.39	1.44	NA	1.35	1.36	1.33	1.31	1.36	1.35	1.34	1.34	1.29
P <sub>2</sub> O <sub>5</sub>	0.37	0.34	0.37	0.38	NA	0.36	0.32	0.31	0.33	0.35	0.34	0.33	0.38	0.33
LOI	19.34	18.82	19.22	17.41	NA	19.19	19.38	19.73	19.39	16.53	18.13	18.20	16.71	17.98
CIA	60.40	71.30	62.40	62.60	NA	64.10	68.10	68.50	68.50	68.80	67.10	69.70	68.20	70.40
ICV	1.12	0.82	1.11	1.08	NA	1.05	1.00	0.98	0.96	0.95	1.02	0.97	1.01	0.91
K <sub>2</sub> O/Na <sub>2</sub> O	0.25	0.40	0.29	0.29	NA	0.29	0.32	0.30	0.31	0.31	0.30	0.31	0.33	0.33
SiO <sub>2</sub> /Al <sub>2</sub> O <sub>3</sub>	1.85	1.57	1.88	1.89	NA	1.77	1.73	1.73	1.71	1.75	1.80	1.77	1.76	1.65
Al <sub>2</sub> O <sub>3</sub> /TiO <sub>2</sub>	25.00	30.56	24.23	24.36	NA	24.95	24.77	25.46	26.37	26.22	24.90	25.40	25.70	27.51
K <sub>2</sub> O/Al <sub>2</sub> O <sub>3</sub>	0.07	0.07	0.07	0.07	NA	0.06	0.06	0.06	0.06	0.06	0.06	0.06	0.06	0.06
MgO/Al <sub>2</sub> O <sub>3</sub>	0.19	0.11	0.19	0.19	NA	0.17	0.16	0.15	0.15	0.14	0.16	0.16	0.17	0.15



*Table 6.1 Cont'd. Trace Element concentration in ppm for Ashtamudi Estuary (Core 3 ) sediment core*

<b>Element (ppm)</b>	<b>0.2 (m)</b>	<b>0.3 (m)</b>	<b>0.4 (m)</b>	<b>0.5 (m)</b>	<b>0.6 (m)</b>	<b>0.7 (m)</b>	<b>0.8 (m)</b>	<b>0.9 (m)</b>	<b>1.0 (m)</b>	<b>1.1 (m)</b>	<b>1.2 (m)</b>	<b>1.3 (m)</b>	<b>1.4 (m)</b>	<b>1.48 (m)</b>
Cr	178	160	183	179	NA	188	190	181	170	177	177	182	182	164
Co	11	12	12	11	NA	12	12	11	11	12	12	12	12	12
Ni	92	102	95	94	NA	100	97	96	91	97	94	97	96	89
Cu	70	65	89	33	NA	78	46	56	63	69	51	64	144	51
Zn	53	56	64	37	NA	61	47	52	61	84	88	89	138	48
Ga	30	44	32	37	NA	38	40	38	36	44	44	42	41	39
Rb	88	109	83	101	NA	97	85	88	77	107	105	97	91	96
Y	18	32	24	21	NA	17	24	20	27	17	15	20	24	17
Zr	36	32	52	33	NA	33	55	50	57	23	29	30	66	33
Nb	10	10	9	11	NA	11	8	9	7	12	12	11	10	10
Ba	220	302	225	256	NA	249	235	242	237	227	221	228	232	222
La	46	47	45	51	NA	52	55	51	50	48	51	49	50	50
Ce	79	93	95	86	NA	94	89	78	77	89	77	82	67	91
Sm	6	5	5	5	NA	6	6	6	6	6	5	5	6	6

Table 6.1 Cont'd. Major Element concentration in weight percentages for Ashtamudi Estuary (Core 4) sediment core

<b>Element (Wt%)</b>	<b>0.1 (m)</b>	<b>0.2 (m)</b>	<b>0.3 (m)</b>	<b>0.4 (m)</b>	<b>0.5 (m)</b>	<b>0.6 (m)</b>	<b>0.7 (m)</b>
SiO <sub>2</sub>	57.87	45.29	47.55	47.64	47.89	43.39	41.62
TiO <sub>2</sub>	0.79	0.81	0.81	0.83	0.80	0.84	0.81
Al <sub>2</sub> O <sub>3</sub>	12.60	16.34	16.43	16.27	15.31	16.45	16.25
MnO	0.02	0.03	0.03	0.03	0.02	0.03	0.02
Fe <sub>2</sub> O <sub>3</sub>	4.64	7.36	7.55	7.85	6.69	7.96	7.92
CaO	7.33	6.50	5.67	6.66	9.87	7.83	8.22
MgO	3.06	4.01	3.68	3.61	3.85	4.14	4.09
Na <sub>2</sub> O	2.77	3.75	3.42	3.53	3.08	3.27	3.18
K <sub>2</sub> O	1.66	1.62	1.60	1.73	1.68	1.59	1.67
P <sub>2</sub> O <sub>5</sub>	0.38	0.47	0.42	0.40	0.45	0.47	0.49
LOI	8.60	13.68	12.62	11.22	10.13	13.86	15.54
CIA	53.62	53.70	55.89	54.67	56.18	56.86	57.00
ICV	1.61	1.47	1.38	1.49	1.70	1.56	1.59
K <sub>2</sub> O/Na <sub>2</sub> O	0.60	0.43	0.47	0.49	0.55	0.48	0.52
SiO <sub>2</sub> /Al <sub>2</sub> O <sub>3</sub>	4.59	2.77	2.89	2.93	3.13	2.64	2.56
Al <sub>2</sub> O <sub>3</sub> /TiO <sub>2</sub>	15.91	20.10	20.34	19.65	19.23	19.67	20.09
K <sub>2</sub> O/Al <sub>2</sub> O <sub>3</sub>	0.13	0.10	0.10	0.11	0.11	0.10	0.10
MgO/Al <sub>2</sub> O <sub>3</sub>	0.24	0.25	0.22	0.22	0.25	0.25	0.25

*Table 6.1 Cont'd. Trace Element concentration in ppm for Ashtamudi Estuary (Core 4) sediment core*

<b>Element (ppm)</b>	<b>0.1 (m)</b>	<b>0.2 (m)</b>	<b>0.3 (m)</b>	<b>0.4 (m)</b>	<b>0.5 (m)</b>	<b>0.6 (m)</b>	<b>0.7 (m)</b>
Cr	154	156	154	157	146	162	164
Co	9	11	11	11	11	12	11
Ni	91	73	66	67	66	71	69
Cu	26	16	28	34	21	48	16
Ga	11	15	17	20	16	14	12
Rb	57	61	74	87	72	55	64
Nb	8	8	9	11	9	6	8
Ba	578	425	432	440	439	368	318
La	30	41	38	35	36	43	42
Pb	48	49	59	72	59	41	47
Ce	60	62	77	61	67	64	86
Sm	5	5	5	5	5	4	5
Th	13	20	22	27	21	23	22

Table 6.1 Cont'd. Major Element concentration in weight percentages for Offshore (Core 5) sediment core

<b>Element (wt%)</b>	<b>0.1 (m)</b>	<b>0.2 (m)</b>	<b>0.3 (m)</b>	<b>0.4 (m)</b>	<b>0.5 (m)</b>	<b>0.6 (m)</b>	<b>0.7 (m)</b>	<b>0.8 (m)</b>	<b>0.88 (m)</b>
SiO <sub>2</sub>	48.13	46.79	45.28	45.48	41.54	45.29	48.20	50.21	49.16
TiO <sub>2</sub>	0.91	0.87	0.87	0.85	0.85	0.99	0.85	0.73	0.83
Al <sub>2</sub> O <sub>3</sub>	15.31	15.57	15.73	15.72	16.25	15.58	14.01	13.63	14.39
MnO	0.03	0.03	0.03	0.03	0.02	0.03	0.03	0.02	0.03
Fe <sub>2</sub> O <sub>3</sub>	6.55	6.60	7.18	7.21	7.33	6.74	6.12	5.74	6.39
CaO	8.32	8.38	8.05	7.92	5.04	8.42	9.52	10.17	9.86
MgO	3.56	3.80	4.13	4.38	4.36	4.23	3.89	3.71	3.85
Na <sub>2</sub> O	3.43	3.26	3.48	3.82	4.33	3.56	3.23	2.85	2.94
K <sub>2</sub> O	1.96	1.81	1.88	1.83	1.55	1.68	1.73	1.65	1.82
P <sub>2</sub> O <sub>5</sub>	0.59	0.62	0.61	0.60	0.58	0.60	0.52	0.51	0.53
LOI	10.91	12.07	12.52	11.93	18.04	12.55	11.65	10.51	9.92
CIA	53.28	55.13	53.82	51.92	50.53	53.49	52.84	54.96	55.27
ICV	1.62	1.59	1.63	1.65	1.44	1.65	1.81	1.82	1.78
K <sub>2</sub> O/Na <sub>2</sub> O	0.57	0.55	0.54	0.48	0.36	0.47	0.54	0.58	0.62
SiO <sub>2</sub> /Al <sub>2</sub> O <sub>3</sub>	3.14	3.01	2.88	2.89	2.56	2.91	3.44	3.68	3.42
Al <sub>2</sub> O <sub>3</sub> /TiO <sub>2</sub>	16.84	17.91	18.15	18.45	19.07	15.80	16.57	18.70	17.38
K <sub>2</sub> O/Al <sub>2</sub> O <sub>3</sub>	0.13	0.12	0.12	0.12	0.10	0.11	0.12	0.12	0.13
MgO/Al <sub>2</sub> O <sub>3</sub>	0.23	0.24	0.26	0.28	0.27	0.27	0.28	0.27	0.27

*Table 6.1 Cont'd. Trace Element concentration in ppm for Offshore (Core 5) sediment core*

<b>Element (ppm)</b>	<b>0.1 (m)</b>	<b>0.2 (m)</b>	<b>0.3 (m)</b>	<b>0.4 (m)</b>	<b>0.5 (m)</b>	<b>0.6 (m)</b>	<b>0.7 (m)</b>	<b>0.8 (m)</b>	<b>0.88 (m)</b>
Cr	144	148	162	165	182	159	151	139	135
Co	10	10	11	11	10	11	10	10	11
Ni	46	57	60	77	81	62	69	60	54
Cu	3	17	15	42	26	46	42	54	25
Ga	14	14	16	15	12	13	12	9	15
Rb	68	68	82	60	66	52	53	53	59
Nb	9	9	11	7	8	7	7	7	7
Ba	619	531	492	472	258	435	509	471	584
La	41	46	35	36	43	50	39	31	40
Pb	56	58	69	47	52	44	44	46	49
Ce	78	68	62	77	70	91	69	79	77
Sm	5	6	5	6	5	6	5	5	5
Th	20	20	23	19	19	22	17	13	17

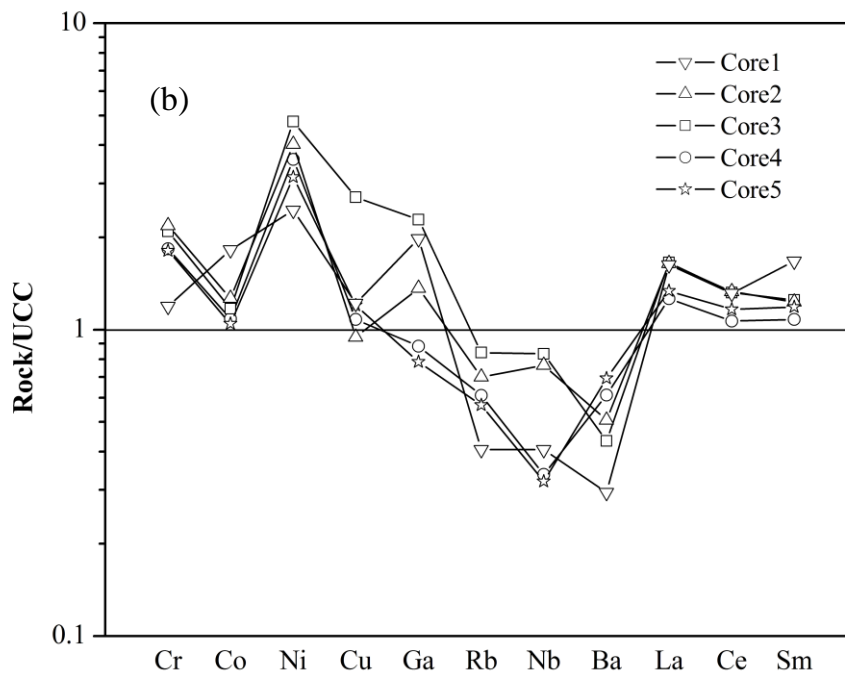
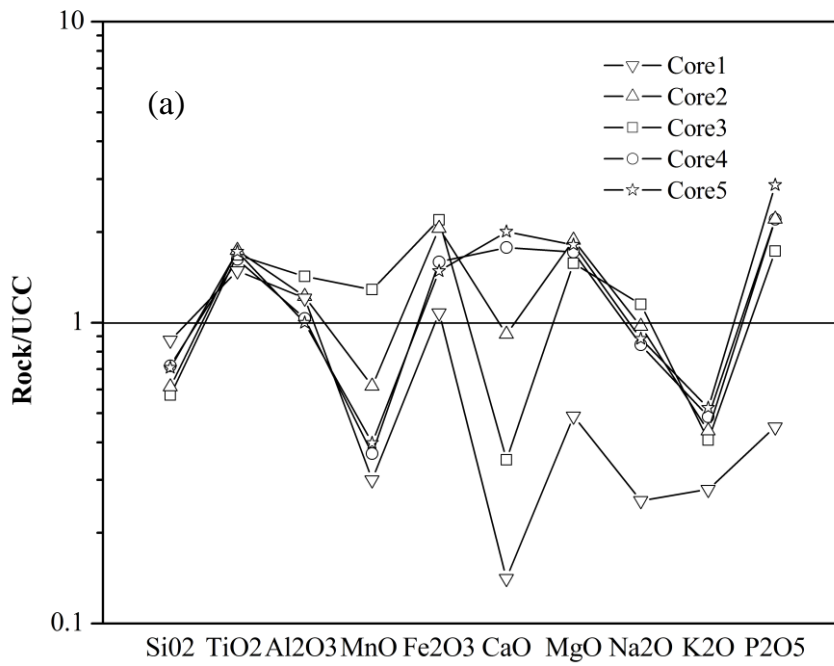


Fig. 6.1 Normalisation of Major elements (a) and Trace elements (b) diagram against Upper Continental Crust (UCC: Taylor and McLennan, 1985; McLennan, 2001)

The coastal plain core (Core 1) sediments show similar trend as estuarine sediments however, MnO, CaO, MgO, K<sub>2</sub>O and P<sub>2</sub>O<sub>5</sub> contents are much depleted than the other core sediments. The offshore sediments (Core 5) also comparable with estuarine sediments, which show higher content of CaO and P<sub>2</sub>O<sub>5</sub>, compare to other sediments and UCC.

The UCC normalised trace element distribution based on Taylor and McLennan (1985) in the core sediments representing the coastal plain, estuary and offshore is shown in figure 6.1b. Core 4 and Core 3 have lower concentrations of Rb, Nb, Ba, Y, Zr and Zn compare to UCC, whereas the Cr and Ni content in these sediments is 4-5 fold higher than the UCC. Core 3 shown higher content of Cr, Ni, Cu, Ga, La, Ce and Sm and are depleted in Rb, Nb, Ba and Zr. Co, Cu, Ce, Sm in Core 4 and Core 2, and Co, Y and Zn in Core 3 are similar to UCC. Pb and Th was only recorded in Core 4 sediments, have higher concentration than UCC. The observed depletion of Zr, and Y in Core 2 is relative to the lack of enrichment of heavy minerals like zircon and monazite by sedimentary sorting. Offshore sediments (Core 5) shows similar trend as shown by Core 4 whereas coastal plain core sediments (Core 1) show a different trend compare to estuarine and offshore sediments. Core 1 sediments show enrichment in Cr, Co, Ni, Cu, Ga, La, Ce and Sm and depletion in Rb, Nb.

SiO<sub>2</sub> and Al<sub>2</sub>O<sub>3</sub> are the two most dominant elements which shows a strong negative correlation ( $r=-0.94$ ) with respect to each other in the Core 4, Core 1, and Core 5 ( $r=-0.88$ ), while the Core 3 and Core 2 does not have any correlation and/or shows weak correlation between SiO<sub>2</sub> and Al<sub>2</sub>O<sub>3</sub>. The negative linear relationships of SiO<sub>2</sub> with other major oxides such as TiO<sub>2</sub>, Al<sub>2</sub>O<sub>3</sub>, Fe<sub>2</sub>O<sub>3</sub>, MnO, MgO, Na<sub>2</sub>O and P<sub>2</sub>O<sub>5</sub> in the sediments of Core 4 indicate that the most of silica being sequestered in quartz (Rahman and Suzuki, 2007). Both Na<sub>2</sub>O and CaO show negative correlation with Al<sub>2</sub>O<sub>3</sub> suggesting concentration of plagioclase in the Core 3 sediments than the other core sediments. Titanium is mainly concentrated in phyllosilicates (Condie et al., 1992) and TiO<sub>2</sub> is relatively immobile compared to other elements during various sedimentary processes and may strongly represent the source rocks (McLennan et al., 1993). Significantly high content of TiO<sub>2</sub> in all the core sediments (average = 0.8

wt.% in Core 4 and Core 3; 0.9 wt. % in Core 2; 0.71 wt. % in Core 1; and 0.86 wt.% in Core 5) indicate the presence of significant amounts of phyllosilicates in these sediments (Dabard, 1990), which has been released from Ti-bearing rocks by physical erosion (Cohen, 2003) through weathering and minerals containing Ti, which are not sensitive to dissolution (Demory et al., 2005). MgO have positive correlation with SiO<sub>2</sub> ( r=0.24) in Core 2 and Core 3 (r=0.17) indicate the presence of biotite while other core sediments shows negative correlation (Moosaviradi et al., 2012). Fe<sub>2</sub>O<sub>3</sub> and MgO exhibits strong positive correlation with Al<sub>2</sub>O<sub>3</sub> (r = 0.9) in the sediments of Core 4 suggests the presence of chlorite and ferromagnesian minerals (e.g., biotite, hornblende) (Moosaviradi et al., 2012). The high correlation coefficients between Fe and Ti (0.79), Fe and Mg (0.89), Fe and Mn (0.83), and Ti and Mg (0.64) in sediments of Core 4 indicate that these elements likely reside in similar mineral phases, probably biotite, muscovite and garnet. Values of Al<sub>2</sub>O<sub>3</sub>/TiO<sub>2</sub> ratio of the sediments are high in all the core sediments (average = 18.9 wt.% in Core 4; 21.2 wt.% in Core 3: 25.7 wt.% in Core 2: 17.65 in Core 5 and Core1 24.31 wt.% ), which indicate the derivation of the detrital materials from a continental source (Fyffe and Pickerill, 1993).

On K<sub>2</sub>O/Na<sub>2</sub>O vs SiO<sub>2</sub>/Al<sub>2</sub>O<sub>3</sub> plot (Fig. 6.3) all the core sediments fall away from the PAAS, UCC and Khondalites. Core 4 sediments fall nearer to intermediate charnockites and all the samples fall on the linear range of TTG, Average Garnet Biotite Gneiss and intermediate Charnockite but overall the sediments are depleted in K<sub>2</sub>O/Na<sub>2</sub>O and SiO<sub>2</sub>/Al<sub>2</sub>O<sub>3</sub> ratios. Core 4 sediments are slightly lower in K<sub>2</sub>O/Na<sub>2</sub>O and SiO<sub>2</sub>/Al<sub>2</sub>O<sub>3</sub> ratios than gneisses, intermediate Charnockites, and Khondalites of the adjacent source area (Kerala Khondalite Belt of southern India; Chacko et al., 1992). Core 5 sediment are clustered nearer to Charnockite, which clearly supports that these sediments are mainly derived from Charnockites. Core 1 sediments are clustered away from the other studied sediments and rock types. However, these sediments show higher content of SiO<sub>2</sub> and K<sub>2</sub>O than the other sediments and some of the sediments show high content SiO<sub>2</sub> and low content of K<sub>2</sub>O. Those three samples recorded very low content of SiO<sub>2</sub> and K<sub>2</sub>O. Considering the somewhat mobile nature of these major elements, the above observations suggest that this felsic to intermediate igneous rocks could be a source for these sediments.



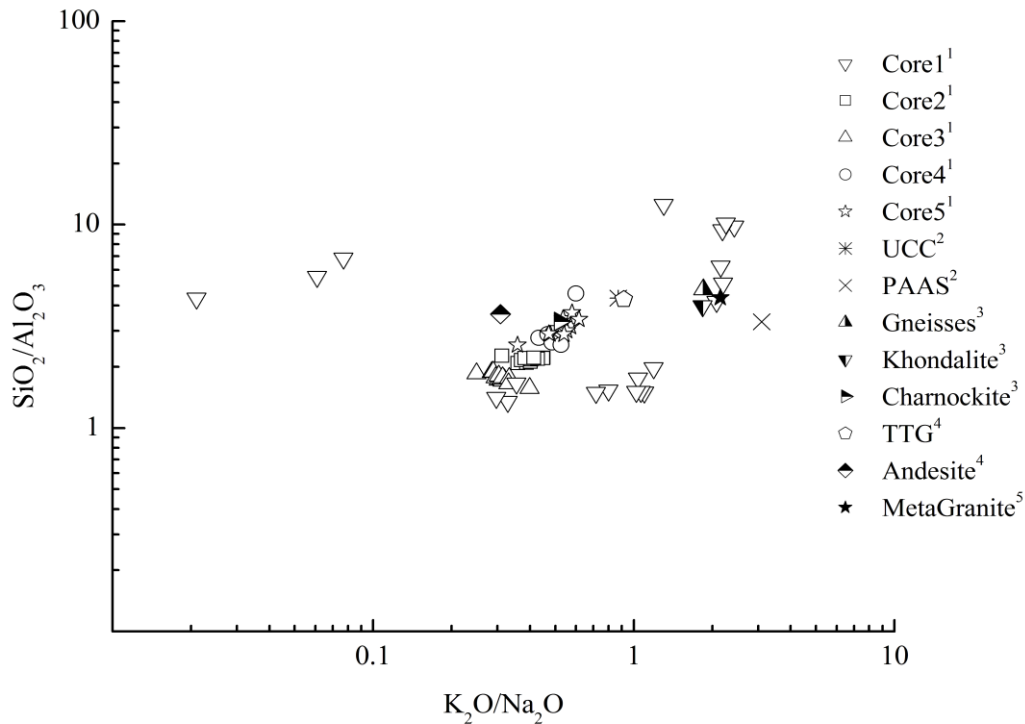


Fig. 6.2  $\text{SiO}_2/\text{Al}_2\text{O}_3$  vs  $\text{K}_2\text{O}/\text{Na}_2\text{O}$  plot for the core sediments<sup>1</sup> representing the coastal plain, estuary and offshore compared with different possible source rocks: <sup>2</sup>Taylor and McLennan (1985); <sup>3</sup>Chacko et al. (1992); <sup>4</sup>Condie (1993); <sup>5</sup>Sreejith and Ravindra Kumar (2013)

### 6.3. Geochemical Classification

Several authors (Pettijohn et al., 1972; Blatt et al., 1980) have proposed the geochemical classification diagrams for terrigenous sedimentary rocks using major elements. However, the modified classification diagram proposed by Herron (1988) facilitates arkoses to be more successfully classified than Pettijohn et al. (1972) diagram do and it is a measure of mineral stability, as the ferromagnesian minerals tend to be amongst the least stable minerals during weathering. The Log ratio of  $\text{SiO}_2/\text{Al}_2\text{O}_3$  indicates mineralogical maturity of sediment (Pettijohn, et al., 1972).  $\text{Fe}_2\text{O}_3/\text{K}_2\text{O}$  ratio is an indication of the mineralogical stability of the sediment (Herron, 1988).

In the Herron (1988; Fig. 6.3) diagram all the core sediments from estuary (Core 2,3,4), plot within Fe- shale field except one sample falls on the field of shale,

whereas coastal plain core sediments (Core 1) show wide distribution plot in the fields of Fe-shale, Fe-Sand, shale, wacke and litharenites which indicates that the chemistry and provenance show wider distribution over the stratigraphic periods. Apart from that, depositional system might be changed from quite environment to high energy environment; during this period more detrital sediments are deposited. Wide variation of  $\text{Fe}_2\text{O}_3/\text{K}_2\text{O}$  and  $\text{SiO}_2/\text{Al}_2\text{O}_3$  ratios in the inland sediments clearly indicates that these sediments are weakly to moderately mature. Offshore sediments (Core 5) typically plot in the Fe-shale field and are comparable with the estuarine core sediments.

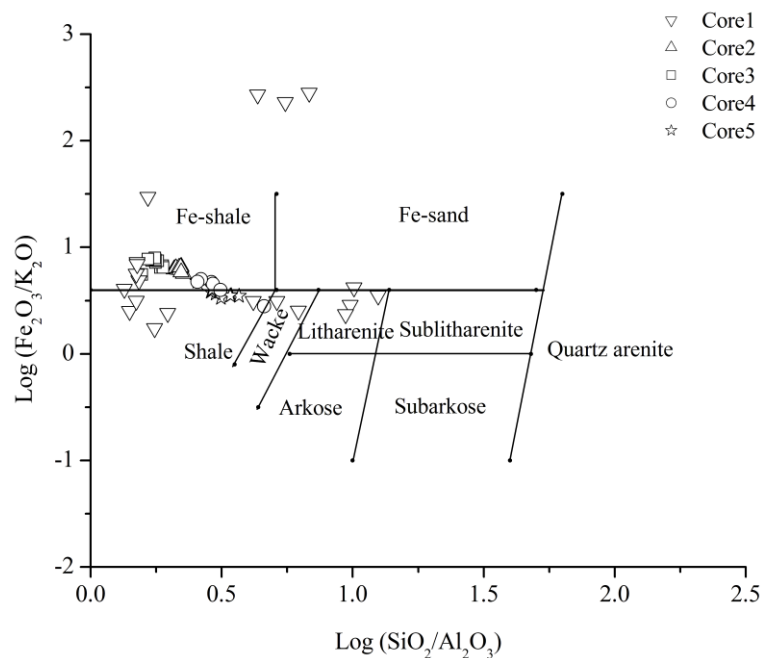


*Fig. 6.3 Geochemical classification diagram of sediment cores representing coastal plain, estuary/lagoon and offshore core sediments (after Herron, 1988)*

## 6.4. Paleoweathering and Sediment Maturity

### 6.4.1. Chemical Index of Alteration

Alteration of sedimentary rocks can be determined by various parameters like chemical index of alteration (CIA, Nesbitt and Young, 1982),  $\text{K}_2\text{O}/\text{Na}_2\text{O}$  (Nesbitt and Young, 1984; Lindsey, 1999; Dey et al., 2009),  $\text{Rb}/\text{Sr}$  (McLennan et al., 1993), and

Th/U ratios (McLennan et al., 1993). These parameters have been successfully used in several studies to identify the intensity of weathering (Hurowitz and McLennan, 2005; Selvaraj and Chen, 2006; Van Staden et al., 2006; Pe-Piper et al., 2008; Zimmermann and Spalletti, 2009; Wani and Mondal, 2010; Armstrong-Altrin et al., 2013; Nagarajan et al., 2013). In order to quantify the degree of weathering in the sediments and infer their possible provenance, the chemical Index of Alteration (CIA) was used (Nesbitt and Young, 1982) and this index was calculated using the molecular proportions as shown in the equation below:

$$\text{CIA} = [\text{Al}_2\text{O}_3 / (\text{Al}_2\text{O}_3 + \text{CaO}^* + \text{Na}_2\text{O} + \text{K}_2\text{O})] \times 100$$

Where, CaO\* is the amount of CaO incorporated in the silicate fraction of the rock. Correction for CaO from carbonate contribution was not done in this study due to the absence of CO<sub>2</sub> value. Thus, to compute for CaO\* from the silicate fraction, the assumption proposed by Bock et al. (1998) was adopted. In this regard, CaO values were accepted only if CaO < Na<sub>2</sub>O; consequently, when CaO > Na<sub>2</sub>O, it was assumed that the concentration of CaO equals to that of Na<sub>2</sub>O. This procedure provides measure of the ratio of the secondary aluminous mineral to feldspar, and forms a basis for the measure of intensity of weathering. This assumption seems to be valid as the sediments of the studied area are devoid of carbonate matter.

A CIA value of 100 indicates strong chemical weathering because all the alkali and alkaline earth elements are completely removed from the weathered sediment. Average upper continental crust (UCC) and unaltered granite rocks have CIA values of about 50 and 47, respectively. Plagioclase and potassium feldspar have a CIA value of 50. Since chemical weathering is tightly related to climate condition, these geochemical proxies have been widely used to reconstruct the paleoenvironmental changes of various marine and terrestrial sediments (Nesbitt and Young, 1982; Nesbitt et al., 1996; Vital and Statterger, 2000; Yang et al., 2004; Singh et al., 2005). The CIA is a measure of the weathering of feldspar minerals and their hydration to form clay minerals. As clay content increases Al should also increase, whereas Ca, K, and Na contents should decrease, leading to higher CIA values. Kaolinite has a CIA value of 100 and represents the highest degree of weathering. Illite is between 75 and 90, muscovite at 75, the feldspars at 50. Fresh basalts have

values between 30 and 45, fresh granites and granodiorites of 45 to 55 (Nesbitt and Young, 1982; Fedo et al., 1995).

The CIA actually reflects changes in the proportion of feldspar and various clay minerals in the weathering product (Nesbitt and Young, 1982). It is well known that aluminous minerals such as kaolinite, gibbsite and beidellite are secondarily formed while Na<sup>+</sup> and Ca<sup>2+</sup> bearing silicate minerals are significantly removed from the weathering profile during intense chemical weathering, resulting in high CIA values in the weathered sediments. As a consequence, CIA values of about 45 to 55 indicate virtually no weathering, whereas the value of 100 indicates intense weathering with complete removal of alkali and alkaline earth elements (McLennan, 1993).

Sediments from coastal plain core (Core 1) show the higher CIA values compared to estuarine and offshore core sediments, which is ranging between 72 and 91 (av. 82). Amongst estuarine core sediments, the average CIA values are recorded higher in Core 3 (av.67) than Core 4 (av. 58) and Core 2 (av.57). The average CIA values of 58 to 67 are consistent with average shale value, which indicate weak to moderate weathering in the source region (Nesbitt and Young, 1982; Nesbitt et al., 1996; Vital and Statterger, 2000; Yang et al., 2004; Singh et al., 2005). The offshore sediments show the lowest CIA values ranges between 53 and 56, which indicates that these sediments are mostly unweathered to weakly weathered (*see*, McLennan, 1993).

The intensity of weathering was also analysed using A-CN-K trilinear plot proposed by Nesbitt and Young (1982), which indicates not only the intensity of weathering but also depicts the relationship between Al<sub>2</sub>O<sub>3</sub> (aluminous clays), CaO+Na<sub>2</sub>O (Plagioclase), and K<sub>2</sub>O (K-feldspar) (Nesbitt and Young, 1984). This diagram also evaluates bulk source rock composition, diagenetic effects, and tectonism in the source area. The samples fall parallel to trend of weathering in the A-CN-K diagram indicating a little or no loss of K during weathering (Fig 6.4). The core sediments of Ashtamudi estuary and surrounding environment form a single trend originating from a bulk source composition near average granodiorite and toward smectite on the A-CN edge. Thus, the data trends along the ideal weathering trend, which theoretically should lie parallel to the A-CN edge. Estuarine (Core 2, 3 4)

sediments show that these sediment undergone weak to moderate weathering rather than intensive. Offshore (Core 5) sediments are clustered near plagioclase and potash feldspar join while coastal plain (Core 1) sediments are clustered near A-apex (CIA 72-91) indicating intensive source area weathering respectively.

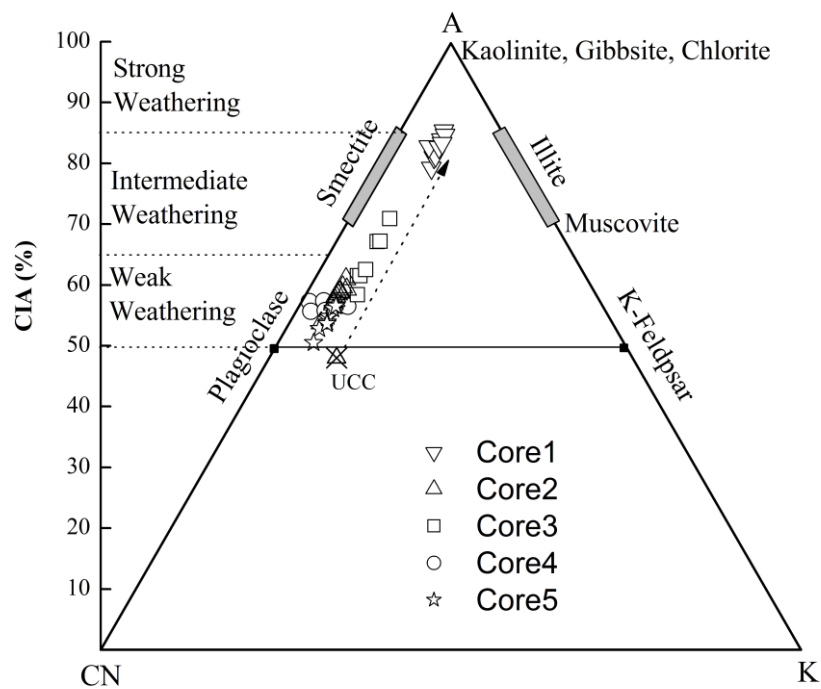


Fig. 6.4 A-CN-K ( $Al_2O_3$ -CaO+Na<sub>2</sub>O+K<sub>2</sub>O) ternary diagram showing the general weathering trend and intensity of weathering in the source region for the coastal plain, estuary and offshore (after Nesbitt and Young, 1984)

The low average CIA values in Core 4 and Core 5 sediments are due to direct input of immature continent detrital minerals into the depositional system, which indicates weak weathering of sediments of Core 2 and Core 3. Sediments of Core 1 are clustered away from the Plagioclase-K-feldspar line and plotted neared to A-apex indicates that Core 1 sediments are intensively weathered than the other core sediments. Intersection of this weathering trend with K-feldspar-plagioclase joint represents source rock composition. Backward projection of the linear trend for the studied sediments in the A-CN-K diagram can be traced to be possible granodioritic – (UCC-Intermediate) source composition.

#### 6.4.2. ICV Relation to Recycling and Weathering Intensity

Cox et al. (1995) proposed the Index of Compositional Variability (ICV), which is an approach toward assessing original detrital mineralogy for characterizing the sediments.

ICV is defined as  $[(\text{Fe}_2\text{O}_3 + \text{K}_2\text{O} + \text{Na}_2\text{O} + \text{CaO} + \text{MgO} + \text{TiO}_2) / \text{Al}_2\text{O}_3]$  and measures the abundance of alumina relative to the other major cations in a rock or mineral. ICV values for clay minerals are in the range of 0.03–0.78, and for feldspars in the range of 0.54–0.87 (Cox et al., 1995). The ICVs of constituent minerals increase, for instance, in the order of kaolinite (~0.03–0.05), montmorillonite (~0.15–0.3), muscovite-illite (~0.3), plagioclase (~0.6), alkali feldspar (~0.8–1), biotite (~8), and amphibole-pyroxene (~10–100) (Cox et al., 1995). Generally non-clay minerals show higher ICV compared to clay minerals. Typical rock forming minerals (feldspars, amphibols and pyroxenes) show ICV values >0.84, whereas typical alteration products such as Kaolinite, illite and muscovite show <0.84 (Cox et al., 1995).

The ICV values for coastal plain core sediments (Core 1) ranges from 0.18 to 0.62 (av. 0.55), except one sample with an ICV value of 1.33. This indicates matured sediments followed by tectonically quiescent or cratonic environments (Weaver, 1989) with minimal uplift and are associated with extensive chemical weathering (Cox et al., 1995), where recycling and concomitant weathering are active. However, intense chemical weathering of first-cycle material may also produce such signatures (Barshad, 1966). First cycle terrigenous sediment formed during intense chemical weathering or with long residence times in soils, however, may also become intensely weathered (Barshad, 1966; Johnsson et al., 1988) and thus form ICVs less than one.

ICV values for Ashtamudi Estuary varies significantly with higher ICV values in Core 4 sediments ranging from 1.38 to 1.70 with mean value of 1.55 than the sediments of Core 2 (1.20-1.31; av.1.26) and Core 3 sediments (0.82-1.11; av. 1.00) respectively. The ICV values of offshore core (Core 5) sediments vary from 1.44 to 1.82 with an average value of 1.67. These ICV values exhibits higher values

than PAAS (ICV=0.85; Taylor and McLennan, 1985) suggesting the predominance of rock forming minerals such as plagioclase, K-feldspar, amphiboles, pyroxenes and lithics over clay minerals as well as tend to be found in tectonically active settings which are characterised by first-cycle deposits (Pettijohn et al., 1987; Van De Kamp and Leake, 1985) in the sediments of Ashtamudi estuary and offshore.

Similarly, the variations in CIA values also indicate the sediment sorting effect. Physical sorting of sediments during transportation and deposition leads to concentration of quartz and feldspar with some heavy minerals in the coarse fraction and more weatherable minerals in the suspended load sediments (Garcia et al., 2004). Long et al. (2012) proposed the chemical maturity and intensity of weathering based on ICV and CIA ratios. ICV value in Core 4 sediments is 1.55 and offshore core (Core 5) sediments (1.67), which is higher than the sediments of Core 2 and Core 3 (1.26 and 1.00 respectively) and PAAS (ICV=0.85). These features suggest the predominance of rock forming minerals such as plagioclase, K-feldspar, amphiboles, pyroxenes and lithics over clay minerals in the sediments of Ashtamudi estuary and offshore. The Ashtamudi estuary core sediments and offshore core sediments have ICV values ranging between 0.82 to 1.60; and 1.44 to 1.82 and CIA ratios from 64 to 78 and 51 to 55. The ICV values are thus greater than PAAS (ICV = 0.85; Taylor and McLennan, 1985), whereas CIA is lower except Core 3. This confirms that the Ashtamudi estuarine sediments and offshore sediments are geochemically immature (Fig. 6.5), and were derived from a weakly to moderately weathered source as discussed above. Sediments from coastal plain (Core 1) shows CIA values ranging between 72 to 91 higher than PAAS and ICV values between 0.18 to 0.67 (except one sample ICV=1.33) lower than PAAS values clearly confirms their intense weathering condition in the source area and high maturity (Fig. 6.5). Overall, several samples have ICV>1, suggesting first cycle input (*e.g.*, Cullers and Podkovyrov, 2000).

#### **6.4.3. Textural maturity**

The ratio between SiO<sub>2</sub> and Al<sub>2</sub>O<sub>3</sub> was also used to know the textural maturity of sediments since the relative enrichment of Al-rich phyllosilicates at the expense of silica rich phases in fine grained sediments are expected (*see for e.g.*, McLennan et

al., 1993; Weltje and Eynatten, 2004). Igneous rocks show a narrow range for  $\text{SiO}_2/\text{Al}_2\text{O}_3$ , from  $\sim 3$  in basic rocks (gabbros and basalts) to  $\sim 5$  in acidic rocks such as granites and rhyolites (Le Maiter, 1976). Thus, decreased  $\text{SiO}_2/\text{Al}_2\text{O}_3$  ratio is related to decreasing in grain size or lower textural maturity (Weltje and Eynatten, 2004).

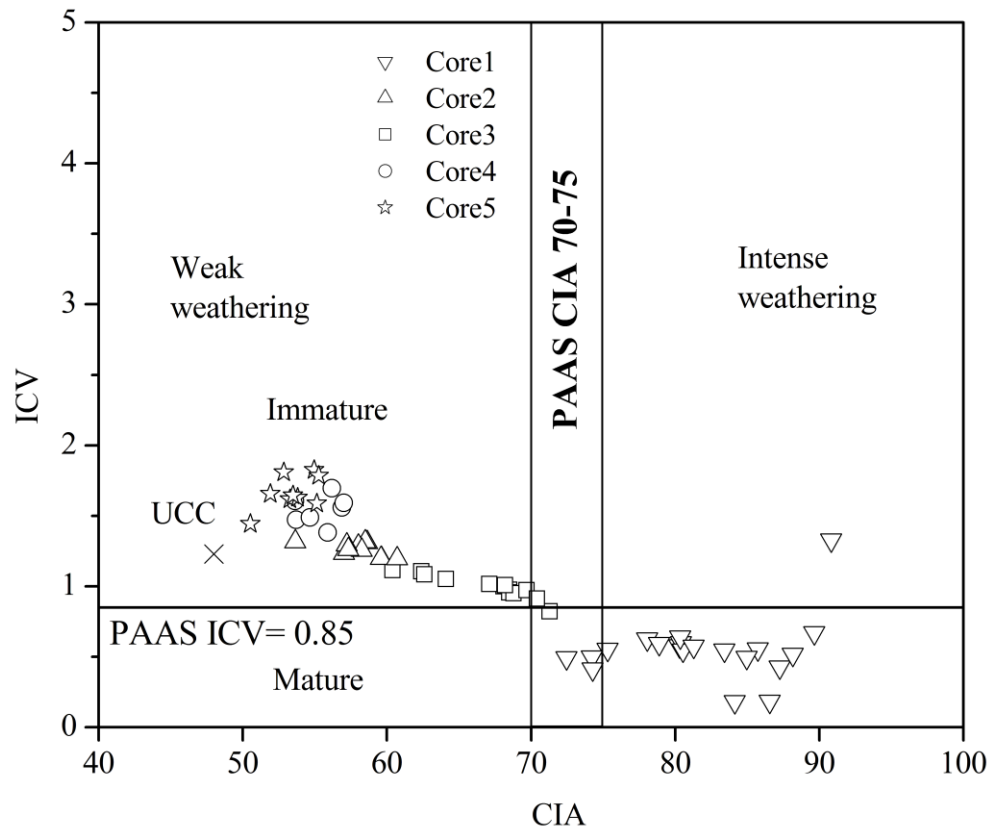


*Fig. 6.5 ICV vs CIA plot shows the maturity and intensity of chemical weathering for the sediment cores representing coastal plain, estuary and offshore (after Long et al., 2012)*

The  $\text{SiO}_2/\text{Al}_2\text{O}_3$  ratio varies between 2.6 and 4.6 (av. 3.3) for Core 4, 1.6 – 1.9 (av. 1.8) for Core 3 and 2.1 – 2.3 (av. 2.2 for Core 2) of estuarine sediments, which is lower than PAAS ( $\text{SiO}_2/\text{Al}_2\text{O}_3 \sim 3.3$ ), indicating low to moderate textural maturity and implies that sediments have undergone a minimal sedimentary cycle. The  $\text{SiO}_2/\text{Al}_2\text{O}_3$  ratio in the offshore varies from 2.6 to 3.7.  $\text{SiO}_2/\text{Al}_2\text{O}_3$  ratio of the coastal plain (Core 1) shows higher variation, which is ranging between 1.3 and 12.5 and decreasing downcore. A total of 10 samples exhibit extreme textural maturity with values ranging



from 4.3-12.5, whereas the remaining 10 samples is lower than PAAS value ranging from 1.34-1.97. The higher content of  $\text{SiO}_2/\text{Al}_2\text{O}_3$  ratio in coastal plain sediments clearly indicates that the sediments are highly matured and are derived from more felsic source, which is evident from the abundant distribution of felsic rocks in the hinterlands (Sreejith and Ravindra Kumar, 2013).

## 6.5. Provenance

Source rocks composition thought to be the dominant factor that controls the composition of sediments derived from them (Taylor and McLennan, 1985). However, secondary processes such as weathering, transport, diagenesis, etc. can have an affect on chemical composition (Cullers et al., 1987; Wronkiewicz and Condie, 1987), and therefore one has to rely on elements that show little mobility under the expected geological conditions.

The ratio between  $\text{Al}_2\text{O}_3$  and  $\text{TiO}_2$  of clastic rocks are widely used to infer the source rock composition (Garcia et al., 1994; Andersson et al., 2004), as this ratio increases from 3 to 8 for mafic igneous rocks, 8-21 for intermediate rocks and 21-70 for felsic rocks (Hayashi et al., 1997). The  $\text{Al}_2\text{O}_3/\text{TiO}_2$  ratios of estuarine Core 4 (15.9-20.3), Core 3 (24.2-30.6), and Core 2 (18.7-22.3) are more or less relatively similar to average  $\text{Al}_2\text{O}_3/\text{TiO}_2$  ratio of PAAS (18.97), which indicates the mixed composition (intermediate igneous rocks). The relative increase in  $\text{Al}_2\text{O}_3/\text{TiO}_2$  ratio in the estuarine sediments ranges from 18.9 to 25.7 indicates the intermediate to felsic source rocks (Girty et al. 1996).

Coastal plain core sediments show high  $\text{Al}_2\text{O}_3/\text{TiO}_2$  ratio (23.6) compared to offshore sediments (17.6) and is comparable with Core 4 sediments, which clearly indicate that coastal plain sediments are mostly derived from felsic source area whereas offshore sediments are mainly derived from intermediate source area. This is further supported by  $\text{TiO}_2$  vs.  $\text{Al}_2\text{O}_3$  plot based on Flyod et al. (1989) (Fig. 6.6), displays that all the analysed rocks are plotted between granite to granite+basalt (offshore sediments, Core 4 and some coastal plain sediment). Other sediments from Core 3, Core 2 and Core 1 are mostly derived from granodiorite to granitic source, which are clustered along granodiorite line and towards granite line (coastal plain

sediments).  $K_2O$  and Rb contents in sediments also can be used as an indicator of source rocks and both elements were applied successfully by many studies (Floyd and Leveridge, 1987). The K and Rb are also sensitive to sedimentary recycling processes and have been widely used as indicators for source composition (Floyd et al., 1989). In the  $K_2O$  vs Rb plot all the samples except six samples from inland sediments fall in the acid+intermediate composition field.

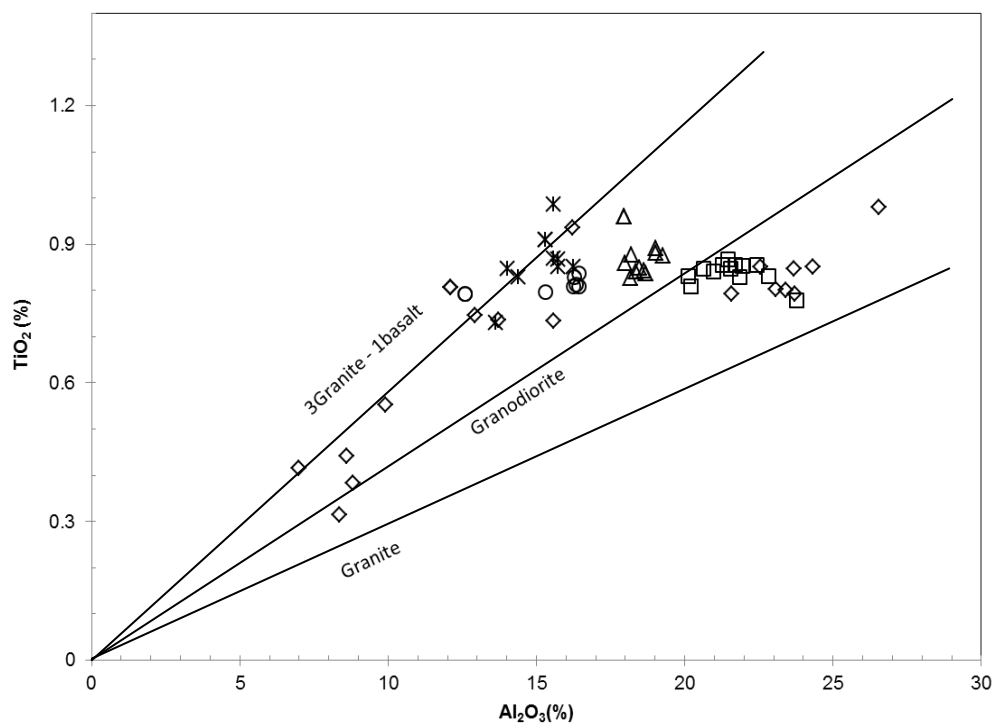


*Fig. 6.6  $TiO_2$  vs  $Al_2O_3$  (after Floyd et al., 1989) bivariate plot showing the possible provenance for the core sediments representing coastal plain, estuary and offshore*

The six samples from Core 1 fall in the basic compositions is due to low content of  $K_2O$  and may be due the fractionation and sorting effect which may be brought more ferromagnesian minerals from the source region to the depositional system. All the core sediments show uniform K/Rb ratios and they plot close to a typical differentiated magmatic suite defined by a trend with K/Rb ratio of 230 (Fig 6.7; Shaw, 1968). The high Rb concentrations (>40 ppm) and the phenomenon shown by the studied samples demonstrates the chemically coherent nature of the sediments and derivation from rocks of intermediate and acidic compositions.

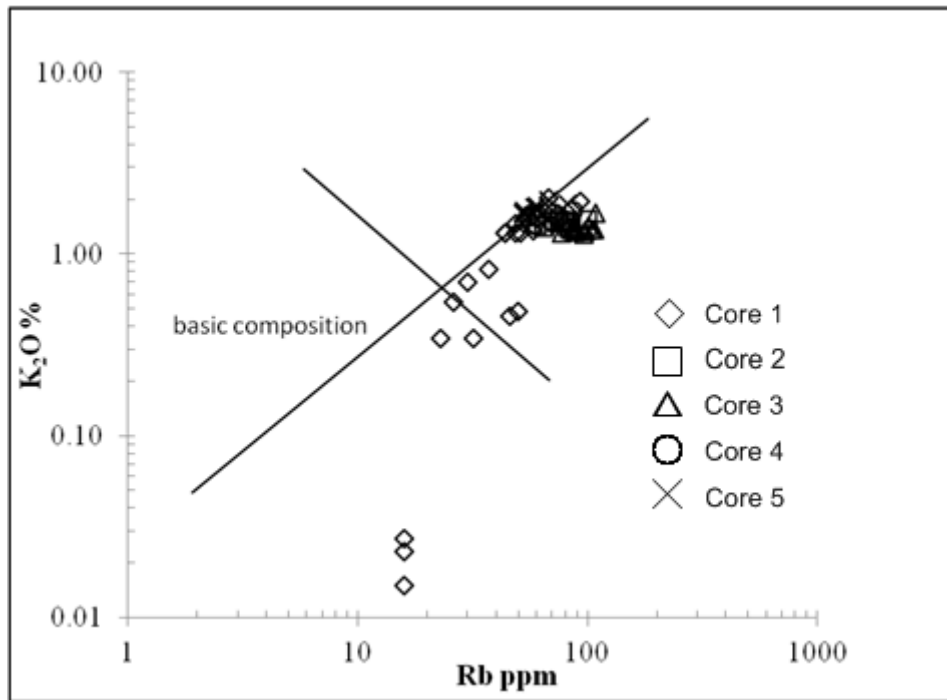


*Fig. 6.7 K<sub>2</sub>O vs Rb plot shows the provenance field for core sediments representing coastal plain, estuary and offshore*

Roser and Korsch (1988) devised a discriminant function diagram, provides a convenient method of viewing stratigraphic variation among sample suites. All the estuarine samples fall within the intermediate igneous provenance field (Fig 6.8) but one sample from core 5 fall on the felsic igneous provenance. This pattern is consistent with derivation from intermediate igneous source terrane. Core 1 sediments are mostly clustered in quartzose sedimentary provenance area which indicates that these sediments may be derived from recycled sources represented by quartzose sediments of mature continental provenance (granitic-gneissic source area), similar to PM derived sediments categorized by Roser and Korsch (1988). However, some of the Core 1 sediments fall in mafic igneous province. Overall, the estuary sediments clustered near the boundary between intermediate igneous rocks and mafic igneous rocks. Fractionation of some immature mafic minerals such as orthopyroxenes and garnets may be derived from the source area, which has elevated the ferromagnesium elements in the studied sediments. In general, the estuarine sediments (Core 2, 3, and 4) mostly derived from intermediate igneous rocks, charnockites, and gneisses and sediments fall in mafic igneous provenance indicates their immaturity.

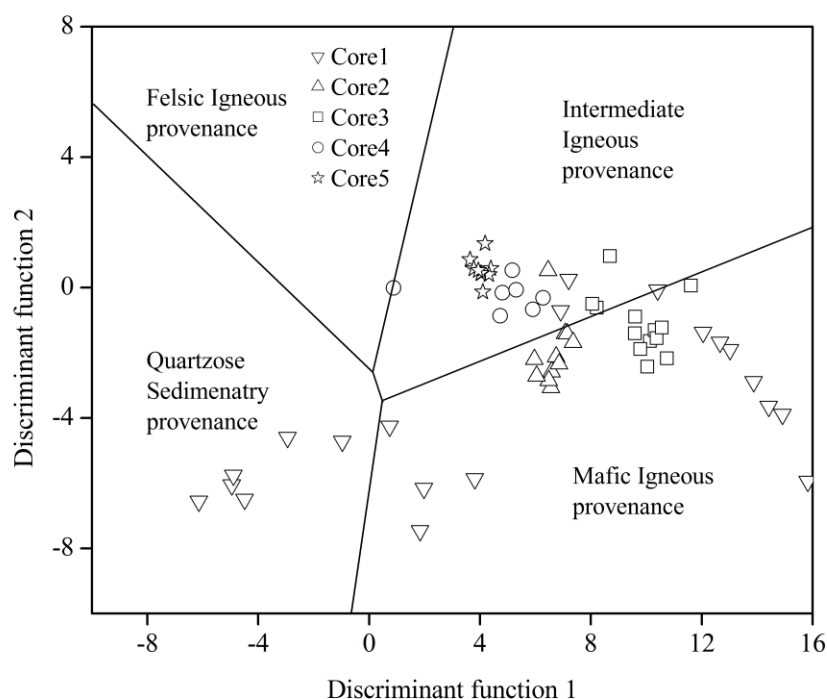


Fig. 6.8 Discriminant function diagram for the provenance signatures of the core sediments for using major elements (after Roser and Korsch, 1988). The discriminant functions are: *Discriminant Function 1* =  $(-1.773.TiO_2) + (0.607.Al_2O_3) + (0.760.Fe_2O_3) + (-1.500.MgO) + (0.616.CaO) + (0.509.Na_2O) + (-1.224.K_2O) + (-9.090)$ ; *Discriminant Function 2* =  $(0.445.TiO_2) + (0.070.Al_2O_3) + (-0.250.Fe_2O_3) + (-1.142.MgO) + (0.438.CaO) + (1.475.Na_2O) + (1.426.K_2O) + (-6.861)$ .

Trace element compositions in sediments could potentially be a source of information to determine the provenance of sediments (Kasper- Zubillaga et al., 2008; Wani and Mondal, 2010; Cao et al., 2012; Armstrong-Altrin et al., 2013; Nagarajan et al., 2013). Trace elements, such as Cr, are powerful in identifying accessory detrital components, such as chromite, commonly derived from mafic to ultramafic sources, including ophiolites, which cannot be readily recognized by petrography alone (Zimmermann and Bahlburg, 2003).

The compatible ferromagnesian trace elements such as Cr, Ni, Co and V behave similarly in magmatic processes, but they may be fractionated during weathering process (Feng and Kerrich, 1990). Mafic to ultramafic igneous rocks have higher contents of Cr, Co, Cu than silicic and intermediate igneous rocks (Brugmann

et al., 1987). Relatively immobile trace elements such as Cr and Ni undergo least fractionation during sedimentary processes. The respective average Cr values of the studied estuarine sediments vary from 156 ppm (Core 4) to 186ppm (Core 2), far above the UCC value of 83 ppm (McLennan, 2001). Cr content in inland and offshore sediments ranges between 100 ppm and 153 ppm respectively. The average Ni content also recorded higher in estuarine (Core 4: 74 ppm, Core 3: 95 ppm; Core 2: 80 ppm), Core 1 (48 ppm) and Core 5 (61 ppm) sediments indicates the mafic and/or ultramafic rocks input from the source area. Though the Cr content is recorded more than 100 ppm estuarine and coastal plain core sediments, offshore core sediments show fluctuations in the Cr content and high Cr content is recorded in certain intervals. This high and variable Cr content is probably a reflection of changing source composition, and the incoming of detrital material of intermediate/basic character (Floyd and Leveridge, 1987). It is also supported by Ni content in these sediments, average Ni content ranges between 74 and 95 ppm in Core 4 and Core 3 respectively. High content of Cr (112-225 ppm) and Ni (50-130 ppm) is reported from the Cauvery River flood plain sediments and have been considered as the result of chemical weathering of mafic source rocks (Singh and Rajamani, 2001). Ni enrichment was observed in Upper Miocene sandstones and was considered that the elevated Cr and Ni content and low Cr/Ni ratios ( $Cr > 100\text{ppm}$ ,  $Ni > 100\text{ppm}$  and Cr/Ni ratios between 1.3 and 1.5) in the sediments suggest the input from the ultramafic source rocks (Garver et al., 1996).

The average Ni content in studied sediments is recorded lower than 100 ppm except some certain intervals and high Cr/Ni ratios indicate that the fractionation of some mafic minerals such as orthopyroxene and garnet from the source area, which can increase Cr and Ni content in the sediments (Armstrong-Altrin et al., 2004). Orthopyroxenes especially hypersthene and garnets are common minerals in charnockites and gneisses in the source area (Chacko et al., 1992; Sreejith and Ravindra Kumar, 2013). The orthopyroxene grains may influence the ferromagnesian budget of sedimentary rocks through breakdown into pyrite, which can scavenge ferromagnesian elements from pore water after breakdown of pyroxenes and hornblende (Armstorng-Altrin et al., 2004, Bock et al., 1998). In addition, there is no wider distribution of ultramafic or mafic rocks in the source region. Therefore, the 4–

5 fold enrichment of Cr and Ni concentration in the sediments compared to the UCC might be related to contribution from the detrital minerals such as orthopyroxenes from Charnockite and garnet from the granulitic terrane and from the Khondalite belt of Kerala. Because, Garnet has very high Cr/Ni ratios and partition coefficients for Ni, Cr, V and Co (Torres-Alvarado et al., 2003; Armstrong-Altrin et al., 2004) can strong fractionate the Ni from other elements. This is well supported by the  $TiO_2$  vs Ni plot (Fig. 6.9) (Floyd et al., 1989) except coastal plain sediments, all estuarine and offshore sediments show constant enrichment in Ni content and show plateau values of  $TiO_2$ , which is comparable with matured sandstones and mudstones and inland sediments are mostly derived from felsic source. However, the estuarine and offshore sediments are mostly immature compared to coastal plain sediments, which is confirmed by ICV ratios and  $SiO_2/Al_2O_3$  ratios. This further indicates that sorting of heavy minerals (Garnet and Orthopyroxenes) may be masked the original provenance signatures. Confirmation of fractionation of garnet from the source rock during transportation would require the study of REE patterns of these sediments and/or petrography of these sediments.

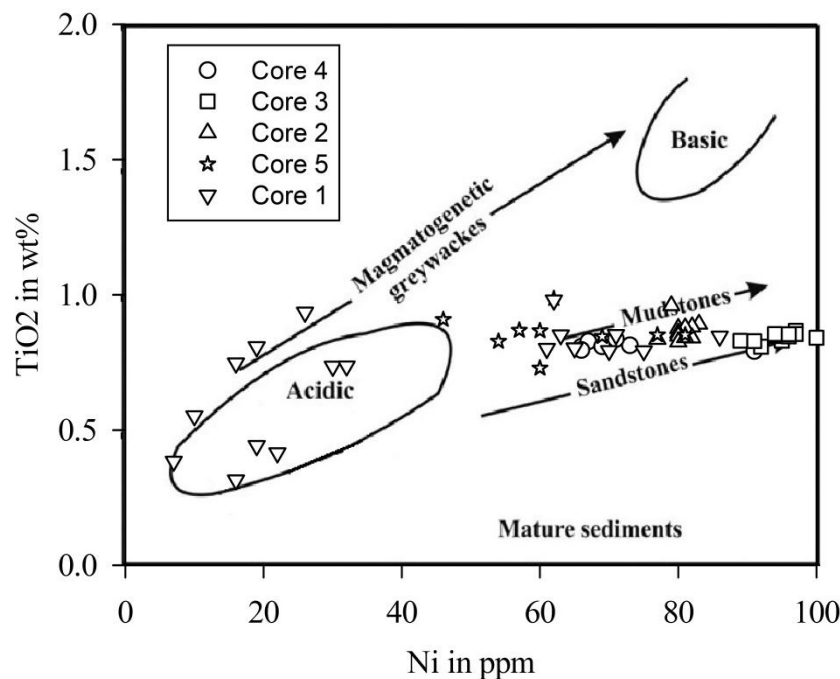


Fig. 6.9  $TiO_2$  vs Ni diagram (after Floyd et al., 1989) for the core sediments representing coastal plain, Ashtamudi estuary and offshore

## 6.6. Environment of Deposition

The relation between  $K_2O/Al_2O_3$  and  $MgO/Al_2O_3$  was used by Roaldset (1978) to differentiate between marine and non-marine clays. Majority of the core samples representing the estuary (Core 2,3,4) and offshore (Core 5) (Fig. 6.10) falls in the marine dominance except the coastal plain core sediments (Core 1), where top 7m sediment samples falls under non-marine or fresh water conditions, 7-11m samples falling along the marginal line of non-marine-marine conditions and from 11m to down the core falls under marine conditions.

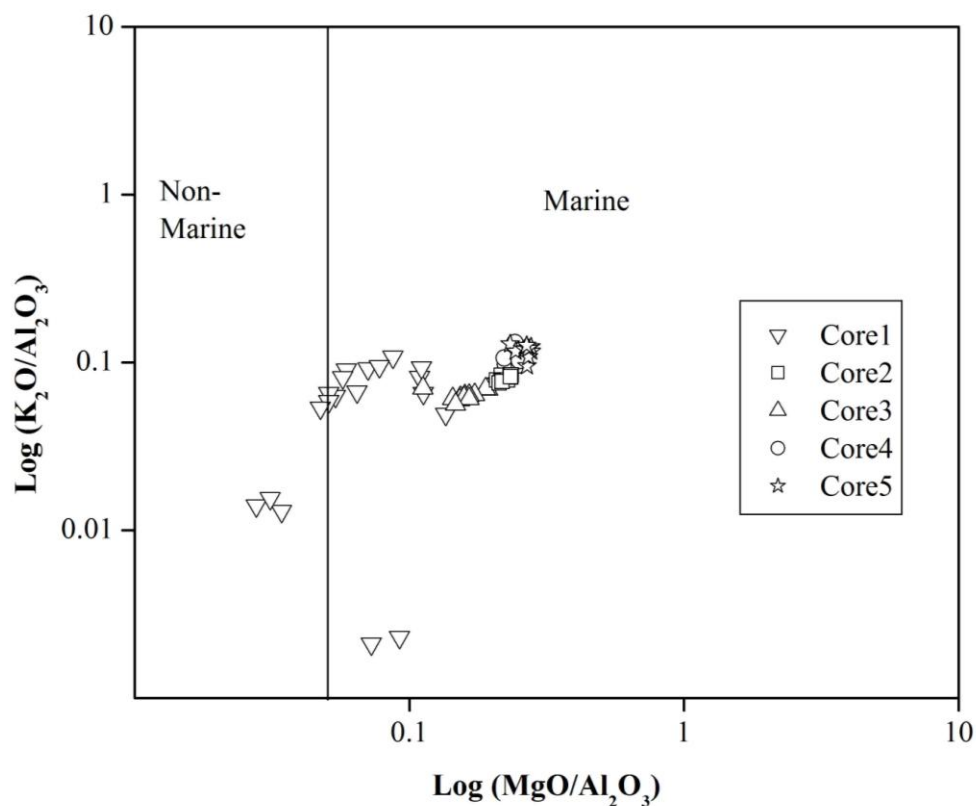


Fig. 6.10  $MgO/Al_2O_3$  and  $K_2O/Al_2O_3$  diagram (after Roaldset, 1978) to differentiate between marine and non-marine clays representing coastal plain, estuary and offshore region

## 6.7. Geoaccumulation Index (Igeo)

The geoaccumulation index (Igeo), (Muller, 1981), was used to quantitatively measure the metal pollution in the core sediments based on a pollution intensity

classification (Igeo Class), consists of seven classes (0-6; Table 6.2). The geoaccumulation index (Igeo) values were calculated for the surface sediments of study area using the equation after (Muller, 1981).

$$I_{\text{geo}} = \log [\text{Me}]_{\text{studied area}} / 1.5[\text{Me}]_{\text{baseline values}}$$

in which, [Me] baseline value represents the metal concentration in the average crust values taken from Wedepohl (1995) since the standard background values for Indian soils are not available. The 1.5 factor is included because of possible variations in the background data due to lithogenic effects (Salomons and Forstner, 1984). The highest class indicates 100 fold enrichment of metal pollution over the baseline values. As shown in Table 6.2, the calculated Igeo values from the core sediments Core 4 as follows -0.27 to -0.53 for Fe, -2.51 to 1.72 for Mn, 1.48 to 1.64 for Cr; -0.42 to 1.16 for Cu, 0.69 to 1.50 for Pb, 1.24 to 1.71 for Ni, and 0.84 to 0.92 for Co respectively. The calculated Igeo values for cores Core 3 and Core 2 are ranges as follows 0.46 to 0.68 and 0.36 to 0.61 for Fe, -0.67 to 0.18 and -1.67 to 1.88 for Mn, 1.61 to 1.86 and -0.03 to 1.86 for Cr; 0.62 to 2.75 and -0.72 to 0.22 for Cu, -1.08 to 0.82 and -5.29 to -2.12 for Zn, 1.67 to 1.87 and 1.46 to 1.57 for Ni, and 0.63 to 0.75 and 0.77 to 0.97 for Co in the sediments of Core 3 and Core 2 respectively.

The average geoaccumulation indexes are less than zero for Mn in AS 05; Mn and Zn in Core 3; and Cu and Zn in Core 2 suggesting that the sediments have not been polluted by these metals. Based on the individual trace metals Igeo values, Core 4 and Core 2 core sediments are categorized as unpolluted to moderately polluted (Igeo class 0-2), whereas Core 3 sediments are categorized as unpolluted to Strongly polluted (Igeo class 0-3). 26% of the elements belong to Igeo class 0; 39% of the elements belong to Igeo class 1 (unpolluted to moderately polluted) and 36% of the elements belong to Igeo class 2 (moderately polluted). The remaining 0.86% of the elements (Cu) in sediments of Core 3 belonged to Igeo class 3 (moderate – extremely polluted). Overall, results from this study indicated that Core 4 sediments are moderately polluted with Cr, Pb and Ni; Core 3 sediments are moderate to strongly polluted with Cr, Cu and Ni and Core 2 sediments are moderate to strongly polluted with Cr and Ni.



Table 6.2 Geoaccumulation index (Igeo) for core sediments of Ashtamudi Estuary

Sample Number	Igeo value (class)						
	<0 (0)	0-1 (1)	1-2 (2)	2-3 (3)	3-4 (4)	4-5 (5)	>5 (6)
Core 4 – 01	Fe, Mn	Cu, Pb, Co	Cr, Ni				
Core 4– 02	Fe, Mn	Cu, Pb, Co	Cr, Ni				
Core 4– 03	Mn, Cu	Fe, Pb, Co	Cr, Ni				
Core 4– 04	Mn	Fe,Cu, Co	Cr, Pb, Ni				
Core 4– 05	Mn	Fe,Cu, Co	Cr, Pb, Ni				
Core 4– 06	Mn, Cu	Fe,Co	Cr, Pb, Ni				
Core 4– 07	Mn	Fe,Pb, Co	Cr, Cu, Ni				
Core 4– 08	Mn, Cu	Fe,Pb, Co	Cr, Ni				
Core 3 – 01	Mn, Zn	Fe,Co	Cr, Cu, Ni				
Core 3 – 02	Mn, Zn	Fe,Co	Cr, Cu, Ni				
Core 3 – 03	Mn, Zn	Fe,Co	Cr, Cu, Ni				
Core 3 – 04	Mn, Zn	Fe,Co	Cr, Ni	Cu			
Core 3 – 05	Mn, Zn	Fe, Cu, Co	Cr, Ni				
Core 3 – 06	Zn	Fe, Mn, Co	Cr, Cu, Ni				
Core 3 – 06	Mn, Zn	Fe, Co	Cr, Cu, Ni				
Core 3 – 07	Mn, Zn	Fe, Co	Cr, Cu, Ni				
Core 3 – 08	Mn, Zn	Fe, Co	Cr, Cu, Ni				
Core 3 – 09	Mn	Fe, Zn, Co	Cr, Cu, Ni				
Core 3 – 10	Mn	Fe, Zn, Co	Cr, Cu, Ni				
Core 3 – 11	Mn	Fe, Zn, Co	Cr, Cu, Ni				
Core 3 – 12		Fe, Mn, Zn, Co	Cr, Ni	Cu			
Core 3 – 13	Mn, Zn	Fe, Co	Cr, Cu, Ni				
Core 2 – 01	Mn, Cu,	Fe, Co	Cr, Ni				
Core 2 – 02	Mn, Cu	Fe, Co	Cr, Ni				
Core 2 – 03	Mn, Cu, Zn	Fe, Co	Cr, Ni				
Core 2 – 04	Mn, Cu, Zn	Fe, Co	Cr, Ni				
Core 2 – 05	Mn	Fe, Cu, Co	Cr, Ni				
Core 2 – 06	Mn, Zn	Fe, Cu, Co	Cr, Ni				
Core 2 – 07	Mn, Zn	Fe, Cu, Co	Cr, Ni				
Core 2 – 08	Mn, Cu, Zn	Fe, Co	Cr, Ni				
Core 2 – 09	Mn, Zn	Fe, Cu, Co	Cr, Ni				
Core 2 – 10	Mn, Zn	Fe, Cu, Co	Cr, Ni				
Core 2 – 11	Mn	Fe, Cu, Co	Cr, Ni				
Core 2 – 12	Mn, Cu	Fe, Co	Cr, Ni				
<b>OP</b>	<b>25.75% (60)</b>	<b>38.63% (90)</b>	<b>35.62% (83)</b>	<b>0.86% (02)</b>			

Igeo value <0 (0) unpolluted, 0-1 (1) from unpolluted to moderately polluted, 1-2 (2) moderately polluted, 2-3 (3) from moderately polluted to strongly polluted, 3-4 (4) strongly polluted, 4-5 (5) from strongly polluted to extremely polluted, >5 (6) extremely polluted

## 6.8. Summary

The geochemical characterisation of sediment cores have been carried out to address the source rock composition, sediment maturity, palaeo-weathering and diagenetic processes. The ICV values for coastal plain core sediments (Core 1) suggesting matured characteristics of sediments which were subjected to tectonically quiescent or cratonic environments with minimal uplift. Extensive chemical weathering, where recycling and concomitant weathering are active is also indicated by the data. ICV values for Ashtamudi Estuary varies significantly with higher values in Core 4 sediments than the sediments of Core 2 and Core 3 sediments. These ICV values exhibits higher values than PAAS (ICV=0.85); suggesting the predominance of rock forming minerals such as plagioclase, K-feldspar, amphiboles, pyroxenes and lithics over clay minerals as well as tend to be found in tectonically active settings which are characterised by first-cycle deposits in the sediments of Ashtamudi estuary and offshore. Ashtamudi estuarine sediments and offshore sediments are geochemically immature, and were derived from a weakly to moderately weathered source. The  $\text{SiO}_2/\text{Al}_2\text{O}_3$  ratio of estuarine sediments, is lower than PAAS ( $\text{SiO}_2/\text{Al}_2\text{O}_3 \sim 3.3$ ), indicating low to moderate textural maturity, implying that Ashtamudi estuary sediments have undergone a minimal sedimentary cycle. The higher content of  $\text{SiO}_2/\text{Al}_2\text{O}_3$  ratio in coastal plain sediments clearly indicates that the sediments are highly matured and are derived from more felsic source, which is evident from the abundant distribution of felsic rocks in the hinterlands. All the core sediments from estuary (Core 2,3,4) indicates that the chemistry and provenance show wider distribution over the stratigraphic periods. Application of discriminant diagrams for the estuarine samples suggest intermediate igneous provenance (see Fig 6.9) suggesting that sediments derived from intermediate igneous provenance. Core 1 sediments are mostly clustered in quartzose sedimentary provenance, few plotting in igneous field. These sediments are interpreted to have derived from recycled sources. Majority of the core samples representing the estuary (Core 2,3,4) and offshore (Core 5), are except the coastal plain core sediments (Core 1), show marine dominance. The geo-accumulation index (I<sub>geo</sub>) values for the surface sediments of study area suggest varying element and concentration levels.

# CHAPTER 7

## DEPOSITIONAL ENVIRONMENTS AND COASTAL EVOLUTION

### 7.1. Introduction

The coastal lands of the study area comprises of different sub-environments, which includes coastal plain, river, estuaries, lagoon, marshes, dunes and beaches. Since each of these environments is characterized by unique sediment characteristics the determination and interpretation of sediment characteristics is particularly important for a better understanding of the evolution of the coastal plain during the Quaternary. Further, the study of sediment characteristics in relation to the depositional features is important in terms of resource exploitation of the various natural resources in the coastal region.

### 7.2. Depositional Environment

The surface sediments of the southern and northern sector transects and its adjoining coastal plain show a wide spectrum of textural classes viz., sand, siltyclay, clayey silt, mud, etc. The coastal plain bordering the river-estuary confluence on the southern sector is covered by coarse sand and gravel dominated sediments whereas the northern sector is covered by fine sand mixed with siltyclay sediments. The coarse sand and gravel representing the top 9 m of the sediment core were deposited under the '*violent to most violent environment*'. Below these depths the sediments were deposited during the '*quite environment*' which is similar to the samples of the estuarine cores. That means below the 9 m depth the depositional conditions are similar. The sediment of the offshore Core 5 falls in the category III indicating '*violent environment*'. Though the samples of the northern coastal sector also show a similar trend in the energy condition the sediments were deposited under a comparatively low energy depositional regime.

In contrast, the ternary plots of sand, silt and clay after Pejrup (1988) showing the inferred depositional environments of the southern coastal plain sediments fall under the *open channel* conditions indicating high energy, whereas the sediments below it falls in the closed basin indicating low energy, which is an indication of

*partially open to restricted estuary*. In the northern coastal plain also the sediments were deposited in almost similar conditions. This indicates that the sedimentation took place under a moderate environmental setting. The river-estuary region of the southern coastal plain is characterised by a faster sedimentation process from the fluvial source because of the early Holocene climatic optimum, whereas the lower part of core is influenced by still-water condition under the rising Holocene sea level rise through the incised estuarine basin.

### **7.3. Relationship between Organic matter and Calcium Carbonate**

There is an intimate relationship between the climate and sedimentation pattern that has a synergistic effect on preservation potential of the organic matter and CaCO<sub>3</sub> in the sediments. Carbonate content of sediments has been found to be a good indicator of the glacial and inter-glacial stages. Generally high concentration of CaCO<sub>3</sub> indicates cooler periods while a lower content indicates warmer period.

The top 9 m of the sediment Core 1 representing the southern transect has less percentage of organic matter and negligible amount of calcium carbonates. At a depth of 11 to 15.5 m the organic matter has increased to as high as 47 % with a range of 7 to 15 %. This anomalous enrichment of organic matter was dated with an age of 42,000 Yrs BP representing the first marine transgression event during the late Pleistocene period in the study area. In the estuary the organic matter and calcium carbonate are varying in all the three cores (Core 2, 3 & 4) as it represents the sink for the fluvial detritus. The offshore region has a calcium carbonate of 9 to 14 % with < 5 % organic matter. The organic matter is less throughout the sediment core of the northern coastal plain. The calcium carbonate content is < 1.5 % up to a depth of 9 m but from 10 m downwards the percentage has increased considerably going even up to 38 % and that can be attributed to the inter-glacial period causing marine transgression. In the lagoon and offshore area the organic matter and calcium carbonates are in varying proportion limited to a maximum of 8 and 15 % respectively.

### **7.4. Geochemical Proxies**

The various major and trace elemental composition of the core sediment and their inter-relationships were studied to understand the depositional environment that

prevailed in the coastal area. Some of the geochemical proxies were used to identify provenance of these sediments. The relation between  $K_2O/Al_2O_3$  and  $MgO/Al_2O_3$  was used to differentiate between the marine and non-marine clays. Majority of the core samples representing the southern transect falls in the marine dominance except the coastal plain core (Core 1), where the top 7 m sediment falls under the non-marine conditions or fresh water conditions, 7-11 m samples falling along marginal line of non-marine -marine (mixed) conditions and from 11 m to down the core falls under marine conditions which further substantiates the late Pleistocene transgression event. The Ashtamudi estuary cores as well as the offshore sediments fall totally in the marine environment.

## **7.5. Bathymetry**

The bathymetry of the Ashtamudi estuary prepared as part of the Ashtamudi Management Plan (Kurian et al., 2001) is used here to understand the bottom configuration of the estuarine basin (Fig. 7.1). Most of the estuary is shallow ( $< 3$  m) with maximum depths of up to 14 m measured in the eastern kayal where the Kallada river debouches into the estuary. Depths in the northern central kayal reach up to 10 m whereas the southern central kayal is very shallow showing a depth of  $< 1$  m. The estuary also has a few deep gorges in the eastern part near to the Kallada river confluence. At present, the estuary is connected with the Sea by a comparatively narrow entrance channel. The present width of the basin is over-sized compared to the narrow channel at the estuarine mouth. It may be conjectured that the present width of the lake is the result of the erosional phase that prevailed during the late Pleistocene period. The bathymetric contours and the presence of many flood tide islands at the estuarine entrance are indicative of the high input of sediments from the nearshore regions. Modelling studies carried out for the Ashtamudi estuary as part of the estuarine management plan do indicate the arrival of sediments from the offshore (Black and Mathew, 2001). All these features indicate that the lake basin has started getting filled up by the transport of sediments from the nearshore region due to tidal flux. In addition, the eastern end of the estuary also started getting filled by the sediments brought through the river channels.

The input of sediment was at much higher rate during the middle Holocene (Padmalal et al., 2013) though the process has slowed down in recent years as

compared to the sediment from the nearshore environments. The incised valley formed on the bed of the estuary started filling at both ends and has intermittently resulted in funnel shaped depression in the eastern part of the estuary. The overall contribution of the sediments from the river catchments region and siltation of estuarine mouth might be responsible for the present configuration of estuarine basin. Much faster arrival of sediment from the offshore might have initiated during the early Holocene transgression event.

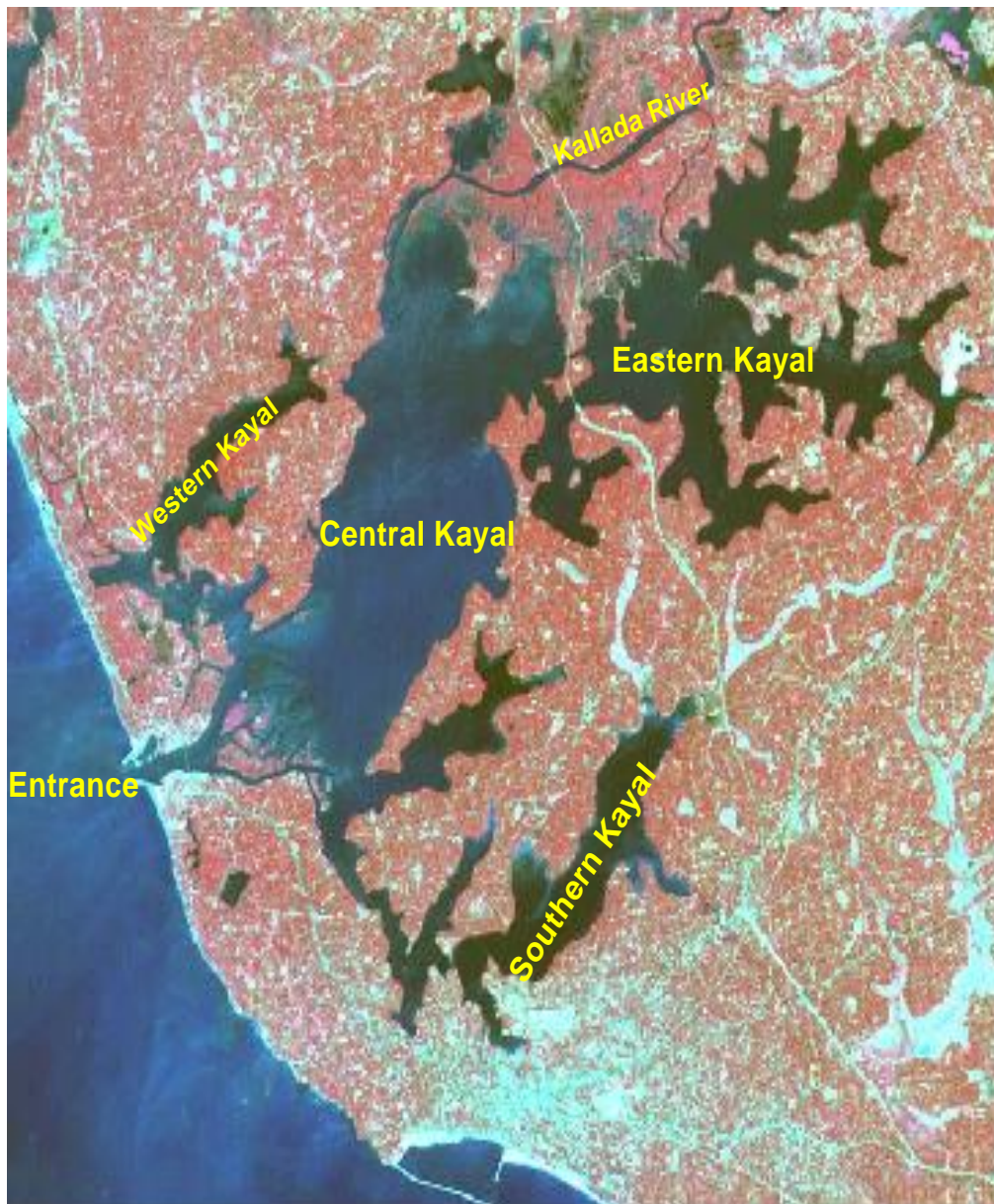


*Fig. 7.1 Kayals of the Ashtamudi estuary*

## 7.6. Holocene sea level changes

Holocene sea level changes documented by Woodroff and Horton (2005) reveal broad similarity in all the locations in the Indo-Pacific region. However, these authors believe that differences do exist, in the timing and magnitude of the Mid-Holocene High Stand (MHHS) and the nature of late Holocene sea level fall across the region. This is probably due to lack of consistent methodology throughout the Indo-Pacific for the analysis of sea level change. When the Indo-Pacific is subdivided into smaller regions, these discrepancies do not disappear, and in some cases the discrepancies are large within a single coastline.

Banerjee (2000) reconstructed the mid Holocene sea level changes for the east coast of India using Radiocarbon and Uranium series methods by dating beach ridges, *Porites* coral colony and intertidal shells at 5 locations. He identified the 1<sup>st</sup> high stand of sea level at 7,300–5,660 Yrs BP and 2<sup>nd</sup> high stand at 4,330–2,500 Yrs BP. Katupotha and Fujiwara (1988) used radiocarbon dating of corals and marine shells at 4 locations along the Srilankan coast and recognized the 1st high stand sea level at 6,485–5,370 Yrs BP and 2<sup>nd</sup> high stand at 2,902–1,558 Yrs BP in mid Holocene.

Ramsay (1995) produced a 9,000 Yrs BP record showing the early Holocene rising sea level (RSL) rise to a mid-Holocene high stand of +3.5 m at 4,650 Yrs BP with RSL subsequently falling below the present levels, but also identified a secondary high stand at 1,610 Yrs BP (+1.5 m) before the attainment of the mean sea level at 900 Yrs BP. The sea-level observations are taken from a 180 km long stretch of coastline in the eastern South Africa, thus reflecting regional RSL influences. It may be observed here that the Holocene sea level changes of the South African and Srilankan coasts show close similarity.

Since, the present study area is in close geographic enclosure with the Sri Lankan coast, it is prudent to extrapolate the Holocene sea level changes to the present study area on the west coast of India. Pluet and Pirazzoli (1991) reconstructed sea level changes during Holocene for both stable and Deltaic regions throughout the world. According to the world Atlas of the Holocene sea level changes (Pluet and Pirazzoli, 1991) the sea level high stand was around 1,200 Yrs BP and the subsequent gradual transgression led to the present mean sea levels attained around 900 Yrs BP.

By correlating the age dates of 940 years at 1.0–1.08 m in Core 2 of the Ashtamudi estuary, the bottom depth is likely to fall within the transgressive phase of the late Holocene sea level.

### **7.7. Evolution of the coast**

The ancient sediments exposed near the shoreline are manifestations of specific environments of deposition. The instantaneous position of the shoreline results from the sea level variations and the rate of subsidence. The present day surface of the continental shelf and the coastal plain has resulted from the eustatic sea level fluctuations during the Quaternary. The rising of sea level results in transgression or landward migration of the shoreline. Conversely, the falling sea level results in seaward migration of the shoreline or regression. However, determination of different aspects of transgression and regression such as the duration of time involved, rate of sediment supply, rate of dispersal and deposition of sediments are seldom achieved with precision. Moreover, it is difficult to assess the relative role of the Eustatic sea level change and tectonic movement responsible for the shoreline evolution.

The paleo-coastline of the study area during the late Pleistocene, early Holocene and LGM during the last 18,000 Yrs BP along with the substrate is shown in figure 7.2. These paleo-coastlines in any part of the globe are formed due to rise and fall of the sea level at different stages during the Quaternary period. There are two stages of which the Stage 1 beginning in the late Pleistocene approximately at 18,000–19,000 Yrs BP, continued progressively through the Holocene to the present. This rise in the sea level is directly related to the melting of polar glaciers called the Stage 2 (Wisconsin). The rate of melting and the proportional sea level rise was not constant through time. Sea level rose quickly during warm periods, but stopped or even temporarily fell during the cold periods.

The evolution of coastal lands of the region has been influenced by regional factors including changes in climate, sea level, and local and regional tectonics as depicted in the conceptual model (Fig. 7.3). There are many pieces of evidences in the study area indicating that the region has been subjected to a series transgression and



regression starting as early as in the late Pleistocene unlike the earlier report as Holocene (Padmalal et al., 2011).

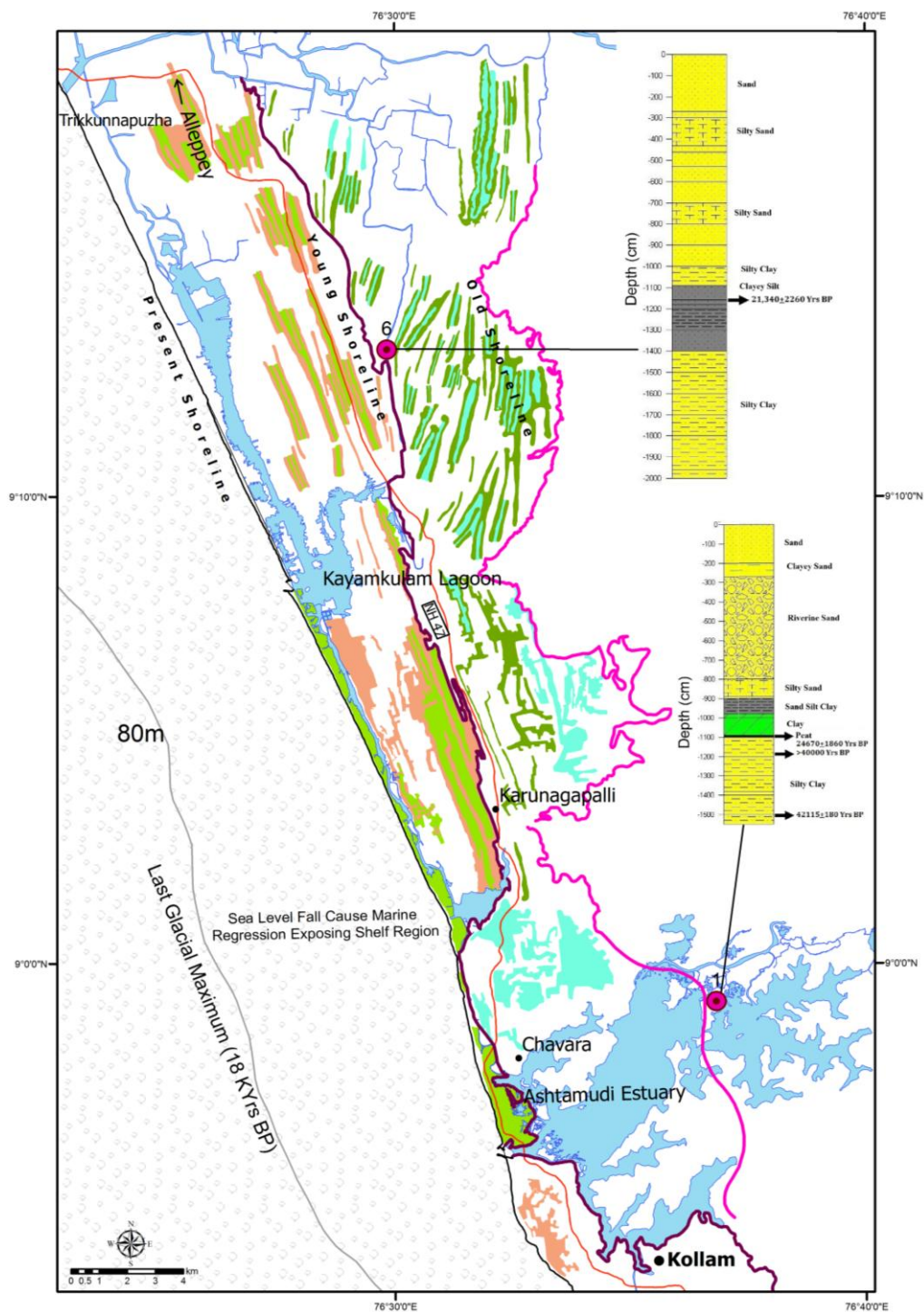
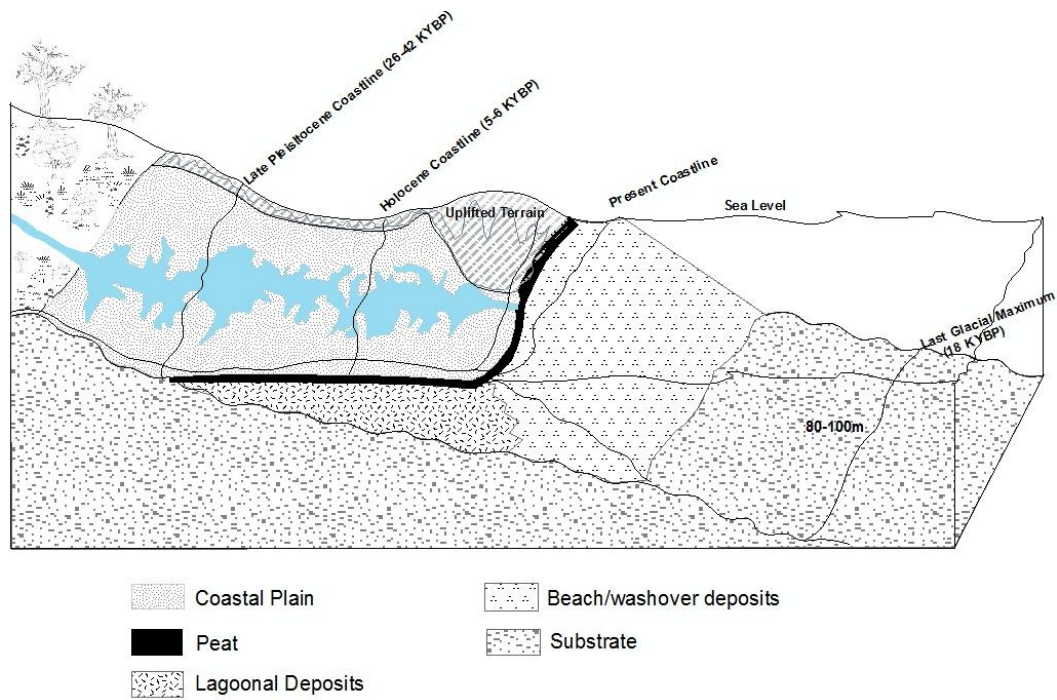


Fig. 7.2 Paleo-shoreline derived from geomorphological signatures and radiocarbon dating during Late Holocene (5,000 to 6,000 Yrs BP) and Late Pleistocene (42,000 Yrs BP). Borehole lithology of 1 & 6 showing peat and corresponding  $^{14}\text{C}$  dates. Sea level fall cause marine regression exposing shelf region even up to 80 m during LGM.



*Fig. 7.3 Conceptual model showing the evolution of the coast during the Quaternary*

The present study, for the first time, reports a peat layer at a depth of 11 m in sediment Core 1 yielded an age  $24,670 \pm 1,869$  Yrs BP and further down at 15.0 m has yielded an age of  $42,115 \pm 180$  Yrs BP representing the old coastline (See also Table. 4.10 in Chapter 4). Many evidences exist in the Kerala coast to reveal that the region was subjected to several spells of sea level rise and falls and the first marine transgression in the study area took place around 42,000 Yrs BP followed by the gradual lowering of sea level corresponding to the Last Glacial Maximum (LGM) which is approximately at 80 to 110 m water depth from the present day shoreline. The high rainfall during >40,000 to 28,000 Yrs BP has brought many depositional and landform features. Some of the depositional features seen are ferruginous yellow clay, white clay or clayey sand, peat etc., on the continental environment.

Following the Flandrian transgression from the LGM the sea level rose rapidly in the late Pleistocene but the rate of sea level rise has slowed down drastically during the progress of the Holocene. The Kallada River, which was part of a major river debouching sediment much inside into the shelf resulted in the development of valleys over the Neogene sediments. These valleys were subsequently broadened during the mid-Holocene period due to heavy precipitation. The Neogene sediments (Quilon and Warkali beds) are exposed on the uplifted southern block of the study area. The

presence of uplifted terrain on the southern side resulting in the river/estuarine entrenchment following the formation of a bay head environment.

There are also reports indicating that the Kallada River was a major deltaic system of which offshore evidences are reported in the geophysical surveys carried out by the National Institute of Oceanography, Goa (*Personal communication*). The formation of bay head delta on the upper part of estuarine basins began in the Early Holocene as is evident from the  $^{14}\text{C}$  age  $8,296\pm 44$  Yrs BP (Padmalal et al., 2011). Based on the new set of  $^{14}\text{C}$  age ranging between 42,000 and 24,000 Yrs BP, the formation of the bay head delta was initiated as early as late Pleistocene.

The intense rainfall witnessed during the early Holocene not only broadened valleys and eroded the sediment when the sea level was much lower during the LGM. The surface exposure of the Quilon bed seen on the periphery of the estuary further substantiates erosion of the Neogene sediments. The rise in the sea level during 5,000 to 6,000 Yrs BP had forced deposition of river-borne materials/alluvium leading to the filling of channels and building of sediments in the river mouth zones. This is evident from the rich deposit of fluvial sediment of nearly 9 m. The characteristics of these sediments are studied applying SEM technique and details are given in Chapter 5. The progradation of the alluvial sediments towards the estuarine zones brought out many separate water bodies in the basin including the formation of many fresh water lakes from the Ashtamudi estuary (Padmalal et al., 2013). The bell shape coastline formed during 6,000 to 5,000 Yrs BP in the study area shows further evidence of progradation of the Holocene coastline.

## **7.8. Evolution of Ashtamudi Estuary**

Palaeo records of sediment cores provide evidence of a prograding coastline indicating the occurrence of Quaternary formations at various elevations along the Kerala coast. Also the formation of a chain of coast-parallel estuaries/lagoons with rivers debouching into them and separated from the sea by spits/bars is reported. Padmalal et al. (2011) and Nair et al. (2010) through sedimentological and palynological analysis of the boreholes samples around the Ashtamudi estuary deciphered a thick sequence of Holocene sediments (20–35.0 m) containing good archives of landform evolution and climate changes. The sediment lithological

variations from the above observations and a detailed sedimentological study along with carbon dating has brought out clear understanding on the evolution of estuary during the Quaternary. In the southern coastal plain bordering the Asthamudi estuary the results of sediment lithology indicates several deposition as well as erosion episodes. The top 7 m is carpeted with fluvial sand of medium to fine grade of angular to sub-angular in nature is considered to be of recent deposition. This is also well documented in the SEM studies. Below 7 to 9 m are medium to coarse sand with occasional gravel and brachiopods shells indicating a change in the deposition scenario of shallow marine to lagoonal and swamp/marsh environment. Overpeck et al. (1996) concluded that the monsoon strength increased suddenly in two steps, 13,000–12,500 Yrs BP and 10,000–9,500 Yrs BP. Most climatic proxies suggest that the stronger monsoon in the early Holocene was associated with the high lake levels; increased flow discharges floods and scouring (Kale et al., 2004). The stronger monsoon during the early Holocene results in the formation incised valley at the entrance of the Kallada River. This was followed by the Holocene transgression event submerging the adjacent coastal plain resulting in the formation of coast perpendicular estuary. The Pleistocene-Holocene boundaries were also encountered in the study area. The Holocene sediment was replaced by 7 to 9 m thick modern sediments which is directly overlying the late Pleistocene of 40,000 Yrs BP.

## CHAPTER 8

### SUMMARY AND CONCLUSIONS

#### 8.1. Summary

The geological and geomorphological signatures of sea level changes during the Quaternary period have been reported in general for the Indian coast by many researchers during the last two decades. However, studies for the Kerala coast, which is known for various coastal landforms such as estuaries, lagoons, backwaters, coastal plains, cliffs and barrier beaches, are limited. The present study deals with sedimentological and geochemical characteristics of late Quaternary sediments and attempts to reconstruct of palaeo-environmental conditions of the central Kerala coast. Different sediment proxies and sediment cores collected from the coastal plain, estuary/lagoon and offshore regions have been used to decipher the sea level changes and palaeo-climatic conditions of the Late Pleistocene-Holocene sediment sequence. The study area is in the Neendakara-Kayamkulam coastal stretch, in central Kerala where the coast is manifested with shore parallel Kayamkulam Lagoon on one side and shore perpendicular Ashtamudi Estuary on the other side. This distinctive feature is suggestive of existence of an uplifted prograded coastal margin followed by barrier beaches, backwater channels, ridge and runnel topography and hence is an ideal site for studying the marine transgression-regression events. The thesis embodies the results obtained on the evolution history of this coastal region. The field and laboratory test results of the sediment cores have also helped in better understanding of the evolutionary history of the Ashtamudi Estuary and its surrounding regions.

The sedimentological study of sediment cores of different coastal environments show a wide spectrum of textural classes comprised of sand, siltyclay, clayey silt, mud, etc. The study reveals that the sediment were deposited in different regime with dominance of terrigenous to marine origin in the southern coastal plain and dominance of marine origin towards north. The Ashtamudi Estuary is composed of silty clay to clayey type of sediments whereas offshore cores are made of siltyclay to relict sand. The study also presents hydrodynamic conditions as well as the depositional environment of the sediment cores based on statistical parameters that decipher the deposition pattern at various levels viz., coastal plain (open to closed

basin), Ashtamudi Estuary (partially open to restricted estuary to closed basin) and offshore (open channel).

The statistical parameters like mean size, standard deviation, skewness and kurtosis for the coastal plain, estuary/lagoon and offshore for both southern and northern transects sediment cores are discussed and down core variations have been deciphered.

The dominant clay minerals observed in the core section are essentially made up of kaolinite and gibbsite with minor occurrence of illite and chlorite. The down core variation of clay mineral intensities have helped in distinguishing the hard desiccated clay (late Pleistocene) from that of the Holocene clay. The Kaolinite mineral peak shows much sharper peak at 10.8 m depth, possibly the Pleistocene-Holocene boundary, indicating the strong crystalline nature of clay and a uniform particle size distribution.

The radiocarbon dating reveals the ages ranging from 42,115 Yrs BP to 940 Yrs BP. The dated organic rich sediments and peat (Core 1) reveal that the black clay sediments rich in organic matter (14%) occurring at the depth of 15.0 to 11.7 m have ages from 42,115 Yrs BP to 40,000 Yrs BP. The peat sample with an organic matter content of 47% occurring at a depth of 11 m, above the black clay, gives an age of 24,670 Yrs BP. The northern coastal plain core has also given similar age of 21,340 yrs BP at a depth of 11.6m. The dates obtained from the study region are therefore of late Pleistocene age. The dates were reconfirmed by conducting blank analysis test at BSIP, Lucknow. The core representing the Ashtamudi Estuary (Core 2) has yielded an age of 940 yrs indicating the sediments to be Recent age.

The result of surface micro-morphological study of quartz grains, selected based on the lithological variation and their environment of deposition, using Scanning Electron Microscope (SEM) techniques, throws light on the processes of transportation and diagenetic history of sediments. The study indicates that the sediments of the southern coastal plain were transported and deposited mechanically under fluvial environment. This was followed by diagenesis under the prolonged marine incursion. In the northern coastal plain, the sediments were transported and deposited under the littoral environment which suggests dominance of marine

incursion through mechanical as well as chemical processes. The surface texture features of the offshore sediments suggest that the quartz grains are of littoral origin and represent the relict beach deposits.

The geochemical characterisation of sediment cores have been carried out to address the source rock composition, sediment maturity, palaeo-weathering and diagenetic processes. The ICV values for coastal plain core sediments (Core 1) suggesting matured characteristics of sediments which were subjected to tectonically quiescent or cratonic environments with minimal uplift. Extensive chemical weathering, where recycling and concomitant weathering are active is also indicated by the data. ICV values for Ashtamudi Estuary varies significantly with higher values in Core 4 sediments than the sediments of Core 2 and Core 3 sediments. These ICV values exhibits higher values than PAAS (ICV=0.85); suggesting the predominance of rock forming minerals such as plagioclase, K-feldspar, amphiboles, pyroxenes and lithics over clay minerals as well as tend to be found in tectonically active settings which are characterised by first-cycle deposits in the sediments of Ashtamudi estuary and offshore. Ashtamudi estuarine sediments and offshore sediments are geochemically immature, and were derived from a weakly to moderately weathered source. The  $\text{SiO}_2/\text{Al}_2\text{O}_3$  ratio of estuarine sediments, is lower than PAAS ( $\text{SiO}_2/\text{Al}_2\text{O}_3 \sim 3.3$ ), indicating low to moderate textural maturity, implying that Ashtamudi estuary sediments have undergone a minimal sedimentary cycle. The higher content of  $\text{SiO}_2/\text{Al}_2\text{O}_3$  ratio in coastal plain sediments clearly indicates that the sediments are highly matured and are derived from more felsic source, which is evident from the abundant distribution of felsic rocks in the hinterlands. All the core sediments from estuary (Core 2,3,4) indicates that the chemistry and provenance show wider distribution over the stratigraphic periods. Application of discriminant diagrams for the estuarine samples suggest intermediate igneous provenance suggesting that sediments derived from intermediate igneous provenance. Core 1 sediments are mostly clustered in quartzose sedimentary provenance, few plotting in igneous field. These sediments are interpreted to have derived from recycled sources. Majority of the core samples representing the estuary (Core 2,3,4) and offshore (Core 5), are except the coastal plain core sediments (Core 1), show marine dominance. The geo-accumulation index (Igeo) values for the surface sediments of the Astamudi Estuary suggest varying element and concentration levels.

## 8.2. Evolution of the coast

The evolution of coastal lands of the region has been influenced by regional factors like climate changes, sea level rise, and local and regional tectonics. These are well depicted in the schematic diagram (see Figure 7.3). Based on these evidences it is suggested that the region was subjected to series of transgression and regression events, starting as early as in the late Pleistocene. This observation is not reported before as earlier reports have suggested the period to be Holocene. The study also records for the first time an age  $24,670 \pm 1,869$  Yrs BP from a peat layer occurring at a depth of 11 m (Core 1) and an age of  $42,115 \pm 180$  Yrs BP for the old coastline recorded from 15.0 m depth. Many evidences are present indicating that the region was subjected to several spells of sea level rise and falls and that the first marine transgression, in the study area, took place around 42,000 Yrs BP. The study suggests that this was followed by the gradual lowering of sea level corresponding to the Last Glacial Maximum (LGM), which is located approximately at 80 to 110 m water depth from the present day shoreline. The study also suggest that high rainfall during  $>40,000$  to 28,000 Yrs BP did bring about many depositional and landform features, including the initiation of incised valley formation.

Following the Flandrian transgression, from the LGM, the sea level rose rapidly during early part of late Pleistocene but the rate of sea level rise has reduced drastically during the progress of the Holocene. The study suggests that Kallada River, which was part of a major deltaic river debouching sediments much inside into the shelf, resulted in the initiation of valley development over the Neogene sediments. These valleys were subsequently widened during the mid-Holocene period due to heavy precipitation. The formation of bay head delta on the upper part of estuarine basins appear to have begun in the Early Holocene as reported from the  $^{14}\text{C}$  age of  $8,296 \pm 44$  Yrs BP (Padmalal et al., 2011).

The intense rainfall witnessed during the early Holocene, broadened the valleys and resulted in erosion of sediments. The sea level was much lower during the LGM. The surface exposure of the Quilon bed seen on the periphery of the estuary further substantiates erosion of the Neogene sediments. The rise in the sea level during 5,000 to 6,000 Yrs BP had forced deposition of river-borne materials/alluvium leading to the filling of channels and building of sediments in the river mouth zones.



This is evident from the rich deposit of fluvial sediment of nearly 9 m. The progradation of the alluvial sediments towards the estuarine zones have brought out many separate water bodies in the basin including the formation of many fresh water lakes from the Asthamudi estuary. The bell shape coastline formed during 6,000 to 5,000 Yrs BP in the study area shows further evidence of progradation of the Holocene coastline.

### **8.3. Evolution of Asthamudi Estuary**

Palaeo records of sediment cores provide evidence for a prograding coastline and occurrence of Quaternary formations at various elevations along the Kerala coast. The study reports the formation of a chain of coast-parallel estuaries/lagoons, separated from the sea by spits/bars. Sedimentological and palynological analysis of the bore hole samples around the Ashtamudi Estuary reveal a thick sequence of Holocene sediments containing good record of landform evolution and climate changes. Detailed sedimentological studies, variations in sediment types and carbon dating have provided new knowledge on the evolution of estuary during the Holocene period. In the southern coastal plain bordering the Asthamudi Estuary the results of sediment litholog indicates several deposition as well as erosion episodes. Grain size study of core samples at different depths is suggestive of changes in the depositional scenario from shallow marine to lagoonal and swamp/marsh environment. Most climatic proxies suggest that the stronger monsoon in the early Holocene was associated with the high lake levels; increased flow discharges floods and scouring. The stronger monsoon during the early Holocene resulted in widening of incised valley at the entrance of the Kallada River. This was followed by the Holocene transgression event which submerged the adjacent coastal plain, resulting in the formation of coast perpendicular estuary. The study has also identified Pleistocene-Holocene boundaries in the study area and recorded that the Holocene sediment was replaced by 7 to 9 m thick modern fluvial sediments, directly overlying the late Pleistocene (40,000Yrs BP) sediments.

#### **8.4. Recommendations for Future Work**

- Studies on inland and offshore Quaternary deposits to develop a high resolution climate prediction system.
- Studies on early and mid Quaternary stratigraphy.
- Studies on fluvial, estuarine and coastal stratigraphy and neo-tectonism.
- Studies on Anthropocene defining the late part of Holocene?

## REFERENCES

- Aditya, S., Sinha, R.N., 1976. Geology and the hydrocarbon prospects of the west coast basin. Workshop on coastal sedimentaries of India south of 18° N. ONGC Madras.
- Agarwal, D.P., Gupta, S.K, Kusumgar, S., 1970. Radiocarbon dates of Quaternary samples. *Current Science* 39, 1, 219-222.
- Agarwal, D.P., Avasia, R.K., Guzdar, S., 1973. A multidisciplinary approach to the Quaternary problems in Maharashtra. *Radiocarbon and Indian Archaeologist*, TIFR, Bombay (3-17 pp.).
- Agarwal, D.P., Kusumgar, S., 1974. Prehistoric chronology and radiocarbon dating in India, MunshiramManoharlal, New Delhi.
- Agrawal , D.P. , Kusumgar, S., 1975. Radiocarbon dates of some Late Quaternary Samples. *Current Science*, 44 (5), 149-151.
- Agrawal, D.P., Krishnamurthy, R.V. , Kusumgar, S., Pant, R.K. , 1979. Physical Research Laboratory Radiocarbon Dates: II. *Current Science*, 48 (5), 190-194.
- Agarwal, J.M., 1990. Sea level variation-through bathymetric data example-Azhikkal on west coast of India. In: sea level variation and its impact on coastal environment. Tamil university Press, Thanjavur (1-6 pp.).
- Ahamed, E., 1972. Coastal Geomorphology of India.Orient. Longman, New Delhi. (222 pp.).
- Algeo, T.J., Maynard, J.B., 2004. Trace element behaviour and redox facies in core shales of upper Pennsylvanian Kansas-type cyclothems.*Chemical Geology*. 206, 289–318.
- Allen, J.R.L., 1970. *Physical Processes of Sedimentation*, 4<sup>th</sup> edn. Allen & Unwin, London, (248 pp.).
- Andersson, P.O.D., Worden, R.H., Hodgson, D.M., Flint, S., 2004. Provenance evolution and chenostartigraphy of a plaeozoic submarine fan-complex: Tanqua Karoo Basin, South Africa. *Mar. Petrol. Geol.* 21, 555-577.

- Armstrong-Altrin, J.S., Lee, Y.I., Verma, S.P., Ramasamy, S., 2004. Geochemistry of sandstones from the upper Miocene Kudankulam Formation, southern India: Implications for provenance, weathering, and tectonic setting. *Journal of Sedimentary Research* 74(2), 285-297.
- Armstrong-Altrin, J.S., Nagarajan, R., Madhavaraju, J., Rosalez-Hoz, L., Lee, Y.I., Balaram, V., Cruz-Martinez, A., Avila-Ramirez, G., 2013. Geochemistry of Jurassic and upper Cretaceous shales from the Molango Region, Hidalgo, eastern Mexico: Implications for source-area weathering, provenance and tectonic setting. *Comptes Rendus Geosci.* 345, 185-202, DOI: 10.1016/j.crte.2013.03.004.
- Baker, H.W., 1976. Environmental sensitivity of submicroscopic surface textures on quartz sand grains - A statistical evaluation. *Journal of Sedimentary Petrology* 46, 871-880.
- Banerjee, M., Sen, P.K., 1987. Palaeobiology in understanding the change of sea level and coast-line in Bengal basin during Holocene period. *Indian Journal of Earth Sciences* 14, 307-320.
- Banerjee, P.K., 2000. Holocene and Late Pleistocene relative sealevel fluctuations along the east coast of India. *Mar. Geol.* 167 (3-4), 243-260.
- Barshad, I., 1966. Factors Affecting the Frequency Distribution of Clay Minerals in Soils. *J. Clays and Clay Minerals* 14, 207-207.
- Bateman, C., 1985. Development and evolution of sedimentary environments during the Holocene in the western coastal plain of Belgium. *Eiszeitalter u. Gegenwart*. 35, 23-32.
- Benoit, J.M., Fitzgerald, W.F., Damman, A.W.H., 1998. The biogeochemistry of an ombrotrophic bog: evaluation of use as an archive of atmospheric mercury deposition. *Environmental Research* 78, 118-133.
- Biscaye, P.E., 1964. Distinction between chlorite and kaolinite in recent sediments by X-ray diffraction. *American Mineralogy* 49, 1281-1289.
- Biscaye, P.E., 1965. Mineralogy and sedimentation in the recent deep-sea clay in the Atlantic and adjacent seas and oceans. *Bulletin Geological Society of America* 76, 803-832.

- Bisutti, I., Hilke, I., Raessler, M., 2004. Determination of total organic carbon - an overview of current methods. *TRAC - Trends in Analytical Chemistry* 23, 10-11, 716-726.
- Black, K., Baba, M., 2001. Developing Management Plan for Ashtamudi estuary, Kollam, India, Technical Memoir (Eds. Black, K., Baba, M.) ASR, New Zealand and Center for Earth Science Studies, Trivandrum, pp. 546.
- Black, K., Mathew, J., 2001. Numerical modelling of circulation, sea levels and pollution/larval dispersal. In: Black, K., Baba, M., (Eds.), Developing a management plan for Ashtamudi estuary, Kollam, India. ASR Ltd., Marine and Fresh water consultants, Hamilton, NewZealand; Centre for Earth Science Studies, Trivandrum, India. pp. 471-500.
- Blackwelder, P.L., Pilkey, O.H., 1972, Electron microscopy of quartz grain surface textures: The U.S. Eastern Atlantic continental margin. *Jour. Sed. Petrology* 42, 520-526.
- Blatt, H.G., Middleton, G.V., Murray, R.C., 1980. *Origin of Sedimentary Rocks*. 2<sup>nd</sup> ed., Prentice-Hall, New Jersey, (634 pp.).
- Bloom, A.L., 1977. Atlas of sea level curves. (Ed.), Dept. Geol. Sci. Cornell Univ. pp. 114.
- Bock, B., McLennan, S.M., Hanson, G.N., 1998. Geochemistry and provenance of the Middle Ordovician Austin Glen Member (Normanskill Formation) and the Taconian Orogeny in New England. *Sedimentol.* 45, 635-655.
- Bowen, D.Q., 1978. *Quaternary Geology*. Pergamon Press, Oxford, (221 pp.).
- Brantley, S.L., Crane, S.R., Crerar, D.A., Hellmann, R., Stallard, R., 1986. Dissolution at dislocation etch pits in quartz. *Geochimicaet. Cosmochimica Acta.* 50, 2349-2361.
- Brugmann, G.E., Arndt, N.T., Hofmann, A.W., Tobschall, H.J., 1987. Noble metal abundances in komatiite suites from Alexo, Ontario, and Gorgona Island, Columbia. *Geochim. Cosmochim. Acta.* 51, 2159-2169.
- Bull, P.A., 1977. Glacial deposits identified by chattermark trails in detritalgarnets: comment. *Geology* 5, 248.

- Bull, P.A., 1978. A quantitative approach to scanning electron microscope analysis of cave sediments, in Whalley, W.B., (Ed.), *Scanning Electron Microscopy in the Study of Sediments*. Norwich, Geo-books, pp. 821-828.
- Bull, P.A., Culver, S.J., Gardner, R., 1980. The nature of the late Palaeozoic glaciation in Gondwana as determined from an analysis of garnets and other heavy minerals: Discussion: *Canadian Journal of Earth Science*, 17.
- Bull, P.A., Culver, S.J., Gardner, R., 1980., Chattermark trails as paleo-environmental indicators. *Geology* 8, 318-322.
- Butzer, K.W., 1980. Holocene alluvial sequence: Problems of dating and correlation. In: Cullinford, R.A., Davidson, D.A., Lewin, J. (Eds). *Time scales in Geomorphology*. John Wiley, New York, pp. 131-142.
- Calvert, S.E., 1990. Geochemistry and origin of the Holocene sapropel in the Black Sea. In: Ittekkot, V. (Ed.), *Facets of Modern Biogeochemistry*. Springer-Verlag, Berlin, pp. 327-353.
- Cao, J., Wu, M., Chen, Y., Hu, K., Bian, L., Wang, L., Zhang, Y., 2012. Trace and rare earth element geochemistry of Jurassic mudstones in the northern Qaidam Basin, northwest China. *Chem. Erde Geochem.*, <http://dx.doi.org/10:1016/j.chemer.2011.12.002>.
- Carver, R.E., 1971. *Procedures in sedimentary petrology* (Ed.). Wiley-Interscience, New York, pp. 653.
- CESS., 1988. *Environmental Geomorphic Atlas Kerala Coastal Zone*, pp. 145.
- CESS., 1998. *Natural Resource Inventory for Hazard Management for Kollam District- A system approach*. Project report submitted to the State Committee on Science, Technology and Environment. Govt. of Kerala, Centre for Earth Science Studies, pp. 70.
- Chacko, T., Ravindra Kumar, G.R., Meen, J.K., Rogers, J.J.W., 1992. Geochemistry of high-grade supracrustal rocks from the Kerala Khondalite Belt and adjacent massif charnockites, south India. *Precambrian Research* 55, 469-489.
- Chakraborti, P., 1991. Subarnarekha delta - a geomorphic appraisal. *Memoir of the Geological Society of India* 22, (25-30 pp.).

- Chamley, H., 1989. *Clay Sedimentology*. Springer Verlag, Berlin (623 pp.).
- Chattopadhyay, S., 2001. Emergence of central Kerala coastal plain- a geomorphic analysis. In: Tandon, S.K., Thakur, B., (Eds.), *Recent advances in geomorphology, Quaternary geology and environmental geoscience: India case studies*, Manisha publication, pp. 287–298.
- Chattopadhyay, S., 2002. Emergence of central Kerala coastal plain-a geomorphic analysis. In: Tandon S.K., Thakur, B., (Eds.) *Recent advances in Geomorphology, Quaternary geology and environmental geoscience: India case studies*, Mnaisha publication, pp. 287-298.
- Chiverrell, R.C., 2001. A proxy record of late Holocene climate change from May Moss, northeast England. *J. Quat. Sci.* 16 (1), 9-29.
- Coch, N.K., Krinsley, D.H., 1971. Comparison of stratigraphic and electron microscopic studies in Virginia Pleistocene coastal sediments. *J. Geol.*, 79, 425-437.
- Cohen, A.S., 2003. *Paleolimnology. The history and evolution of lake systems*. Oxford University Press, New York, 1st Edition (500 pp.), ISBN: 0-19-513353-6.
- Condie, C.K., Noll, P.D.Jr., Conway, C.M., 1992. Geochemical and detrital mode evidence for two sources of Early Proterozoic sedimentary rocks from the Tonto Basin Supergroup, central Arizona. *Sediment. Geol.* 77, 51-76.
- Cox, R., Lowe, D.R., Cullers, R.L., 1995. The influence of sediment recycling and basement composition on evolution of mudrock chemistry in the southwestern United States. *Geochimica et Cosmochimica Acta* 59(14), 2919-2940.
- Cronin, T.M., 1999. *Principles of Paleoclimatology*, Columbia University Press, New York.
- Cullen, J.L., 1981. *Palaeogeogr., Palaeoclimat., Palaeoecol.* 35, 121-144.
- Cullers, R.L., Barrett, T., Carlson, R., Robinson, B., 1987. Rare earth element and mineralogic changes in Holocene soil and stream sediment: a case study in the Wet Mountains, Colorado, USA. *Chem. Geol.* 63, 275-297.

- Cullers, R.L., Podkovyrov, V.N., 2000. Geochemistry of the Mesoproterozoic Lakhanda shales in southeastern Yakutia, Russia: implications for mineralogical and provenance control, and recycling. *Precambrian Res.* 104(1-2), 77-93.
- Curry, J.R., Moore, D.G., 1971. Growth of the Bengal Deep - Sea Fan and denudation in the Himalayas. *Geol. Soc. Am. Bull.* 82, (563-573 pp.).
- Dabard, M.P., 1990. Lower Brioverian formations (Upper Proterozoic) of the Armorican Massif (France): geodynamic evolution of source areas revealed by sandstone petrography and geochemistry. *Sedim. Geol.* 69, 45-58.
- Dalrymple, R.W., Zaitlin, B.A., Boyd, R., 1992. Estuarine facies models: conceptual basis and stratigraphic implications. *J. Sediment. Petrol.* 62 (6) 1030-1046.
- Damodaran, K.T., Sajan, K., 1983. Carbonate content of sediments in the Ashtamudy lake, west coast of India. *Indian Journal of Marine Sciences*, 12, pp. 228-230.
- Davies, J.L., 1964. A morphogenic approach to world shorelines. *Z. Geomorphol.* 8(1), 27-42.
- De la Vega, A.C., Keen, D.H., Jones, R.L., Wells, J.M., Smith, D.E., 2000. Mid-Holocene environmental changes in the Bay of Skaill, Mainland Orkney, Scotland: an integrated geomorphological, sedimentological and stratigraphical study. *J. Quat. Sci.* 15, 509-528.
- Demory, F., Oberhänsli, H., Nowaczyk, N.R., Gottschalk, M., Wirth, R., Naumann, R., 2005. Detrital input and early diagenesis in sediments from Lake Baikal revealed by rock magnetism. *Global and Planetary Change* 46, 145-66.
- Dewers, T., Ortoleva, P., 1990. Force of crystallization during the growth of siliceous concretions. *Geology* 18, 204-207.
- Dey, S., Rai, A.K., Chaki, A., 2009. Palaeoweathering, composition and tectonics of provenance of the Proterozoic intracratonic Kaladgi-Badami basin, Karnataka, southern India: evidence from sandstone petrography and geochemistry. *J. Asian Earth Sci.* 34, 703-715.
- Doornkamp, J.C., Krinsley, D.H., 1971. Electron microscopy applied to quartz grains from a tropical environment, *Sedimentology* 17, 89-101.



- Dunn, D.A., Moore, T.C., Keigwin, L.D., 1981. Atlantic-type carbonate stratigraphy in the late Miocene Pacific. *Nature* 291, 225–227.
- EDGI, 1998. The encyclopedia district of gazettiers of India, southern zone, (S.C. Bhatt, Ed.), Gyan Publishing house, New Delhi 2, (701-1293 pp.).
- Edwards, R.J., 2001. Mid-to late Holocene relative sea-level change in Poole Harbour, southern England. *J. Quaternary Sci.* 16 (3), 221-235.
- El Wakeel, S.K., Riley, J.P., 1957. Determination of organic carbon in the marine muds. *J. Cons.perm.int. Explor. Mer.* 22, 180-183.
- Fairbanks, R.G., 1989. A 17,000-year glacio-eustatic sea level record: influence of glacial melting rates on the younger Dryas event and deep-ocean circulation. *Nature* 342, 637-642.
- Fairbridge, R.W., 1961. Eustatic changes in sea level. In: Ahrews, L.H., Press, F., Rankama, K., Runcom, S.K. (Eds.) *Physics and Chemistry of the Earth*, New York, Pergamon, 4, pp. 99-185.
- Fairbridge, R.W., 1983. The pleistocene-holocene boundary, *Quaternary Science Reviews* (215-244 pp.).
- Farooqui, A., Vaz, G.G., 2000. Holocene sea-level changes and climatic fluctuations: Pulicat Lagoon: A case study. *Curr. Sci.* 79 (10), 1484–1488.
- Fedo, C.M., Nesbitt, H.W., Young, G.M., 1995. Unraveling the effects of potassium metasomatism in sedimentary rocks and paleosols, with implications for paleoweathering conditions and provenance. *J. Geol.* 23 (10), 921-924.
- Feng, R., Kerrich, R., 1990. Geochemistry of fine grained clastic sediments in the Archaean Abitibi greenstone belt, Canada: implication for provenance and tectonic setting. *Geochim. Cosmochim. Acta* 54, 1061-1081.
- Fitpatrick, K.T., Summerson, C.H., 1971. Some observations on electron micrographs of quartz sand grains, *Ohio Journal Science* 71, 106-119.
- Floyd, P.A., Leveridge, B.E., 1987. Tectonic environments of the Devonian Gramscatho basin, south Cornwall: framework mode and geochemical evidence from turbidite sandstones. *J. Geol. Soc. London* 144 (4), 531-542.

- Floyd, P.A., Winchester, J.A., Park, R.G., 1989. Geochemistry and tectonic setting of Lewisian clastic metasediments from the early Proterozoic Loch Maree Group of Gairloch, N.W. Scotland. *Precambrian Research* 45, 203-214.
- Folk, R.L., 1954. The distinction between grain size and mineral composition in sedimentary rock nomenclature. *J. Geol.* 62 (4), 344-359.
- Folk, R.L., 1980. *Petrology of Sedimentary Rocks*. Austin, Texas, U.S.A. Hemphill Publishing Co., 2nd edition, (184 pp.).
- Folk, R.L., Ward, W.C., 1957. Brazos River bar: a study in the significance of grain size parameters. *J. Sediment. Petrol.* 27 (1), 3-26.
- Fournier, R., 1960. Solubility of quartz in water in the temperature interval from 25 oC to 300 0C, *GSA Bull.*, 71, 1867-1868.
- Friedman, G.M., 1961. Distinction between dune, beach and river sands from their textural characteristics. *J. Sediment. Petrol.* 3 (4), 514-529.
- Friedman, G.M., 1979. Differences in size distributions of populations of particles among sands of various origins. *Sedimentology* 26, 3-32.
- Fyffe, L.R., Pickerill, R.K., 1993. Geochemistry of Upper Cambrian Lower Ordovician black shale along a north eastern Appalachian transect. *Geological Society of America Bulletin* 105, 897-910.
- Garcia, D., Fonteilles, M., Moutte, J., 1994. Sedimentary fractionations between Al, Ti, and Zr, and the genesis of strongly peraluminous granites. *J. Geol.* 102 (4), 411-422.
- Gardner, J.V., 1982. High-resolution carbonate and organic-carbon stratigraphies for the late Neogene and Quaternary from the western Caribbean and eastern equatorial Pacific. In: Prell, W.L., Gardner, J.V., et al., (Eds.) *Init. reports Deep Sea Drilling Projects Reports and Publications (DSDP)*, Washington (U.S. Govt. Printing Office) 68, pp. 347-364.
- Garver, J.I., Royce, P.R., Smick, T.A., 1996. Chromium and nickel in shale of the Taconic Foreland: A case study for the provenance of fine-grained sediments with an ultramafic source. *Journal of Sedimentary Research* 66, 100-106.

- Gaudette, H.E., Flight, W.R., Toner, L., Folger, D.W., 1974. An inexpensive titration method for determination of organic carbon in recent sediments. *Journal of sedimentary petrology* 44 (1), 249-253.
- Gerdes, G., Petselberger, B.E.M., Scholz-Bottcher, B.M., Streif, H., 2003. The record of climatic change in the geological archives of shallow marine, coastal, and adjacent lowland areas of northern Germany. *Quat. Sci. Rev.* 22 (1), 101–124.
- Gibbs, R.J., 1965. Error due to segregation in quantitative clay mineral X-ray diffraction mounting techniques. *American Mineralogy* 50 (5-6), 741–751.
- Girty, G.H., Ridge, D.L., Knaack, C., Johnson, D., Al-Riyami, R.K., 1996. Provenance and depositional setting of Paleozoic chert and argillite, Sierra Nevada, California. *J. Sedim. Res.* 66, 107-118.
- Goodsite, M.E., Rom, W., Heinemeier, J., Lange, T., Ooi, S., Appleby, P.G., Shotyk, W., Van der Knaap, W.O., Lohse, C. H., Hansen, T.S., 2001. High-resolution AMS <sup>14</sup>C dating of post-bomb peat archives of atmospheric pollutants. *Radiocarbon* 43(2B), 495–515.
- Goring-Morris, A.N., Belfer-Cohen, A., 1998. The Articulation of Cultural Processes and Late Quaternary Environmental Changes in Cisjordan, *Paléorient* 23, 71-93.
- Goudie, A.S., 1981. *The Human impact Man's role in environmental Change*, Blackwell Publishers, Oxford (326 pp.).
- Govil, P.K., 1985. X-ray fluorescence analysis of major, minor and selected trace elements in new IWG reference rock samples. *Journal of the Geological Society of India*, 26, 38-42.
- Gratz, A.J., Manne, S., Hansma, P.K., 1991. Atomic force microscopy of atomic-scale ledges and etch pits formed during dissolution of quartz. *Science* 251, 1343-1346.
- Gravenor, C.P., 1979. The nature of the Late Paleozoic glaciation in Gondwana as determined from an analysis of garnets and other heavy minerals. *Canadian Journal of Earth Sciences* 16, 1137-1153.
- Griffin, J.J., Windom, H., Goldberg, E.D., 1968. The distribution of clay minerals in the World Ocean. *Deep-Sea Research.* 15, 433-459.

- Guzder, S.J., 1980. Quaternary environment and stone age cultures of the Konkan, Coastal Maharashtra, Deccan College, Pune.
- Haneesh, V., 2001. Sea level variations during the late Quaternary and coastal evolution along the northern Kerala, south west of India. Ph.D. thesis submitted to Cochin University of Science and Technology, Cochin, Unpublished (184 pp.).
- Hashimi, N.H., Gupta, M.V.S., Kidwai, R.M., 1978. Sediments and sedimentary processes on the continental shelf off Bombay. *Mahasagar* 11, 51-161.
- Hashimi, N.H., Nair, R.R., 1986. Climatic aridity over India 1000 years ago: evidence from feldspar distribution in the shelf sediments. *Paleogeog. Paleoclimatol. Paleoecol.* 53, 309-319.
- Hashimi, N.H., Nigam, R., Nair, R.R., Rajagopalan, G., 1995. Holocene sea level fluctuations on western Indian Continental margin: An update, *Jour. Geol. Soc. India* 46, 157-162.
- Hayashi, K., Fujisawa, H., Holland, H.D., Ohmoto, H., 1997. Geochemistry of  $\approx 1.9$  Ga sedimentary rocks from northeastern Labrador, Canada. *Geochimica et Cosmochimica Acta* 61(19), 4115-4137.
- Holland, P.E., Holmes, M.A., 1997. Surface textural analysis of quartz sand grains from ODP Site 918 off the southeast coast of Greenland suggests glaciation of southern Greenland at 11 Ma: *Palaeogeography, Palaeoclimatology, Palaeoecology* 135, 109-121.
- Herron, M.M., 1988. Geochemical classification of terrigenous sands and shales from core or log data. *Journal of Sediment Petrology* 58(5), 820-829, doi: 10.1306/212F8E77-2B24-11D7-8648000102C1865D.
- Hicks, B.D., 1985. Quartz dissolution features: An experimental and petrofabric study (unpublished MS thesis). University of Missouri-Columbia, Columbia, (114 pp.).
- Higgs, R., 1979. Quartz grain surface features of Mesozoic- Cenozoic sands from the Labrador and Western Greenland continental margins. *Journal of Sedimentary Petrology* 49, 599-610.

- Hodgson, A.V., Scott, W.B., 1970. The identification of ancient beach sands by the combination of size analysis and electron microscopy. *Sedimentology* 14, 67-75.
- Hurowitz, J.A., McLennan, S.M., 2005. Geochemistry of Cambro-Ordovician Sedimentary Rocks of the Northeastern United States: Changes in Sediment Sources at the Onset of Taconian Orogenesis. *Jour. Geol.* 113, 571-587.
- Hurst, A.R., 1981. A scale of dissolution for quartz and its implication for diagenetic processes in sandstones. *Sedimentology* 28, 451-459.
- Hutchinson., Mcheman., 1947. Soil and plant analysis by Piper. The University of Adelaide (368 pp.).
- IPCC, 2007. The Intergovernmental Panel of Climate Change, The Fourth Assessment Report (AR4), Climate Change, Cambridge Univ. Press, Oxford.
- Jacob, K., Sastri, V.V., 1952. Miocene foraminifera from Chavara near Kollam, Travancore, *Rec. Geot. Surv. India*, 32, (65-67 pp.).
- Jacob, Z., 2008. Luminescence chronologies for coastal and marine sediments. *Boreas* 37, 508-535.
- Jayalakshmi, K., Nair, K.M., Kumai, H., Santhosh, M., 2004. Late Pleistocene-Holocene palaeoclimatic history of the southern Kerala basin, southwest India. *Gondwana Res.* 7 (2), 585-594.
- Jelgersma, S., 1966. Sea level changes during the last 10, 000 years. In: proceedings of the International symposium on World climate 8,000 to 0 BC, Royal Meteorological Society London 54-70.
- Johnsson, M.J., Stallard, R.F., 1988. First-cycle quartz arenities in the Orinoco River basin, Venezuela and Colombia. *Journal of Geology* 96, 263-277.
- Joshi, V.U., 2009. Grain surface features of alluvial sediments of upper Pravara basin and their environmental implications. *Jour. Geol. Soc. India* 74, 711-722.
- Kabata-Pendias, A., Pendias, H., 2001. Trace elements in soils and plants (3rd ed.). Boca Raton, FL, CRC Press (505 pp.).
- Kale, V.S., Kshirsagar, A.A., Rajaguru, S.N., 1984. Late Pleistocene Beach rock from Uran Maharashtra India. *Curr. Sci.* 53, 317-319.

- Kale, V.S., Rajaguru, S.N., 1985. Neogene and Quaternary transgressional and regressional history of the west coast of India, An overview, Bull Deccan college, Res. Inst. 44 (153-165 pp.).
- Kale, V.S., Gupta, A., Singhvi, A.K., 2004. Late Pleistocene-Holocene palaeohydrology of Monsoon Asia, Jour. Geol. Soc. India 64 (10), 403-417.
- Kasper-Zubillaga, J.J., Carranza-Edwards, A., Mortonbermea, O., 2008. Heavy Minerals and Rare Earth Elements in Coastal and Inland Dune Sands of El Vizcaino Desert, Baja California Peninsula, Mexico. Marine Georesources & Geotechnology 26(3), 172-188.
- Katupotha, J., Fujiwara, K., 1988. Holocene sea level change on the southwest and south coasts of Sri Lanka. Palaeogeography, Palaeoclimatology, Palaeoecology 68, 189-203.
- Kerr, A.R., 2008. Geology: A time war over the period we live. Science 319, 5862, 402 - 403.
- Koinig, K.A., Shotyk, W., Lotter, A.F., Ohlendorf, C., Sturm, M., 2003. 9000 years of geochemical evolution of lithogenic major and trace elements in the sediment of an alpine lake - the role of climate, vegetation, and land-use history. J. Paleolimnol. 30 (3), 307-320.
- Krauskopf, K.B., 1956. Dissolution and precipitation of silica at low temperatures. Geochim. Cosmochim. Acta. 10, 1-26.
- Krinsley, D.H., Takahashi, T., 1962. Applications of electron microscopy to geology. Transactions of the New York Academy of Sciences. Series II, 25, pp. 3-22.
- Krinsley, D.H., Takahashi, T., Silberman, M.L., Newman, W.S., 1964. Transportation of sand grains along the Atlantic shore of Long Island, New York. An application of electron microscopy. Marine Geology, 2, 100-120.
- Krinsley, D.H., Donahue, J., 1968. Environmental interpretations of sand grain surface textures by electron microscopy. Geological Society of America Bulletin 79, 743-748.

- Krinsley, D.H., Margolis, S.V., 1969. A study of quartz sand grains surface textures with the scanning electron microscopes. *Trans. N.Y. Acad. Sci.*, 31, 457.
- Krinsley, D.H., Margolis, S., 1971. Grain surface texture, in Carver, R.E., (ed.), *Procedures in Sedimentary Petrology*. New York, Wiley, pp. 151-180.
- Krinsley, D.H., Doornkamp, J.C., 1971. Electron microscopy applied to quartz grains from a tropical environment. *Sedimentology* 17, 89-101.
- Krinsley, D.H., Doornkamp, J.C., 1973. *Atlas of quartz sand surface textures*. Cambridge, England, Cambridge University Press (91 pp.).
- Krinsley, D., Smalley, I., 1973. Shape and nature of small sedimentary quartz particles. *Science* 180, 1277-1279.
- Krinsley, D.H., Friend, P., Klimentidis, R., 1976. Eolian transport textures on the surface of sand grains of Early Triassic age: *Geological Society of America Bulletin*, 87, pp. 130-132.
- Krinsley, D.H., McCoy, F.W., 1977. Significance and origin of surface textures on broken sand grains in deep sea sediments. *Sedimentology* 24, 857-862.
- Krinsley, D.H., Marshall, J.R., 1987. Sand grain textural analysis: an assessment. In: Marshall, J.R., (Ed.), *Clastic particles: Scanning Electron Microscopy and Shape Analysis of Sedimentary and Volcanic Clasts*. New York, Van Nostrand-Reinhold, pp. 2-15.
- Krishnan Nair, K., 1987. Geomorphological and Quaternary geological studies along the coastal plain in parts of Cannanore and Kasargod districts, Kerala. *J. Geol. Soc. India* 29, 433-439.
- KSUB, 1995. Land resource of Kerala state, Kerala state land use board.
- Kumaran, K.P.N., Limaye, R.B., Nair, K.M., Padmalal, D., 2008. Palaeoecological and palaeoclimate potential of subsurface palynological data from the Late Quaternary sediments of South Kerala Sedimentary Basin, southwest India. *Curr. Sci.* 90 (4), 515-526.
- Kurian, N.P., Mathew J., Harish, C.M., Shahul Hameed, T.S., Prakash, T.N., 2001. In: Kerry, B., Baba, M., (Eds.), *Developing a management plan for Ashtamudi estuary, Kollam, India*. Bathymetry of Ashtamudi estuary, ASR Ltd., Marine

- and Fresh water consultants, Hamilton, New Zealand; Centre for Earth Science Studies, Trivandrum, India, pp. 329-340.
- Kurup, B.M., Thomas, K.V., 2001 In: Black, K., Baba, M., (Eds.), Developing a management plan for Ashtamudi estuary, Kollam, India. Fisheries resources of the Ashtamudi estuary. pp. 514-541.
- Kuttiyamma, V.J., 1980. Studies on the prawn and prawn larvae of the Kayamkulamlake and the Cochin backwaters. Bull. Dept. Marine Sci. Univ., Cochin (1-38 pp.).
- Lamb, H.F., Gasse, F., Benkaddour, A., Hamount, N., van der Kaars, S., Perkins, W.T., Pearce, N.J., Roberts, C.N., 1995. Relation between century scale Holocene arid intervals in tropical and temperate zones. *Nature* 373, 134-137.
- Lario, J., Zazo, C., Plater, A.J., Goy, J.L., Dabrio, C., Bolja, F., Sierro, F.J., Lllque, L., 2000. Particle size and magnetic properties of Holocene estuarine deposits from the Doñana National Park (SW Iberia): evidence of gradual and abrupt coastal sedimentation. *Z. Geomorphol* 45 (1), 33-54.
- Lario, J., Spencer, C., Plater, A.J., Zazo, C., Goy, J.L., Dabrio, C.J., 2002. Particle size characterisation of Holocene back-barrier sequences from North Atlantic coasts (SW Spain and SE England). *Geomorphol.* 42 (1-2), 25–42.
- Leduc, J., Bileudeau, G., Vernal, A., Mucci, A., 2002. Distribution of benthic foraminiferal populations in surface sediments of the Saguinay Fjord, before and after the 1996 flood. *Palaeogeogr. Palaeoclimatol. Palaeoecol.* 180 (1-3), 207–223.
- Le-Ribault, L., 1975. L'exoscopie. Methode et applications. Compagnie Francaise des petroles, Notes et Memoires, 12, (231 pp.).
- Limaye, R.B., Kumaran, K.P.N., Nair, K.M., Padmalal, D., 2010. Cyanobacteria as potential biomarkers of hydrological changes in the Late Quaternary sediments of South Kerala Sedimentary Basin, India, *Quaternary International* 213(1–2), 79-90.
- Lindsey, D.A., 1999. An evaluation of alternative chemical classifications of sandstones. USGS Open File Report 99-34, pp. 23.



- Long, X., Yuan, C., Sun, M., Xiao, W., Wang, Y., Cai, K., Jiang, Y., 2012. Geochemistry and Nd isotopic composition of the Early Paleozoic flysch sequence in the Chinese Altai, Central Asia: Evidence for a northward-derived mafic source and insight into Nd model ages in accretionary orogen. *Gond. Res.* 22, 554-566.
- Lowe, J., Walker, M., 1997. *Reconstructing Quaternary Environments*, Addison, Wesley, Longman, London, (446 pp.).
- Ly, C., 1978. Grain surface texture in environmental determination of late Quaternary deposits in New South Wales, *Jou. Sed. Petrol.* 48, 1219-1226.
- Madhavaraju, J., Lee, Y.I., Armstrong-Altrin, J.S., Hussain, S.M., 2006. Microtextures on detrital quartz grains of upper Maastrichtian-Danian rocks of the Cauvery Basin, Southeastern India: implications for provenance and depositional environments. *Geosciences Journal* 10, 23-34.
- Madhavaraju, J., Ramasamy, S., Mohan, S.P., Hussain, S.M., Gladwin GnanaAsir, N., Stephen Pitchaimani, V., 2004. Petrography and surface textures on quartz grains of Nimar Sandstone, Bagh Beds, Madhya Pradesh - Implications for provenance and depositional environment. *Journal of the Geological Society of India* 64, 747-762.
- Mahaney, W.C., Kalm, V., 1995. Scanning Electron Microscopy of Pleistocene tills in Estonia, *Boreas* 24, 13-29.
- Mahaney, W.C., 1998. Scanning electron microscopy of Pleistocene sands from Yamal and Taz peninsulas, Ob River estuary, northwestern Siberia. *Quaternary International*, 45-46, pp. 49-58.
- Mahaney, W.C., Kalm, V., 2000. Comparative SEM study of oriented till blocks, glacial grains and Devonian sands in Estonia and Latvia. *Boreas* 29, 35-51.
- Mahaney, W.C., 2002. *Atlas of Sand Grain Surface Textures and Applications*. Oxford University Press, (237 pp.)
- Mallik, T.K., Suchindan, G.K., 1984. Some sedimentological aspects of Vembanad Lake, Kerala, west coast of India. *Indian Jour.Mar.Sci.* 13, 159-163.
- Manickam, S., Barbaroux., 1987. Variations in the surface texture of suspended quartz grains in the Loire River: A SEM Study. *Sedimentology* 34, 495-510.

- Manjunatha, B.R., Shankar, R., 1992. A note on the factors controlling the sedimentation rate along the western continental shelf of India. *Mar. Geol.* 104, 219-224.
- Manker, J.P., Ponder, R.F., 1978. Quartz grain surface features from fluvial environments of north-eastern Georgia. *Journal of Sedimentary Petrology* 2, 243-256.
- Manson, C.C., Folk, R.L., 1958. Differentiation of beach, dune and aeolian flat environments by size analyses, Mustang Island, Texas. *J. Sed. Petrol.* 28 (2), 211-226.
- Margolis, S., 1968. Electron microscopy of chemical solution and mechanical abrasion features on quartz sand grains. *Sedimentary Geology* 2, 243-256.
- Margolis, S.V., Kennett, J.P., 1971. Cenozoic glacial history of Antarctica recorded in sub-antarctic deep-sea cores. *Am. Jour. Sci.* 271, 1-36.
- Margolis, S.V., Krinsley, D.H., 1971. Sub-microscopic frosting on eolian and subaqueous quartz sand grains. *Geological Society of America. Bulletin* 82, 12, pp. 3395-406.
- Margolis, S.V., Krinsley, D.H., 1974. Processes of formation and environmental occurrence of microfeatures on detrital quartz grains. *Amer. Jour. Sci.*, 274, 449-464.
- Marshall, J.R., 1987. *Clastic particles Scanning Electron Microscopy and shape analysis of sedimentary and volcanic clasts.* Van Nostrand, Reinhold Company, New York (346 pp.).
- Martinez-Cortizas, A., Pontevedra-Pombal, X., Garcia-Rodeja, E., N6voa-Muiioz, J. C., Shotyk, W., 1999. Mercury in a Spanish peat bog, archive of climate change and atmospheric metal deposition, *Science* 284, 939- 942.
- Mascarenhas, A., Paropakari, A.L., Babu, C.P., 1993. On the possibility of allochthonous peat on the inner shelf off Karwar. *Curr. Sci.* 64 (9), 684-687.
- Mathai, J., Nair, S.B., 1988. Stages in the emergence of the Cochin-Kodungallur coast - evidence for the interaction of marine and fluvial process. *Proc. Indian. Nat. Sci. Acad.* 54A (3), (439-447 pp.).

- McLennan, S.M., 1989. Rare earth elements in sedimentary rocks; influence of provenance and sedimentary processes, In: Lipin, B.R., McKay G.A., (Eds.), *Geochemistry and Mineralogy of Rare Earth Elements*, Rev. Mineral 21, pp. 169-200.
- McLennan, S.M., Taylor, S.R., 1991. Sedimentary rocks and crustal evolution: tectonic setting and secular trends. *J. Geol.* 99 (1), 1-21.
- McLennan, S.M., 1993. Weathering and global denudation. *J. Geol.* 101 (2), 295-303.
- McLennan, S.M., 2001. Relationships between the trace element composition of sedimentary rocks and upper continental crust. *Geochemistry, geophysics, geosystems* 2(4), 1021. <http://dx.doi.org/10.1029/2000GC000109>.
- Meher-Homji, V.M., Gupta, H.P., 1999. A critical appraisal of vegetation and climate changes during quaternary in the Indian Region. *Proc. Indian Natl. Sci. Acad.* B65, pp. 205-244.
- Merh, S.S., 1992. Quaternary Sea Level Changes along Indian Coast. *Proceedings of Indian National Sciences Academy* 58, 5, (461pp.).
- Mikkel, S., Henderson, J.B., 1983. Archean chemical weathering at three localities on the Canadian shield. *Precamb. Res.*, 20, 189-224.
- Milliman, J.D., Troy, P.J., Balch, W.M., Adams, A.K., Li Y.H., Mackenzie, F.T., 1999. Biologically mediated dissolution of calcium carbonate above the chemical lysocline? *Deep-Sea Res.* 46, 653-1669.
- Mohana Rao, K., Durgaprasada Rao, N.V.N., Rao, T.C.S., 1990. Holocene sea levels on Visakhapatnam shelf, east coast of India, Paper presented at National Seminar on Continental Margins of India at Andhra University, Visakhapatnam, India.
- Mohana Rao, K., Rajamanickam, G.V., Rao, T.C.S., 1989. Holocene Marine transgression as interpreted from bathymetry and sand grain- size parameters off Gopalpur. *Proc. Indian Acad.Sci. (Earth Planet Sci.)*.98, 2, (173-181 pp.).
- Mohana Rao, K., Rao, T.C.S., 1994. Holocene sea-levels of Visakhapatnam shelf, east coast of India. *J. Geol. Soc. India* 44, 685-689.

- Moiola, R.J., Weiser, D., 1968. Textural parameters: an evaluation. *Sediment. Petrol.* 38 (1), 45-53.
- Moosaviradi, et al., 2012. Geochemistry of Lower Jurassic Sandstones of Shemshak Formation, Kerman Basin, Central Iran : Provenance, Source Weathering and Tectonic Setting.
- Morner, N.A., 1976. Eustatic changes during the last 8000 years in view of radiocarbon calibration and new information from the Kattegatt region and other northwestern European areas: *Palaeogeog, Palaeoclimatol, Palaeoecol.* 19, (63-85 pp.).
- Muller, G., 1981. The heavy metal pollution of the sediments of Neckars and its tributary: A stocktaking, *Chem. Zeit.* 105, 157-164.
- Nagarajan, R., Roy, P.D., Jonathan, M.P., Rufino, Lozano-Santacruz., Franz L. Kessler., Prasanna, M.V., 2013. Geochemistry of Neogene sedimentary rocks from Borneo Basin, East Malaysia. Paleo-weathering, provenance, and tectonic setting. *Chemie der Erde - Geochemistry*, 1-8. <http://dx.doi.org/10.1016/j.chemer.2013.04.003>.
- Nair, S., 1971. Some observation on the hydrology of Kayamkulam estuary, *Bull. Dept. Biol. Oceano; Cochin University*, 5, (87-96 pp.).
- Nair, R.R., 1974. Holocene sea levels of the western continental shelf of India. *Proc. Indian Acad. Sci.* 79, (197-203 pp.).
- Nair, R.R., 1975. Nature and origin of small scale topographic prominence on the western continental shelf of India. *Ind. Jour. Marine. Sci.* 4, 25-29.
- Nair, R.R., Hashmi, N.H., Kidwai, R.M., Gupta, M.V.S. Paropkari, A.L., Ambre, N.V., Muralinath, A.S., Mascarenhas, A., D Costa, G.P., 1978. Topography and sediments of the Western Continental Shelf of India-Vengurla to Mangalore. *Indian Jour. Mar. Sci.* 7, 224-230.
- Nair, R.R., Hashimi, N.H., 1980. Holocene climatic inferences from the sediments of the western Indian continental shelf. *Proc. Ind. Acad.Sci.* 89, 3, (299-315 pp.).
- Nair, N.B., Azis, P.K.A., Dharmaraj, K., Arunachalam, M., Krishnakumar, K. and Balasubramanian, N.K. 1983. Ecology of Indian Estuaries: Part I- Physico-

- chemical features of water and sediment nutrients of Ashtamudi estuary. *Indian J. Mar. Sci.* 12, 143-150.
- Nair, N.B., Azis, P.K.A., 1987. Hydrobiology of Ashtamudi estuary: a tropical backwater system in Kerala, *Proc. Nat. Sem. Estuarine Mnagement*, Nair, N.B., (Ed.) National committee on science technology and environment, Government of Kerala, Trivandrum (268-280 pp.).
- Nair, N.J.K., Nalinakumar, S., Regunathan, P.K., Suresh Babu, D., 1988. Environmental geomorphic atlas Kerala, coastal zone. Project report submitted to Centre for Earth Science Studies report (PRT 88-5) (145 pp.).
- Nair, N.M., 1990. Structural trend line patterns and lineaments of the Western Ghats, South of 13° latitude. *Jour. Geol. Soc. of India* 35, 99-105.
- Nair, K.M., Padmalal, D., 2004. Quaternary geology and geomorphologic evolution of the south Kerala sedimentary basin, west coast of India. In: *Earth System Science and Natural Resources Management, Silver Jubilee Compendium*, Centre for Earth Science Studies. pp. 69-81.
- Nair, K.M., Padmalal, D., Kumaran, K.P.N., 2006. Quaternary Geology of South Kerala Sedimentary Basin - An outline, *Journal of Geological Society of India* 67, 165-179.
- Nair, K.M., Kumaran, K.P.N., Padmalal, D., 2009. Tectonic and hydrologic control on Late Pleistocene - Holocene landforms, palaeoforest and non forest vegetation: Southern Kerala, Project Completion Report, Kerala State Council for Science, Technology and Environment, Thiruvananthapuram, pp. 83.
- Nair, K.M., Padmalal, D., Kumaran, K.P.N., Sreeja, R., Limaye., Ruta B., Srinivas, R., 2010. Late Quaternary evolution of Ashtamudi-Sasthamkotta Lake systems of Kerala, south west India. *J. Asian Earth Sci.* 37 (4), 361-372.
- Nambiar, A.R., Rajagopalan, G., 1995. Radiocarbon dates of sediment cores from inner continental shelf off Taingapatnam, southwest coast of India. *Curr.Sci.* 68 (11), 1133–11137.
- Nameroff, T.J., Calvert, S.E., Murray, J.W., 2004. Glacial-interglacial variability in the eastern tropical north Pacific oxygen minimum zone recorded by redox-

sensitive trace metals. *Paleoceanography* 19 (1), doi: 10.1029/2003PA000912.  
ISSN: 0883-8305.

Narayana, A.C., Priju, C.P., Chakrabarti, A., 2001. Identification of a palaeodelta near the mouth of Periyar river in central Kerala, *Journal of the Geological Society of India* 57, 545-547.

Narayana, A.C., Priju, C.P., Rajagopalan, G., 2002. Late Quaternary peat deposits from Vembanad Lake (lagoon), Kerala, south-west coast of India. *Current Science* 83 (3), 318-321.

Narayana, A.C., Priju, C.P., 2004. Evolution of coastal landforms and sedimentary environments of the late Quaternary period along central Kerala, southwest coast of India. *J. Coast. Res. SI* 39, 1898–1902.

Narayana, A.C., Priju, C.P., 2006. Landforms and shoreline changes inferred from satellite images along the central Kerala coast. *J. Geol. Soc. India* 68, 35-49.

Narayana, A.C., 2007. Peat deposits of the west coast of India: implications for environmental and climate changes during Late Quaternary, *J. Coast. Res. SI* 50, 683–687.

Nelson, D.W., Sommers, L.E., 1996. *Methods of Soil Analysis. Part 3. Chemical Methods.* Soil Science Society of America, Book Series no. 5, (961-1010 pp.).

Nesbitt, H.W., Young, G.M., 1982. Early Proterozoic climates and plate motions inferred from major element chemistry of lutites. *Nature* 299, 715-717.

Nesbitt, H.W., Young, G.M., 1984. Prediction of some weathering trends of plutonic and volcanic rocks based on thermodynamic and kinetic considerations. *Geochimica et Cosmochimica Acta* 48, 1523-1534.

Nesbitt, H.W., Young, G.M., McLennan, S.M., Keays, R.R., 1996. Effects of chemical weathering and sorting on the petrogenesis of siliciclastic sediments, with implications for provenance studies. *J. Geol.* 104 (5), 525-542.

Neuendorf, K.K.E., J.P. Mehl, Jr., Jackson, J.A., 2005. *Glossary of Geology* (5th ed.). Alexandria, Virginia, American Geological Institute. ISBN 0-922152-76-4, (779 pp.).

- Niyogi, D., 1968. Morphology and evolution of Subernarekha delta, India. *TridsskriftSaertrkyafGeografisk* 67, 230–241.
- Niyogi, D., 1971. Morphology and evolution of Balasore shoreline, Orissa. *Studies in Earth Sciences, West Commemoration Volume, Today and Tomorrow Publishers, New Delhi* (289–304 pp.).
- Nordstrom, C., Margolis, S., 1972. Sedimentary history of central California shelf sands as revealed by scanning electron microscopy. *Jour. Sed. Petrology*, 42, 527-536.
- Orr, E.D., Folk, R.L., 1983. New scents on the chattermark trail: Weathering enhances obscure micro fractures. *Journal of Sedimentary Petrology* 53, 121–129.
- Orr, E.D., Folk, R.L., 1985. Chattermarked garnets found in soil profiles and beach environments. *Sedimentology* 32, 307–308.
- Overpeck, J., Anderson, D., Trumbore, S., Prell, W.L., 1996. The southwest Indian monsoon over the last 18000 years. *Clim. Dynam.* 12 (3), 213–225.
- Padmalal, D., Kumaran, K.P.N., Nair, K.M., Baijulal, B., Limaye, R.B., Vishnu Mohan, S., 2011. Evolution of the coastal wetland systems of SW India during the Holocene: evidence from marine and terrestrial archives of Kollam coast, Kerala, *Quaternary Inter.* 237 (1), 123-139.
- Padmalal, D., Maya, K., Vishnu Mohan, S., 2013. Late Quaternary climate, sea level changes and coastal evolution - A case study from SW India, *Monograph, Published by Centre for Earth Science Studies, Thiruvananthapuram, (164 pp.)*, ISBN 81-901842-1-0.
- Pandarinath, K., Verma, S.P., Yadava, M.G., 2004. Dating of sediment layers and sediment accumulation studies along the western continental margin of India: a review. *Inter. Geol. Rev.* 46 (10), 939-956.
- Partridge, T.C., Scott, L., Hamilton, J.E., 1999. Synthetic reconstructions of southern African environments during the Last Glacial Maximum (21-28 kyr) and the Holocene Altithennal, (8-6 kyr), *Quaternary International* 57/58, 207-214.
- Pascoe, E.H., 1964. *A manual of the geology of India and Burma.* Govt. of India, Delhi, 3rd Edition.

- Paterson, M.S., 1978. Experimental rock deformation: The brittle field. New York, Springer-Verlag (254 pp.).
- Paulose, K.V., Narayanaswami, S., 1968. The Tertiaries of Kerala coast. Mem. Geol. Soc. India, No.2, (300-308 pp.).
- Pejrup, M., 1988. The triangular diagram used for classification of estuarine sediments: A new approach. In: de Boer, P.L., (Ed.), Tide Influenced Sedimentary Environment and Facies. Riedal Publishing, pp. 289-300.
- Pe-Piper, G., Triantafyllidis, S., Piper, D.J.W., 2008. Geochemical identification of clastic sediment provenance from known sources of similar geology: the Cretaceous Scotian Basin, Canada. Jour. Sediment. Res. 78, 595-607.
- Peterknecht, K.M., Tietz, G.F., 2011. Chattermark trails: surface features on detrital quartz grains indicative of a tropical climate. Journal of Sedimentary Research 81, 153-158.
- Pettijohn, F.J., 1963. Chemical composition of sandstones – excluding carbonate and volcanic sands, in Data of Geochemistry 6th edn. US Geological Survey Professional Paper 440S.
- Pettijohn, F.H., Potter, P.E., Siever, R., 1972. Sand and Sandstone. Springer-Verlag, New York. (618 pp.).
- Pettijohn F.J., Potter, P.E., Siever R., 1987. Sand and Sandstone. Springer, New York. (553 pp.).
- Pirazzoli, P.A., 1976. Les Variations du Niveau Marin Depuis 2000 Ans. Memoris du Laboratoire de Geomorphologie de l'Ecole Pratique des Hautes Etudes, Dinard, France, no.30, (1-421 pp.).
- Pirazzoli, P.A., 1991. World Atlas of Holocene Sealevel Changes. Elsevier Oceanography Series 58, Elsevier, Amsterdam (300 pp.).
- Pisharody, P.R., 1992. Keralathile Kalavastha (Climate in Kerala). State institute of Language Publ. (26 pp.) [in Malayalam].
- Pisias, N.G., Prell, W.L., 1985. High resolution carbonate records from the hydraulic piston cored section of Site 572. In: Mayer, L., Theyer, F., et al., Init. Repts., DSDP, 85, Washington (U.S. Govt. Printing Office) (711-722 pp.).



- Pluet, J., Pirazzoli, P., 1991. World Atlas of Holocene Sea-Level Changes. Elsevier, Vol. 58.
- Poppe, L.J., Williams, S.J., Paskevich, V.F., 2005. USGS east coast sediment analysis: procedures, database, and GIS data. US Geol. Surv. Open-File Report -1001.
- Posamentier, H.W., Jervey, M.T., Vail, P.R., 1988. Eustatic controls on clastic deposition - Conceptual framework. In: Wilgus, C.K., Hastings, B.S., et al. (eds.). Sea level changes: An Integrated Approach. Society of Economic Paleontologists and Mineralogists. Special Publication. 42, (109-124 pp.).
- Powar, S.D., Venkataramana, B., Mathai, T., Mallikarjuna, C., 1983. Progress report, Unpublish. Geol. Surv. India, Trivandrum.
- Prabhakar Rao, G., 1962. Some aspects of the placer deposits of south Kerala in relation to the geomorphic evolution of the west coast of India. Ph. d. thesis submitted to the Andhra University (Unpublished) (199 pp.).
- Prakash, T.N., Varghese, A.P., 1987. Seasonal beach changes along Quilon District Coast, Kerala. Jour. of Geol. Soc. India, 29, 390-398.
- Prakash, T.N., 2000. Sediment distribution and placer mineral enrichment in the innershelf of Quilon, SW coast of India, Indian Journal of Marine Sciences 29, 120-127.
- Prakash, T.N., Muraleedharan Nair, M.N., Kurian, N.P., Vinod, M., 2001. In: Black, K., Baba, M., (Eds.) Developing a management plan for Ashtamudi estuary, Kollam, India. Geology and Sediment characteristics, pp. 341-361.
- Prell, W.L., Murray, D.W., Clemens, S.C., Anderson, D.M., 1992. Evolution and variability of the Indian ocean summer monsoon: evidence from the western Arabian Sea drilling program; Geophysical. Monograph 70, pp. 447-469.
- Prentice, I.C., Jolly, D., (with BIOME 6000 participants), 2000. Mid-Holocene and glacial-maximum vegetation geography of the northern continents and Africa. J. Biogeogr., 27, 507-519.
- Priju, C.P., Narayana, A.C., 2007. Evolution of Coastal Landforms and Sedimentary Environments of the Late Quaternary Period along Central Kerala, Southwest Coast of India, Journal of Coastal Research 39, 1898-1902.

- Prithviraj, M., Prakash, T.N., 1991. Surface Microtextural study of detrital quartz grains off inner shelf sediments off Central Kerala coast. *Indian Journal of Marine Science* 20, 3-16.
- PWD, 1976. Water Resources of Kerala. Public Works Department, Govt. of Kerala (60 pp.).
- Qasim, S.Z., 2002. *Indian Estuaries*. Allied Publishers, New Delhi (189-200 pp.).
- Raha, P.K., Roy, S.K.S., Rajendran, C.P., 1983 A new approach to the lithostratigraphy of the cenozoic sequence of Kerala, *Jour. Geol. Soc. India*, 24, 114-115.
- Rahman, M.H., Ahmed, F., 1996. Scanning electron microscopy of quartz grain surface textures of the Gondwana Sediments, Barapukuria, Dinajpur, Bangladesh. *Journal of the Geological Society of India* 47, 207-214.
- Rahman, M.J.J., Suzuki, S., 2007. Geochemistry of sandstones from the Miocene Surma Group, Bengal Basin, Bangladesh: implications for Provenance, tectonic setting and weathering. *Geochemical Journal* 41, 415-428.
- Rajan, T.N. (with nine others), 1992. Report on the Geotechnical investigations off Kodungallur and Ponnani, Kerala. Unpublished GSI Report.
- Rajendran, P., 1979. Environment and stone age cultures of north Kerala. Ph.D. Dissertation, University of Poona, Pune. (Unpublished) (145 pp.).
- Rajendran, C.P., Rajagopalan, G., Narayanaswamy, N., 1989. Quaternary geology of Kerala: evidence from radiocarbon dates. *J. Geol. Soc. India* 33, 218-222.
- Ramanujam, C.G.K., 1987. Palynology of the Neogene Warkalli beds of Kerala state of South India. *Jour. Pal. Soc. India* 32, 26-42.
- Ramsay, P.J., 1995. 9000 years of sea-level change along the southern African coastline. *Quaternary Inter.* 31 (5), 71-75.
- Rao, V.P., Rao, Ch.M., Mascarenhas, A., Rao, K.M., Reddy, N.P.C. Das, H.C., 1992. Changing sedimentary environments during Pleistocene-Holocene in a core from the eastern continental margin of India. *J. Geol. Soc. India* 40, 59-69.

- Rao, P.C., Thamban, M., 1997. Dune Associated Calcretes, Rhizoliths and Paleosols from the Western Continental Shelf of India. *Jour. Geol. Soc. India* 49, 297-306.
- Rao, P.C., Wagle, B.G., 1997. Geomorphology and surficial geology of the western continental shelf and slope of India: A review. *Current Science* 73, No. 4, 330-350.
- Rao, V.P., Nair, R.R., Hashimi, N.H., 1983. Clay mineral distribution on the Kerala continental shelf and slope. *Jour. Geol. Soc. India.* 24, 540-546.
- Rao, V.P., Rajagopalan, G., Vora, K.H., Almeida, F., 2003. Late Quaternary sea level and environmental changes from relic carbonate deposits of the western margin of India, *Proc. Ind. Acad. Sci. (Earth Planet. Sci.)* 112(1), pp. 1-25.
- Reddy, N.P.C., Rao, N. V.N. D.P., Dora, Y.L., 1992. Clay mineralogy of inner shelf sediments off Cochin, west coast of India. *Ind. Jour. Mar. Sc.* 21, 2, 152-154.
- Reddy, N.P.C., Rao, N.V.N.D.P., 1992. A mid-Holocene strandline deposit on the innershelf of Cochin, West coast of India. *Jour. Geol. Soc. India.* 39, 205-211.
- Riboulleau, A., Baudin, F., Deconinck, J.F., Derenne, S., Largeau, C., Tribouvillard, N., 2003. Depositional conditions and organic matter preservation pathways in an epicontinental environment: the Upper Jurassic Kashpir Oil Shales (Volga basin, Russia). *Palaeogeography, Palaeoclimatology, Palaeoecology*, 197, 171-197.
- Rimmer, S.M., Thompson, J.A., Goodnight, S.A., Robl, T., 2004. Multiple controls on the preservation of organic matter in Devonian-Mississippian marine black shales: Geochemical and petrographic evidence. *Palaeogeography, Palaeoclimatology, Palaeoecology*, 215, 125-154.
- Roaldset, E., 1978. Mineralogical and chemical changes during weathering, transportation and sedimentation in different environments with particular references to the distribution of Yttrium and lanthanide elements, Ph.D. Thesis, Geol. Inst., Univ. of Oslo, Norway (unpublished).
- Robinson, G.W., 1949. *Soils*, Wiley, New York , (22 pp.).

- Roser, B.P., Korsch, R.J., 1988. Provenance signatures of sandstone–mudstone suites determined using discrimination function analysis of major-element data. *Chem. Geol.* 67, 119-139.
- Rothwell, R.G., Rack, F.R., 2006. New techniques in sediment core analysis: an introduction. In: Rothwell, R.G., (Ed.), *New techniques in sediment core analysis*. Special Publications. Geological Society, London, pp. 1-29.
- Sabu, J., Thiruvikramji, K.P., 2002. Kayals of Kerala coastal land and implications to Quaternary sea-level changes. In: Narayana, A.C. (Ed.), *Late Quaternary Geology of India and Sea Level Changes*, Memoir No. 49. Geol. Soc. India 51-64.
- Sahu, B.K., 1964. Depositional mechanisms from the size analysis of clastic sediments. *J. Sediment. Petrol.* 34 (1), 73-83.
- Salomons, W., Forstner, U., 1984. *Metals in the hydrocycle*. Springer-Verlag, Berlin, Heidelberg, New York, ISBN 3540127550.
- Samsuddin, M., 1986. Textural differentiation of foreshore and breaker zone sediments on the northern Kerala coast, India. *Sed. Geol.* 46 (1-2), 135-145.
- Samsuddin, M., 1991. Sedimentology and mineralogy of the beach strand plain and innershelf sediments of the northern Kerala coast. Ph.D. thesis submitted to the Cochin University of Science and Technology, Cochin, Unpublished (160 pp.).
- Samsuddin, M., Ramachandran, K.K., Dora, Y.L., 1992. Quartz grain surface textures and depositional history of beach and strand plain sediments along the northern Kerala coast. *Jour. Geol. Soc. India* 40, 501-508.
- Samsuddin, M., Ramachandran, K.K., John Mathai., Jayaprasad, B.K., Neelakandan, V.N., 2008. *Natural Resources and Environmental Atlas of Kerala., Alapuzha and Kollam District*.
- Satkunas, J., Stancikaite, M., 2009. Pleistocene and Holocene palaeo-environments and recent processes across NE Europe, *Quaternary International* 207, 13.
- Sawarkar, A.P., 1969. Gold bearing alluvial gravels of Nilambur valley, Kozhikode district, Kerala. *Indian Minerals* 23 (3), 1-19.

- Schnitzer M., 1978. Humic substances: chemistry and reactions. In: Schnitzer M, Khan SU (Eds.) Soil organic matter. Elsevier, Amsterdam, pp. 1-64.
- Schulz, M.S., White, A.F., 1999. Chemical weathering in a tropical watershed, Luquillo Mountains, Puerto Rico III: quartz dissolution rates, *Geochimica et Cosmochimica Acta* 63, 337–350.
- Schumm, S.A., 1969. Geomorphic implications of climate change. In: Chorley, R.J., (Ed.), *Introduction to Fluvial Processes*, Methuen, London (202–210 pp.).
- Selby, M.J., 1985. *Earth's Changing Surface-An Introduction to Geomorphology*. Clarendon, Oxford (607 pp.).
- Selvaraj, K., Chen, C.T.A., 2006. Moderate chemical weathering of subtropical Taiwan: constraints from solid-phase geochemistry of sediments and sedimentary rocks. *J. Geol.* 114, 101-116.
- Selvaraj. K., Ram Mohan, V., 2003. Textural variation and depositional environments of innershelf sediments, off Kalpakkam, South-East coast of India. *Journal of Geological Society of India* 61, 449-462.
- Semeniuk, V., Searle, D.J., 1985. Distribution of calcrete in Holocene coastal sands in relationship to climate, southwestern Australia. *Journal of Sedimentary Research* 55, 86-95.
- Sen, P.K., 1985. The genesis of flood in the lower Damodar catchment. In: Sen P.K., (ed.) *The concepts and methods in Geography*. The University of Burdwan, Burdwan (71-85 pp.).
- Setlow, L.M., Karpovich, R.P., 1972. Glacial microtextures on quartz and heavy mineral sand grains from the littoral environment. *Journal of Sedimentary Petrology* 42, 864–975.
- Setty, A.P.M.G., Madhusudhana Rao, C., 1972. Phosphate, carbonate and organic matter distribution in sediment cores of Bombay- Saurashtra coast, India. 24th IGC., Section 8.
- Shajan, K.P., 1998. Studies on Late Quaternary sediments and sea level changes of the central Kerala coast, India. Ph. D., Thesis, Cochin University of Science and Technology, Cochin, Kerala, Unpublished (101 pp.).

- Shaji, E., 2003. Groundwater management studies of Kollam district, Kerala (AAP 2000-2011). Central Ground Water Board, Ministry of Water Resources, Government of India, (113 pp.).
- Shaw, D.M., 1968. A review of K-Rb fractionation trends by covariance analysis. *Geochim. Cosmochim. Acta* 32, 573-602.
- Shepard, F.P., 1954. Nomenclature based on sand-silt-clay ratios. *J. Sediment. Petrol.* 24 (3), 151-158.
- Shepard, F.P., 1964. Sea level changes in the past 6000 years, possible archaeological significance, *Science* 143, 3606, 574-576.
- Shotyk, W., Weiss, D., Appleby, P.G., Cheburkin, R., Frei, M., Gloor, J.D., Kramers, S.R., W.O.van der Knaap, 1998. History of atmospheric lead deposition since 12,370 14Cyr BP recorded in a peat bog profile, Jura Mountains, Switzerland. *Science* 281, 1635-1640.
- Simon, B., 2007. Grain size distribution and statistic package for the analysis of un consolidated sediments by sieving or laser granulometer. Gradistat programme (Ver. 4.0).
- Singh, P., Rajamani, V., 2001. Geochemistry of the floodplain sediments of the Kaveri River, southern India, *Journal of Sedimentary Research* 71, 50-60.
- Singh, S.K., Sarin, M.M., France-Lanord, C., 2005. Chemical erosion in the Eastern Himalaya: major ion composition of the Brahmaputra and  $\delta^{13}\text{C}$  of dissolved inorganic carbon. *Geochim. Cosmochim. Acta* 69, 3573-3588.
- Sinha, R., Tandon, S.K., Gibling, M.R., Bhattacharjee, P.S., Dasgupta, A.S., 2005. Late Quaternary geology and alluvial stratigraphy of the Ganga basin. *Himalayan Geology*, 26, 223-240.
- Soman, K.I., 1997. *Geology of Kerala*: Published by Geological Society of India.
- Soumya, W., Tresa Radhakrishnan, Radhakrishnan, S., 2011. Sediment Characteristics along the Ashtamudi Estuarine System, *International Journal of Biological Technology* 2(3), 11-16.

- Spencer, C.D., Plater, A.J., Long, A.J., 1998. Rapid coastal change during the mid-to late-Holocene: the record of barrier estuary sedimentation in the Romney marsh region, south-east England. *Holocene* 8 (2), 143-163.
- Sreejith, C., Ravindra Kumar, G.R., 2013. Petrogenesis of high-K metagranites in the Kerala Khondalite Belt, southern India: a possible magmatic-arc link between India, Sri Lanka, and Madagascar, *Journal of Geodynamics* 63, 69-82, <http://dx.doi.org/10.1016/j.jog.2012.10.002>.
- Srinivasa Rao, P., Krishna Rao, G., Rao, N.V.N.D.P., Swamy, A.S.R., 1990. Sedimentation and sea level variations in Nizampatnam Bay, east coast of India. *Ind. Jour.Mar. Sci.* 19, 261-264.
- Srivastava, S.P., Arthur, M., Clement, B., 1989. Morphology and surface texture of quartz grains from odp site 645, Baffin Bay Michel Cremer and Philippe Legigan. *Proceedings of the Ocean Drilling Program, Scientific Results, Vol. 1*, pp. 21-30.
- Stanley, D.J., Nir, Y., Galili, E., 1998. Clay mineral distributions to interpret Nile Cell provenance and dispersal: III. Offshore margin between Nile delta and northern Israel. *Journal of Coastal Research* 169-217.
- Stanley, D.J., Hait, A.G., 2000. Holocene Depositional Patterns, Neotectonics and Sundarban Mangroves in the Western Ganges-Brahmaputra Delta. *Journal of Coastal Research* 16(1), 26-39.
- Subramanian, V., 1975. Origin of surface pits on quartz as revealed by scanning electron microscopy. *J. Sediment. Petrol.* 45, 530-534.
- Suchindan, G.K., Samsuddin, M., Ramachandran, K.K., Haneeshkumar, V., 1996. Holocene coastal landforms along the northern Kerala coast and their implications on sea level changes, Paper presented in International seminar on Quaternary sea level variations, shore line displacement and coastal environment, held at Tamil University Thanjavur (72 pp.).
- Sukhtankar, R.K., Pandian, R.S., 1990. Evaluation of sea level rise on the shore zone areas of the Maharashtra coast. In: sea level variation and its impact on coastal environment. Tamil university Press, Thanjavur (329-338 pp.).

- Swain, M.V., 1979. Microfracture about scratches in brittle solids. Royal Society of London, Proceedings, ser. A, 366, pp. 575-597.
- Swain, A.M., Kutzbach, J.E., Hastenrath, S., 1983. Quat. Res. 19, 1–17.
- Tanner, W.F., 1991a. Suite statistics: the hydrodynamic evolution of the sediment pool. In: Syvitski, J.P.M., (Ed.), Principles, methods and application of particle size analysis, Cambridge, Cambridge University Press, pp. 225-236.
- Tanner, W.F., 1991b. Application of suite statistics to stratigraphy and sea-level changes. In: Syvitski J.P.M., (Ed.), Principles, methods and application of particle size analysis, Cambridge, Cambridge University Press, pp. 283-292.
- Taylor, S.R., McLennan, S.M., 1985. The Continental Crust: its composition and evolution. Blackwell Scientific Publication, Oxford. (301 pp.).
- Tertian, R., Claisse, F., 1982. Principles of quantitative X-ray fluorescence analysis. Heyden, London, U.K. (385 pp.).
- Thrivikramji, K.P., Ramasarma, M., 1981. Implication of sedimentary structural facies of a calcareous sand body at Kovalam, Kanyakumari District, Tamil Nadu. Jour. Geol. Soc. India 24, 203-207.
- Tomkins, J.D., Dermot, A., Scott, F.L., Warwick, F.V., 2007. A simple and effective method for preserving the sediment–water interface of sediment cores during transport. J. Paleolimnol, DOI 10.1007/s10933-007-9175-1.
- Torres-Alvarado, I.S., Verma, S.P., Palacios-Berruete, H., Guevara, M., Gonzálezcastillo, O.Y., 2003. DC-BASE: a database system to manage Nernst distribution coefficients and its application to partial melting modeling. Computers and Geosciences 29, 9, 1191-1198.
- Trefethen, J.M., 1950. Classification of sediments. American Journal of Science, 248, 55-62.
- Udayaganesan, P., Angusamy, N., Gujar, A.R., Rajamanickam, G.V., 2011. Surface microtextures of quartz grains from the central coast of Tamil Nadu. Journal of Geological Society of India 77, 26-34.



- Umitsu, M., Buman, M., Kawase, K., Woodroffe, C.D., 2001. Holocene paleoecology and formation of the Shoalhaven River deltaic-estuarine plains, southeast Australia. *Holocene* 11 (4), 407-418.
- USGS, 2006. Surficial sediment character of the Louisiana offshore continental shelf region: a GIS Compilation. U.S. Geological Survey, Open-File Report (1195 pp.).
- Valdiya, K.S., Narayanan, A.C., 2007. River response to neotectonic activity, Example from Kerala. India. *J. Geol. Soc. India* 70, 427-443.
- Van Campo, E., 1986. Monsoon fluctuations in two 20,000 yr BP Oxygen-isotope/pollen records off southwest India. *Quaternary Res.* 26 (3), 376-388.
- Van De Kamp, P.C., Leake, B.E., 1985. Petrography and geochemistry of feldspathic and mafic sediments of the northeastern Pacific margin. *Transactions of the Royal Society of Edinburgh: Earth Sciences* 76, pp. 411-449.
- Van Staden, A., Naidoo, T., Zimmermann, U., Germs, G.J.B., 2006. Provenance analysis of selected clastic rocks in Neoproterozoic to lower Paleozoic successions of southern Africa from the Gariep Belt and the Kango Inlier. *South African Jour. Geol.* 109, 215-232.
- Wani, H., Mondal, M.E.A., 2010. Petrological and geochemical evidence of the Paleoproterozoic and the Meso- Neoproterozoic sedimentary rocks of the Bastar craton, Indian Peninsula: Implications on paleoweathering and Proterozoic crustal evolution. *Jour. Asian Earth Sci.* 38(5), 220-232.
- Washmi, H.A., Gheith, A.M., 2003. Recognition of diagenetic Dolomite and chemical Surface Features of the Quartz Grains in Coastal Sabkha Sediments of the Hypersaline Shuaiba Lagoon, Eastern Red Sea Coast, Saudi Arabia. *J. KAU: Mar. Sci.* 14, 101-112.
- Weaver, C.E., 1989. Clays, muds and shales, *Developments in Sedimentology*. Elsevier, Amsterdam, (819 pp.).
- Wedepohl, K.H., 1971. Environmental influences on the chemical composition of shales and clays. In: Ahrens, L.H., Press, F., Runcorn, S.K., Urey, H.C. (Eds.), *Physics and Chemistry of the Earth*. Pergamon, Oxford, pp. 305-333.

- Wedepohl, K.H., 1995. The composition of the continental crust, *Geochimica et Cosmochimica Acta* 59, 217-239.
- Velde, B., 1995. Origin and mineralogy of clays. *Clays and the environment*, Berlin, Springer-Verlag. (356 pp.).
- Weltje, G.J., Von Eynatten, H., 2004. Quantitative Provenance Analysis of Sediments: Review and Outlook. *Sedimentary Geology* 171, 1-11.
- Verma, K., Sudhakar, M., 2006. Evidence of reworking and resuspension of carbonates during last glacial maximum and early deglacial period along the southwest coast of India. *J. Earth Syst. Sci.* 115 (6), 695-702.
- Werne, J.P., Lyons, T.W., Hollander, D.J., Formolo, M.J., Sinningh-Damsté, J.S., 2003. Reduced sulfur in euxinic sediments of the Cariaco Basin: sulfur isotope constraints on organic sulfur formation. *Chemical Geology* 195, 159-179.
- White, J.W.C., Ciais, P., Figge, R.A., Kenny, R., Markgraf, V., 1994. A high-resolution record of atmospheric CO<sub>2</sub> content from carbon isotopes in peat. *Nature* 367, 153-156.
- Williams, M.A.J., Faure, H., 1980. In: Balkema I Rotterdam A.A., (Ed). *The Sahara and the Nile*.
- Williams, M.A.J., Clarke, M.F., 1984. Late Quaternary environments in North-Central India, *Nature*, 308, 633-35.
- Williams, M.A.J., Clarke, M.F., 1995. Quaternary geology and prehistoric environments in the Son and Belan Valleys, north-central India. *Geol. Soc. India Memoir* 32, 282-308.
- Vincent, P., 1986. Differentiation of modern beach and coastal dune sands-a logic regression approach using the parameters of the hyperbolic distribution. *Sedimentary Geol.* 49 (3-4), 167-176.
- Vital, H., Statterger, K., 2000. Major and trace elements of stream sediments from the lowermost Amazon River. *Chem. Geol.* 168 (1-2), 151-168.

- Von Eynatten, H., Gaupp, R., 1999. Provenance of Cretaceous synorogenic sandstones in the Eastern Alps: constraints from framework petrography, heavy mineral analysis and mineral chemistry. *Sed. Geol.* 124 (1-4), 81-111.
- Woodroffe, C.D., 1983. Development of mangrove forests from a geological perspective. In: Teas H.J., (Ed.), *Biology and Ecology of Mangroves*, pp. 118.
- Woodroffe, S.A., Horton, B.P., 2005. Holocene sea-level changes in the Indo-Pacific. *J. Asian Earth Sci.* 25 (1), 29-43.
- Wronkiewicz, D.J., Condie, K.C., 1987. Geochemistry of Archaean shales from the Witwatersrand Supergroup, South Africa. Source-area weathering and provenance. *Geochim. Cosmochim. Acta* 51, 2401-2416.
- Yang, S.Y., Jung, H.S., Li, C.X., 2004. Major elements geochemistry of sediments from Chinese and Korean River. *Geochimica et Cosmochimica Acta* 33 (1), 99-106.
- Ybert, J.P., Mareschi Bissa, W., Martins Catharino, E.L., Kutner, M., 2003. Environmental and sea-level variations on the southeastern Brazilian coast during the Late Holocene with comments of pre-historic human occupation. *Palaeogeogr. Palaeoclimatol. Palaeoecol.* 189 (1-2), 11-24.
- Yim, W.W.S., Higlens, A., Huang, G., Radtke, U., 2008. Stratigraphy and optically stimulated luminescence dating of sub-aerially exposed Quaternary deposits from two shallow bays in Hong Kong, China. *Quaternary Inter.* 183 (1), 23-39.
- Zimmermann, U., Bahlburg, H., 2003. Provenance analysis and tectonic setting of the Ordovician deposits in the southern Puna basin, NW Argentina. *Sedimentology* 50, 1079-1104.
- Zimmermann, U., Spalletti, L.S., 2009. Provenance of the Lower Paleozoic Belcarce Formation (Tandilia System, Buenos Aires Province, Argentina): Implications for paleogeographic reconstructions of SW Gondwana. *Sediment. Geol.* 219, 7-23.

## PUBLICATIONS

- Tiju I. Varghese**, Prakash, T.N., Nagendra, R., Samsuddin, M., 2010. Studies of sub-crop sediments in southern Kerala; Implications to sea level changes Coastal processes in a critically eroding sector of south west Coast of India. Proceedings, Indian National Conference on Coastal Processes, Resources and Management, Thiruvananthapuram, pp. 362-368.
- Tiju I. Varghese**, Prakash, T.N., Nagendra, R., 2012. Depositional environment of inland, lagoon and offshore sediments of Kayamkulam area, Kerala National Seminar on Coastal Zone- Processes, Resources & Social Relevance held at School of Marine Sciences, Cochin University of Science and Technology (CUSAT), Cochin, p9.
- Tiju I. Varghese**, Prakash, T.N., Shahul Hameed, T.S., 2014. Morphological changes and sediment characterization in tsunami affected innershelf, southern Kerala, India. Indian Journal of Geo-Marine Sciences (In Press).
- Tiju I. Varghese**, Prakash, T.N., Nagendra, R., 2014. Micromorphological Characteristics and Depositional history of Coastal plain sediments, southern Kerala, SW India. Journal of Geological Society of India (Under Review).